AN APOLLO APPLICATIONS PROGRAM DATA RELAY TERMINAL DESIGN STUDY

FINAL REPORT

NASA Contract No. NAS W-1982 • FEBRUARY 1970

HUGHES
HUGHES AIRCRAFT COMPANY
SPACE SYSTEMS DIVISION

SSD 00058R

FEBRUARY 1970

AN APOLLO APPLICATIONS PROGRAM DATA RELAY TERMINAL DESIGN STUDY

FINAL REPORT

NASA Contract No. NAS W-1982

The support of the
National Aeronautics and Space Administration
during the performance of this study
is hereby acknowledged.

HUGHES
HUGHES AIRCRAFT COMPANY
SPACE SYSTEMS DIVISION

SSD 00058R

CONTENTS

		Page
1.	INTRODUCTION	1-1
2.	DRT REQUIREMENTS	
	2.1 Operational Concept	2-1
	2.2 Communication Signals	2-1
	2.3 Carrier Frequencies	2-5
	2.4 Spectrum Spreading	2-5
	2.5 DRT Antenna Subsystem	2-5
	2.6 Orbital Constraints	2-6
	2.7 OA Altitude and Stabilization Constraints	2-6
	2.8 Operational Constraints	2-7
	2.9 Operational Life	2-7
	2.10 OA Interfaces	2-8
	2.11 Booster Interface	2-9
	2.12 Intelsat IV Interface	2-9
	2.13 Ground Equipment Interface	2-9
3.	DRT DESCRIPTION AND PERFORMANCE	
	3.1 Configuration	3-1
	3.2 Functional Description	3-2
	3.3 Communications Performance	3-9
	3.4 Power and Weight Summary	3-11
4.	SUBSYSTEMS	
	4.1 Transmitter/Receiver	4-1
	4.2 Telemetry Signal Selector and Multiplexer	4-7
	4.3 Antenna	4-9
	4.4 Antenna Positioning Subsystem	4-25
	4.5 Telemetry, Command, and Manual Control	4-41
	4.6 Thermal Design	4-41
5.	SUPPORTING STUDIES	
	5.1 Signal Multiplexing	5-1
	5.2 Link Performance Analysis	5-5
	5.3 Carrier Spreading	5-17
	5.4 Antenna Acquisition and Tracking	5-19

5.5 TWT Selection 5-37
5.6 Antenna Selection 5-37
5.7 Antenna Fabrication 5-41
5.8 Selection of Antenna Positioner Tradeoffs 5-43
5.9 Thermal Analysis 5-51

APPENDICES

A. Selection of Intelsat IV Transponder Channels and Frequencies A-1
B. AAP/SWS Space Terminal Structural Design Criteria and Requirements B-1
C. Gimbal Angles for Low Altitude Satellite Antenna Tracking a Synchronous Satellite C-1

1. INTRODUCTION

This report presents the results of a study for the design of a Data Relay Terminal (DRT) to be incorporated into a Saturn Workshop (SWS) as part of the Apollo Applications Program (AAP). This study was performed by the Space Systems Division of Hughes Aircraft Company for the National Aeronautics and Space Administration, Headquarters, under Contract NASW-1982.

At the inception of this study on 13 October 1969, it was anticipated that the subject DRT would be incorporated into the first SWS. Contact was established with McDonnell Douglas Aircraft Corporation (MDAC) through a resident NASA representative, and a cooperative effort was initiated by MDAC for the purpose of defining the physical interface between the DRT and the SWS. However, in November 1969, it was established by NASA that the DRT would not be implemented on the first SWS, nor were any definitive plans established for its subsequent implementation. As a result of this decision, the MDAC team was no longer in a position to make firm commitments on how and where to mount the DRT and the final selection from two proposed DRT configurations was deferred. The two configurations, both described in Section 3 of this report, are essentially similar, differing primarily in detail as to the attachment location and the antenna deployment boom.

It was also decided by NASA that the DRT design study should be completed so that a preliminary design would be available should a future requirement for such a terminal be established. This report documents that design, as well as a summary of the analyses and tradeoffs supporting the design. The overall design requirements and constraints are summarized in Section 2. The DRT configuration and performance are described in Section 3, followed by more detailed descriptions of the DRT subsystems in Section 4. Supporting studies are summarized in Section 5, with additional detail provided in the appendices.

2. DRT REQUIREMENTS

2.1 OPERATIONAL CONCEPT

The DRT for the AAP serves as one end of a communication link connecting the orbital assembly (OA) to the Mission Control Center at Houston (MCC-H), as conceptually depicted in Figure 2-1. Voice and digital command would be provided on the uplink (MCC-H to OA), and voice and digital telemetry on the downlink (OA to MCC-H); communication in both directions would utilize a single repeater channel leased from Comsat on an Intelsat IV communication satellite. The link is completed on the ground with one or two Comsat ground terminals connected to MCC-H by leased land lines.

In typical operation, two Intelsat IV satellites would be employed, with the orbit geometry shown in Figure 2-2. Using the Atlantic and Pacific satellites stationed at the longitudes currently projected by Comsat, visibility of a communication satellite by the DRT on the SWS will be continuous or near-continuous, depending on the desired clearance of the main-beam of the DRT radiation pattern above the earth. Interruptions in service will occur only upon transfer of the link from one Intelsat IV to the other, or when the DRT antenna pattern is effectively shadowed by the OA.

2.2 COMMUNICATION SIGNALS

2.2.1 Uplink Signals

The uplink shall be capable of transmitting either a voice signal alone, or a voice signal plus a command signal, from MCC-H to the OA whenever visibility to an Intelsat IV satellite exists and the DRT antenna has acquired the satellite. In the event of degraded link performance, the voice signal shall have priority over the command signal.

2.2.1.1 Voice Signal Characteristics

The voice channel shall have a quality equivalent to a test tone-to-noise ratio (TT /N) not less than 20 dB. This channel will be used with 12 dB clipped speech.

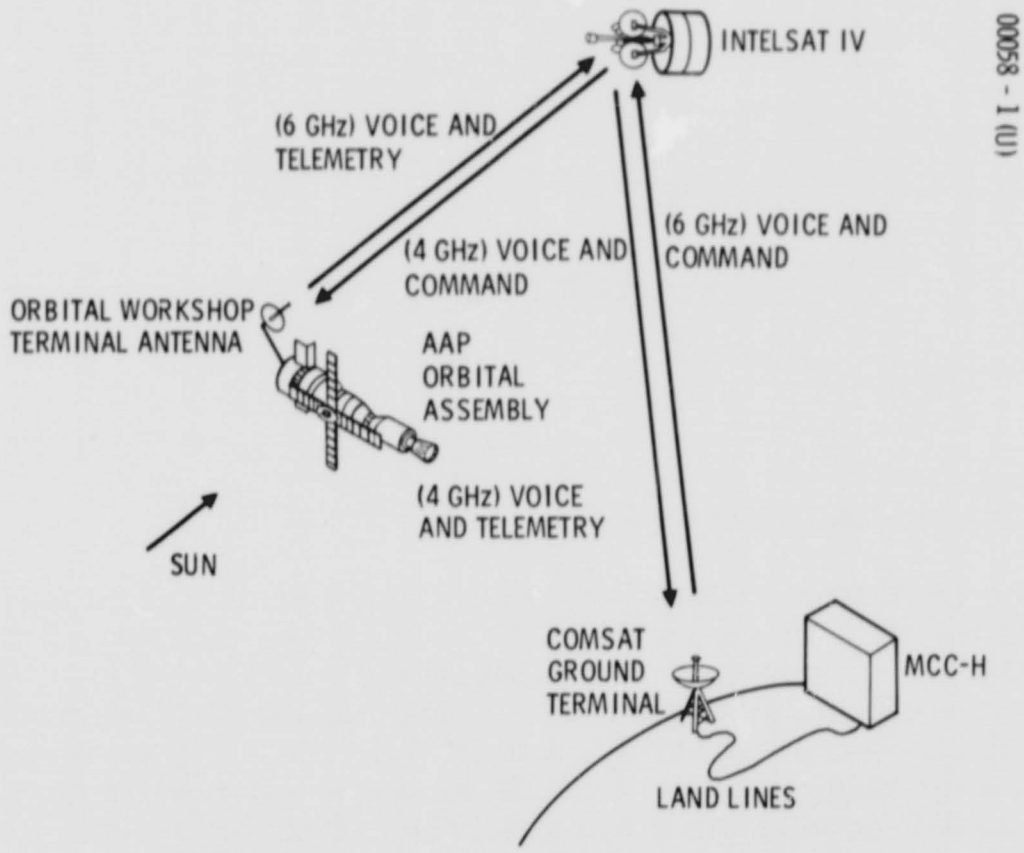

Figure 2-1. Mission Concept

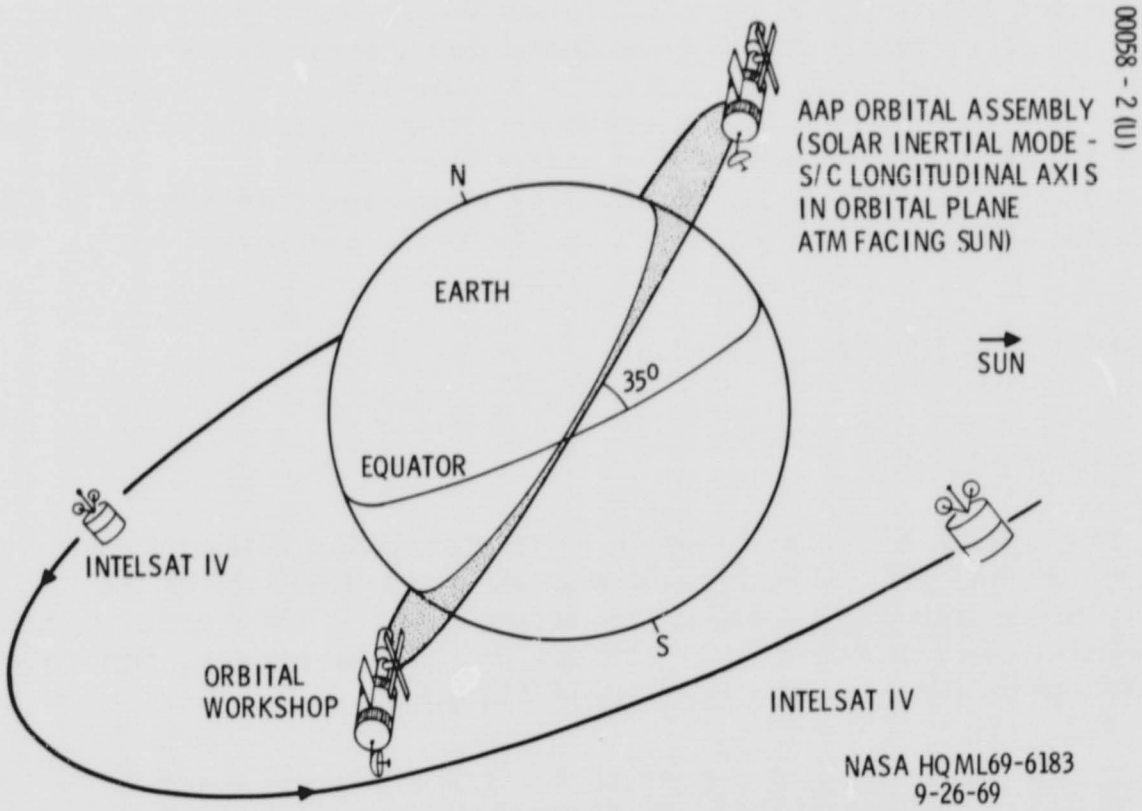

Figure 2-2. Orbit Geometry

2.2.1.2 Command Signal Characteristics

The command signal format, consisting of a 1 kHz sine wave algebraically summed with a phase-shifted 2 kHz sine wave, is shown in Figure 2-3. This signal channel shall contribute a bit error rate not exceeding one part in 10^6.

2.2.1.3 Uplink Multiplexing*

The two uplink signals shall be combined by frequency division multiplexing, retaining the voice signal at baseband.

2.2.2 Downlink Signals

The downlink shall be capable of transmitting voice alone, or voice plus any one of the three telemetry signal channels specified below, whenever the communication link is operative. In the event of degraded link performance, the voice signal shall have priority over any of the telemetry signals.

2.2.2.1 Voice Signal Characteristics

The downlink voice signal shall have the same quality as specified for the uplink voice, in paragraph 2.2.1.1.

2.2.2.2 Telemetry Signal Characteristics

The telemetry signal input to the DRT will consist of seven binary non-return to zero (NRZ) pulse trains, as defined below. These signals will be grouped by the DRT into three telemetry channels, A, B, and C, as follows:

Telemetry Channel	Telemetry Signals
A	1
B	2
C	3, 4, 5, 6, and 7

*This requirement was established for reasons described in Section 5.1.

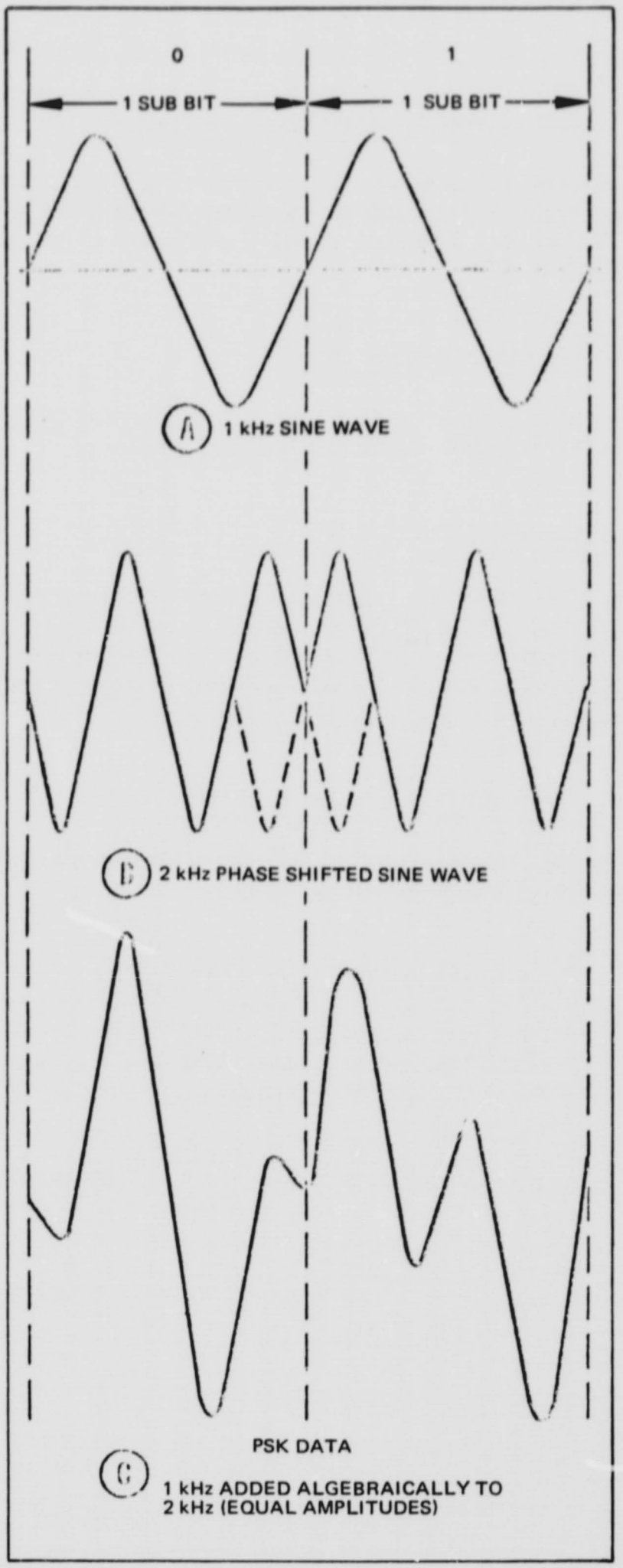

00058-3(U)

Figure 2-3. Command Signal Format

Telemetry Signal	Bit Rate, kilobits/sec
1	51.2
2	72.0
3	1.6
4	4.0
5	5.12
6	5.12
7	5.12 or 5.76

For purposes of multiplexing the several signals that make up telemetry channel C, it shall not be assumed that any of the telemetry signals is synchronous with respect to any other telemetry signal.

The downlink data channel shall contribute an error rate not exceeding one part in 10^4.

2.2.2.3 Downlink Multiplexing (RF)*

The downlink voice and the selected telemetry channel shall be modulated onto separate carriers and combined at the RF level for transmission to MCC-H.

2.3 CARRIER FREQUENCIES**

The link employing the DRT shall be capable of operating on either of two adjacent Intelsat IV transponder channels from the group of channels designated 9 through 12, inclusive.

2.4 SPECTRUM SPREADING†

Whenever the DRT is transmitting, the downlink RF signal shall be spread over a 32 MHz bandwidth. The remaining bandwidth of the Intelsat IV transponder employed shall be reserved for the uplink signal and for a guard band separating the uplink and downlink signals.

2.5 DRT ANTENNA SUBSYSTEM

The DRT shall contain a single antenna. The antenna will include a rigid parabolic reflector with a cassegrainian feed.††

---

*This requirement was established as described in Section 5.1.
**This requirement was established as described in Appendix A.
†This requirement was established as described in Section 5.3.
††This requirement was established as described in Section 5.6.

2.5.1 Antenna Size

The parabolic reflector shall have a diameter of 15 feet unless such a diameter cannot be accommodated within the S-II/S-IVB separation clearance envelope, in which case the diameter will be as large as can be so accommodated. (An official separation clearance envelope has not been available to this study. Based upon separation criteria proposed by MDAC to NASA, there will be no difficulty in accommodating the specified 15 foot diameter antenna.)

2.5.2 Antenna Tracking

The DRT shall be capable of automatically steering its antenna so as to track an earth-synchronous communication satellite in a near-equatorial orbit whenever the uplink signal has been acquired and the incident radiation from such uplink signal exceeds the threshold for usable communication.

In response to antenna steering/scanning commands originated by a real-time computer in the OA, the DRT shall be capable of recognizing the presence of an appropriate uplink signal, and of locking on to such uplink signal and transferring the operation of the DRT to its tracking mode when the uplink signal is so recognized. For purposes of acquisition, the uplink signal shall be a carrier whose nominal frequency shall have been precompensated to negate the doppler frequency shift resulting from the velocity of the OA relative to the cooperating communication satellite.

2.5.3 Acquisition Time

Provided that an appropriate uplink signal is present inside a 10 degree by 10 degree region covered by the steering/scanning commands provided by the OA computer, link acquisition shall be accomplished within a period of 3 minutes from the time the first steering command is provided.

2.6 ORBITAL CONSTRAINTS

The DRT shall be capable of operating any time the OA is in a circular orbit of 200 to 250 n. mi. and inclined from 35 to 55 degrees, and the orbit may be in any orientation relative to the earth or sun.

2.7 OA ALTITUDE AND STABILIZATION CONSTRAINTS

2.7.1 Vehicle Altitude

The DRT shall be capable of normal operation when the OA is in either the sun inertial mode or the perpendicular-to-orbit plane (POP) mode, both defined below.

The sun inertial mode of the OA is one in which its X (longitudinal) axis is in the orbit plane and its Z axis (active surface of the solar panels) is directed toward the sun.

In the POP mode, the X axis is perpendicular to the orbit plane, and the Z axis is directed away from the earth.

2.7.2 Vehicle Rates

The DRT shall be capable of operating at the body rates existing while either of the attitude modes defined in Section 2.7.1 are in effect. (A definitive specification of vehicle attitude and attitude rates was not available for this study. However, it is not anticipated that the vehicle excursions in either of the defined modes would have a significant effect on DRT performance.)

2.7.3 Reactions With OA

The slewing of the antenna shall not impose a torque on the OA in excess of 50 ft-lb, nor shall the integrated torque on the OA exceed 500 ft-lb/sec.

2.8 OPERATIONAL CONSTRAINTS

2.8.1 Command Operation

Power on, power off and all switchable functions of the DRT shall be operable by command from the SWS command subsystem. Operation of the DRT by command shall be the primary mode of operation.

2.8.2 Manual Operation

Backup manual command capability shall be provided, with controls and status displays contained on the DRT control panel. A manual acquisition override capability shall be provided. Displays shall be limited to data necessary to properly perform all of the control functions provided.

2.9 OPERATIONAL LIFE

The DRT shall be capable of operating continuously or intermittently in an in-orbit environment for 1 year. Upon resuming operation after a period of shutdown, a warmup sequence causing a delay of not more than 1 hour shall be acceptable.

2.10 OA INTERFACES

2.10.1 Location of DRT

The DRT shall be located at the aft end of the SWS, except for the DRT control panel and the baseband processing unit which will be inboard in a location to be established. (Specific attach points and permissible stowed and deployed configuration envelopes have been explored with MDAC but have not been finalized since the DRT is not to be incorporated in the first SWS.)

2.10.2 Power

The DRT shall consume not more than 250 watts drawn from a nominal 28 volt dc bus. Except for transients specified below, the DRT shall be capable of operation over a bus voltage range of 25 to 30 volts. Operation of the DRT shall not be affected by transients in the form of spikes up to 50 volts in magnitude and up to 10 microseconds in duration, or to load switching excursions to as low as 22 volts or as high as 33 volts, with a recovery time of 1 second.

2.10.3 Thermal

Thermal control of the outboard portions of the DRT shall be self-contained and independent of the OA.

2.10.4 Apollo Telescope Mount (ATM) Computer

Upon demand, the ATM computer will provide a sequence of antenna positioning commands starting with initial acquisition pointing and followed by a series of offset positions which generate a 10 degree by 10 degree square scan pattern. The initial acquisition pointing command relative to an inertial coordinate reference shall have an error not to exceed 5 degrees. The error in successive scanning commands relative to the initial acquisition pointing command shall not exceed 0.1 degree.

(Specific details as to the number of signal lines between the ATM computer and the DRT, and the formats of such signals, have to be defined.)

2.10.5 DRT Housekeeping Telemetry and Command

Commands to and telemetry data originating within the DRT will be accommodated by the SWS telemetry and command subsystems. Interconnections will be by hard wire, not to exceed 100 wire pairs.

2.10.6 Harnessing

All signal and power cabling to the DRT, and the cabling between the inboard and outboard portions of the DRT, will be provided by one or more elements of the OA. (Specific details have to be defined.)

2.11 BOOSTER INTERFACE

Although an official load specification for the DRT was not available to this study, a loads estimate was obtained from MDAC. These preliminary loads are defined in Appendix B of this report.

2.12 INTELSAT IV INTERFACE

The design of the DRT and of the communication link in which the DRT is employed shall be compatible with the performance of Intelsat IV communication satellites as specified in "Exhibit A, Intelsat IV Satellite Specifications," as revised or amended through 15 December 1969.

2.13 GROUND EQUIPMENT INTERFACE

The design of the DRT and of the communication link in which the DRT is employed shall be essentially compatible with a standard Comsat ground terminal ($G/T = 40.7$ dB/°K) and commercial telecommunication standards. Use of special interface units to provide signal multiplexing, signal formatting, etc., will be acceptable where existing facilities are inadequate.

3. DRT DESCRIPTION AND PERFORMANCE

3.1 CONFIGURATION

The DRT consists of a 15 foot diameter cassegrainian antenna, with a five-horn feed attached to an electronic equipment compartment mounted to the rear of the parabolic reflector; the antenna-equipment compartment assembly is coupled to a positionable boom through a set of elevation-over-azimuth gimbals.

The equipment compartment contains the receiver, transmitter, and antenna positioner electronics. In addition, a DRT control panel and a baseband processing unit are remotely located inboard on the OA. Two configuration variants have been designed. The first (Figure 3-1), has the boom attached to the skirt structure of the SWS. The other (Figure 3-2) is attached to the SWS thrust structure. Except for details of the boom design and its attachment to the SWS, the two variants are essentially the same. Final selection of a mounting location was inhibited by an incomplete definition of other equipment to be located in this area and the indefinite plans for the DRT. However, both approaches shown are feasible.

In the stowed position, during launch and ascent into orbit, the antenna, equipment compartment, and gimbals are supported on the SWS thrust structure. In orbit, the boom is extended and placed in one of its two operating positions, permitting steering of the antenna so that it can be pointed toward an Intelsat IV satellite. With the two boom positions, the antenna provides essentially spherical space coverage, being limited only by vehicle obscuration and distortion of the antenna pattern as a result of parasitic excitation. The total coverage loss is estimated as a cone with its apex at the SWS centered along the +X axis, and with a half-angle of 5 to 10 degrees. (A definitive determination of the coverage loss requires antenna pattern definition and measurements beyond the scope of this study.)

As shown in both configuration variants, the deployed boom positions are parallel to the vehicle Y axis. This is a convenient location since, with the vehicle in the sun inertial mode, the line of site to an Intelsat IV satellite avoids the DRT antenna zenith by at least 26 degrees for the specified range of OA orbits. For the skirt-mounted boom, this location may be inconvenient because of the location of other equipment; therefore, an offset

of about 15 degrees was proposed by MDAC personnel. This is satisfactory as the zenith offset would remain in excess of 10 degrees. (When an antenna must track a target passing through its zenith, infinite rates are required to maintain track. The DRT tracking loop has been designed with a rate limit on the order of 4 deg/min; this limit will not be reached if the zenith is avoided by at least 6 or 7 degrees. If it becomes necessary to track closer to the zenith, occasional short interruptions in service might occur, and the feasibility of an upward shift of the tracking rate limit should be explored.)

The antenna diameter was maximized consistent with stowage of a rigid reflector in the available space of the interstage adapter. The upper bound on diameter was essentially established by the dynamic envelope required to ensure a nonimpacting separation of the booster.*

By placing the equipment compartment directly behind the antenna reflector, long RF transmission lines with multiple rotary joints are avoided. The compartment is detachable from the antenna to provide access to units. With the antenna feed attached to the compartment, access to components is achieved without disturbing the RF transmission lines.

3.2 FUNCTIONAL DESCRIPTION

A simplified block diagram of the DRT is shown in Figure 3-3. Starting with the receive function, the antenna with its five-horn feed provides a sum channel signal (Σ) and azimuth and elevation difference signals (Δ-Az and Δ-El). The azimuth and elevation difference signals are chopped and interleaved in the Az-El switching unit and coupled to the sum channel signal to provide a modified monopulse signal in which the azimuth and elevation pointing errors appear as amplitude modulation of the sum channel signal. The combined signal is then amplified in a tunnel-diode preamplifier and heterodyned to IF before entering a frequency tracking AM receiver, where the AM pointing error information is detected and fed to the Az-El demodulator for separation of the two pointing error signals.

An acquisition signal, not shown in the monopulse tracking circuitry of the simplified block diagram, indicates when a tracking signal has been acquired, causing the antenna positioner electronics to enter the track mode.

---

*At the start of this study, estimates of the separation envelope were based upon a single separation retro engine failure. However, subsequent estimates with a single retro failure indicated that there would be negative clearance even without a DRT, and the SWS contractor has since recommended that the design be based upon no retro engine failure. As a result, it might be feasible to employ a slightly greater antenna diameter. However, it was decided that the selected 15 foot diameter provided a reasonable margin should more refined estimates of the separation envelope further reduce the space available.

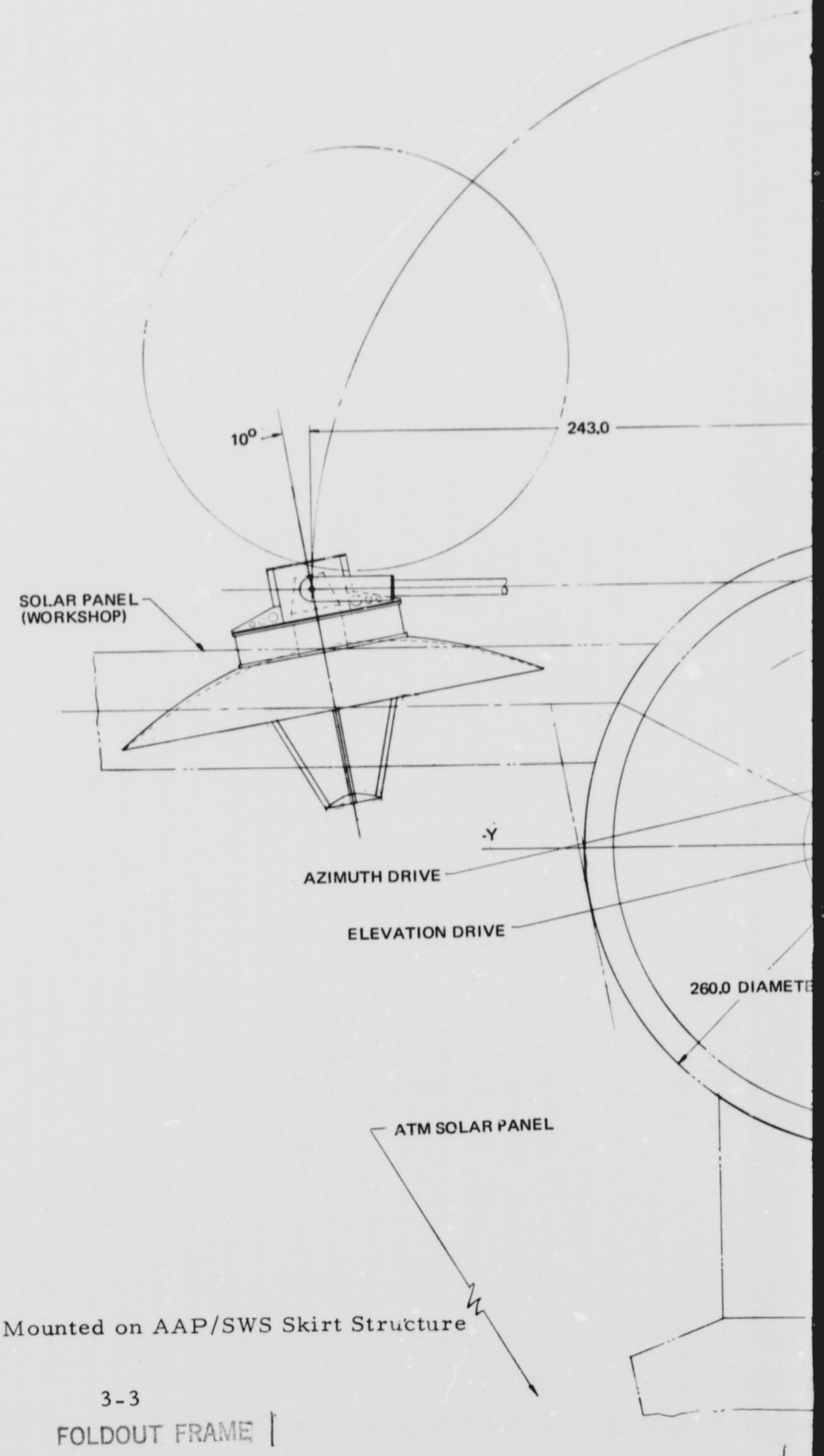

Figure 3-1. DRT Mounted on AAP/SWS Skirt Structure

FOLDOUT FRAME

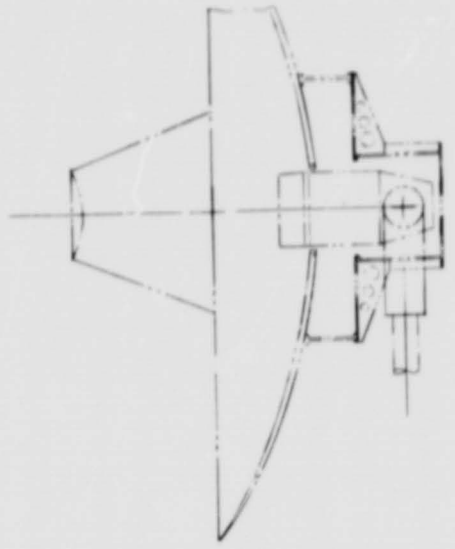

FOLDOUT FRAME 2

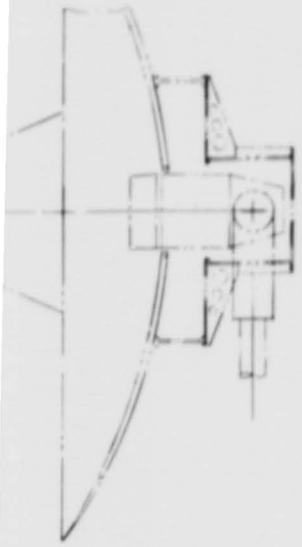

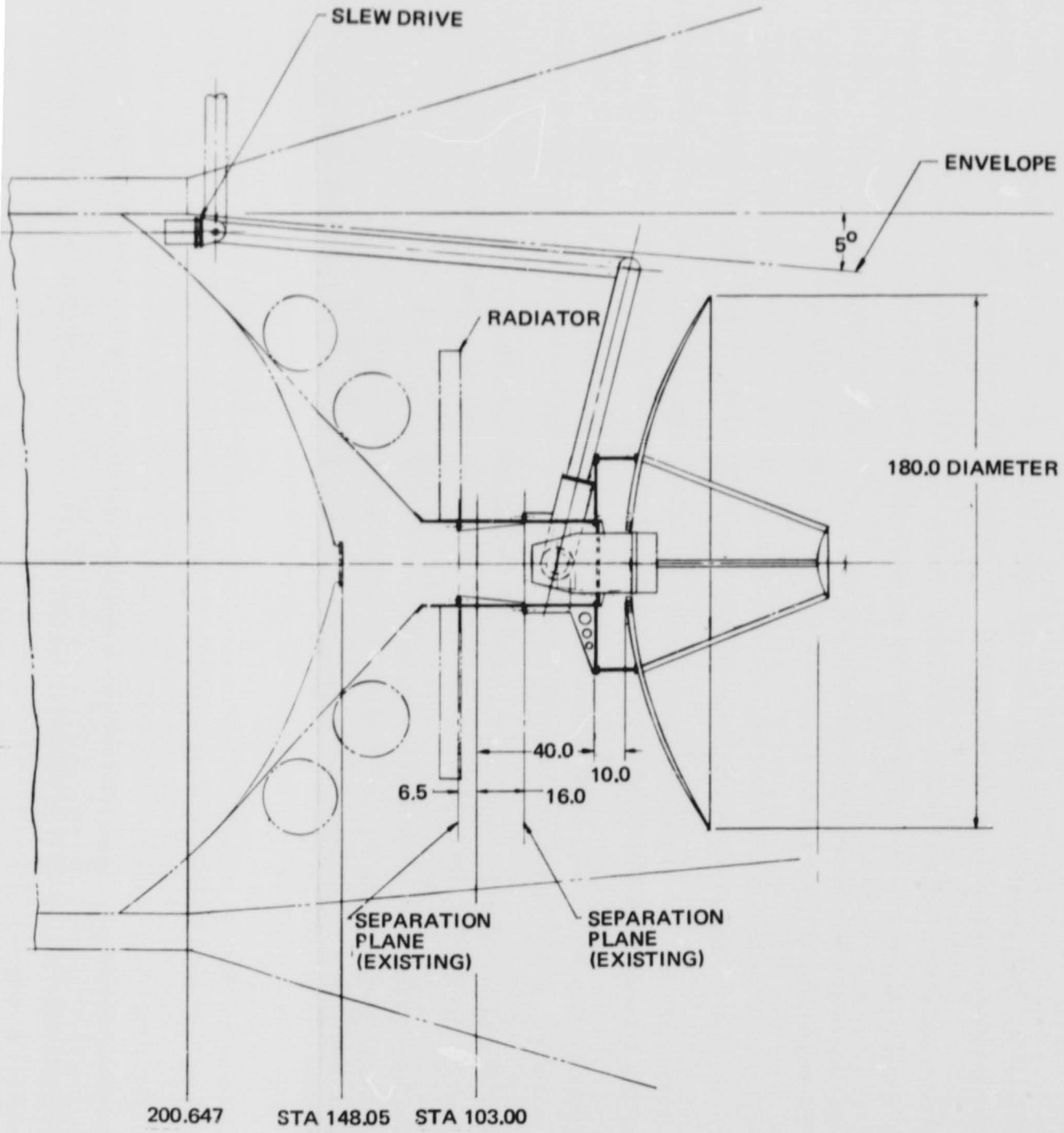

FOLDOUT FRAME 3

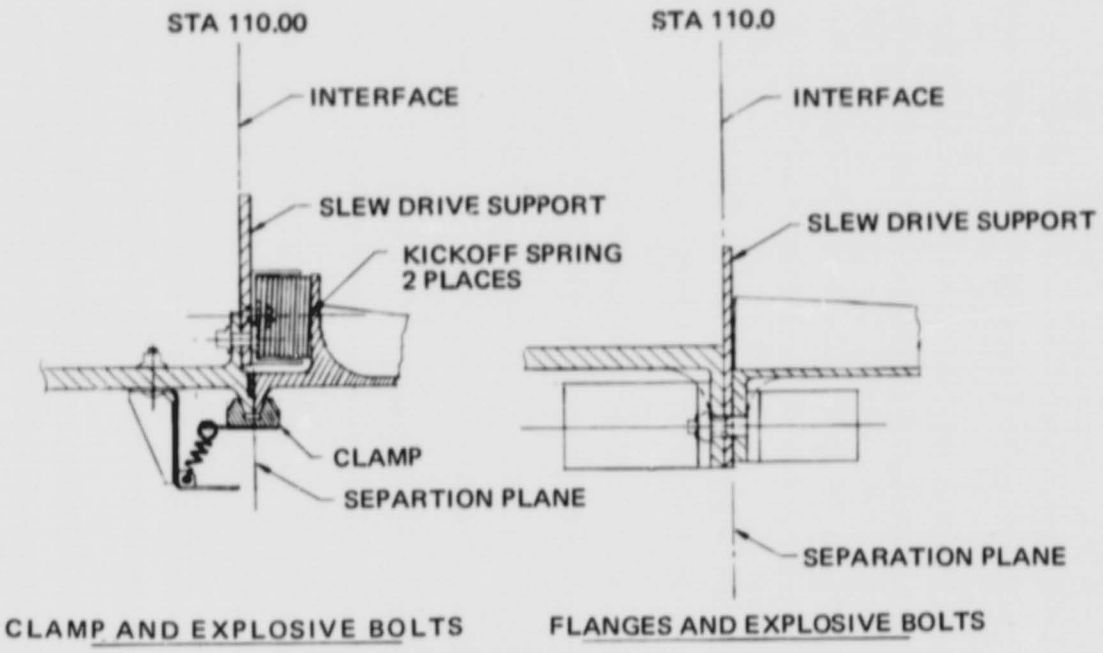

CLAMP AND EXPLOSIVE BOLTS FLANGES AND EXPLOSIVE BOLTS

VIEW B

(POSSIBLE SEPARATION MECHANISMS)
SCALE: 1/1

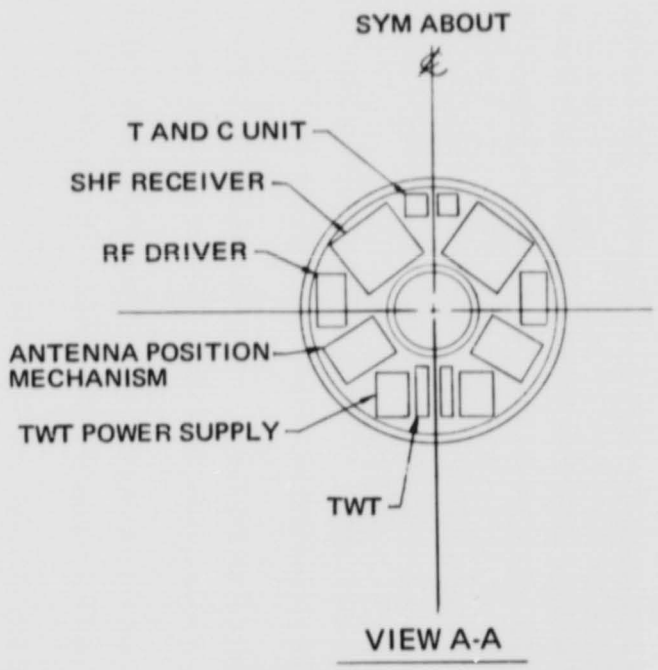

VIEW A-A

(ELECTRONIC EQUIPMENT SHELF)

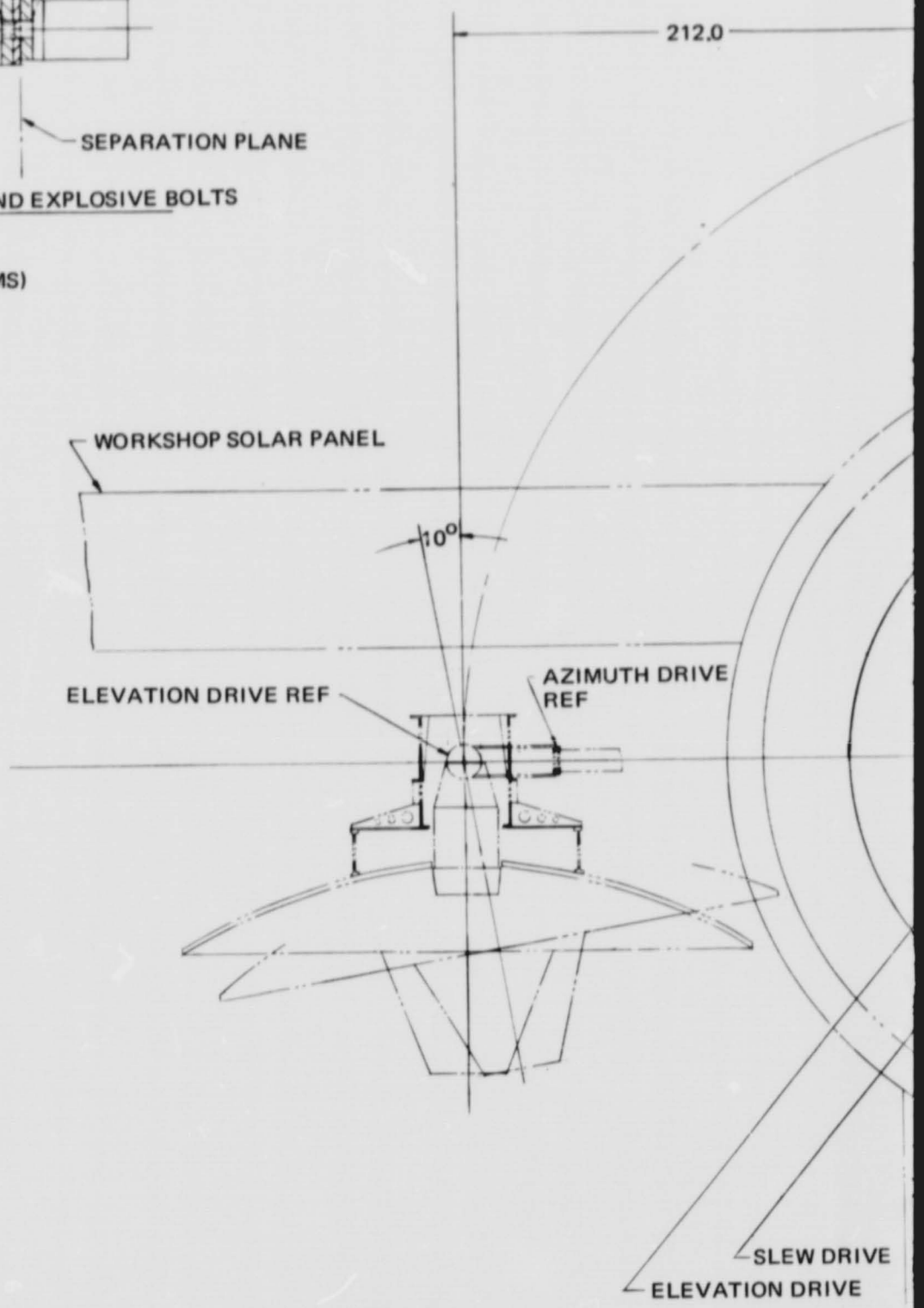

Figure 3-2. DRT Mounted on AAP/SWS Thrust Structure

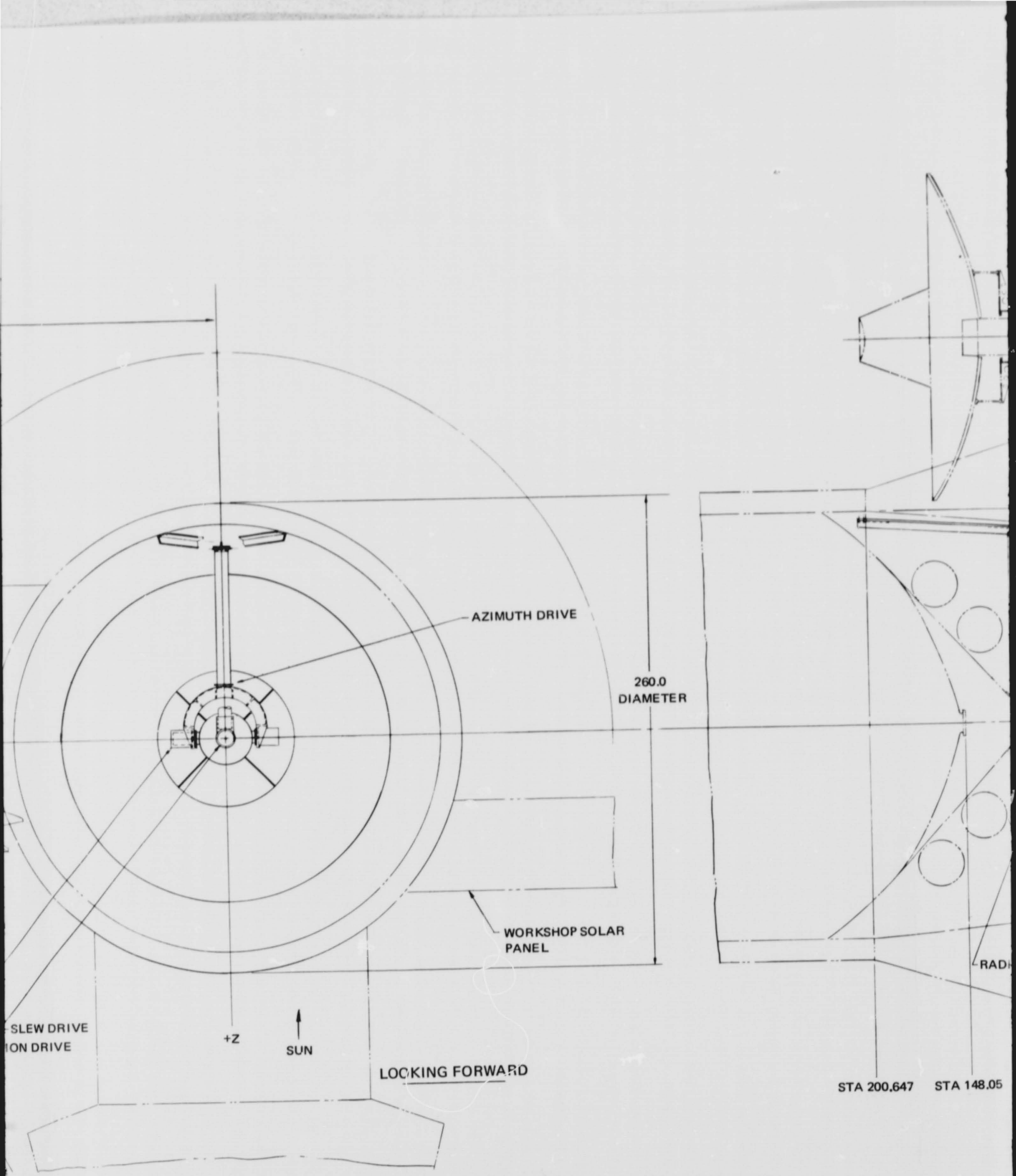

FOLDOUT FRAME 2

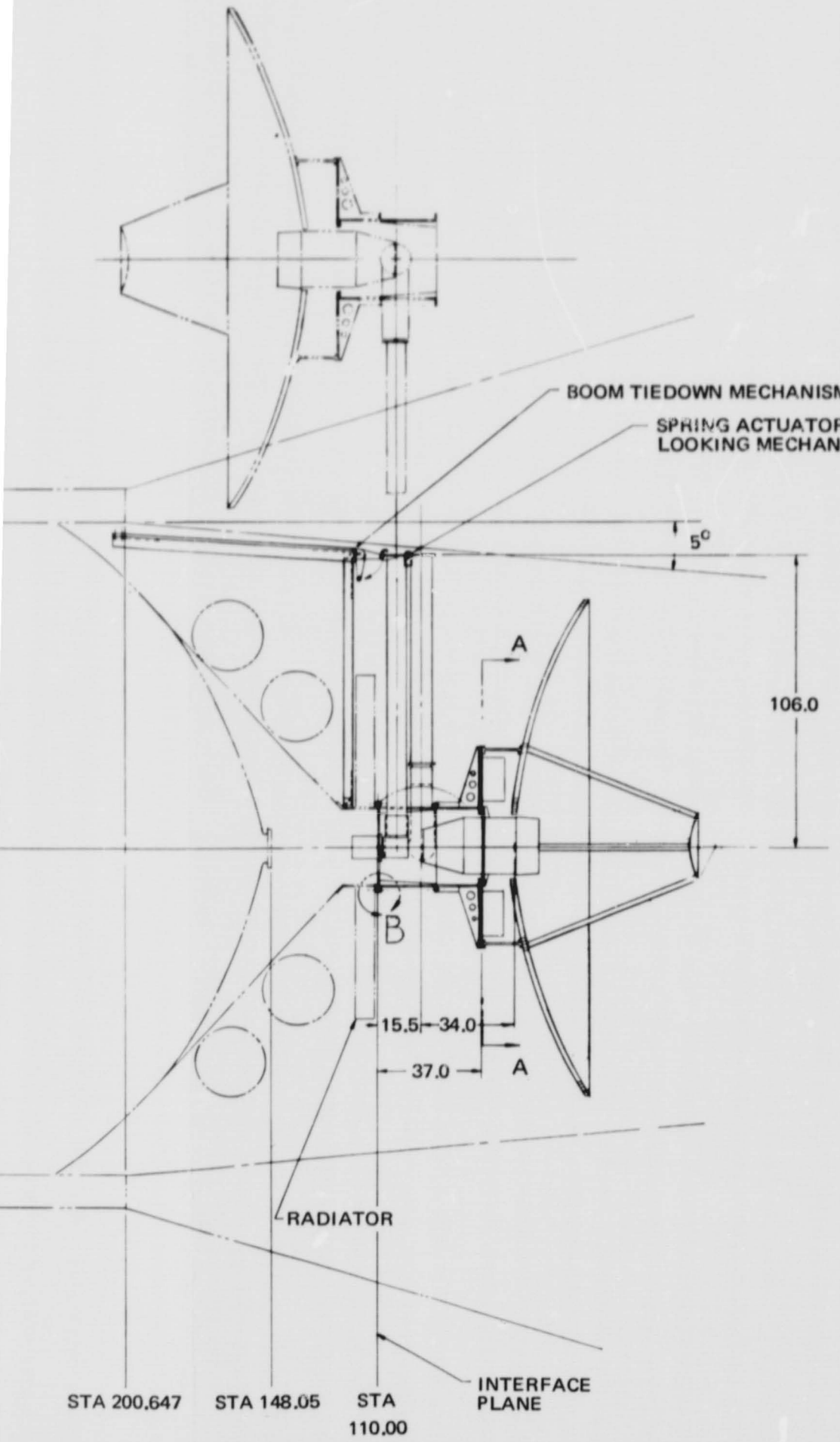

FOLDOUT FRAME 3

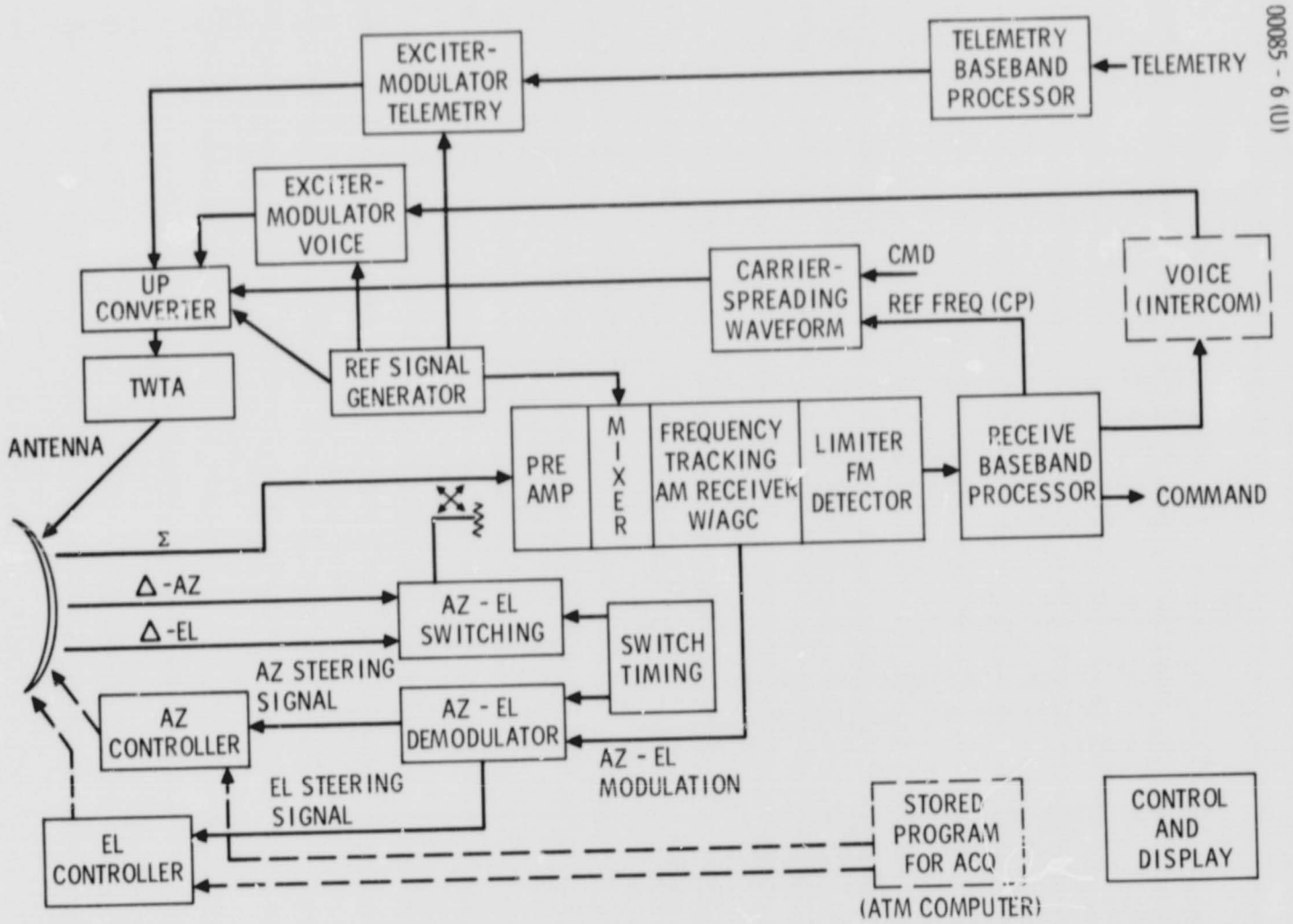

Figure 3-3. AAP DRT Simplified Block Diagram

PRECEDING PAGE BLANK NOT FILMED.

TABLE 3-1. UPLINK POWER BALANCE

Ground to Intelsat IV	
Multiplexed onto single RF carrier, FM	3.1 kHz voice, 20 dB TT/N with 12 dB clipping 1 kilobit/sec data, Gemini format, bit error rate = 10^{-6}
RF output from earth station, watts	48
Path loss to Intelsat IV, dB	-200.8
*Path loss uncertainty due to weather, dB (ground station power control recommended to compensate for weather)	-2.5
Intelsat IV to DRT	
ERP from Intelsat IV, dBw (9.5 degrees off-axis, with backoff)	14.6
*Path loss to DRT, dB for worst orbit geometry, i.e., when ready for handover to other Intelsat IV	-197.1
DRT antenna gain, dB	42.3
DRT antenna pointing loss, dB (for tracking error = 0.05 degree)	-0
T_r of DRT, °K	1120
DRT C/N obtained, dB	10
DRT C/N required, dB	10
Margin, dB (for * limit conditions occurring concurrently)	0

In this mode, the Az and El steering signals drive the Az and El gimbal controllers to position the antenna so as to null the steering signals.

When the tracking signal is not present, the antenna is steered in response to pointing/scanning commands originating in the ATM computer. Switching between track and acquisition modes is controlled automatically by the state of the acquisition signal.

Going back to the frequency tracking receiver, the output for the communication channel is limited and FM detected, and the voice and command signals are separated in the receive baseband processor, from which they are distributed to the OA users.

For signals originating in the OA, the voice channel and the selected telemetry channel each modulate a separate carrier. If the multi-data stream telemetry channel C is selected, it is first multiplexed into a single digital data stream in the telemetry baseband processor.

The two signal carriers are combined and shifted to the transmission frequency (nominally 6 GHz) in the upconverter, which is followed by a 20 watt traveling-wave tube (TWT) power amplifier. The signal then goes to the antenna, where it is fed to the center horn in the feed.

To reduce the level of radiant power incident upon the earth's surface, the upconverter is driven by a carrier-spreading waveform derived from a reference frequency obtained from the received signal.

Detailed descriptions of the various subsystems and units are given in Section 4.

3.3 COMMUNICATIONS PERFORMANCE

The overall design of the up and down links is significantly influenced by their common usage of a single Intelsat IV transponder. Preliminary considerations, discussed in detail in Section 5.2, indicate that the uplink requires substantially more Intelsat IV effective isotropic radiated power (EIRP) than does the downlink. However, to assure the availability of the low power level required by the downlink, it is necessary to operate the Intelsat IV transponder in a quasi-linear mode, so that the total EIRP from the repeater satellite utilized by these links is substantially below the single-carrier beam-edge power level of 22 dBw nominally available. The satellite power utilized for the uplink (14.6 dBw), as shown in Table 3-1, corresponds to a backoff of the Intelsat IV repeater of 6.4 dB, allowing 1 dB loss for operation 1 degree beyond the nominal Intelsat IV beam edge of 8.5 degrees.

As indicated in Table 3-1, the ground station RF power required to drive the uplink is 48 watts, assuming a ground terminal antenna gain of 61.5 dB. Uplink power control will be required to compensate for attenuation

TABLE 3-2. DOWNLINK POWER BALANCE

DRT to Intelsat IV		
Two separate RF carriers	3.1 kHz voice, FM, 20 dB TT/N with 12 dB clipping	72 kilobits/sec data, biphase modulation, bit error rate = 10^{-4}
RF output from TWT, watts	3.5	16.5
Line losses to antenna, dB	-0.7	-0.7
RF input to antenna, dBw	4.8	11.5
DRT antenna gain, dB	45.8	45.8
DRT antenna pointing loss, dB (sum of tracking error plus transmit-receive boresight error = 0.1 degree)	-0.0	-0.0
*Path loss to Intelsat IV, dB, for worst orbit geometry, i.e., when ready for handover to other Intelsat IV	-200.7	-200.7
*Intelsat IV maximum pointing error, dB (0.3 degree at 9.5 degrees off-axis)	0.4	0.4
Intelsat IV to Ground		
ERP from Intelsat IV, dBw (at 8.5 degrees off-axis)	-13.2	-6.6
Path loss to ground station, dB	-197.0	-197.0
Ground station G/T, dB/°K	40.7	40.7
*Ground station G/T loss due to weather, dB	-6	-6
Ground station C/N obtained, dB	10	9
Ground station C/N required, dB	10	9
Margin, dB (for * limit conditions occurring concurrently)	0	0

due to weather. (Although no margin is shown for the uplink, such margin can obviously be obtained by increasing the ground transmitter power; caution must be taken, however, not to overdrive the Intelsat IV transponder as this will degrade the downlink.)

With the Intelsat IV repeater backed off as indicated above, and with the available DRT transmitter power of 20 watts allocated between the two downlink signals, as shown in Table 3-2, the downlinks show zero margin when three statistically or time varying worst case conditions are considered simultaneously. These conditions are a worst case pointing error of the Intelsat IV satellite, extreme orbit geometry, and a 6 dB degradation of the ground terminal receiver due to weather. While it is difficult to estimate the joint probability of occurrence of these conditions, it is obviously small, and it is further offset by the fact that their simultaneous occurrence virtually coincides with the point at which operation is transferred between the two Intelsat satellites employed in the link. Since the two communication satellites are serviced by ground terminals located on opposite coasts of the United States, the simultaneous occurrence of severe weather degradation at both terminals is negligibly small. A positive margin could be achieved under these conditions by an increase in DRT antenna size or transmitter power, but the resulting increase in cost and/or complexity does not seem justified.

3.4 POWER AND WEIGHT SUMMARY

Electrical power required for operation of the DRT is estimated to be about 160 watts, as shown in Table 3-3. A peak power demand substantially higher than the average level could occur because of the slewing power required during handover from one Intelsat IV to the other if the DRT were permitted to transmit during handover. However, the normal operation is to inhibit transmission during this period to avoid inadvertent illumination of the earth's surface by the mainbeam. When transmission during handover is so inhibited, the peak power demand will not be much greater than the average power, even when slewing two gimbals simultaneously.

The overall weight of the terminal is estimated at 750 pounds, including about 10 percent for contingency. Component weights are shown in Table 3-4.

Equipment and structural weight estimates are based on a minimum cost design approach rather than a minimum weight approach. Should weight become a more significant design constraint, reductions are potentially available in the structure and in the antenna and boom positioning mechanisms.

TABLE 3-3. ESTIMATED ELECTRICAL POWER REQUIREMENTS

Subsystem/Item	Power, watts	
Communication subsystem		118
Communication receiver	8	
Tracking receiver	5	
Baseband processor	3	
Frequency performance	10	
Transmitter	90	
Control panel	2	
Antenna positioning subsystem		42
Gimbal drive	26	
Boom positioner	16	
Estimated average power required		160

TABLE 3-4. SATURN WORKSHOP TERMINAL PRELIMINARY ESTIMATED WEIGHTS

Subsystem/Item	Weight, pounds	
Communication subsystem		100
Communication receiver (2)	20	
Tracking receiver	10	
Transmitter (2)	42	
Diplexer and circuits	2	
Baseband processor (2)	6	
Control panel	10	
Frequency reference generator (2)	10	
Antenna (15 foot diameter)		209
Main reflector	160	
Subreflector	14	
Feed	35	
Antenna position control		125
Antenna positioner (2)	66	
Boom positioner	33	
Servo controller (2)	16	
Crew control and display	10	
Wire harness		50
Equipment wiring	25	
Power leads	10	
Signal leads	15	
Structure		175
Equipment support	105	
Deployment boom	60	
Separation mechanism	10	
Thermal control		20
Insulation blankets	10	
Paint and finishes	10	
Contingency, (10 percent)		71
Total terminal weight		750

4. SUBSYSTEMS

4.1 TRANSMITTER/RECEIVER

A detailed block diagram of the DRT transmitter/receiver is shown in Figure 4-1. The transmit channel is virtually fully redundant, as are those portions of the receive channel which operate on the uplink communication signals. This degree of redundancy, although relatively inexpensive in comparison to the total cost of implementing the DRT, is probably overly conservative in view of the 1 year operational life requirement. A detailed reliability analysis, beyond the scope of this study, is desirable to determine how much, if any, of the redundancy should be retained. Two factors favoring a reduction in redundancy are the demonstrated reliability of comparable equipment in other space programs and the existence of alternate means of communication with the OA.

The functional operation of the transmitter and receiver were generally described in Section 3.2 and will not be repeated here. However, the description of these units will track the signal flow.

Transmitter

Starting with signals originating in the OA, the incoming voice and selected telemetry channel signals are fed to exciter modulators. (The selection and multiplexing of telemetry signals is performed in the signal selector and multiplexer, described in Section 4.2.)

The exciter-modulators are conventional voltage-controlled crystal oscillator (VCXO) configurations, provided redundantly for both the voice function (71 MHz) and the data function (70 MHz). In the event of voice-only transmission, the voice boost switch can increase the level of the voice carrier to drive the TWT at full power.

The outputs from the exciter-modulators are combined and upconverted to the transmit frequency. The use of a common upconverter stage permits the sharing of a single harmonic chain between the voice and data channels, enables simplified switching between transmission frequencies, and provides a large frequency multiplication factor for convenient carrier spreading of both channels.

The configuration of the transmit reference generator is governed by the requirements of good frequency stability to facilitate acquisition and abiiity to spread the carrier over 32 MHz. The baseline design, using a straightforward harmonic chain, is shown in Figure 4-2. However, even with its large frequency multiplication factor of 576, carrier spreading to 32 MHz by phase modulation requires a modula'ing frequency of about 200 kHz.

An alternate implementation of the transmit reference generator is shown in Figure 4-3; it is based on a 1 GHz solid-state signal source that is either phase-locked to a quartz crystal or is unlocked and frequency modulated. As the carrier spreading modulation is direct FM, the deviation is independent of the modulating frequency. There is, however, some question as to whether sufficient deviation can be obtained; commercially available signal sources of this type are quoted at ±0.1 percent deviation, whereas ±0.4 percent is desired here – a performance stretch which may well be realizable.

Before implementation of the DRT, a more detailed study should be performed for selecting the configuration of the transmit reference generator.

Following the reference generator, the combined carriers are amplified in a 20 watt TWT amplifier. The TWT is operated at saturation, and almost full power is obtained because the telemetry carrier is at a much higher level than the voice carrier. (In fact, when the two signals are combined, the voice signal must be at a level disproportionately higher than would be required in a linear system in order to overcome the effect of small carrier suppression in the presence of a large carrier input to a saturated TWT. This provides an automatic enhancement of the voice signal should the telemetry signal carrier be absent.)

The output of the TWT amplifier is filtered and fed to the antenna (described in Section 4.3). A power monitor has been included to provide a measurement of the RF power being fed to the antenna.

There is complete redundancy in the transmitter, with cross-strapping provided between the exciter-modulators and the transmit reference generators, and again between the reference generators and the TWT amplifiers. With this type of cross-strapping, normal operation can be maintained with the failure of any combination of one each of these three units. (As indicated earlier, this level of redundancy may be excessive relative to the operational life requirements of 1 year.)

Receiver

For incoming signals, the monopulse difference channel signals from the antenna are multiplexed in an azimuth-elevation switching unit and combined with the sum channel signal in a 15 dB coupler in the receiver input assembly. (A detailed discussion of the operation of the time-shared monopulse tracking system is provided in Section 5.4.)

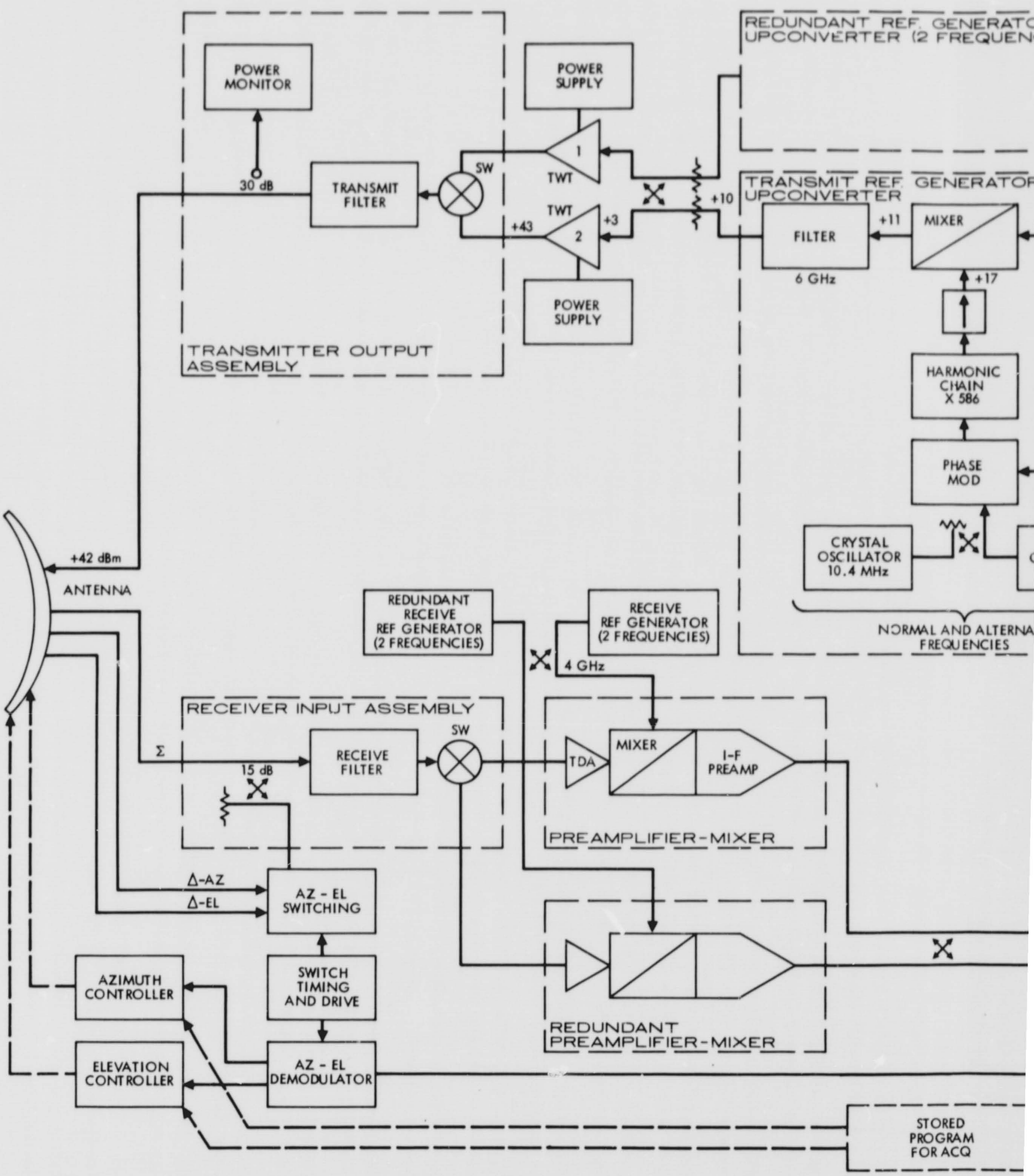

Figure 4-1. DRT Detailed Block Diagram

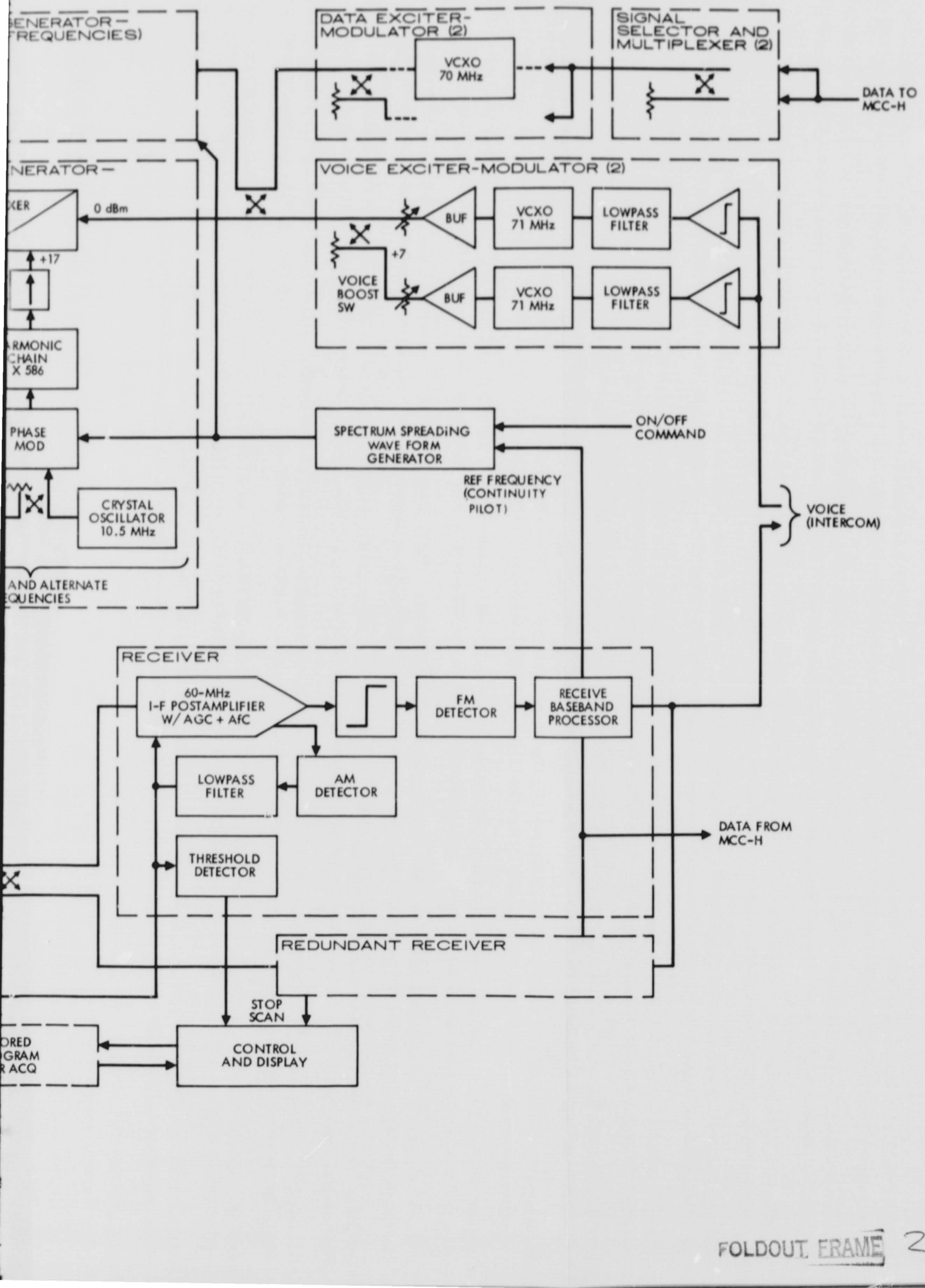

FOLDOUT FRAME 2

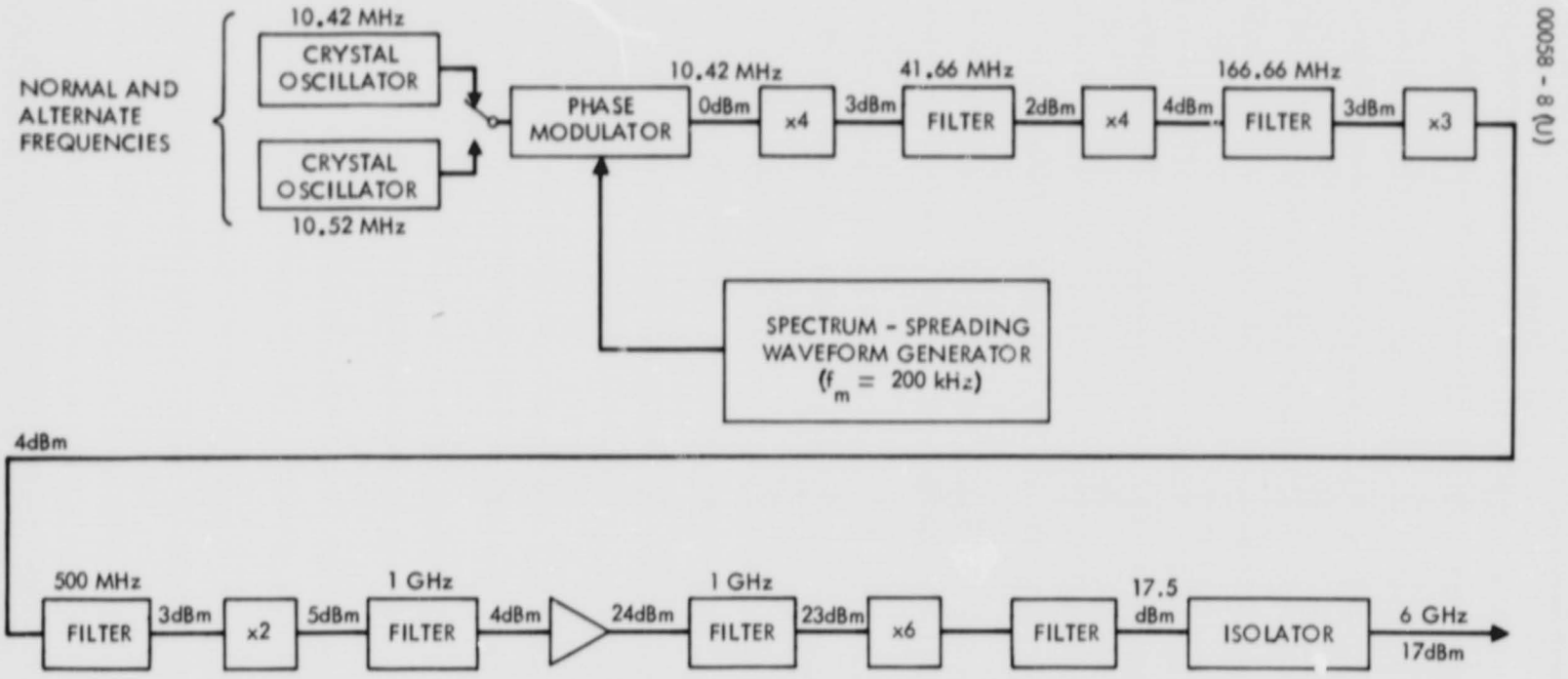

Figure 4-2. Transmit Reference Generator

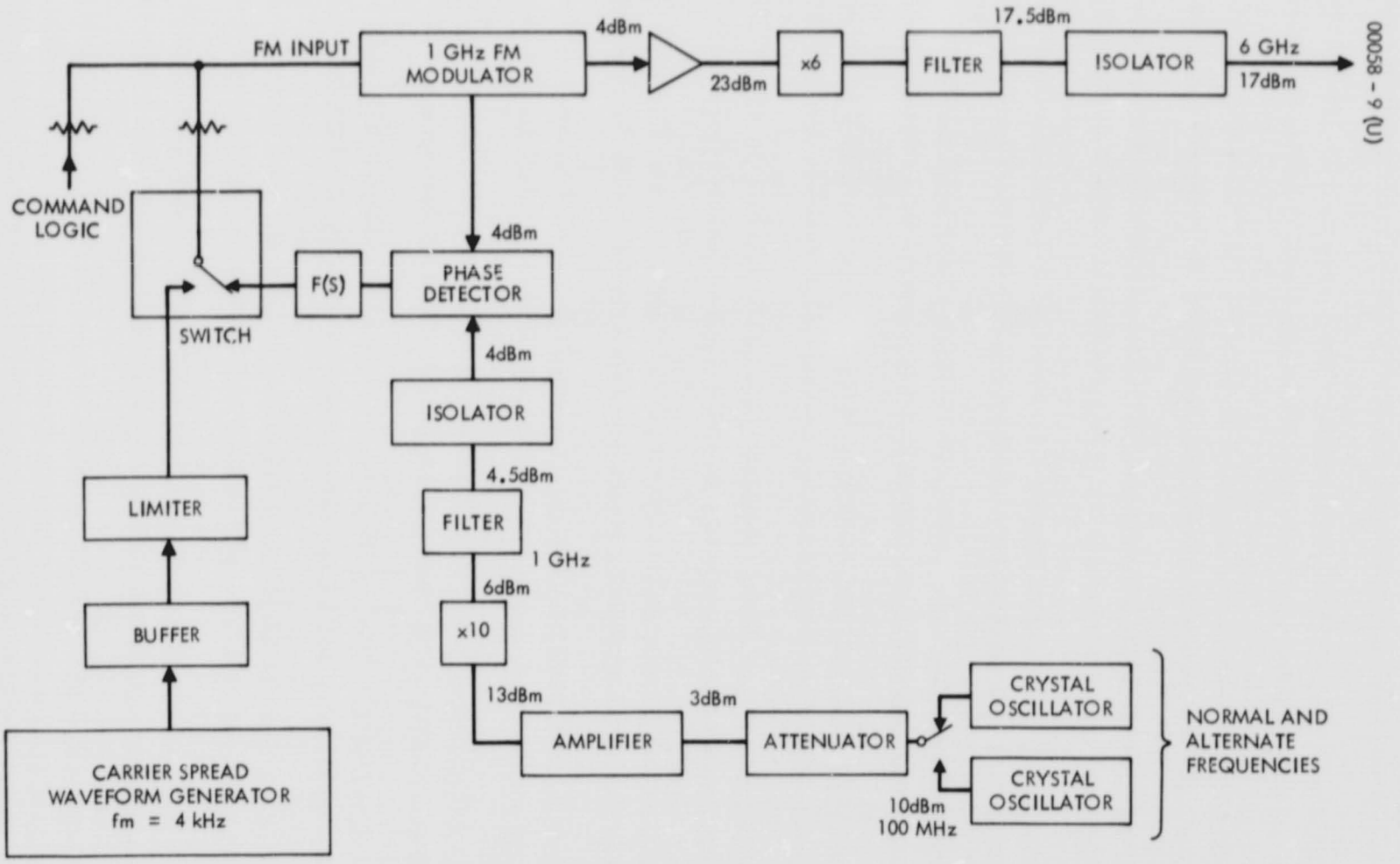

Figure 4-3. Alternate Transmit Reference Generator

PRECEDING PAGE BLANK NOT FILMED.

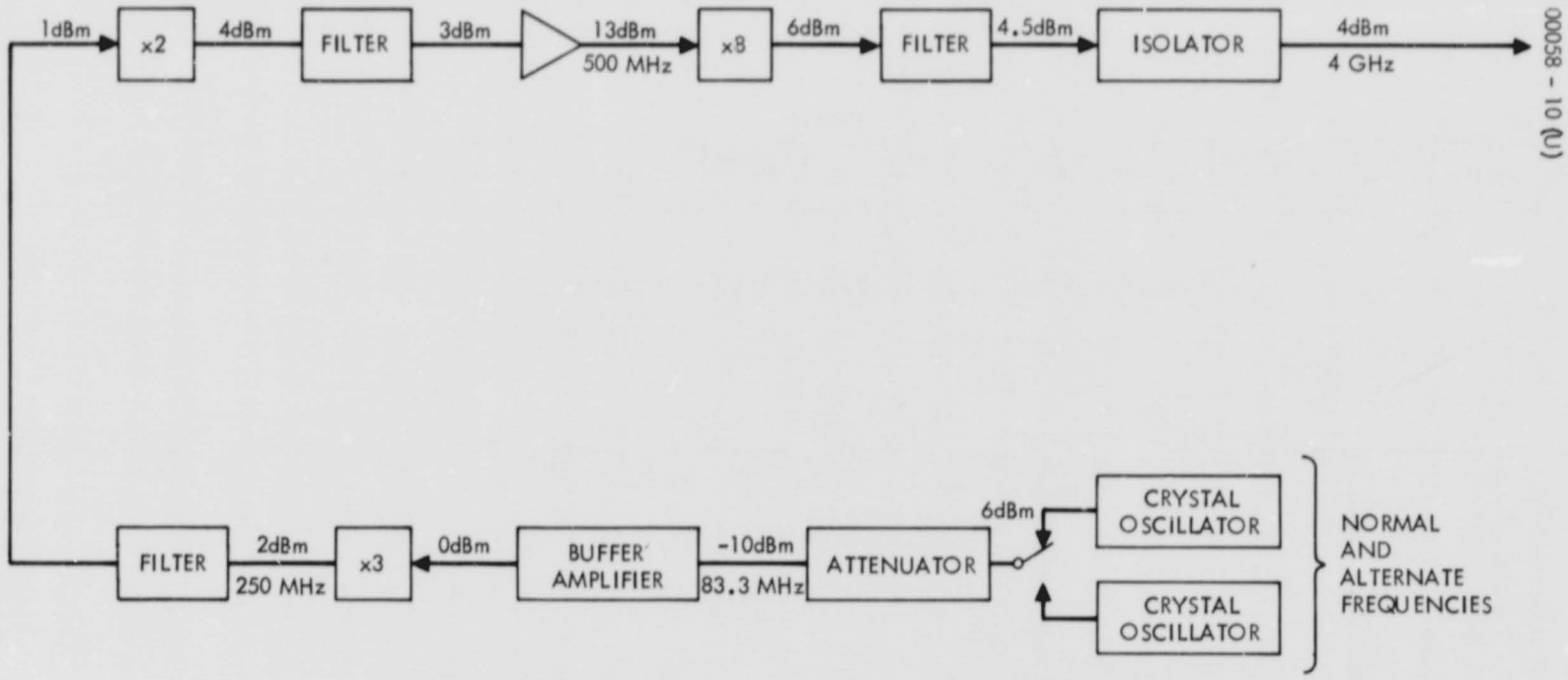

Figure 4-4. Receive Reference Generator

The combined sum and difference signal is then amplified in a tunnel-diode preamplifier before being downconverted to IF. A tunnel-diode preamplifier was selected in preference to a more sensitive parametric amplifier. Although higher sensitivity in the DRT receiver would permit a reduction of the required antenna size for purposes of receiving information, the penalty of a smaller antenna would be felt in the higher RF power required of the downlink transmitter. From the point of view of cost, weight, and raw power consumption, the design consisting of a 15 foot dish, a tunnel-diode preamplifier, and a 20 watt TWT is considered to be close to optimal.

Except for the monopluse tracking circuitry, the receiver is composed largely of conventional circuitry. The receive reference generator design is shown in Figure 4-4. AGC is included in the receiver at the IF level to permit proper processing of the AM tracking signals. A threshold detector provides a positive indication of the presence of a tracking signal. The presence of such a signal is used to transfer operation from acquisition mode to track mode. Loss of the track signal causes the logic to automatically revert to the acquisition mode.

The doppler shift of the received signal (4 GHz) is on the order of ±100 kHz. It is proposed that this frequency shift be substantially cancelled through programmed precompensation by the ground terminal. (This approach has been informally discussed with Comsat Corporation personnel, and implementation on their end appears to be straightforward.) The expected buildup of other residual (i.e., uncompensated) frequency errors is sufficiently small to ensure that, during acquisition, the (unmodulated) uplink carrier will always be within the receiver passband. With uplink modulation present, however, the bandwidth occupied by the modulated carrier will be roughly equal to the total frequency uncertainty; for this reason, the frequency tracking capability of the receiver ensures that the modulation spectrum will always be centered in the passband.

The clipper and FM detector operating on the received communication signal, and the receive baseband processor are all conventional circuits.

4.2 TELEMETRY SIGNAL SELECTOR AND MULTIPLEXER

The telemetry signal selector and multiplexer consist of a four-position command-operated selector switch and a digital encoder. The four switch positions correspond to the four signal transmission modes specified in Section 2.2.2, namely, voice alone or voice-plus-telemetry channels A, B, or C. The input to the switch for channels A and B is simply telemetry signals 1 and 2. For channel C, the input to the selector is the output of the digital encoder, which is the multiplexed combination of telemetry signals 3 through 7.

The multiplexing of telemetry signals 3 through 7 is accomplished by a simple sampling scheme operating at a bit rate of 72 kilobits/sec, which is the same as the data rate on telemetry channel 2. An alternate approach of putting each of these signals on a separate subcarrier before combining onto a single carrier was considered; the subcarrier oscillators to accomplish this are straightforward designs but are, in totality, no simpler than the digital encoder selected, and the penalty in RF bandwidth is excessive.

The sampling format is shown in Figure 4-5. Signals 4, 5, 6, and 7 are sampled four times per minor frame, and signal 3 is sampled once per minor frame. There are 20 bits in a minor frame, 3 of which (F, R, A or $\overline{F}$, $\overline{R}$, $\overline{A}$) are used for frame synchronization. The frame rate is, therefore, 72×10^3 bits/sec $\div$ 20 bits/frame = 3.6×10^3 frames/sec, and the signal sampling rates are $4 \times 3.6 \times 10^3$ samples per second for signals 4 through 7, and $1 \times 3.6 \times 10^3$ samples per second for signal 3.

The corresponding sampling rate, in samples per bit, is given in Table 4-1. Because it is assumed that the 72 kilobits/sec sampling rate and the 5 NRZ bit streams are all relatively asynchronous, this sampling method will result in an apparent random jitter at the bit transitions when these bit streams are demultiplexed and reconstructed. This effect is shown in Figure 4-5 for a representative bit stream which is being sampled at the rate of approximately 2.6 samples/bit. The peak-to-peak magnitude of this random jitter, expressed as a percentage of the bit period, is the reciprocal of the samples per bit for a given channel. The jitter values for each channel are also given in the table. It can be seen that the worst jitter, ±22.2 percent, occurs on signal 3. Commercially available bit synchronizers can operate on this level of jitter.

TABLE 4-1. ENCODER PERFORMANCE SUMMARY

Signal Number	Bit Rate kilobits/sec	Sample per Bit	Maximum Jitter, percent of Bit
3	1.6	2.25	±22.2
4	4.0	3.6	±13.9
5	5.12	2.82	±17.7
6	5.12	2.82	±17.7
7	5.76 or 5.12	2.5 or 2.82	±20.0 or 17.7

A preliminary design implementation is shown in Figure 4-6. A fully redundant encoder system can be packaged in a volume of 61 cubic inches, weighing 1.5 pounds and consuming 1.0 watt.

4.3 ANTENNA

4.3.1 General Design Description

The selected cassegrain antenna design is shown in Figure 4-7. It was selected in preference to a prime-focus feed design for the following reasons:

1) The cassegrain has approximately 2 dB higher gain.

2) Depth of the cassegrain is only 60 percent that of the prime-focus.

3) RF transmission losses of the prime-focus are about 0.5 dB higher.

4) Integration and final assembly of the feed with the main reflector and electronics are substantially simpler.

The cassegrain antenna design consists of a main reflector, a subreflector, and a five-horn feed assembly. The main reflector is a paraboloid, and the subreflector is a modified hyperboloid. The subreflector converts the spherical wave emerging from the feed to the equivalent of a spherical wave emerging from the focus of the main reflector. The paraboloid then converts the spherical wave to a plane wave.

The antenna is designed so that the feed is attached to the equipment compartment at four points, which, in turn, is attached to the main reflector. There is no direct mechanical support between the feed and the main reflector; the feed extends through a 21 inch diameter clearance hole in the reflector. Alignments needed to make the feed mechanical axis coincide with the main reflector axis are done by adjustment at the 73 inch diameter mounting circle. The subreflector will be aligned optically in the shop for coincidence of its axis to the main reflector axis. It is expected that the electrical axis of the beam (defined as the intersection of the monopulse null planes) will be within 1/8 degree of the main reflector axis. The measured boresight bias error will be compensated in the acquisition mode for pointing the beam peak at an Intelsat IV satellite.

The antenna design is similar to a cassegrain antenna previously developed at Hughes.* The cassegrain geometry and the five individual horns in the feed are the same as for the earlier antenna, thereby providing a high confidence that the antenna will perform as designed.

---

* R. T. Clark and P. A. Jensen, Experimental Cassegrain-Fed Monopulse Antenna System, NASA Contractor Report CR-720, May 1967.

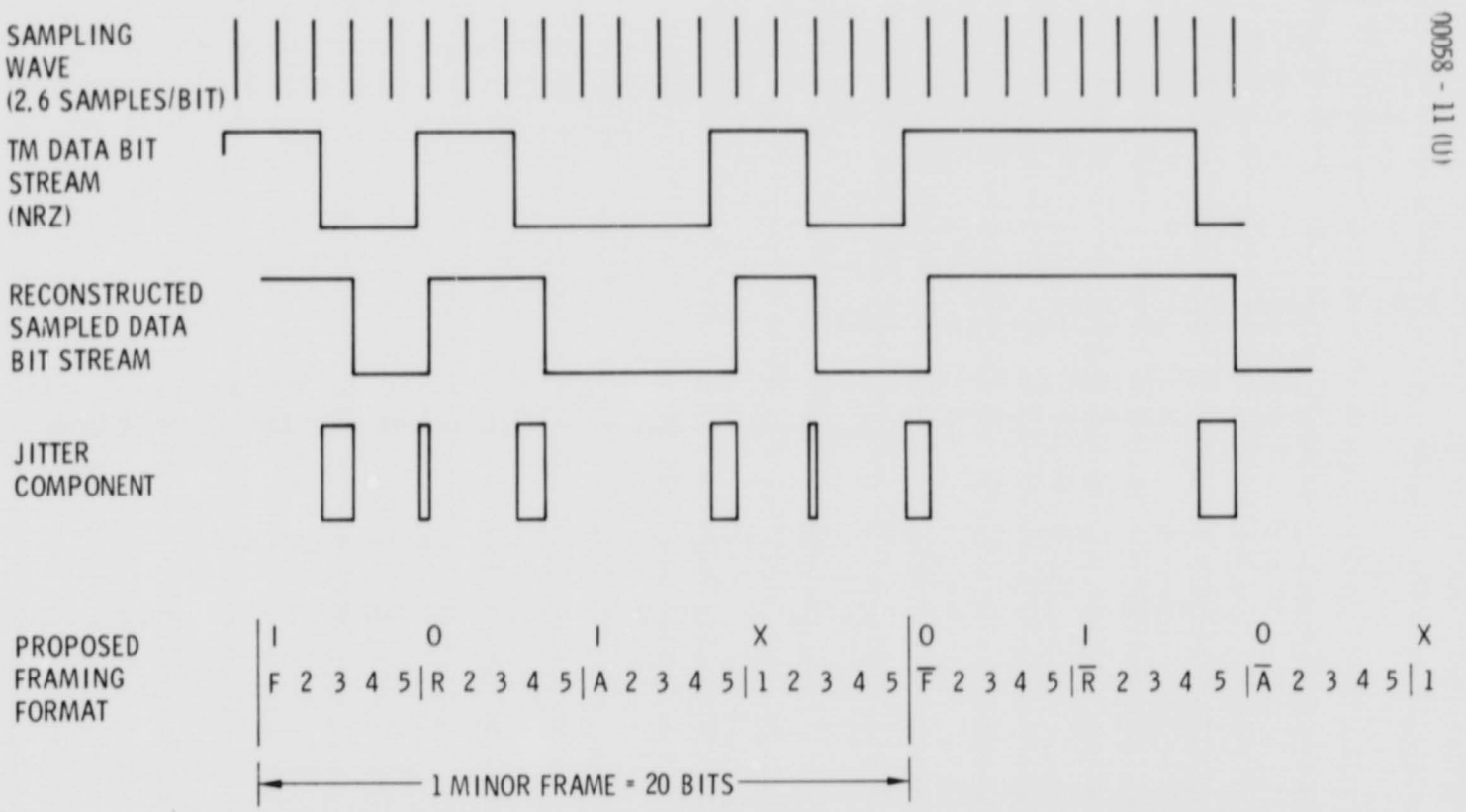

Figure 4-5. Sampling Frame Format

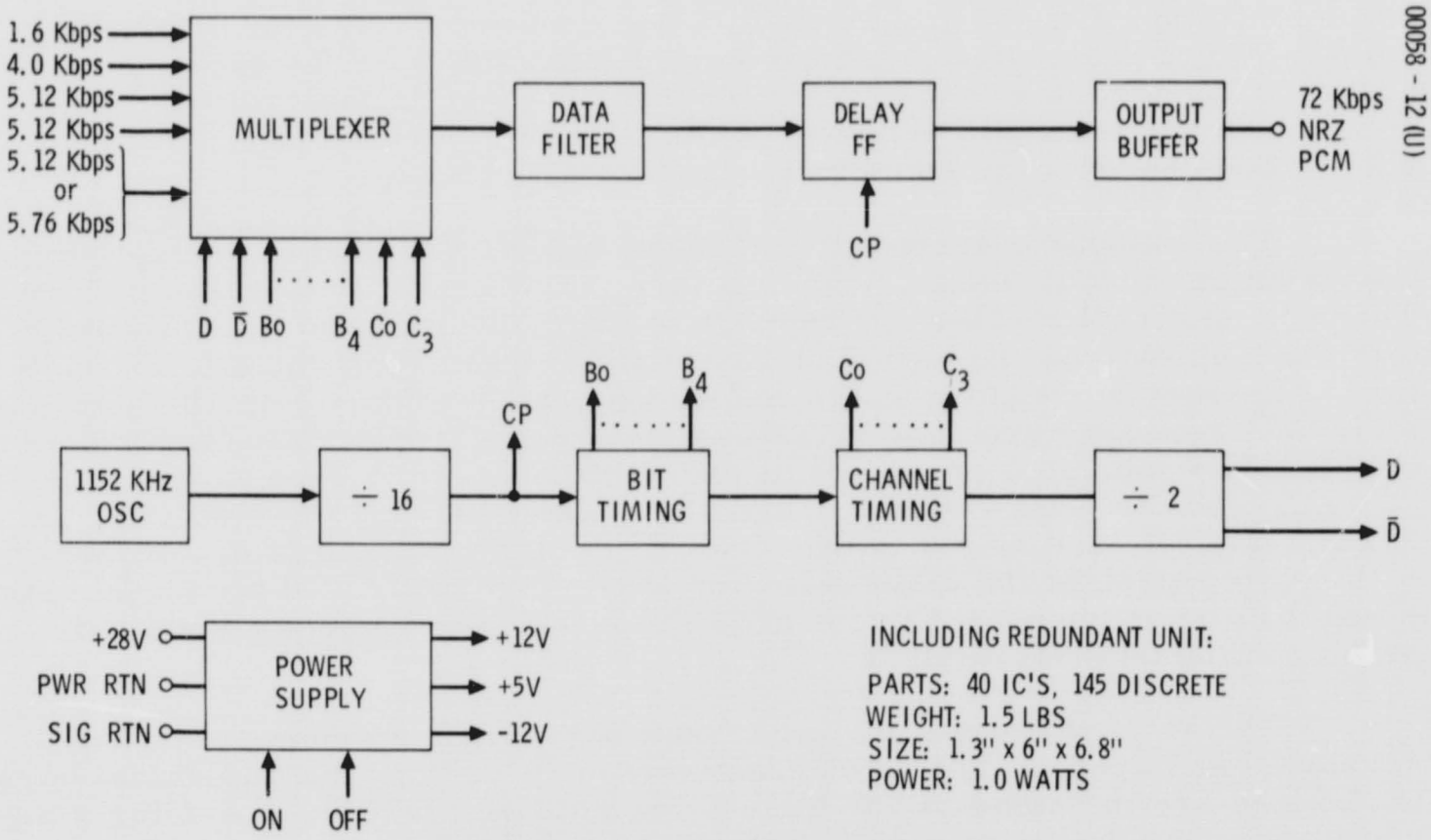

Figure 4-6. Digital Encoder

00058-13(U)

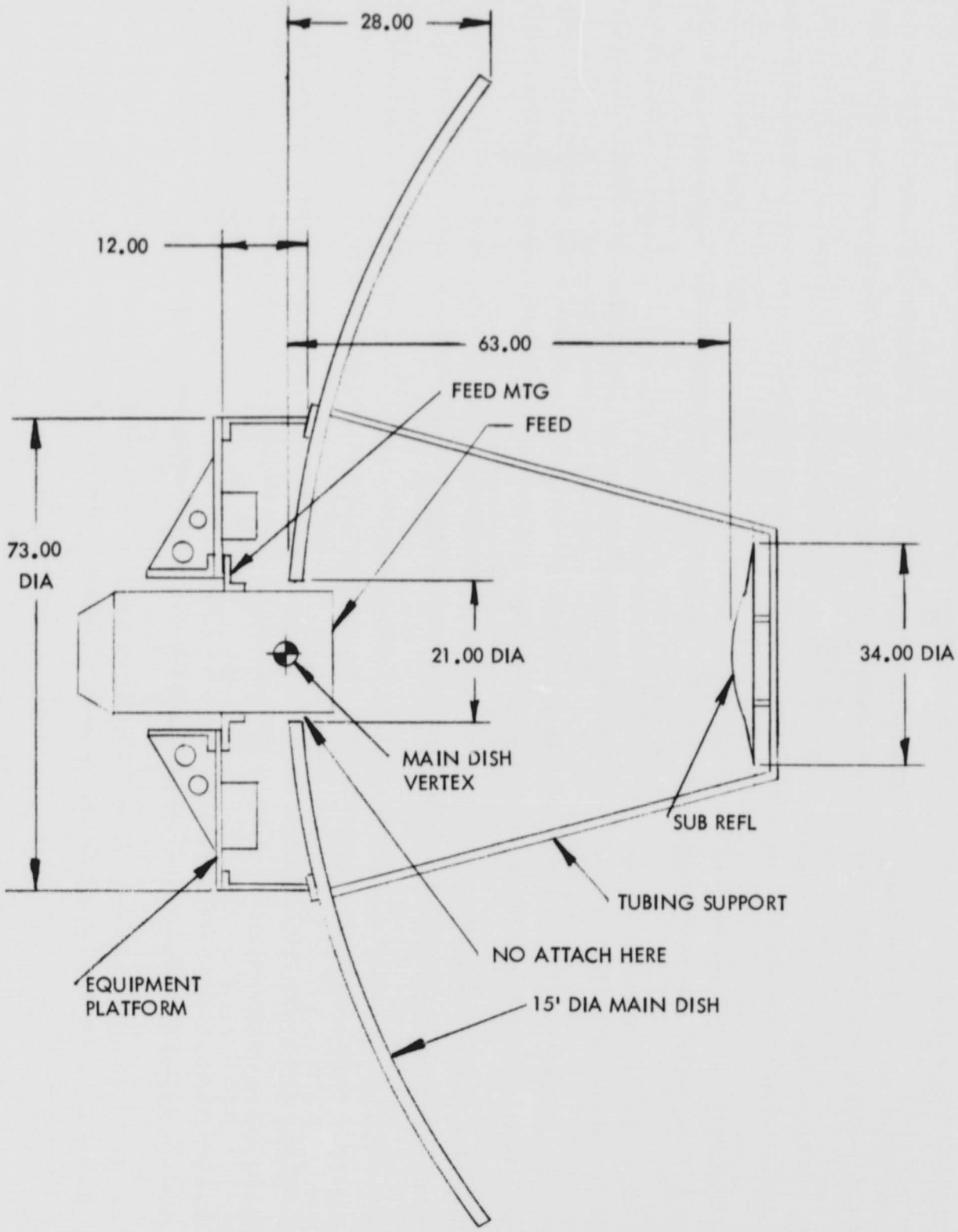

Figure 4-7. Proposed Cassegrain Antenna for AAP Space Terminal

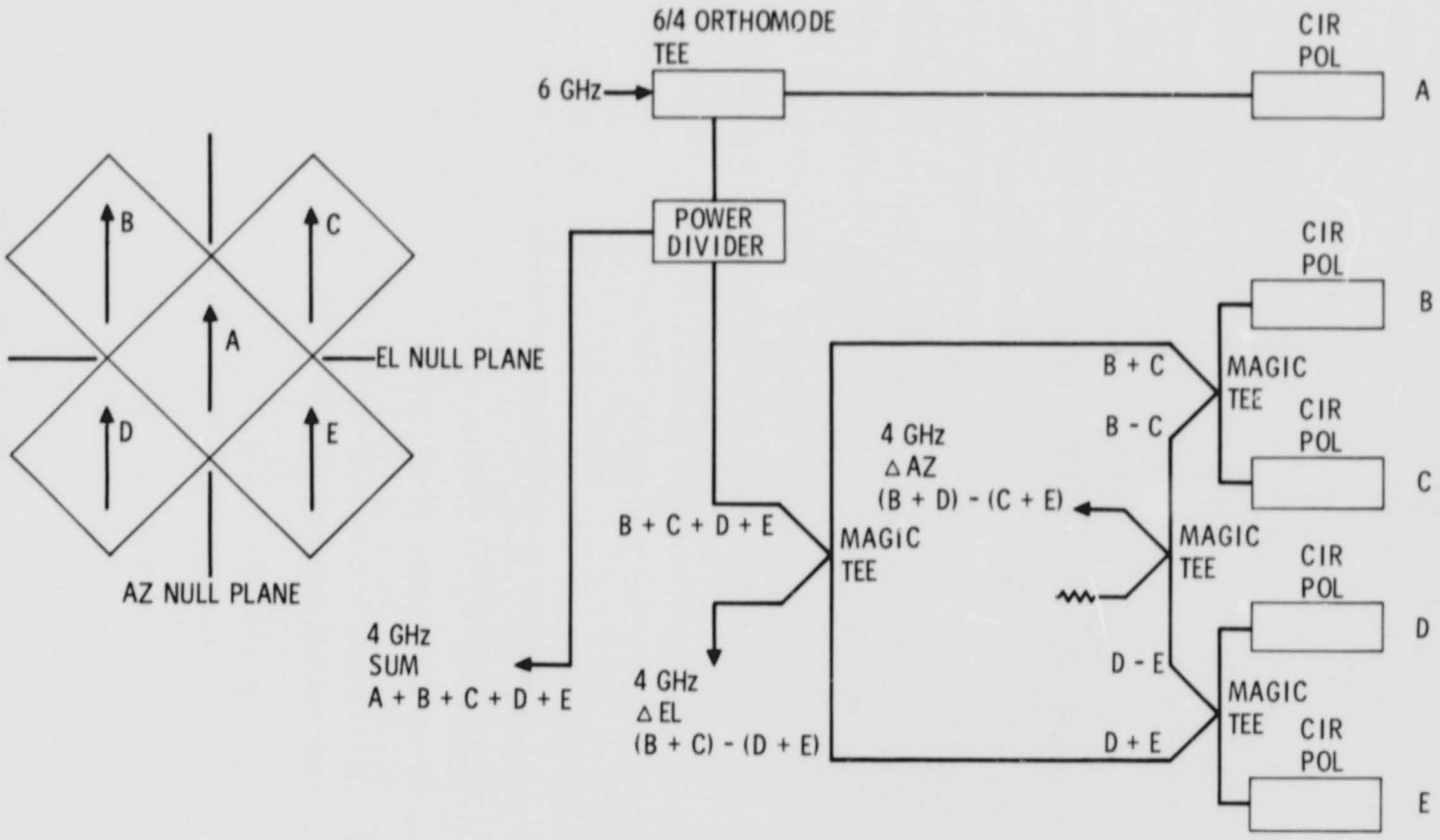

Figure 4-8. Five-Horn RF Feed Circuitry

4.3.2 Feed Design

The feed is designed to simultaneously operate at 6 GHz for transmit and at 4 GHz for receive and monopulse tracking; a feature of the design is efficient operation at both frequencies.

The receive sum channel aperture utilizes all five horns, the receive difference channels use the four outside horns, and the transmit channel uses only the center horn aperture. Control of the aperture size of the individual horns, and amplitude and phase control at the common aperture of the five horns, results in an average beamwidth at 6 GHz equal to the average beamwidth at 4 GHz.

The RF circuitry at 4 GHz consists of a power divider feeding a diagonal plane monopulse comparator and the center horn. The power divider splits the power so that 75 percent goes to the center horn and 25 percent to the comparator (and subsequently to the outer horns). Five circular polarizers are used to convert to right circular polarization. The RF circuitry and its combining operations are shown in Figure 4-8. (The normalizing subscripts are not shown.) The comparator combines the signals from the four outside horns to form the two difference (error) channels. The power dividers add the signal from the center horn, after it has been properly phased, to the sum signal from the comparator to obtain the receive sum channel. The transmit signal is coupled to the center horn through the 6/4 orthomode tee. Because the transmit signal polarization incident on the polarizer is orthogonal to the receive polarization, the output of the polarizer will give left circular polarization. The 6/4 orthomode tee does not allow coupling between the 4 and 6 GHz ports. The mechanical configuration of the feed is shown in Figure 4-9. A large part of the development of this feed was performed in the work reported in NASA Report CR-720.

The only components of the feed that need further development are the 6/4 orthomode tee, the power divider, and the circular polarizer for the center horn. The horns, magic tees, and polarizers for the outer horns will be identical to the existing design.

4.3.3 Cassegrain Design

The cassegrain design establishes the location and contour of the hyperboloid and the proper position of the feed. For an antenna main dish diameter of 180 inches, an F/D ratio of 0.4, and a hyperboloid half-angle of 11.8 degrees, the position of the hyperboloid is as shown in Figure 4-7. The feed protrudes in front of the paraboloid vertex by 9 inches. This is identically the geometry of the cassegrain antenna described in NASA Report CR-720, which also includes details of its mathematical analysis.

The complete subreflector consists of a hyperboloid plus a splash plate. The hyperboloid itself is 24 inches in diameter, and the splash plate is a ring with a radial length of 5 inches tilted 18.4 degrees and added to the

outer edge of the basic hyperboloid. The purpose of the splash plate is to improve the efficiency of the antenna system by redirecting, to the main dish, some of the spillover which goes past the edge of the hyperboloid.

4.3.4 Performance

The estimate of performance of this design, based on the measured results described in NASA Report CR-720, is summarized in Table 4-2. This estimate is based on the assumption that the assigned frequencies for AAP/DRT would be two adjacent channels centered at the frequencies of 6.35 and 4.12 GHz. The expected gain over the transmit and receive bands is 45.8 and 42.3 dB, respectively.

TABLE 4-2. EXPECTED PERFORMANCE OF CASSEGRAIN ANTENNA

Parameter	Transmit	Receive
Frequency, MHz	6350 ±38	4120 ±38
Polarization	LHCP*	RHCP**
Gain (sum-beam peak), dB	45.8	42.3
Ellipticity, dB	2.0	2.0
Sidelobe level (sum), dB		
Maximum (first)	<-16	<-16
$5° < \theta < 10°$	<-30	
$\theta > 10°$	<-35	
Sum peak-to-difference peak, dB		6.0
Monopulse null depth, dB (reference to sum peak)		>35
Beamwidth (3dB), degrees	0.65	1.00

* Left hand circularly polarized.
** Right hand circularly polarized.

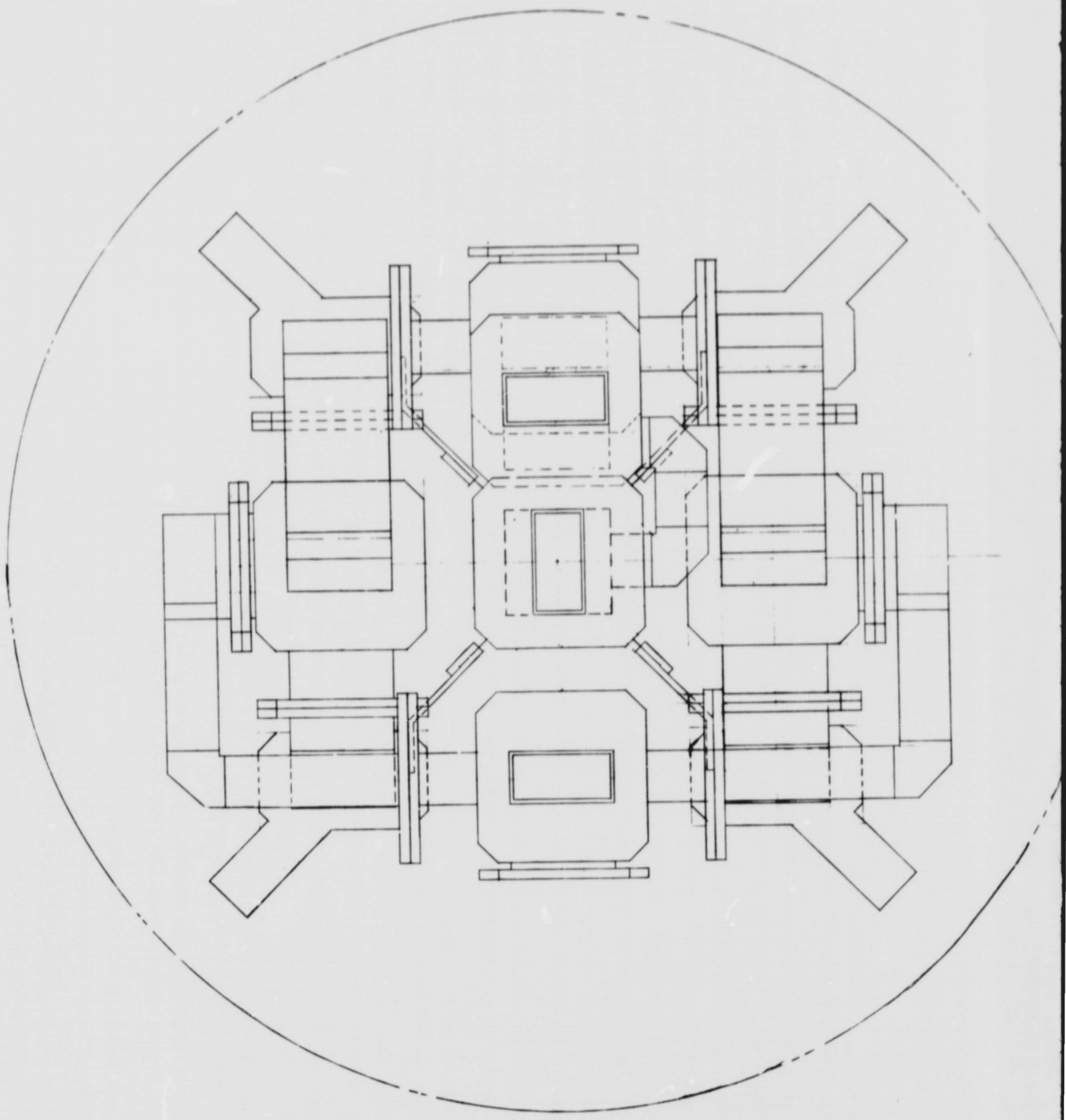

Figure 4-9. Antenna Feed Layout for AAP Space Terminal

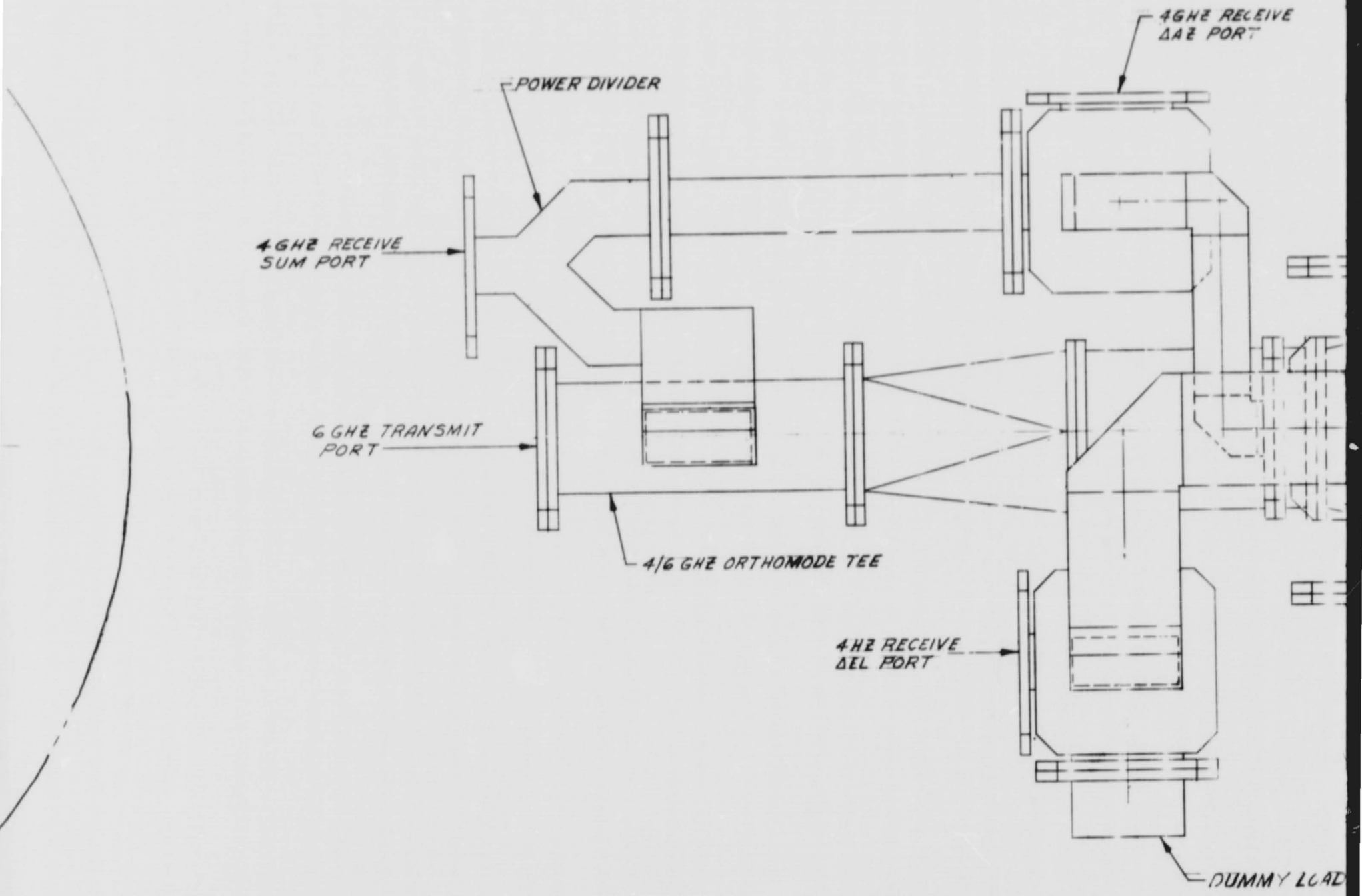

FOLDOUT FRAME 2

FOL

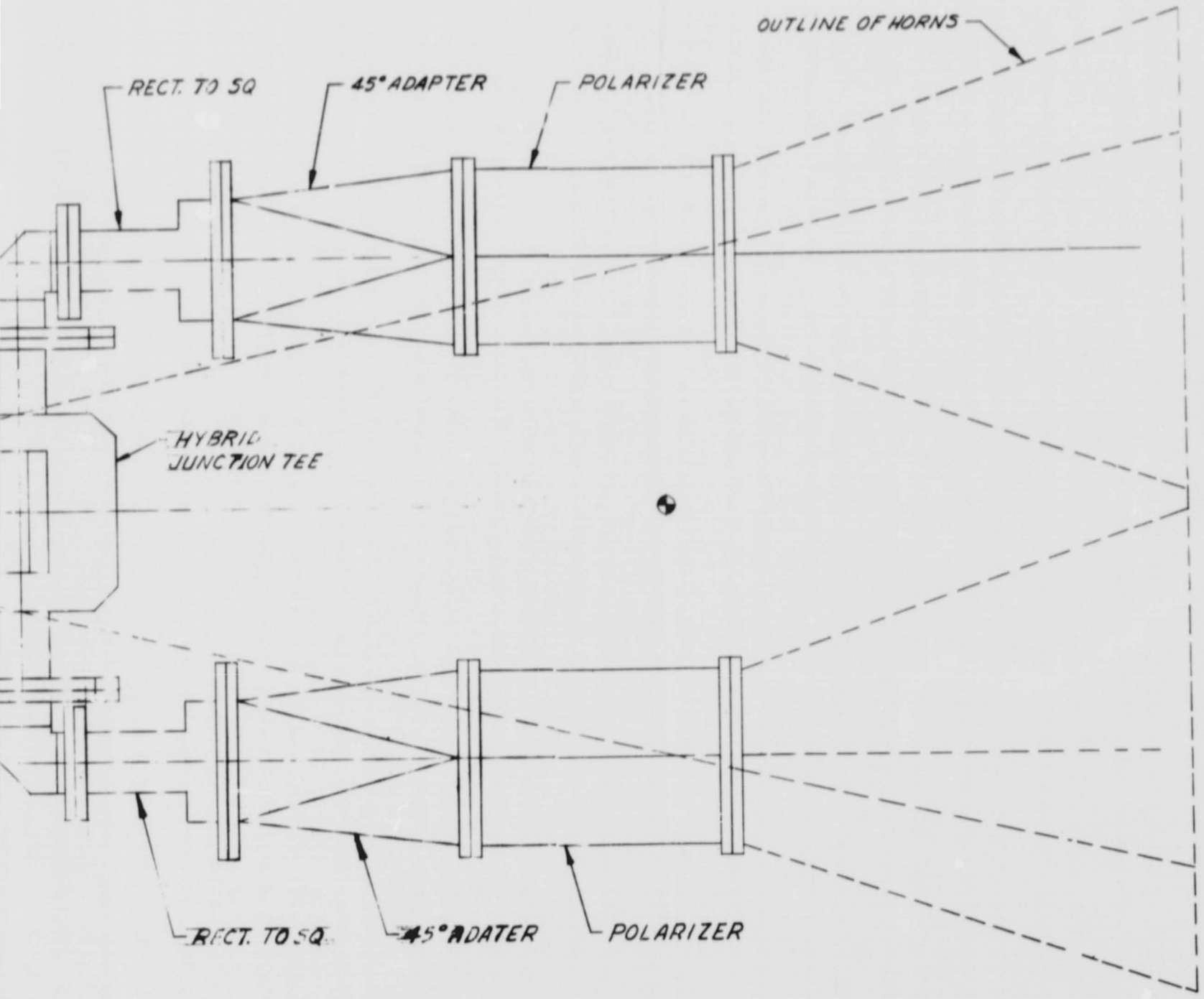

FOLDOUT FRAME 3

OUT FRAME

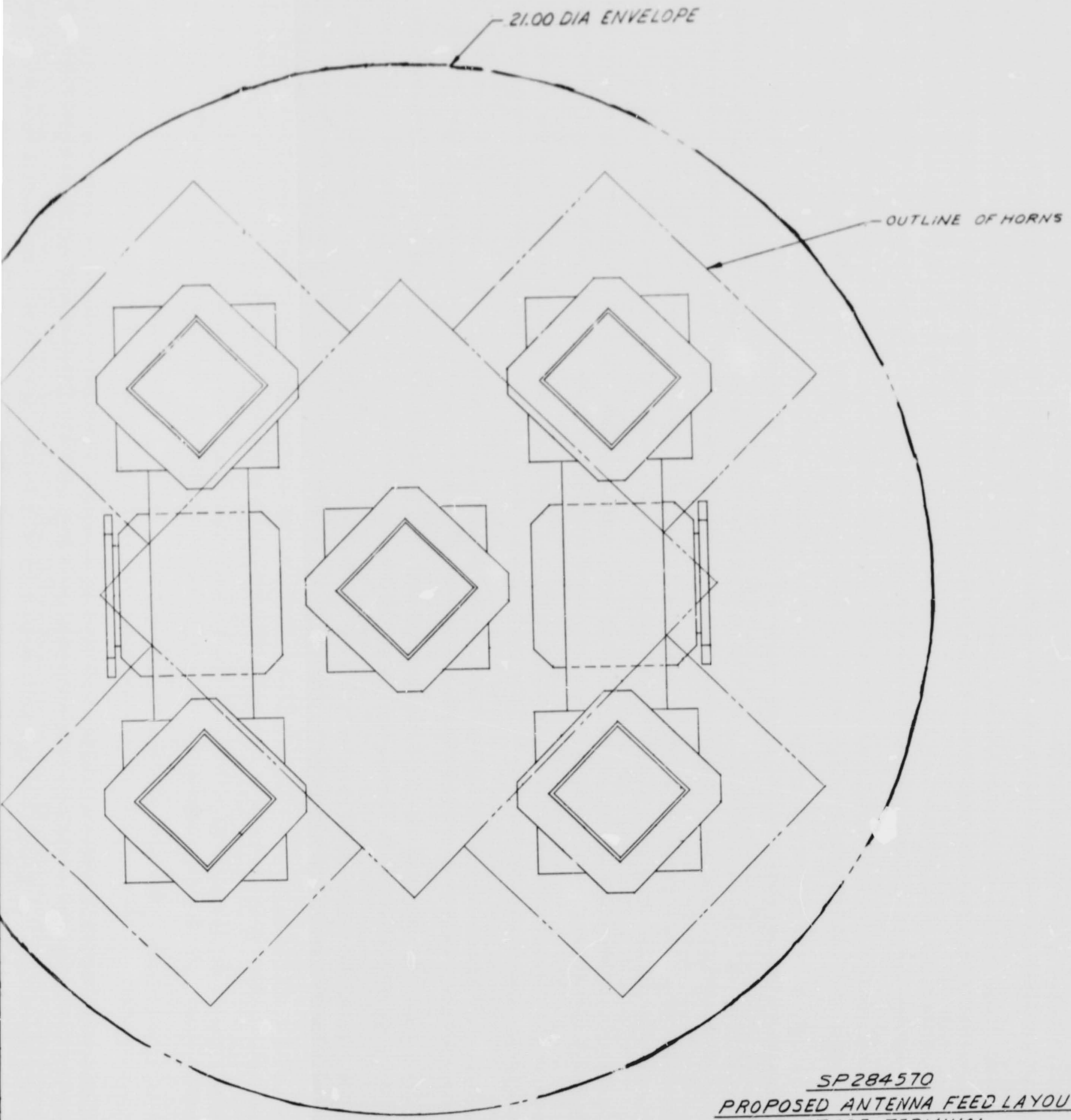

SP284570
PROPOSED ANTENNA FEED LAYOUT
AAP SPACE TERMINAL
SCALE: 1/1 DATE 9 DEC 1969
SHEET 1 OF 2

FRONT VIEW

FOLDOUT FRAME 4

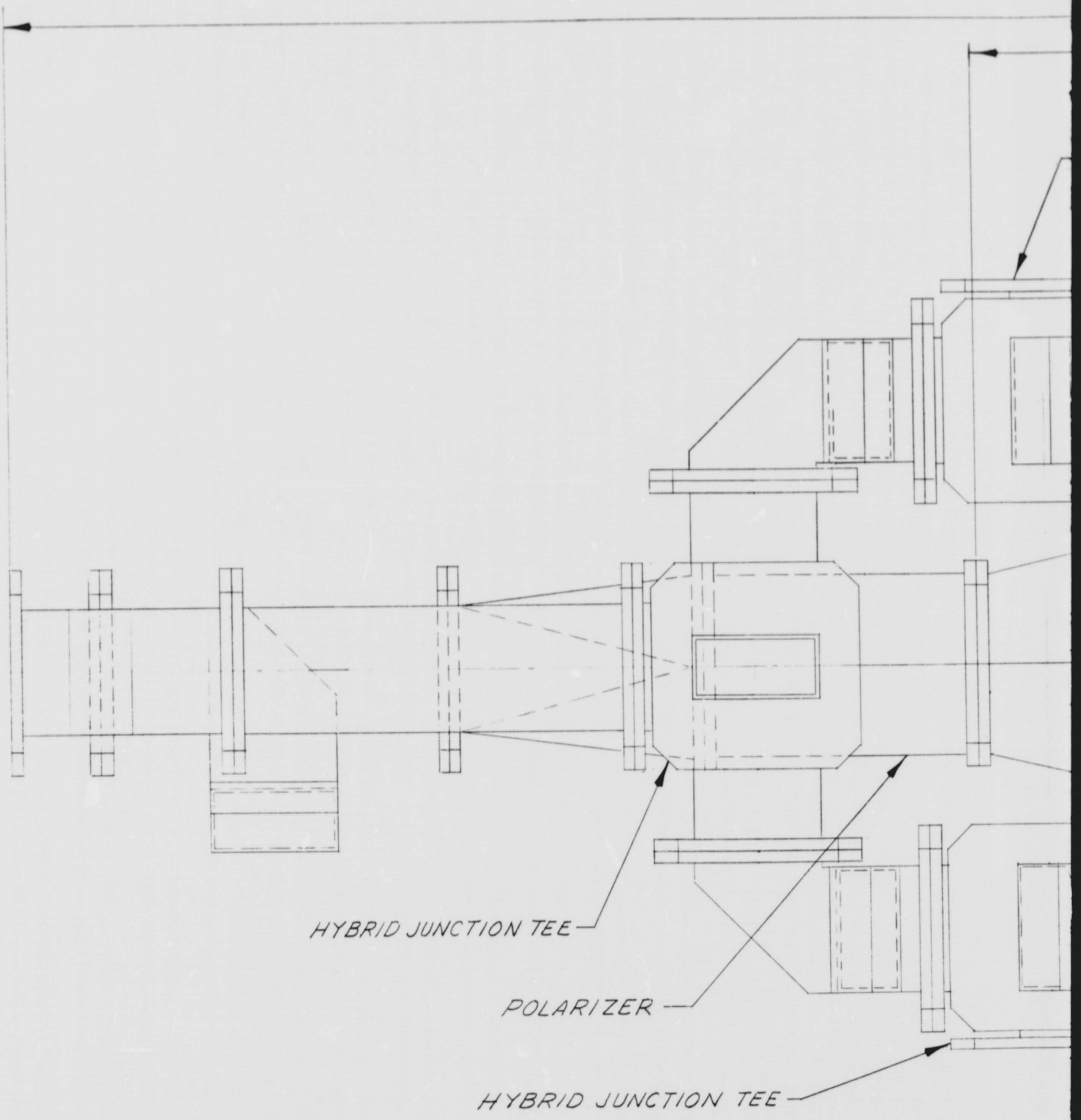

PRECEDING PAGE BLANK NOT FILMED.

FOLDOUT FRAME 1

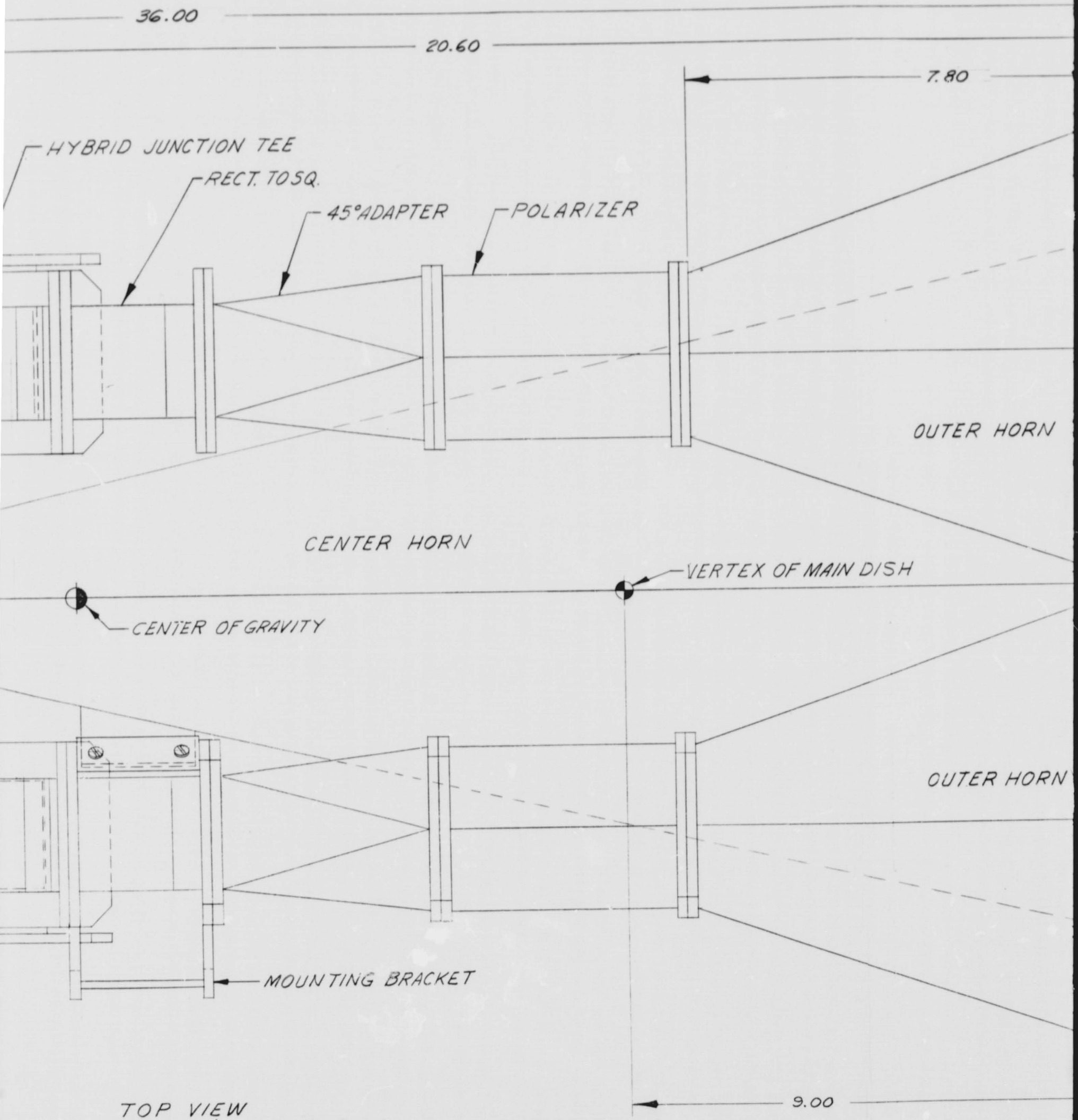

TOP VIEW
SCALE: 1/1

FOLDOUT FRAME 2

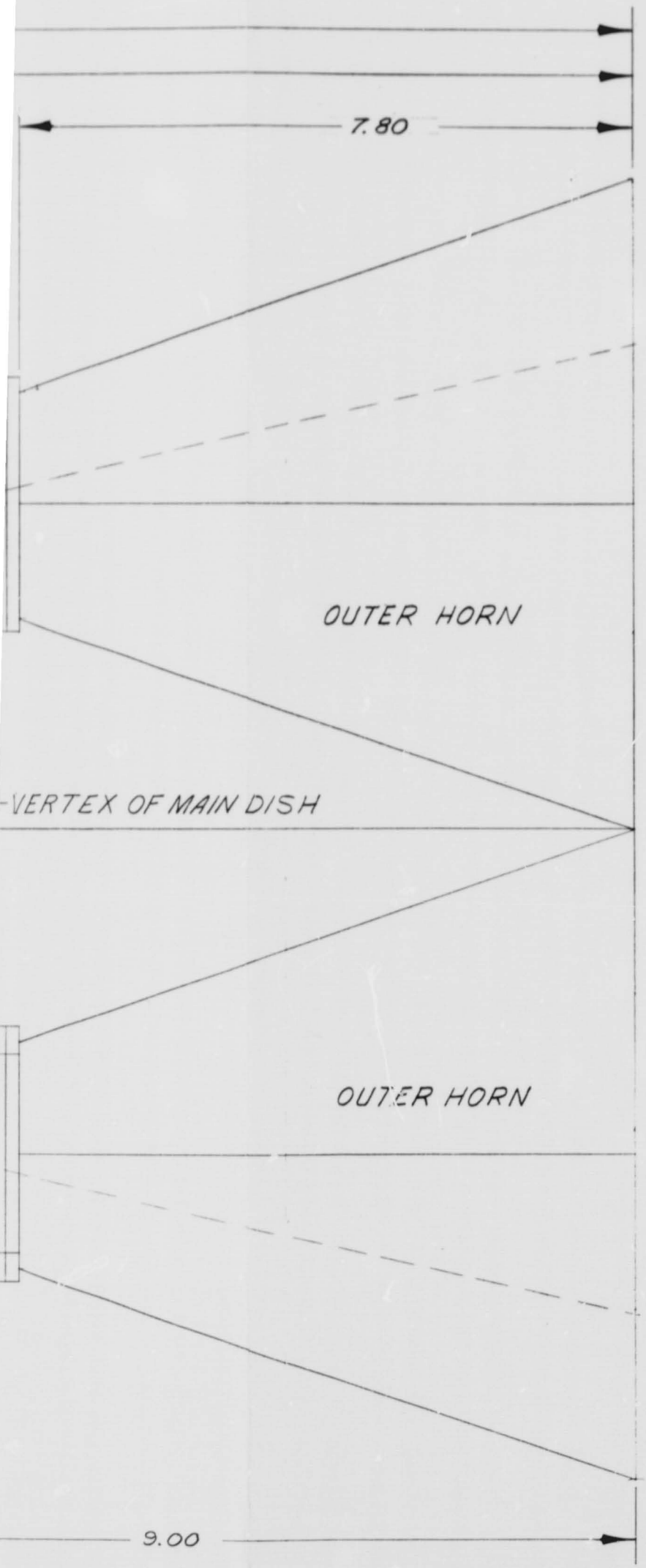

SP 284570
PROPOSED ANTENNA FEED LAYOUT
AAP SPACE TERMINAL
DATE 9 DEC 1969
SHEET 2 OF 2

FOLDOUT FRAME 3

The sidelobe levels were determined by examining computed secondary patterns, the secondary patterns measured at 4 GHz, as given in NASA report CR-720, and the patterns of other cassegrain designs with beamwidths of approximately 1 degree. It should be cautioned that the far-out sidelobes, which are at levels lower than -35 dB, are difficult to predict to an accuracy of better than perhaps ±5 dB. This is because of the dependence of these sidelobes on the detailed construction of the reflector edges, the quadripod support for the subreflector and the exact characteristics of the feed primary pattern. With these considerations in mind, maximum sidelobe level estimates are shown in Table 4-2. It may be possible to decrease the -35 dB sidelobes somewhat by eliminating the splash ring from the subreflector. However, elimination of this ring would probably decrease the gain by approximately 0.5 dB. The true sidelobe level can only be established by measurement with the final mechanical configuration.

Losses used in arriving at the expected gains are shown in Table 4-3. The aperture efficiency and spillover were taken from NASA report CR-720. The blockage losses were computed from Ruze.* The loss from thermal distortion was estimated from computed main dish (paraboloid) distortions. A visual examination of the computed thermal distortions of the reflector indicated that a cubic error existed. The cubic error has three effects: it causes the beam to shift, the sidelobe levels to increase, and the nulls to fill in. In a tracking antenna only, the latter two effects cause a gain loss, which is the only loss shown in the budget.

A computed secondary radiation pattern at 4.1 GHz is shown in Figure 4-10. This pattern was computed using an average of measured primary feed patterns. Typical measured secondary patterns at 4.1 GHz are shown in Figure 4-11 with the splash ring on the hyperboloid, and in Figure 4-12 without the splash ring. An examination of the measured patterns shows that it is reasonable to expect that a decrease in the sidelobe level at 6 GHz could be realized by eliminating the splash ring. However, as stated earlier, this decrease could only be confirmed by measurements at 6 GHz.

---

*John Ruze, "Feed Support Blockage Loss in Paraboloid Antennas," Microwave Journal, December 1968, pp. 76-80.

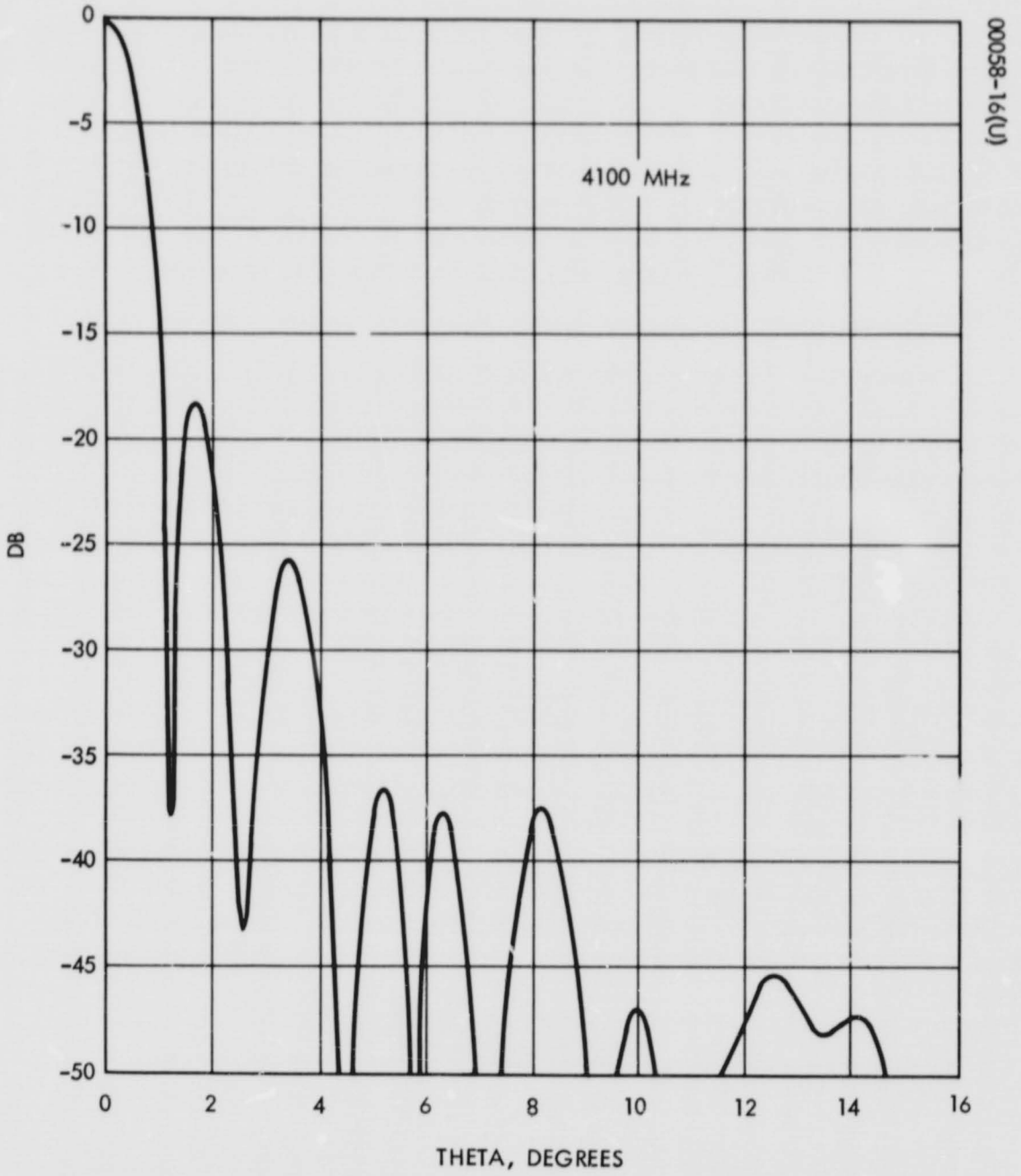

Figure 4-10. Calculated Radiation Pattern of Five-Horn Feed With Splash Ring

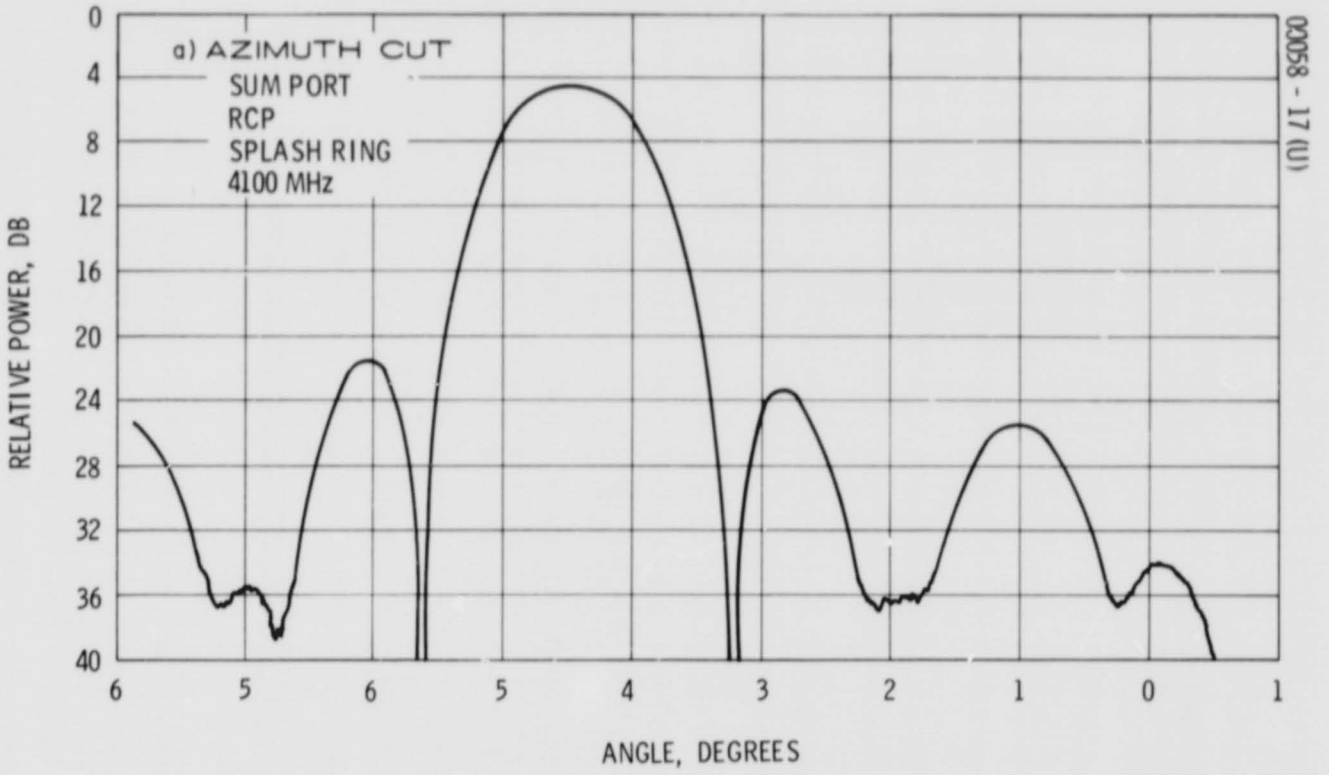

Figure 4-11. Measured Radiation Pattern of Five-Horn Feed With Splash Ring

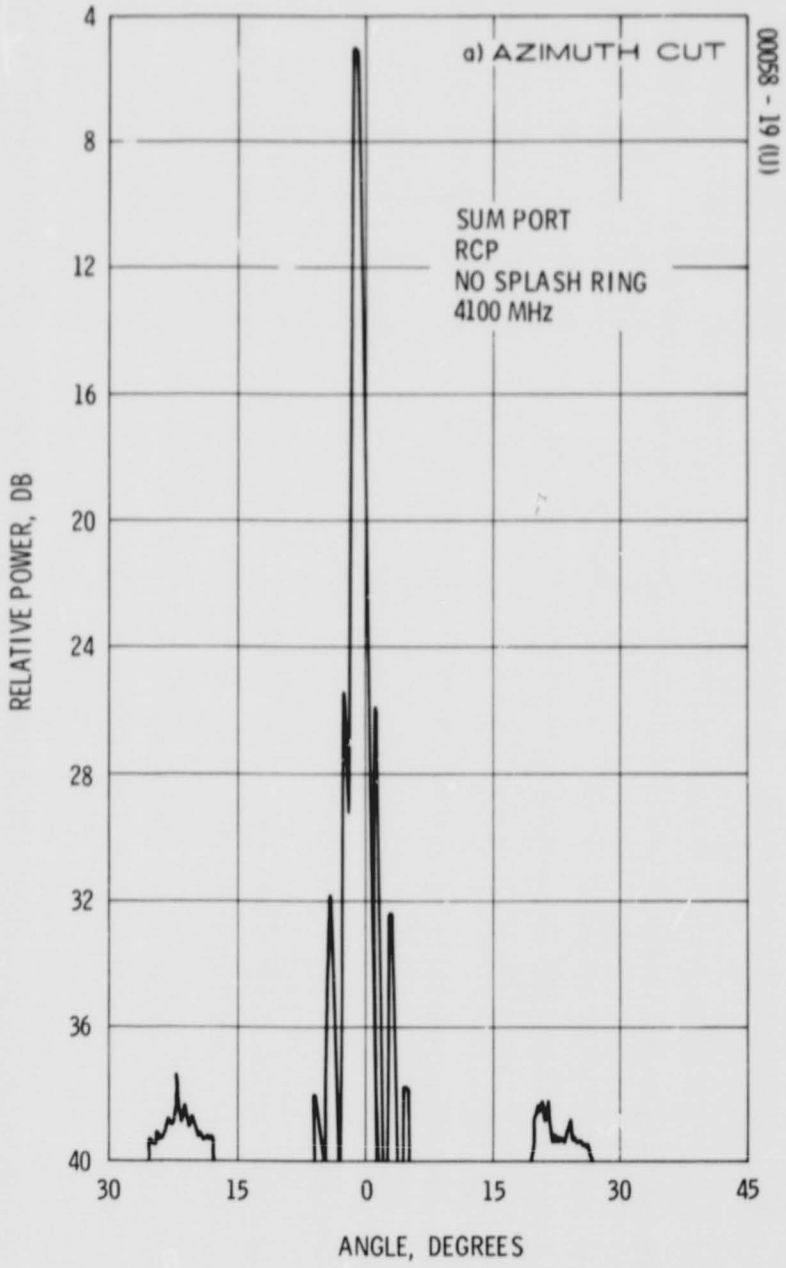

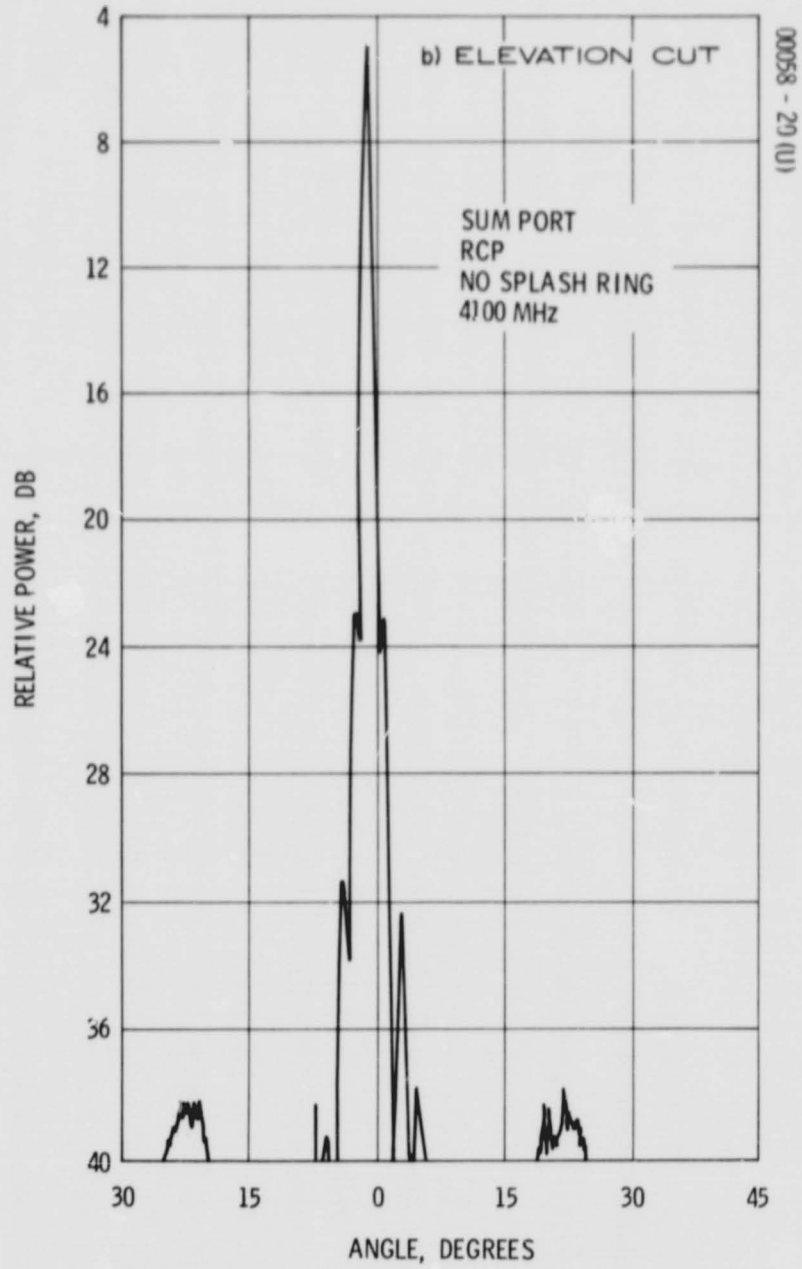

Figure 4-12. Measured Radiation Pattern Without Splash Ring

TABLE 4-3. ANTENNA LOSS BUDGET AND EXPECTED GAINS, dB SUM PEAK

Parameter	Frequency, MHz	
	6350 ±38	4120 ±38
Area gain	49.6	45.9
Losses		
Aperture efficiency	1.0	0.9
Spillover	0.7	0.7
Hyperboloid blockage	0.5	0.5
Strut (hyperboloid support) blockage	0.2	0.2
Reflector rms surface error (σ_M = 0.040 inch, σ_S = 0.015 inch)	0.4	0.2
Reflector thermal distortion	0.3	0.3
RF circuit (two magic tees, 4 foot waveguide polarizer, power divider, 6/4 orthomode tee)	0.4	0.5
Cross-polarized power	0.3	0.3
Total	3.8	3.6
Expected gain	45.8	42.3

TABLE 4-4. POSITIONER REQUIREMENTS

Gimbal limits, degrees	Elevation ±100 Azimuth ±190 Boom 0 and 180
Rates	Track on El and Az 0 to 1.6 deg/min Slew on all axes 180 deg < 2 minutes (150 deg/min)
Commands	Acquisition mode – slew to present position indicated by binary word
Accuracy, degrees	Tracking ±0.05 Slew ±0.20
Temperature, °F	Gimbals -90 to +150 sinks Electronics 0 to +100 operating -65 to +140 nonoperating
Weight, pounds	33 for each drive (three per vehicle) 9 for each control electronics (two per vehicle)
Power	23.5 to 28.5 volts dc 30 watts time average 80 watts peak worst case
Brake	Maintain position with power off system
Position readout	Provide gimbal shaft position in binary word
Reliability	Safety margins compatible with manned systems
Load properties	Approximately 550 pounds El and Az inertia 310 slug-ft^2 Boom < 20 foot length
Ground test	Bearings to withstand full loads, including counterbalance Gimbals to operate with 14 ft-lb unbalance to allow for simplified counterbalance system Track mode – 10 volt/deg error signal for El and Az gimbals

4.3.5 Structural Design

4.3.5.1 Main Reflector

The main reflector is a honeycomb structure of constant thickness, 0.012 inch thick epoxy glass covers on a 1.5 inch thick aluminum flexcore. A 21 inch diameter hole in the center of the dish permits the cassegrain feed to illuminate the subreflector. Syntactic foam fill in the core gives "bump" resistance at the inner and outer diameter edges, and provides an anchor for the metallic inserts used in attaching the support ring structure on the back of the dish and the subreflector support tubes on the front surface.

4.3.5.2 Subreflector

The subreflector is a solid epoxy glass cloth laminate approximately 0.1 inch thick. Four metallic inserts on the backside of the subreflector attach it to the quadripod tubes. The RF surface is vacuum-deposited aluminum.

4.3.5.3 Quadripod

The four subreflector support tubes are 1 inch diameter thin-wall epoxy glass tubes. Longitudinal graphite fibers increase the strength and stiffness of the tubes. The small tube diameter minimizes RF pattern perturbations.

4.3.5.4 Thermal Finish

All external surfaces of the antenna elements are painted black for thermal control.

4.4 ANTENNA POSITIONING SUBSYSTEM

4.4.1 Requirements

The antenna positioner subsystem includes the motors, drives, support bearings, position indicators, and the control electronics to direct the antenna. There are three drives: the elevation and azimuth drives used for closed-loop tracking of the antenna, and the boom drive used for open-loop repositioning of the entire boom and antenna.

The positioner requirements are summarized in Table 4-4. The specified limits are based on a requirement for greater than hemispherical coverage from a single boom position so that boom repositioning will be required only at handover. The 180 degree rotation of the boom provides full spherical coverage with overlap.

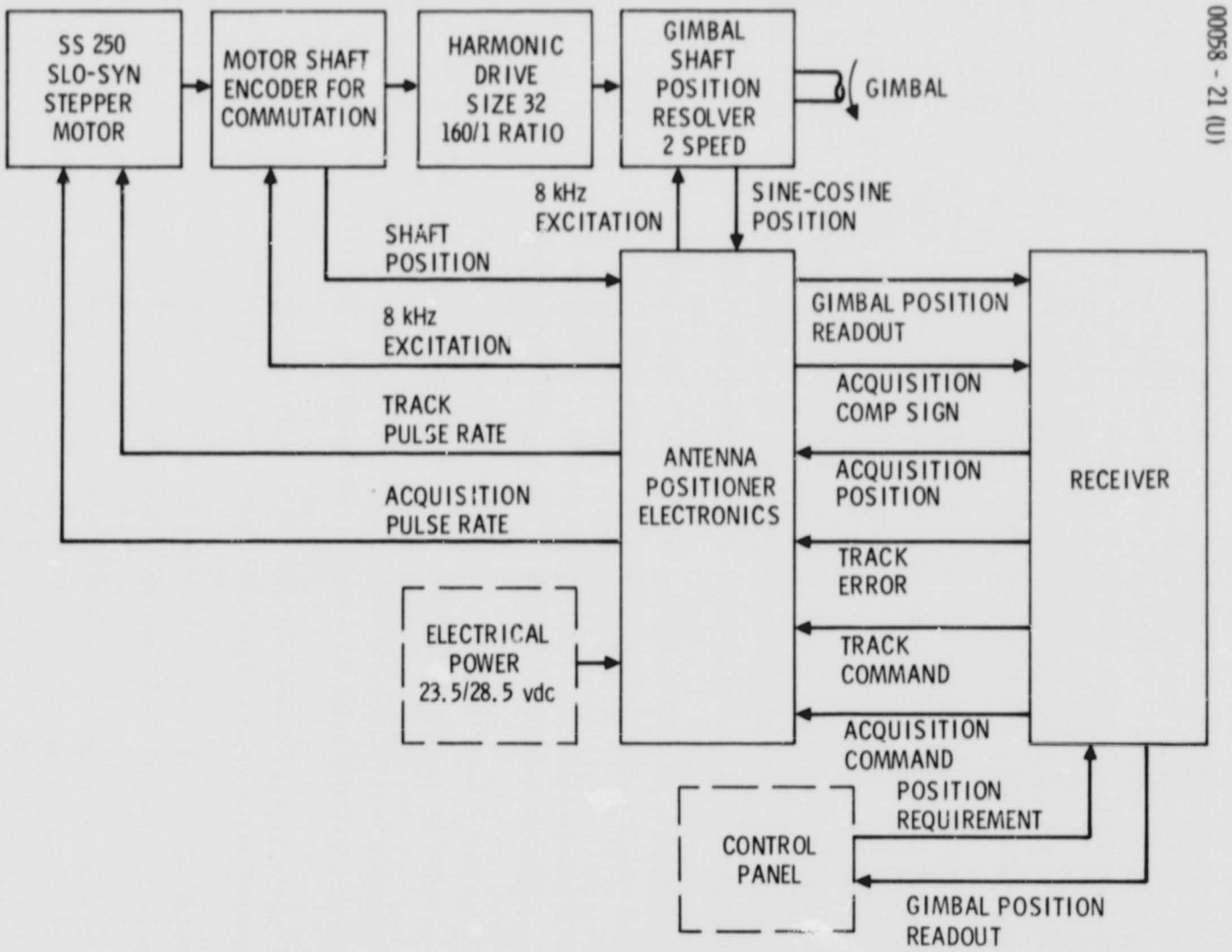

00058 - 21 (U)

Figure 4-13. Antenna Positioner Subsystem Block Diagram

The rate requirements shown in Table 4-4 are adequate near the zenith, where the azimuth drive has its highest rate requirement. (The time-averaged rate is approximately 0.4 deg/min.)

The specified tracking accuracy is consistent with the overall antenna pointing error used in link performance estimates. The accuracy requirement on slewing is imposed to ensure acquisition.

The passive braking requirement provides for locking the antenna in a desirable position without continuous power when the DRT is shut down; it also protects the OA in the event of a power failure to the antenna positioners.

The ground test conditions size the ball bearings so as to withstand the forces and moments encountered during assembly, test setup, and ground handling. The requirement of 14 ft-lb for ground test permits an unsophisticated unloading test rig by allowing for a drive with enough torque to overcome a partially unbalanced moment. This capability is important for a demonstration of two axes working simultaneously in a closed-loop system.

4.4.2 Subsystem Operation

Identical positioner mechanisms are used for the elevation, azimuth, and boom drives. A block diagram of a typical gimbal positioner is shown in Figure 4-13. The antenna positioner electronics (APE) is mounted on the back of the main antenna reflector in the equipment compartment.

The selected motor is a Slo-Syn SS 250 stepper with a step increment of 1.8 degrees, which is reduced through a 160/1 harmonic drive. The drive output is connected directly to the output shaft, which rotates in steps of approximately 0.01 degree.

The stepper motor is designed to perform open-loop stepping by inputting a series of pulses. However, with open-loop stepping, operation is severely limited if the load inertia inhibits the motor from advancing as fast as the driving pulse rate. If, in fact, the rotor position is not in phase with the current pulse sequence, the rotor may even reverse direction for a step. To overcome this difficulty, an encoder is mounted directly on the motor shaft and digitally commutates the stepper motor coils. This commutation technique permits full torque of the motor to be applied at any phase of the step cycle, just as in a dc brush motor. Even when the step transition is very slow, the encoder prevents switching of the coils until the rotor has advanced to a position for the next coils to be effective.

The encoder for commutation is shown in the block diagram of Figure 4-13. This encoder output could be used to accumulate the gimbal position by bit-counting in a register. However, should power be interrupted, the register would lose count and the antenna would have to be positioned to a mechanical stop to reinitialize the count, which can be difficult and time-consuming. Instead, a direct readout resolver has been provided for each gimbal shaft positioner.

TABLE 4-5. TORQUE BUDGET

Elevation and Azimuth Drives	Flight Track	Ground Test Track	Flight Slew	Ground Test Slew
Cables and bearings	19.7*	20.7	19.7	20.7
One step windup	139.0	139.0	0	0
Unbalanced moment	0	168.0	0	168.0
Acceleration	0	0	8.3	8.3
Total required	158.7	327.7	28.0	197.0
Torque available worst case	884.0	884.0	605.0	605.0
Torque margin	5.6/1	2.7/1	21.6/1	3.10/1
Boom drive				
Cables and bearings	Track not required on boom		19.7	20.7
Unbalanced moment			0	168.0
Acceleration			68.0	68.0
Total required			87.7	256.7
Torque available worst case			605.0	605.0
Torque margin			6.9/1	2.36/1

*All torque values in in-lb.

The gimbal shaft resolver puts out sine and cosine signals to indicate actual position. It has two sets of windings, which provide signals corresponding to x1 speed and x72 speed. These signals generate the six most significant bits from the x1 speed winding, and the remaining six bits from the x72 speed winding. These are summed to form a 12 bit word corresponding to actual shaft position, for comparison with the commanded position and for visual readout at the control panel.

In operation, when an acquisition command is received from the receiver, the computer will provide a pointing command consisting of a digital word for each axis. The APE compares the present shaft position with the commanded position to determine the number of steps required to reposition. A motor encoder bit register is initialized, and the gimbal is slewed at 150 deg/min (225 pulses/sec) until the register accumulates the required count. This method utilizes only the motor encoder in the loop rather than the gimbal resolver because of the position lag of the gimbal output shaft, thereby eliminating certain slew stability problems that could arise as a result of the low natural frequency of the structure. When the motor encoder register equals the commanded position register, the desired motor position has been reached; but the "completed response" signal is delayed to allow the gimbal shaft oscillations to damp out.

When the completed response signal is given, a new position command is issued by the computer and the process repeats until the tracking receiver recognizes the presence of a received signal and issues a command to transfer to tracking mode. At this point, the stopping time and mechanical lag of the antenna is important. The estimated overshoot is approximately 0.4 degree, which is within the pull-in range of the receiver.

When the system is in the track mode, the motor coils are turned off between stepping commands to conserve power. The motor is pulsed at a low rate with 0.150 second current pulses. Typically, the target rate is about 0.4 deg/min, which requires a current pulse every 1.7 seconds. This means the coils of each drive are energized less than 10 percent of the time. In operation, whenever the error signal exceeds a predetermined deadband, the electronics waits a short period and executes one pulse. The pulse winds up the harmonic drive by one step and then shuts off power. The magnetic brake action of the motor maintains the position, and the drive unwinds the antenna to its new position, advancing it by a 0.01 degree step. The control loop analysis is described in Section 4.4.4.

The torque budget is shown in Table 4-5; allowances for both ground testing and flight operation are included. The ground test environment includes the possible unbalance moment imposed because of unloading tolerances, and a slight increase in expected bearing friction due to the attendant higher bearing loads. The indicated worst case available torque assumes a motor winding temperature of 75°F above the hottest sink condition. (This condition can occur only after a 15 minute period of slewing for initial acquisition; normally, the motor coil temperature is close to that of the sink, in which case the available torque is 25 percent greater than shown in Table 4-5.

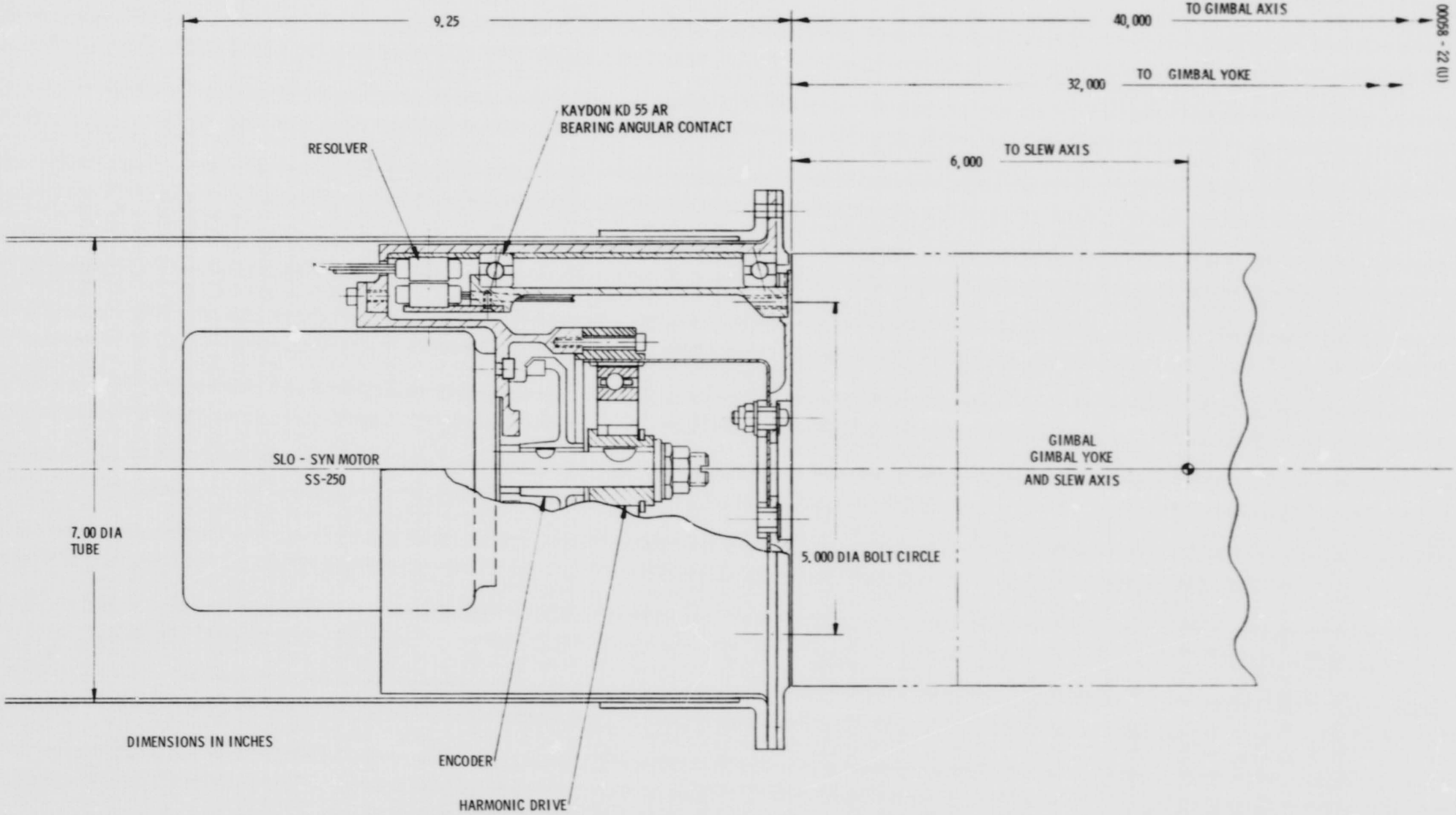

Figure 4-14. Antenna Positioning Drive Assembly

The torque available for the lowest temperature condition is about double that listed. This higher torque is of little significance during tracking because the typical displacement increment is one step at a time. During slew, however, the structural system winds up, and the maximum torque level of about 100 ft-lb could be applied to the OA. If this should present a problem to the OA control system, current limiting could be added to the APE to limit the maximum torque.

The total impulse to the OA is of concern only when slewing the boom because of its large inertia compared to the two gimbals. The requirement to slew the boom 180 degrees in less than 2 minutes results in an acceleration impulse of

$$\frac{2\theta J}{t} = \frac{2(\pi/2)\ 6500\ \text{slug-ft}^2}{60\ \text{seconds}} = 340\ \text{ft-lb-sec}$$

which is well below the allowable 500 ft-lb-sec.

4.4.3 Mechanical Components

The positioner is shown in Figure 4-14, installed in a tube, as it would be for the azimuth drive. In the elevation drive, the same design would be mounted in one of the yoke arms. The opposite arm of the yoke would contain only a matching housing, shaft, and bearing assembly. Since none of the axes have complete rotational freedom, slip rings are not required. The wires, including coaxial cables, are bundled with sufficient slack to allow the required rotary freedom.

A flexible coaxial cable would be used around linkages, and semirigid coaxitube elsewhere. Hughes has conducted tests to determine the forces required to bend Rockbestos flexible coaxial cable at four temperatures, extending down to -250°F. The coldest cable condition for this application is estimated to be -90°F. Since the actual cable harness configuration may differ from the test setup, a factor of two has been applied to the data, and a total of 10.5 in-lb of torque has been budgeted for the bending of the two coaxial cables and the wire bundle.

The positioner shaft ball bearings are Kaydon KD55AR. The 5.50 inch inside bore allows compact packaging of the drive elements. A thin-wall bearing was selected to minimize bearing and positioner housing weight. The bearing has a static rating of 17,100 pounds in the thrust direction and 5900 pounds in the radial direction. These capacities are generous for flight loads since the main weights are locked directly to structure during launch. However, in the 1 g test environment, the radial forces will reach 42 percent of this capacity. The bearings will be preloaded in the thrust direction to approximately 100 pounds to provide radial stiffness and a consistent thrust position despite temperature changes. The resulting levels of bearing friction are a small item in the torque budget and are beneficial to system damping.

A Slo-Syn SS 250 permanent magnet stepper motor has been selected. The permanent magnets provide a residual holding torque of 2.2 in-lb with no power applied. The power-on detent is 18.8 in-lb at room temperature, and the stepping torque is 14 in-lb at low pulse rates and 10 in-lb at 225 pulses/sec. The torque values shown in Table 4-5 are lower than these because they reflect the worst case effect of winding temperature. The motor is bifilar wound, resulting in four coils that are sequenced in pairs to advance the rotor in 1.8 degree increments. Since bifilar wound motors have twice as many winding turns as standard wound types, they have more resistance per winding and lower current ratings. This reduces the low-speed torque but raises the high-speed torque since the L/R time constant is reduced.

Although the SS 250 motor has not yet been space-qualified, Hughes has space-qualified a smaller size of the same design, the SS 25. The changes needed on the commercial SS 25 were developed jointly with the manufacturer (Superior Electric Company); the same changes will be incorporated into the SS 250.

The motor commutation encoder was designed and developed at Hughes for use with the smaller size Slo-Syn motor. Since the step increment is identical and the environment is less severe, the identical design would be used in this application. The motor commutation circuitry will also be identical. The encoder is a variable reluctance differential transformer wound on E-shaped cores. As a toothed wheel, mechanically fastened to the motor shaft, passes the windings, the transformer output changes from 0 to 1. There are two E-cores, displaced from each other by one step, to provide directional information from the lead or lag of the core outputs. The two secondaries of each E-core are differentially wound and spaced so that each detects either the in-phase or the out-of-phase relationship with the toothed wheel. The E-cores and the toothed wheel are formed from 2 mil silicon-iron laminated sheet bonded into stacks. This construction of laminations reduces eddy current losses at the 8 kHz carrier frequency. The device has all inputs to and outputs from the stator, and, therefore, requires no contacting parts and a very low level of power. It has been operated over the temperature extremes of -250° to 180°F in vacuum.

The reduction drive is a size 1M harmonic drive from United Shoe Machinery Corporation. The 160/1 ratio drive is incorporated in the shaft and housing design, as shown in Figure 4-14. This reduction ratio was selected to give the resolution required at the output shaft during tracking. The size 1M is dynamically rated at 160 ft-lb on the output, with a static torque rating twice this value.

The lubrication used throughout is MoS_2 powder burnished into the metal surfaces in accordance with an established Hughes procedure. The life requirement of these positioners is well within the demonstrated capability of MoS_2 in vacuum. The elements of the harmonic drive, ball bearing races for the motor, harmonic drive, and shaft bearings are all disassembled and burnished. The ball separators in all bearings are machined from Duroid material to replenish MoS_2 to the bearing elements during their life.

The two-speed resolver is a conventional design used in many rotating assemblies. The factors leading to its selection are described in Section 5. 8. The accuracy requirement is such that established manufacturing methods can be used with some relaxation over the tolerances presently held on similar resolvers for another Hughes program.

The elements of the positioner are housed in a steel shaft and housing, as shown in Figure 4-14. The shaft wall thickness is sized to provide the required bending stiffness. The wall thickness of the housing could be thinner and still satisfy the stiffness criteria; but as the housing is also the major thermal path for motor heat, its cross-section cannot get too small.

4. 4. 4 Control Loop

A diagram of the positioner control loop is shown in Figure 4-15. There are two operational modes: the acquisition mode, for which the outer antenna loop is open, and the tracking mode, for which that loop is closed. All switches shown are controlled by signals from the tracking receiver.

4. 4. 4. 1 Acquisition

The position control mode has only an inner loop closed around the stepper motor, and commands originate from the pulse rate generator. For either the azimuth or elevation drives, position changes are commanded by gating the 225 pulse/sec rate for the duration necessary to accumulate N pulses, where

$$N = \frac{\text{desired angular position change}}{\text{step size (0. 01125 degree)}}$$

A different pulse rate will be used for the boom drive. This method of driving the position loop at a fixed rate limits load acceleration and thus windup of the structure. Initializing of the command position registers is provided by the resolver output.

4. 4. 4. 2 Tracking Loop

The tracking loop, when closed, derives a feedback loop from the receiver electronics, which puts out a signal proportional to the pointing error of the antenna. A deadband is provided to avoid unnecessary hunting and to keep the motor duty cycle to a minimum.

4. 4. 4. 3 Control Loop Parameters

Table 4-6 shows the preliminary control loop parameters. The two most critical parameters are the gain, K_V, and the bandpass (low-pass-corner frequency). A value for K_V of 1 deg/sec per degree of error was selected so that the loop would follow the expected rates within the allowable error. The bandpass corner frequency, selected to get good response when transferring from acquisition to track mode, is about the upper stability

TABLE 4-6. POSITIONER CONTROL LOOP PARAMETERS

Parameter	Value	Calculation	Comments
Forward loop gain K_V	1.0 deg/sec/deg	$\frac{3 \text{ deg/min} \times 1/60}{0.05 \text{ deg}}$	Minimum = $\frac{\text{maximum expected rate}}{\text{error allowable}}$ Maximum must allow gain margin
Dead space	±0.02 degree	>0.016 degree	Must be greater than 1σ noise level to minimize oscillations
Bandpass	~1 rad/sec	$\frac{< \omega_n \text{ structure}}{10}$	Low-pass corner frequency must be low enough to minimize error and to be well below structure frequency, yet high enough to allow the selected forward loop gain (i.e., leave enough phase margin)
Compensation	$\frac{1}{0.5S + 1}$	>Bandpass $< \frac{\omega n \text{ structure}}{5}$	Allows rolloff at structural frequency (detailed study required at hardware stage)
Rate saturation	4 deg/min tracking		Want maximum tracking rate low to control transients
Torque limit	50 ft–lb		Vehicle requirement

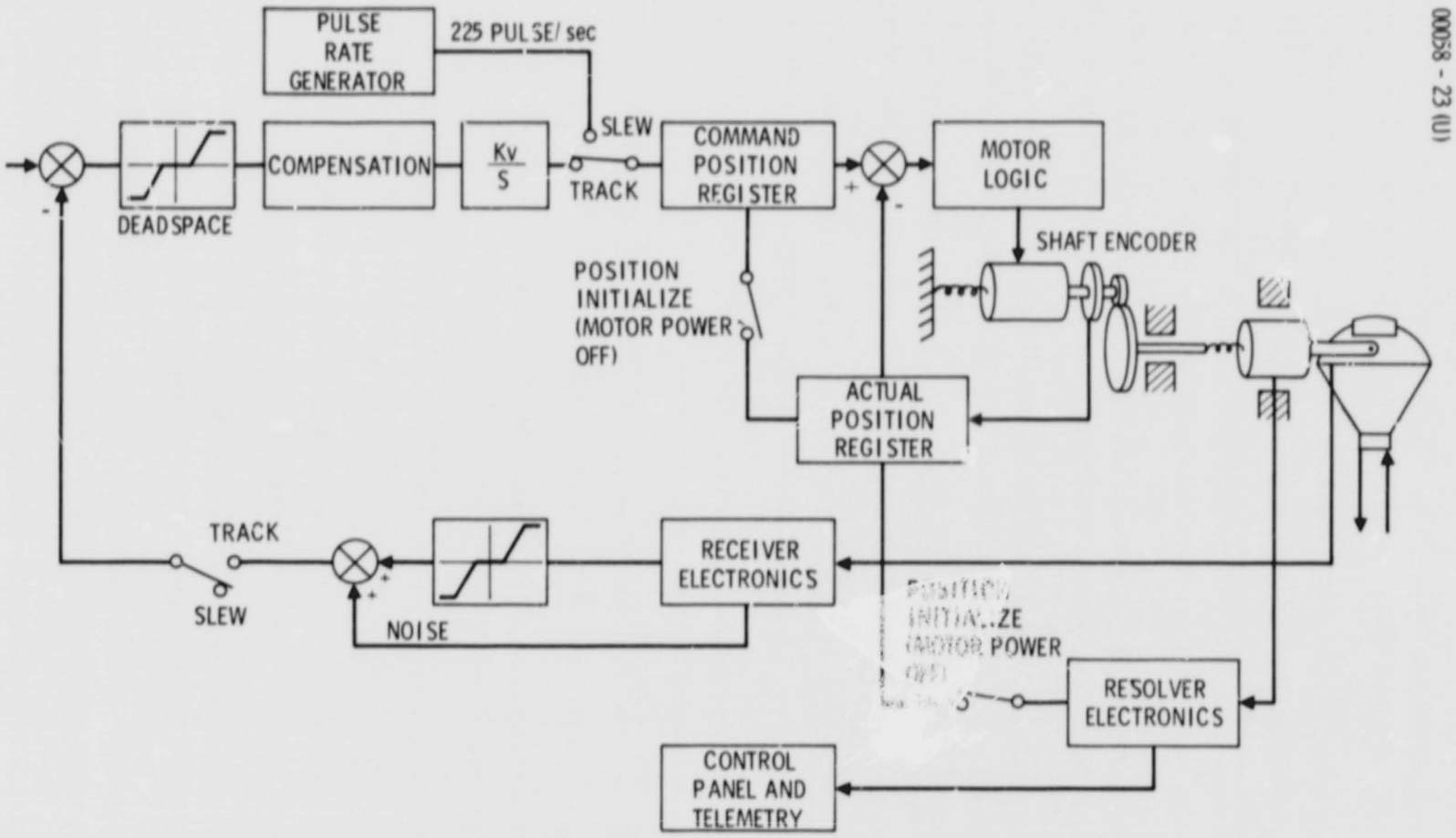

Figure 4-15. Antenna Positioner Control Loop Block Diagram

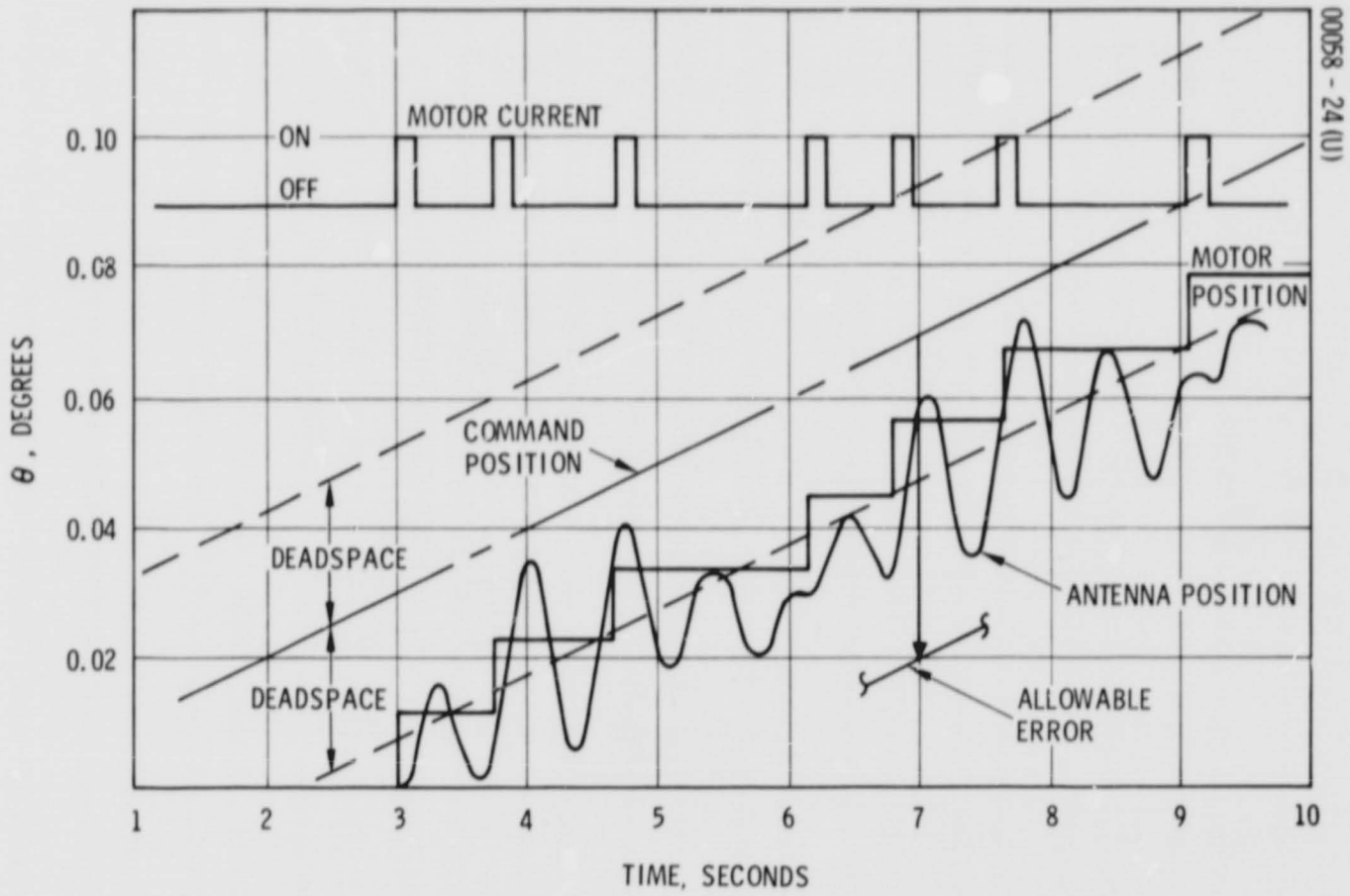

Figure 4-16. Control Loop Tracking Performance

limit for the calculated structural natural frequencies of 10 rad/sec. For this reason, some compensation is required in the tracking loop; the compensation shown in Table 4-6 was selected for the preliminary investigation. A more detailed analysis, beyond the scope of this study, will be required to verify the control loop parameters.

Rate saturation is provided to minimize transients during the transfer from acquisition to tracking. Peak tracking rates are substantially less than the 4 deg/min limit, so there is ample margin.

4.4.4.4 Typical Response

Figure 4-16 is a plot of the response of the tracking loop at a command rate of 0.6 deg/min. This response demonstrates the on-off duty cycle of the motor and the dynamics of the flexible antenna structure. As shown, the system stays well within the allowable error.

4.4.5 Antenna Positioner Electronics (APE)

A block diagram of the motor control circuitry for the elevation and azimuth gimbal drives is shown in Figure 4-17. The commands to the APE are as follows:

1) Acquisition—Discrete command from tracking receiver; logical 1 indicates that APE should enter acquisition mode and logical 0 indicates reception of tracking signal.

2) Track—Discrete command from receiver; logical 1 indicates that track mode has been entered and that analog receiver track voltage is valid. This is logically the negation of the acquisition signal but is implemented so that transfer in either direction is triggered by the presence of the appropriate signal, rather than presence or absence of a single signal.)

3) Tracking Error—Analog voltage from receiver indicating instantaneous error. Maximum input is ±10 volts, with 10 volts corresponding to 1 degree error.

4) Slew Position—Serial digital word containing magnitude portion indicating new slew position, address portion indicating appropriate gimbal drive, and parity bit. Serial command is received least significant bit first. Magnitude portion of command is 14 bits long.

5) Position Boom—Pulse command initiates program for repositioning boom.

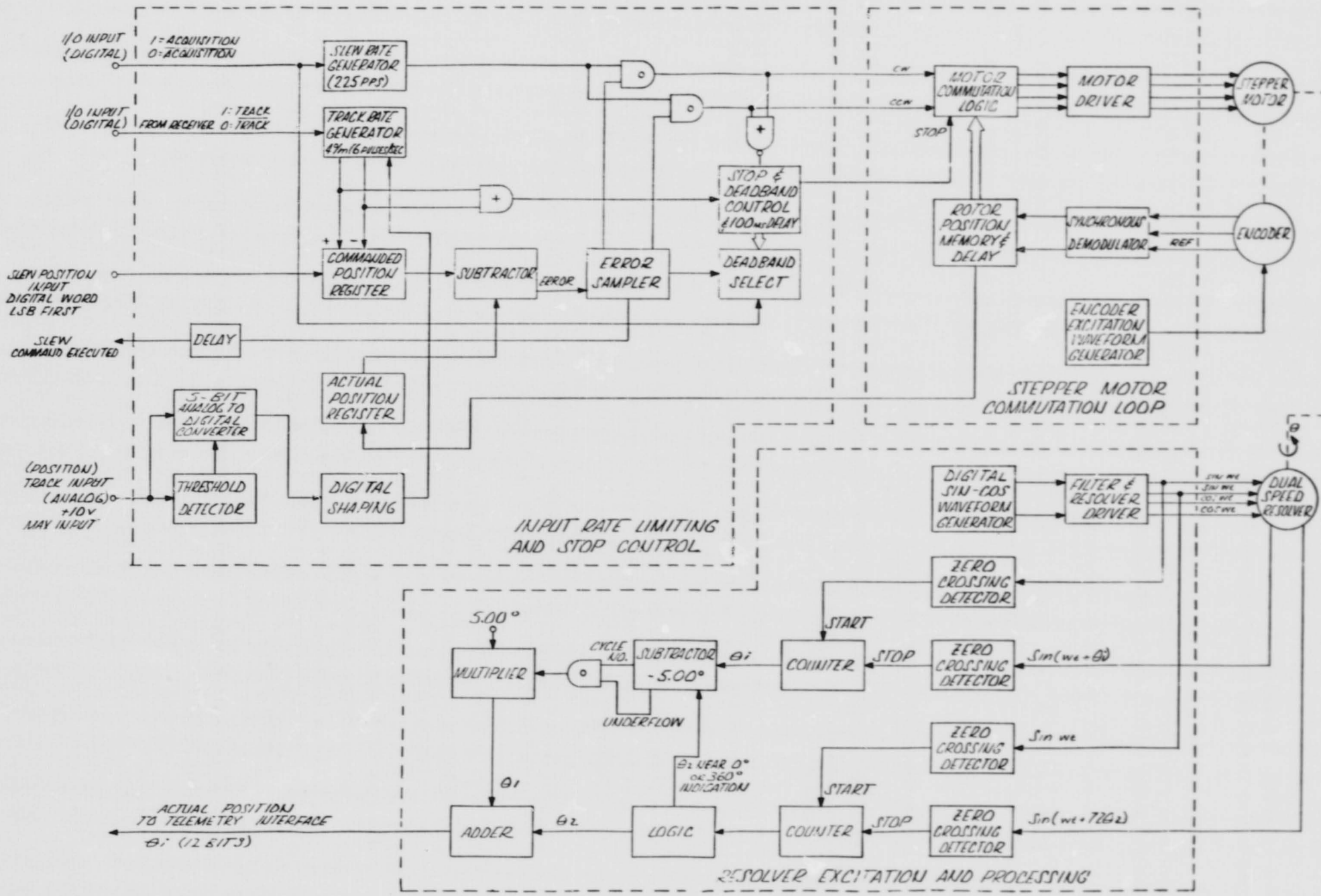

Figure 4-17. Antenna Positioner Electronics

The outputs from the motor control are as follows:

1) Slew Command Executed – Logical signal indicates that slew position command has been executed (i. e. , that error went to zero). Its output is delayed to ensure that the drive has stopped moving. A "slew-command-executed" output does not indicate that error is zero but simply that it was driven to zero. (Overshoots may cause the error to be non-zero at the time the signal is given.)

2) Actual Position Output – Twelve bit serial data word representing processed resolver output indicating actual position of the load. This output is available from all three drives.

The track mode is selectable for either the azimuth or the elevation drives (the boom drive has no track function). In this mode, the load can be positioned at rates up to 4 deg/min. When the receiver steering signal output is greater than 1 volt (i. e. , the error is greater than 0. 1 degree), the track rate will saturate at its maximum value of 4 deg/min. For receiver inputs less than 1 volt, rates are proportional to input voltage.

In the acquisition mode, position commands are provided from the OA computer, which result in load movements at 150 deg/min (225 motor pulses/sec). When the position command has been executed and the drive has stopped, the "slew command executed" output is enabled.

The boom positioning drive has only one mode of operation. This is initiated by a pulse command, which causes a rate profile to be generated in the APE. This, in turn, results in an acceleration of the boom to a rate of 150 deg/min, followed by a deceleration to zero rate, so that 180 degrees of boom travel is accomplished with minimum acceleration within the allowable boom transfer time.

The APE is split into three major categories, as shown in Figure 4-17.

1) Input rate limiting and stop control

2) Motor commutation loop

3) Resolver excitation and processing

Input rate limiting and stop control are achieved by position feedback from the stepper motor commutation loop, which updates the contents of the actual position register and provides the basis for position control of the motor. Rate control is mechanized by limiting the commanded rates. To provide position control, the contents of the "actual position" register are subtracted from the contents of the "commanded position" register. The difference is the error, which is sampled by the error sampler. The error sampler determines whether the error is positive, negative, or zero. If it

is positive or negative, the sampler provides direction control commands to the motor commutation logic to drive the motor until the error is equal to zero. The stop command overrides direction control commands. When a stop command has been executed, a deadband is enabled such that small motor movements resulting from deenergization of the motor windings do not cause direction commands. When further position commands are received from the computer, the deadband is reduced to zero and the new input commands are executed.

The stepper motor commutation loop consists of the magnetic encoder, demodulator, rotor position memory, and motor commutation logic. Motor position is sensed by an encoder mounted on the motor shaft. The encoder provides two outputs, each a double-sideband suppressed-carrier waveform whose carrier phase is dependent on rotor position relative to the stator. These two signals are demodulated to produce a two bit binary signal. The present states of the two signals are stored in the rotor position memory. The motor commutation logic samples this "present rotor position" information, and at the occurrence of any of the three input commands (CW, CCW, or STOP), the logic selects the proper set of motor windings to be energized for the desired motor action.

The dual-speed resolver is mounted at the load end of the drive for accurate determination of load position. The resolver is excited by sine and cosine waveforms of constant amplitude, with outputs of the form sin $(\omega t + \theta_i)$ from the single-speed winding and sin $(\omega t + 72\theta_i)$ from the multiple speed winding. Processing of these outputs to obtain θ_i is accomplished as follows. The first six bits of the angle θ_i are found from the single-speed output, as determined by a gated phase measurement in an electronic counter. The last six bits are found using the multiple speed output in a counter similar to that used in the single-speed channel. The two six bit numbers are added to form the 12 bit representation of the angle.

4. 4. 6 Positioner Weight and Power

The weight breakdown for each positioner is shown in Table 4-7. The 33. 0 pound unit weight is used in each of the three functions: azimuth, elevation, and boom. The dummy positioner used to support the other half of the elevation gimbal weighs approximately 16 pounds; only the shaft, housing, and ball bearings are required in this unit.

Power demands are shown in Table 4-8. The worst case effects of motor winding temperature and voltage level variation are shown. The track power is shown for the nominal bus voltage level and for nominal temperature. (The justification for the 10 percent duty cycle during track is explained in Section 4. 4. 2).

TABLE 4-7. POSITIONER WEIGHT BREAKDOWN

Component	Description	Weight, pounds
Housing (2 pieces)	17-4 PH stainless steel	9. 9
Shaft	17-4 PH stainless steel	4. 0
Cover plate	2024-T4 aluminum	0. 8
Ball bearings (2)	Kaydon 440C steel	2. 1
Bearing spacer and retainer	17-4 PH stainless steel	2. 0
Slo-Syn motor SS 250	Stepper motor, including bearings	6. 5
Motor encoder	Digital commutator	0. 8
Harmonic drive	Size 32, 160/1 ratio	2. 4
Shaft angle instrument	Dual-speed resolver	3. 0
Miscellaneous	Bolts, nuts, and washers	1. 5
Total		33. 0

4. 5 TELEMETRY, COMMAND, AND MANUAL CONTROL

Preliminary requirements for telemetry, command, and manual override are summarized in Table 4-9; they total 50 telemetry items and 32 commands. To be on the safe side, however, it seems prudent to size the T&C interface for a 25 percent growth over the presently identified T&C parameters.

Although normal operation of the SWS microwave terminal is fully automatic and fully commandable from the ground, on-board manual override control is provided. Potential items for inclusion on the on-board control and display panel are also shown in Table 4-9. The final selection of displays and controls to be included in the DRT control panel must be established by NASA and/or the AAP integration contractor.

4. 6 THERMAL DESIGN

Thermal control of all DRT components will be achieved passively. The aft end of the electronics package will be painted black ($\alpha^* = 0.96$, $\epsilon = 0.85$) and serve as the radiator. Superinsulation (30 sheets) will be used to minimize radiation interchange with the cylinder walls and the dish. The antenna dish will be painted black on both sides. Any thermal finish with $\alpha/\epsilon \leq 1.1$ will provide adequate thermal control of the feed support tubes. The gimbal assembly housing will require a finish with $\alpha/\epsilon \leq 0.5$. Thermal requirements and performance are summarized in Table 4-10.

TABLE 4-8. POSITIONER POWER DEMAND

Slew current (one-axis)					
Winding temperature, °F		-90	116	225	
Motor current peak, amperes		2.0	1.4	1.0	
Electronics standby, amperes		0.4	0.4	0.4	
Electronics slew addition, amperes		0.7	0.7	0.7	
Total amperes		3.1	2.5	2.1	
Slew power (one-axis), watts					
23.5 volt bus		73	59	49	
26.0 volt bus		80	65	54	
28.5 volt bus		88	71	60	
Power track 0.4 deg/min				One-axis, amperes	Two-axis, amperes
Motor - mean temperature	1.4 ampere x 10 percent duty =			0.14	0.28
Electronics standby				0.40	0.40
Electronics drive addition	0.7 ampere x 10 percent duty =			0.07	0.14
				0.61	0.82
Power - 26 volt bus, watts				16	21
Positioner system average power, watts (90 percent track, 10 percent slew)					26

TABLE 4-9. SUMMARY OF REQUIREMENTS FOR TELEMETRY, COMMAND, AND MANUAL OVERRIDE

Requirement	Status Telemetry	Analog Telemetry	Digital Telemetry	On-Off Command	Digital Magnetic Command	Manual Override Control
Off				X		X
Standby: Both TWT HV OFF	X			X		X
TWT HV 1 - ON/2 - OFF	X			X		X
2 - ON/1 - OFF	X			X		X
TWT helix current - 1		X				
- 2		X				
RF power monitor		X				
Reference generator/upconverter						
1 - ON/2 - OFF	X			X		X
2 - ON/1 - OFF	X			X		X
Upconverter drive - 1		X				
- 2		X				
Voice exciter-modulator						
1 - ON/2 - OFF	X			X		X
2 - ON/1 - OFF	X			X		X
Data exciter modulator						
1 - ON/2 - OFF	X			X		X
2 - ON/1 - OFF	X			X		X
Carrier spreading ON	X			X		X
OFF				X		
Digital multiplexer						
1 - ON/2 - OFF	X			X		X
2 - ON/1 - OFF	X			X		X
Signal selector modes:						
Voice only (at full transmit pwr)	X			X		X
Voice + 72 kilobits/sec (ATM)	X			X		X
Voice + 51.2 kilobits/sec (AM or CSM)	X			X		X
Voice + composite of 5 tape recorder channels	X			X		X
Frequency 1	X			X		X
Frequency 2	X			X		X
Temperatures		6				
Preamplifier/mixer						
1 - ON/2 - OFF	X			X		X
2 - ON/1 - OFF	X			X		X
Mixer drive - 1		X				
- 2		X				
Receive reference generator						
1 - ON/2 - OFF	X			X		X
2 - ON/1 - OFF	X			X		X
Receiver 1 - ON/2 - OFF	X			X		X
2 - ON/1 - OFF	X			X		X
AGC bus - 1		X				
- 2		X				
AFC voltage - 1		X				
- 2		X				
Stop scan	X					
Continuity pilot	X					
Az shaft encoder data				X		
El shaft encoder data				X		
Az-El pointing data (→ATM computer)				X	X	
Acquisition status:						
Tracking	X			X		X
Look-up pointing data	X			X		X
Slew to estimated Az-El	X			X		X
Acquisition unsuccessful (from ATM)	X			X		X
Totals	30	17	3	31	1	30

TABLE 4-10. THERMAL CONTROL SUMMARY

Component	Thermal Design	Control Requirements	Predicted Temperature, °F		
			Description	Maximum	Minimum
Electronics package	Black radiator	Operational	. Power on	95	45
	(α* = 0.96, ϵ = 0.85)	0/+100	. Power off	0	-20
	30 layers of silicon	Survival	(Boresight pointed at sun)		
		-40/+140			
Antenna	Both sides black	Acceptability of bulk temperatures and ΔTs determined by stress and distortion analysis	Gradient, °F/in	50	μ_o
Dish			Bulk temperature	180	-90
			ΔT across dish	225	μ_o
			ΔT through core	30	μ_o
Feed support	Assumed black for worst case ΔTs		Bulk temperature	190	-150
			ΔT between strut	225	μ_o
Gimbal assembly	α/ϵ = 0.5	-200° to +200°F	Bulk temperature	150	- 90

5. SUPPORTING STUDIES

5.1 SIGNAL MULTIPLEXING

5.1.1 General

Both the uplink and the downlink require the simultaneous transmission of voice and digital data. Either link could be serviced by a single carrier with the two baseband signals combined at a level below the carrier or by two carriers with each baseband signal modulating its own carrier. The selected design approach employs a single carrier on the uplink, with the voice and command data frequency division multiplexed, as is commonly done when combining multiple voice channels, and two carriers on the downlink.

In general, the use of separate RF carriers (two in each direction) will minimize the transmitter power needed to send voice-plus-data, provided the intermodulation loss is not significant. Frequency division multiplexing of signals onto a single carrier inevitably requires guardbands within the baseband, resulting in increased overall RF bandwidth, and thus adds effective noise at the detector. The added noise requires added carrier power to obtain the C/N ratio needed for proper operation. For either RF or baseband multiplexing, cost and complexity come out roughly the same for the sample configurations checked; so the choice rests mainly on performance and convenience. The specific considerations which led to the selected approach for each link are discussed below.

5.1.2 Uplink

For the uplink, multiplexing of the voice and command signal at the baseband level was selected largely because of advantages in providing a good signal for DRT antenna acquisition and tracking. In tracking, some simplification of the receiver is accomplished since it does not have the problem of distinguishing between two uplink carriers. For acquisition, the absence of voice and command, assuming that the 1 kHz command reference signal is maintained, provides the DRT with a strong narrowband signal which, when compensated to cancel the predictable doppler shift, will always fall inside the receiver bandwidth.

The spectrum of the selected frequency division multiplexing scheme is shown in Figure 5.1-1. By placing voice at the bottom of the baseband, it is given priority status in the event of equipment or path degradation. The

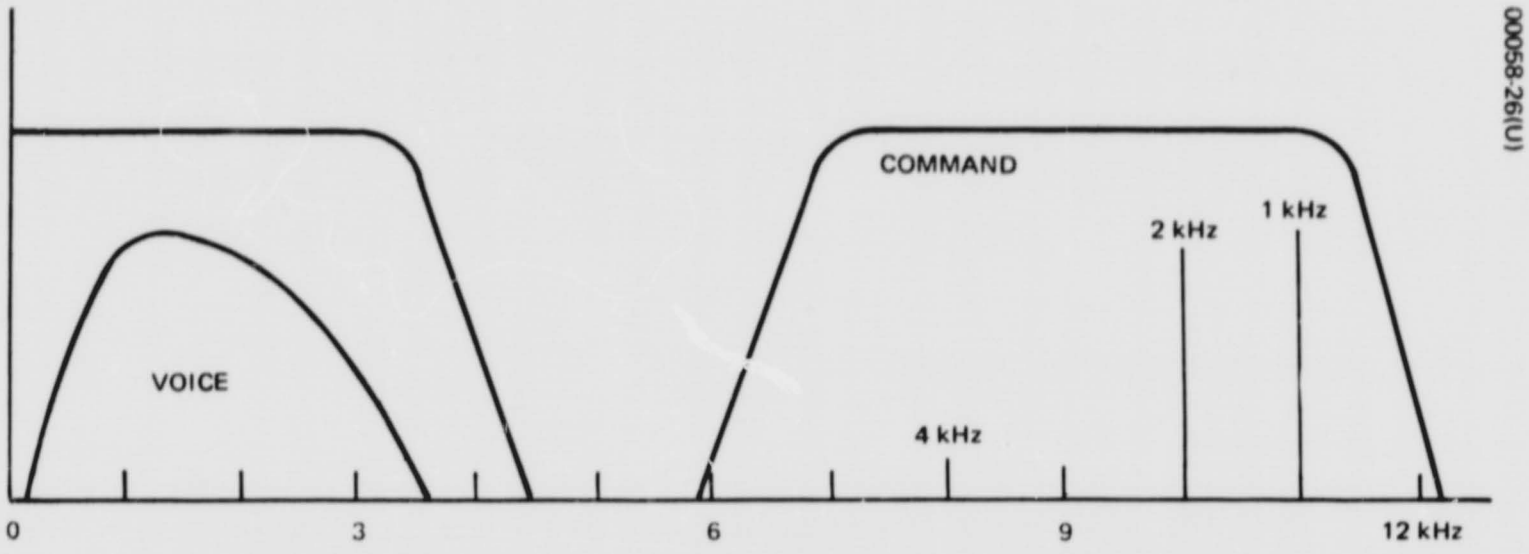

Figure 5.1-1. Uplink FDM Signal Spectrum

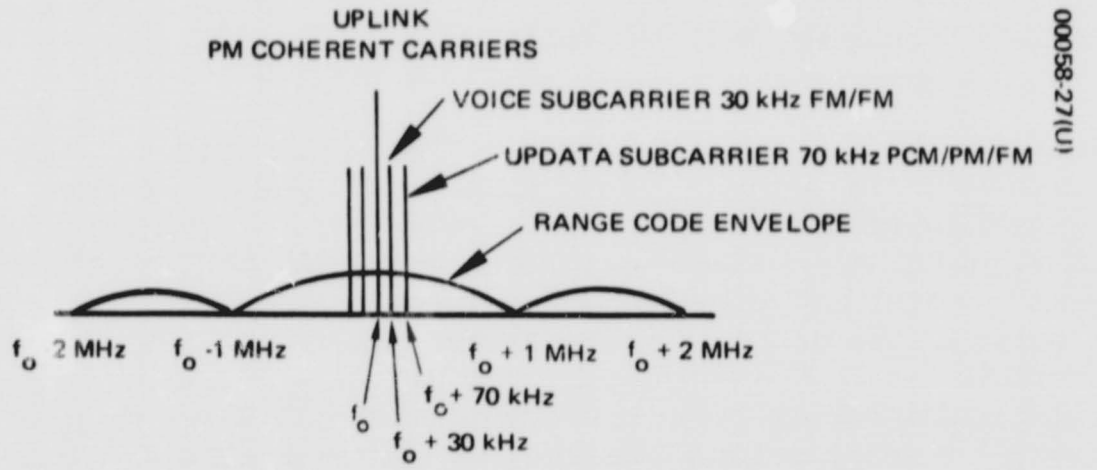

Figure 5.1-2. Unified S Band Uplink

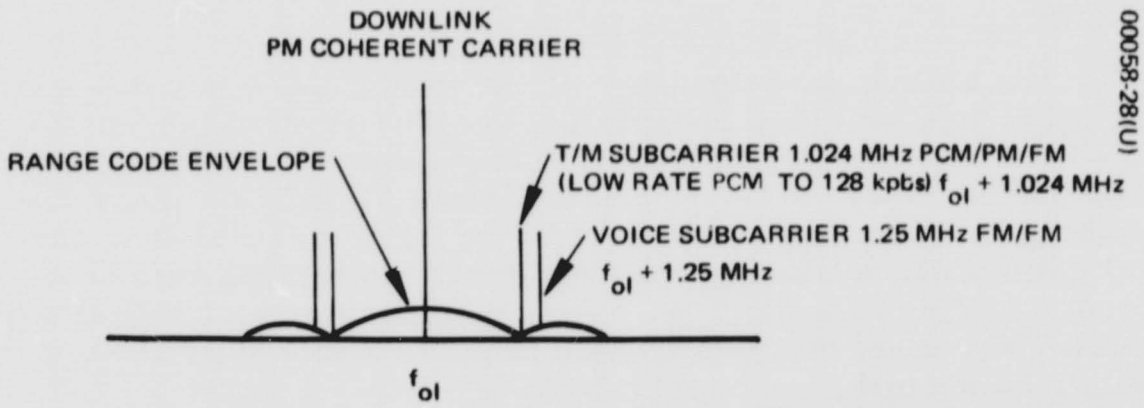

Figure 5.1-3. Unified S Band Downlink

data waveform (Gemini command format) is coherently translated as the lower sideband with a suppressed carrier at 12 kHz. The 1 and 2 kHz components of the Gemini command format are coherently related to each other and to the 12 kHz suppressed carrier, the latter being derived from the twelfth harmonic of the incoming 1 kHz reference tone. Channel filtering permits the retention of the second harmonic (4 kHz) of the biphase-modulated 2 kHz signal. At the DRT, the 11 kHz baseband signal will be filter iso-lated and coherently offset (12/11) to synchronize the locally regenerated subcarrier for demultiplexing the data.

An alternate single-carrier approach uses a multiplexing format developed for the unified S band (USB) system. The signal format used in the USB system is shown in Figure 5.1-2; in addition to carrying voice and command, a ranging signal is included. Since ranging is not a requirement for this application, and it is estimated that the bandwidth required is sub-stantially greater than that required for the scheme described above, this was not a preferred choice.

Although the single carrier requires slightly greater power than does a two-carrier approach, it was selected to simplify acquisition and because uplink power is not a critical parameter at either the ground terminal or the Intelsat IV transponder. As discussed in Section 5.2, a critical parameter in the uplink path is the operating point of the Intelsat IV transponder. Since the uplink requires much greater power from the satellite transponder than does the downlink, precautions must be taken to ensure that the uplink signal does not overdrive the repeater and in so doing impair the operation of the downlink. As shown in the link analyses of Section 5.2, the backoff level of the repeater is sufficient to provide virtually full gain to the downlink path.

5.1.3 Downlink

Single-carrier multiplexing is possible for the downlink; however, the disparity in bandwidth needed by the voice and data channels requires that either the data be placed at the bottom of the baseband (with voice on a sub-carrier) or that both data and voice be on subcarriers (as shown for the USB downlink scheme in Figure 5.1-3). In both cases, the multiplexing penalty in occupied bandwidth and carrier power is appreciable, and the voice func-tion, with its voice-over-data priority status, is not especially well sheltered against possible baseband equipment malfunctions.

The selected downlink arrangement calls for separate RF carriers for voice and data. Both carriers have separate exciter-modulators but share the output-TWT stage of the DRT transmitter. In normal operation, the data carrier is the larger carrier, with the voice drive adjusted to com-pensate for the small-signal suppression incurred by the voice carrier in the TWT. If the data carrier is commanded off, the now unsuppressed voice carrier will automatically rise 5 to 6 dB. More voice boost is possible by separate command.

TABLE 5.2-1. LINK PARAMETERS - LINKS TO INTELSAT IV (6 GHz)

Parameter	Voice - SWS to Earth *	72 kilobits/sec - SWS to Earth *	Voice + 1 kilobit/sec - Earth to SWS
Transmitter output, dB	5.5	12.2	19.3
Line/diplex loss, dB	-0.7	-0.7	
Transmit antenna gain, on axis, including pointing loss, dB	+45.8	+45.8	+61.5
ERP	+50.6	+57.3	+80.8**
(Weather attenuation) dB	-	-	-
Reference range loss (to subsatellite point), dB	-199.5	-199.5	-199.5
Delta-range loss, dB	-1.40	-1.40	-1.25
Polarization loss, dB	-0.2	-0.2	-0.2
Intelsat IV antenna gain, on-axis,	+20.7	+20.7	+20.7
off-axis loss	-4.85	-4.85	-4.10
Intelsat IV pointing loss (0.3 degree)	-0.35	-0.35	-0.35
Intelsat IV received carrier, dB	-135.0	-128.3	-103.9
(Intelsat IV maximum temperature = 2690°K) Intelsat IV maximum noise power density, dBW/Hz	-194.3	-194.3	-194.3
Intelsat IV effective (min.) amplification, dB	+105.0	+105.0	+105.0
Intelsat IV antenna gain, on-axis, dB	+20.7	+20.7	+20.7
Intelsat IV off-axis loss, dB	-4.10	-4.10	-4.85
Intelsat IV pointing loss (0.3 deg), dB	-0.35	-0.35	-0.35
Intelsat IV carrier ERP, dBW	-13.75	-7.05	+16.6
Intelsat IV noise density ENPD, dBW/Hz	-73.05	-73.05	-73.8

* Downlinks from SWS to Intelsat IV not affected by weather.

** Uplink power control required to compensate for weather.

5.2 LINK PERFORMANCE ANALYSIS

The performance of the DRT working through an Intelsat IV communication satellite repeater and a Comsat ground station is considered in this section. The relationships of the various parameters involved are expressed in equation form, and the detailed calculation results are presented in Tables 5.2-1 and 5.2-2. It is seen that the three communication channels considered, namely, voice and telemetry from the OA, and voice plus command from earth, have ample margins operating under clear weather conditions. Under adverse weather conditions, there is a slight deficiency in the downlink channels, with the most severe being that in the telemetry channel (-0.8 dB).

The uplink power from the earth station must not be allowed to exceed specifications. This signal, being dominant in the repeater, establishes the effective gain of the repeater. Should the signal become too strong, the effective gain of the repeater could easily drop to a level that would degrade the downlink signals from the SWS. To avoid this, uplink power control must be effected.

The tightest situation presented in the power budgets assumes the simultaneous occurrence of the following limit conditions:

1) Weather corresponds to earth station G/T loss of 6 dB

2) Maximum Intelsat IV pointing error of 0.3 degree

3) OA in worst orbit location, i.e., ready for handover to other Intelsat

4) Comsat earth station in most disadvantageous location (highly probable)

Hardware parameters for the Comsat terminal and the DRT are assumed to be specification minima, so there are no negative equipment tolerances to contend with. Thus, any path having better conditions than the limit shown will result in a correspondingly positive link margin.

5.2.1 FM Working Parameters

The test-tone-to-noise ratio $(TT/N)_o$ at the output of an FM discriminator is related to the carrier-to-noise ratio (C/N)i at its input by

$$(TT/N)_o = \frac{3}{2} \cdot \frac{\Delta F_p^2}{b^3} \cdot B \cdot \left(\frac{C}{N}\right)_i \cdot K, \left(\left(\frac{C}{N}\right)_i \gg 1\right) \qquad (1)$$

TABLE 5.2-2. LINK PARAMETERS - FROM INTELSAT IV (4 GHz)

Parameter	Voice - SWS to Earth		72 kilobits/sec - SWS to Earth		Voice + 1 kilobit/sec - Earth to SWS *
	Clear	Weather	Clear	Weather	
Intelsat IV carrier ERP, dBW	-13.75	-13.75	-7.05	-7.05	+16.6
Intelsat IV noise density ENPD, dBW/Hz	-73.05	-73.05	-73.05	-73.05	-73.8
Reference minimum range loss, dB	-195.7	-195.7	-195.7	-195.7	-195.7
Delta-range loss, dB	-1.25	-1.25	-1.25	-1.25	-1.40
Polarization loss, dB	-0.2	-0.2	-0.2	-0.2	-0.2
(Weather attenuation), dB	0.0	-1.6	0.0	-1.6	0.0
Receiving antenna gain, on-axis (including pointing loss), dB	+57.7	+57.7	+57.7	+57.7	+42.3
Received carrier power, dBW	-153.2	-154.8	-146.5	-148.1	-138.4
Received noise power density, dBW/Hz (SWS T = 1120°K) (Earth station T = 50°+Wthr) 0° to 90°	-212.5	-214.1	-212.5	-214.1	-228.8
Receiver noise power density, dBW/Hz	-211.6	-207.1	-211.6	-207.1	-198.1
Total effective NPD, dBW/Hz	-209.0	-206.3	-209.0	-206.3	-198.1
Signal bandwidth, dB/Hz	41.0	41.0	48.6	48.6	46.9
Excess noise degradation, dB	1.0	1.0	1.0	1.0	1.0
Total effective noise power, dBW	-167.0	-164.3	-159.4	-156.7	-150.2
C/N effective, dB	13.8	9.5	12.9	8.6	11.8
C/N required, dB	10.0	10.0	9.4	9.4	10.0
Margin, dB	+3.8	-0.5	+3.5	-0.8	+1.8

* Uplink power control required to compensate for weather.

where

B is the IF bandwidth

b is the test tone frequency (usually the highest baseband frequency to be transmitted)

ΔF_p is the peak frequency deviation

K is a compensating factor for preemphasis improvement, multichannel loading, and channel weighting

The minimum IF bandwidth (B) required, according to Carson's rule, is equal to twice the sum of the peak deviation and the test tone, i.e.,

$$B = 2(\Delta F_p + b) = 2\,b(M + 1) \tag{2}$$

where

$$M \triangleq \frac{\Delta F_p}{b}$$

Equations 1 and 2 may be combined to give

$$(TT/N)_o = 3\,K\left(\frac{C}{N}\right)_i M^2\,(M + 1) \tag{3}$$

Solving Equation 3 for the specified $(TT/N)_o$ = 20 dB and assuming a value of 2 dB for K and a simple FM discriminator requiring (C/N)i = 10 dB, then M = 1.025.

Link	b [Hz]	B [Hz]	dB Hz
Up voice and command multiplex	12.0	48.6	46.9
Down voice	3.1	12.6	41.0

Note that the noise in the IF is considered to be of flat spectrum with a density (one-sided)

$$n_o = k\,T_r\ [w\ Hz^{-1}] \tag{4}$$

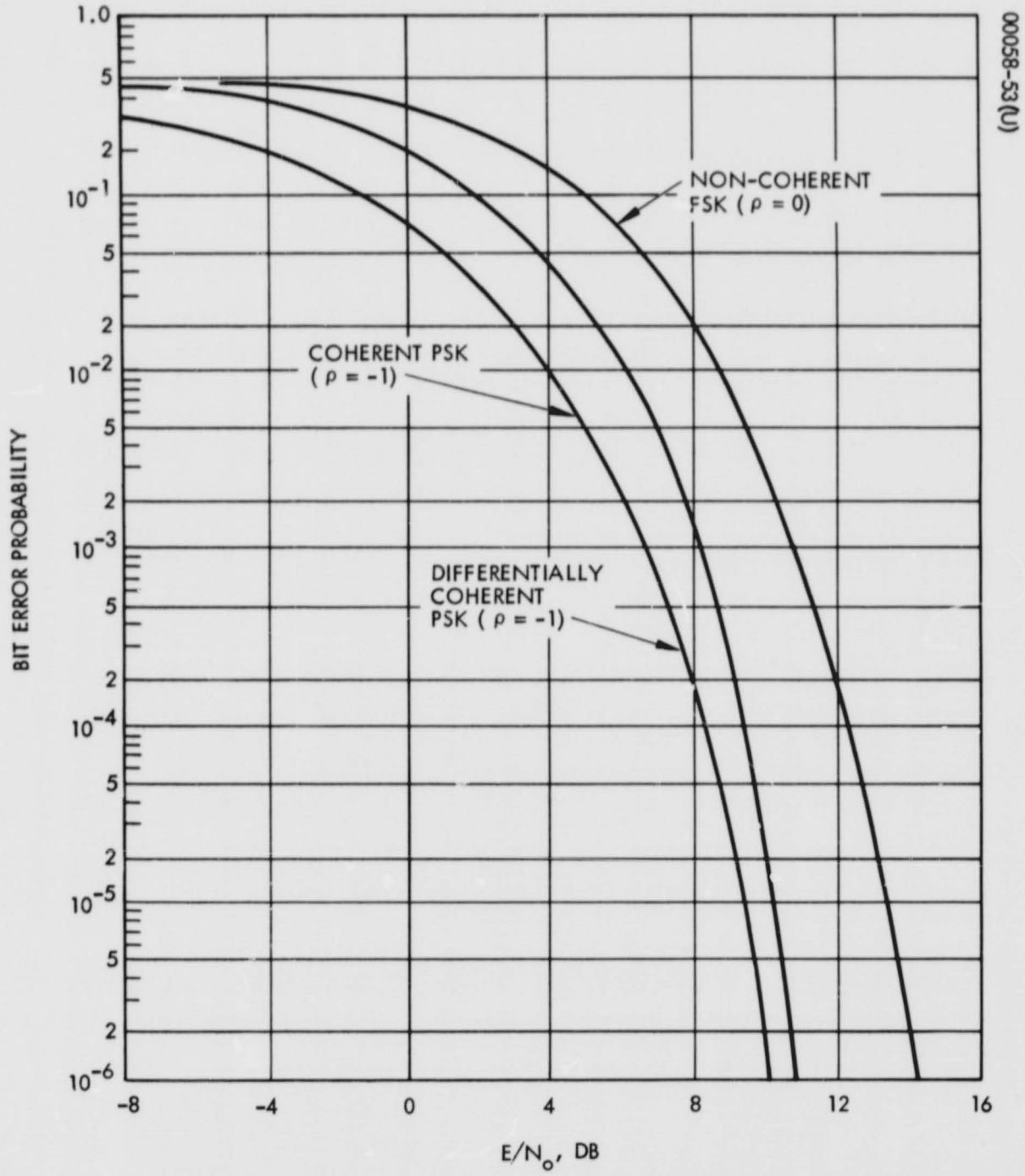

Figure 5.2-1. Probability of Bit Error Versus Normalized Signal Power to Noise Power Ratio

where

$k = -228.6$ dBw Hz^{-1} $^{\circ}K^{-1}$ (Boltzmann's constant)

and

T_r = effective noise temperature of receiver at IF*

An excess noise degradation of 1 dB is to be included to compensate for the increased bandwidth due to the rolloff characteristic of the IF amplifier.

5.2.2 Digital Link Parameters

Of the several alternative telemetry signals stipulated in Section 2.2.2.2, the 72 kilobits/sec serial data stream is the limiting case. The link calculations assume a required $E/n_o = 9.4$ dB for a worst case error rate of 10^{-4} (see Figure 5.2-1), assuming differentially encoded PSK. This is also the required C/N in the input of the decision threshold [output of the (digital) low pass filter] effective noise bandwidth. A basic bandwidth of 1 Hz per bit/sec is assumed; thus, a signal bandwidth of 72 kHz (48.6 dB Hz) is required. Practical implementation of digital demodulators cannot obtain the theoretical figure given. A 1 dB allowance is made for degradation due to excess noise.

5.2.3 Comsat Station Parameters

The Comsat minimum earth station specification of $G/T = 40.7$ dB/°K (in clear weather) is assumed, with a weather margin taken as a 6 dB degradation of the effective G/T. (Any other assumption would not allow definition of the station parameters without also defining a "standard" demodulator and repeater C/n_o.)

The noise at the input of the ground station demodulator is a combination of the noise due to the Intelsat IV receiver and the noise due to the ground receiver itself. The carrier-to-noise ratio (power) at this point may be expressed (inverted) as

$$\left(\frac{N}{C}\right)_i = \frac{(n_o A G)_{rptr} L (a G H)_{rcvr} + k H [T_{rcvr} + T_o(1 - a)]}{(C A G)_{rptr} L (a G)_{rcvr}} \qquad (5)$$

*Sometimes Equation 1 is written without the factor 2 in the denominator. This is because the spectral density in the IF is considered to be $N_o = 1/2\ k\ T_r = 1/2\ n_o$ (two-sided).

where

n_o = repeater noise power density, w Hz^{-1}

A = repeater internal gain

G = antenna gains, as indicated

H = demodulator effective noise bandwidth, Hz

T = receiver effective temperature, measured at antenna flange, ^oK

C = carrier level as received at the repeater, watts

a = weather attenuation

T_o = 290° K (ambient temperature)

L = path loss

Simplifying and rearranging slightly yields

$$\left(\frac{N}{C}\right)_i = H\left\{\left(\frac{n_o}{C}\right)_{rptr} + \frac{k}{(C\ A\ G)_{rptr}}\frac{}{L}\left(\frac{T}{G}\right)\left[\frac{1}{a} + \frac{T_o}{T_{rcvr}}\left(\frac{1}{a} - 1\right)\right]\right\} \qquad (6)$$

where the bracketed weather quantity [ ] = -6 dB. Cool receivers allow use of smaller antennas in obtaining the specified G/T, but then the antenna-receiver combination will be more sensitive to the impact of weather (a).

A maser receiver of 50° K is assumed. Thus,

G_{rcvr} = 57.7 dB gain

T_{rcvr} = 50° K = 17 dB° K

a = 1.6 dB

Scaling the receiver antenna gain by the square-of-the-frequency ratio, assuming constant efficiency (approximately 43 percent for an 85 foot antenna),

G_{xmt} = 61.5 dB gain

5.2.4 Saturn Workshop Parameters

Characteristics of the workshop antenna are given in Section 4.3. The effective gains are given below.

Antenna Gain:

45.8 dB at 6350 MHz (transmit)

42.3 dB at 4120 MHz (receive)

The workshop receiver is assumed to be of the form shown in Figure 5.2-2, yielding a net effective receiver temperature at the antenna flange of approximately 1120°K = 30.5 dB°K.

The DRT transmitter is assumed to be a 20 watt TWTA (see Section 5.9 for selection criteria).

5.2.5 Intelsat IV Characteristics

Figures 5.2-3 and 5.2-4 present current Intelsat IV characteristics, where specifications require optimization for coverage at 8.5 degrees off-axis. At this point, the antenna gain is 4 dB below its dB on-axis value. The ERP is specified at not less than 22 dBW at ±8.5 degrees off-axis. Since the area of prime interest for the workshop project ranges to ±9.5 degrees, the added off-axis losses are taken into account.

Since the locations of both earth and SWS stations strongly affect system loss calculations, the effective gain of the Intelsat antenna is treated separately from the gain of the Intelsat repeater. Figure 5.2-4 is therefore plotted against coordinates of input to repeater (dBW) versus repeater output (dBW). Actual performance in orbit is likely exceed the values shown; the transfer characteristics given represent the specification minima.

The maximum allowable repeater effective temperature of 2690°K = 34.3 dB°K was derived from Intelsat IV specifications.

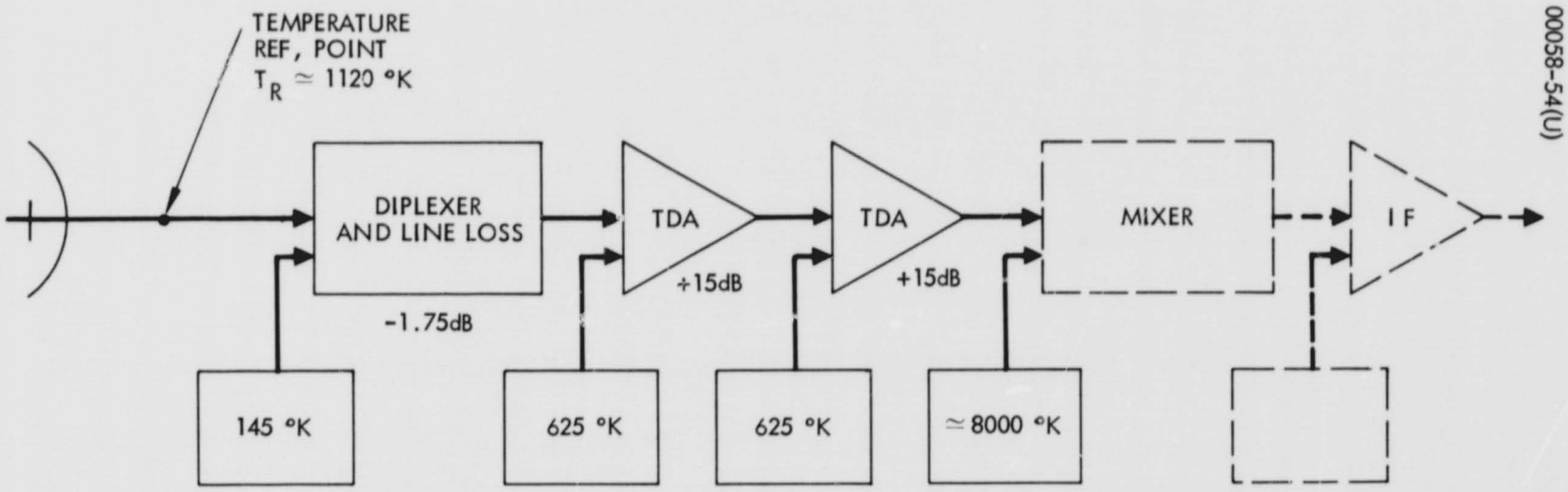

Figure 5.2-2. Receiver Noise Temperature Model

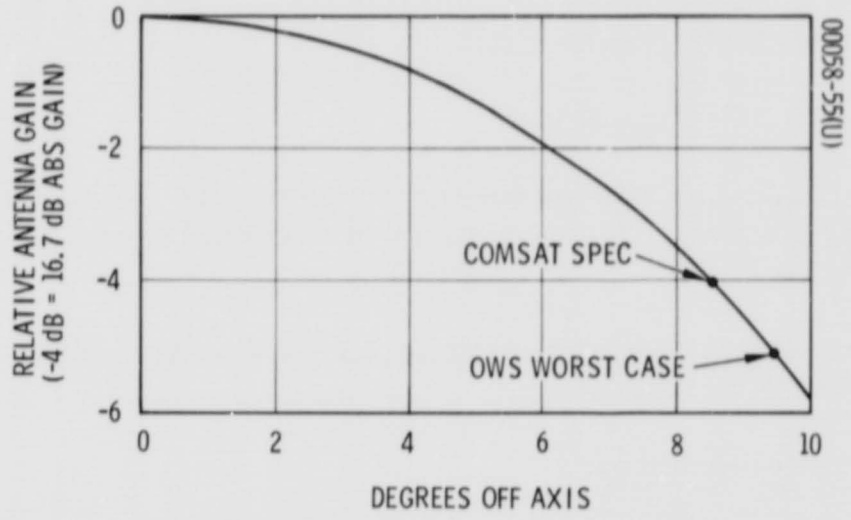

Figure 5.2-3. Intelsat IV Earth Coverage Antenna Pattern

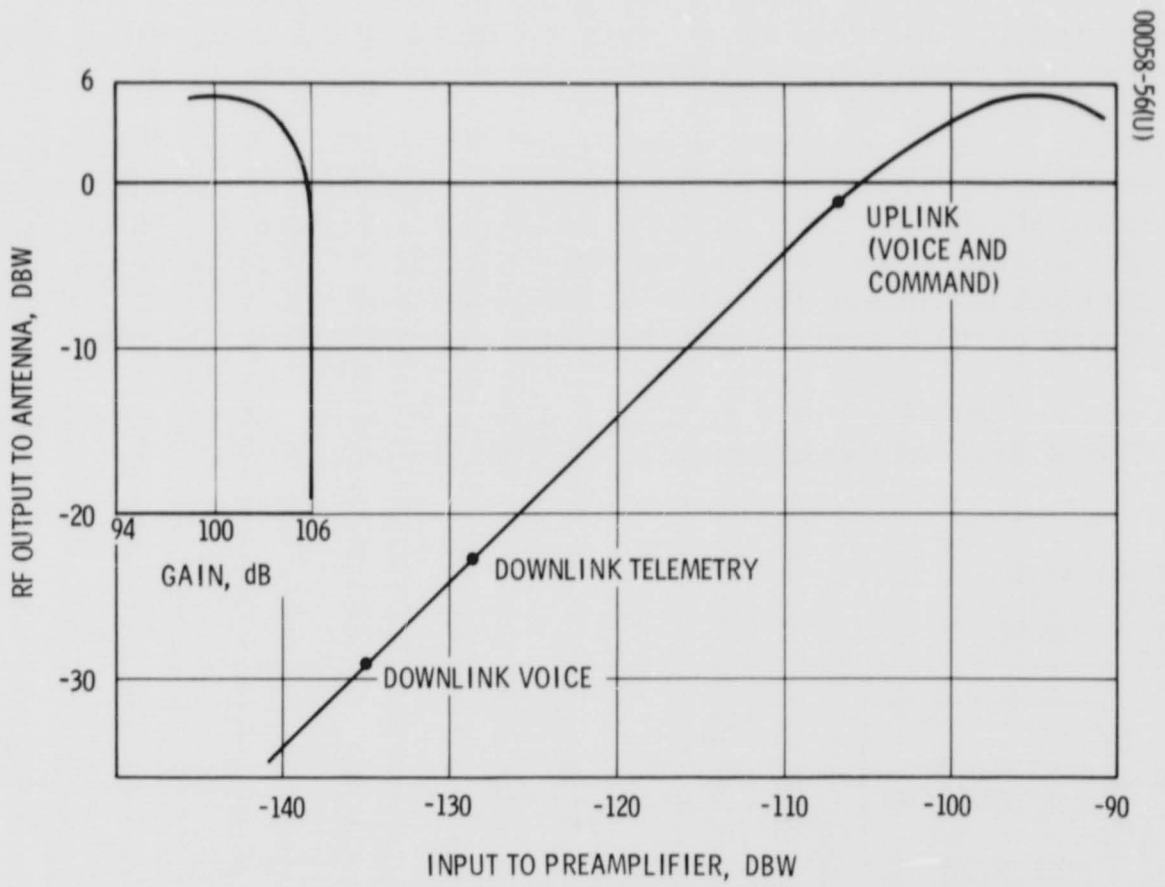

Figure 5.2-4. Intelsat IV Transfer Characteristic

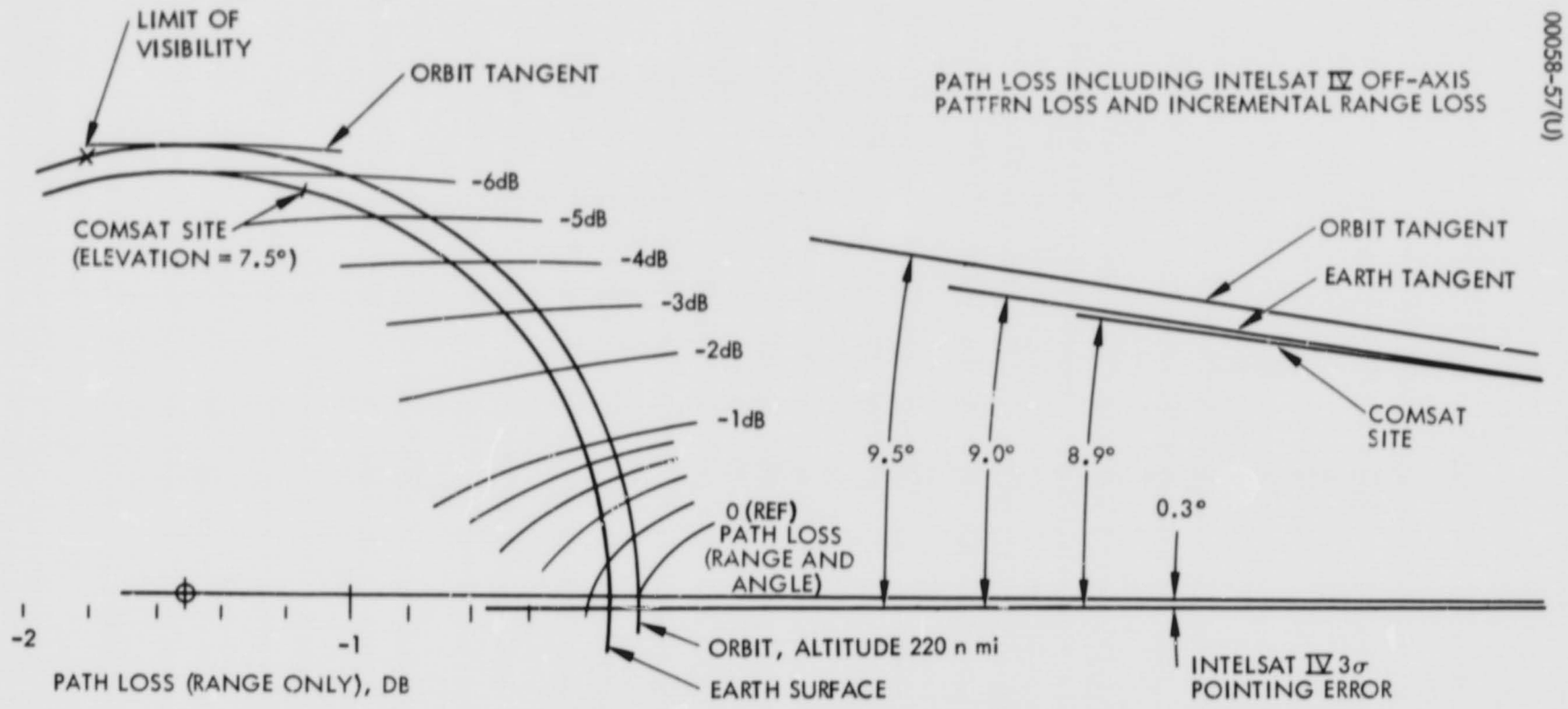

Figure 5.2-5. Path Geometry

5.2.6 Link Geometry

Path losses for the system analysis must include the effects of frequency, range, and Intelsat IV pointing accuracy. The result, illustrated in Figure 5.2-5, is frequency-independent since the Intelsat IV transmit and receive antennas are designed to provide congruent coverage, and range is defined relative to the OA orbit at the Intelsat subsatellite point. The assumed worst case location for the Comsat earth station includes a 7.5 degree line of sight elevation. Calculated values for the specific paths of interest are summarized in Table 5.2-3.

5.2.7 Definition of Link Power Balances

Satisfaction of the link requirements within reasonable power limits and available TWT amplifiers for the DRT, plus the constraints inherent with Intelsat IV, when working into a 15 foot antenna, hinges strongly upon the fact that both the DRT and Intelsat TWTs will be operating in an essentially single-signal mode, with the Intelsat channel TWT operating backed off about 6 dB from single-signal maximum power rating.

TABLE 5.2-3. LOSS VALUES RELATIVE TO SUBSATELLITE POINT (AND REFERENCE CONTOUR)

Loss		Comsat Station	SWS
Off-axis loss	Intelsat IV pointing error = 0 degree	-4.10 dB	-4.85 dB
	Intelsat IV pointing error = 0.3 degree	-4.45 dB	-5.20 dB
Incremental range loss (over that to subsatellite point)		-1.25 dB	-1.40 dB

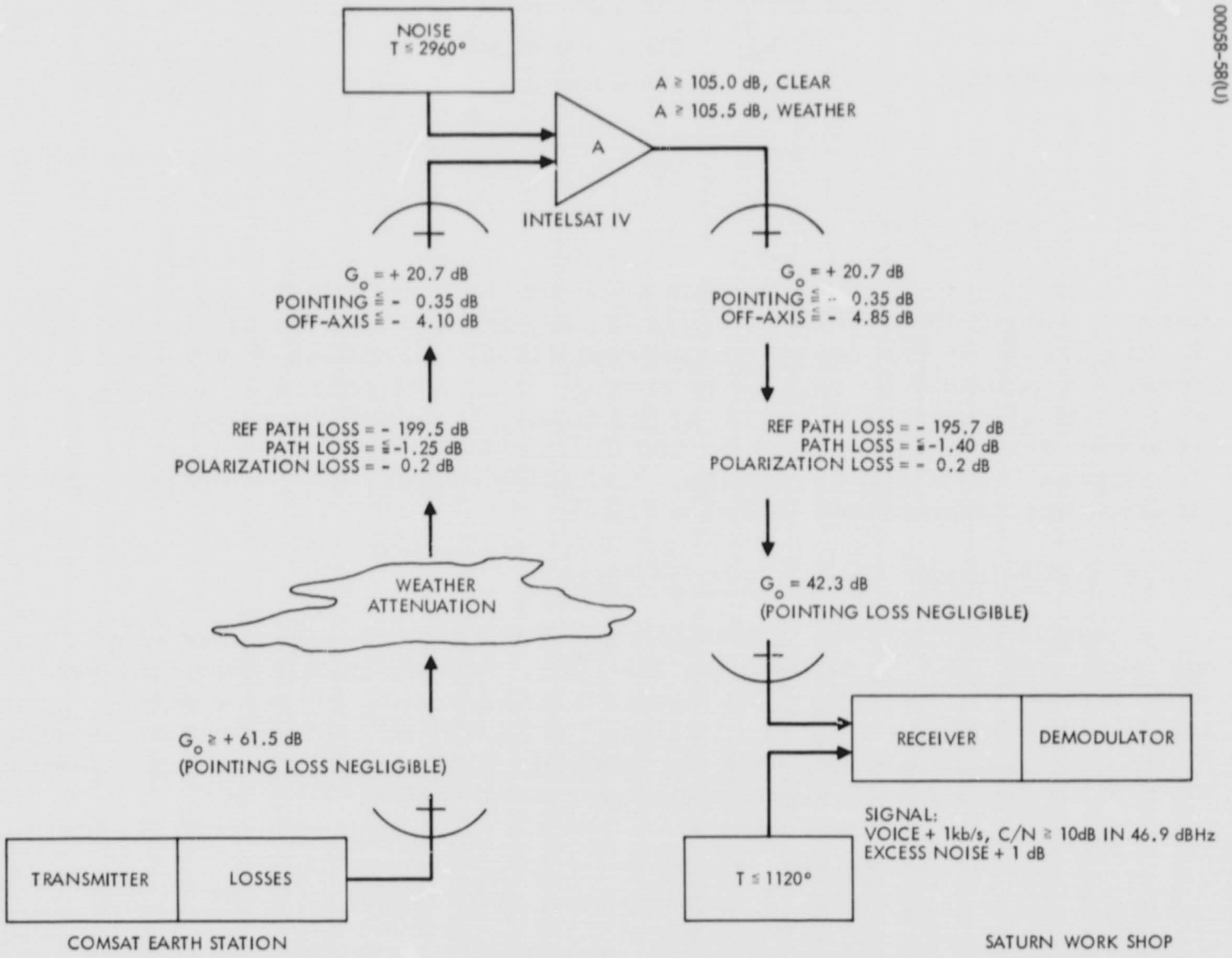

00058-58(U)

a) Uplink

The operating points for the three carriers are illustrated in the transfer curve in Figure 5.2-4. The 24+ dB difference between the uplink carrier and the (72 kilobits/sec) downlink carrier leaves the Intelsat TWT in an essentially single-signal mode of operation. Suppression of the smaller signals should not be noticeable with the tube operating so much below saturation. Similarly, there will be no discernable loss due to intermodulation products.

The TWT in the DRT is presumed to be operating fully saturated. Again, however, the near 7 dB difference in the level of the two downlink carriers leaves this tube also in an essentially single-signal mode. Small-signal suppression will be evident but can easily be compensated through increasing voice-carrier drive to the point that it takes the desired share of signal power at the TWT output.

Figures 5.2-6a and 5.2-6b present a pictorial compilation of the parameters previously derived as they relate to the up and downlinks.

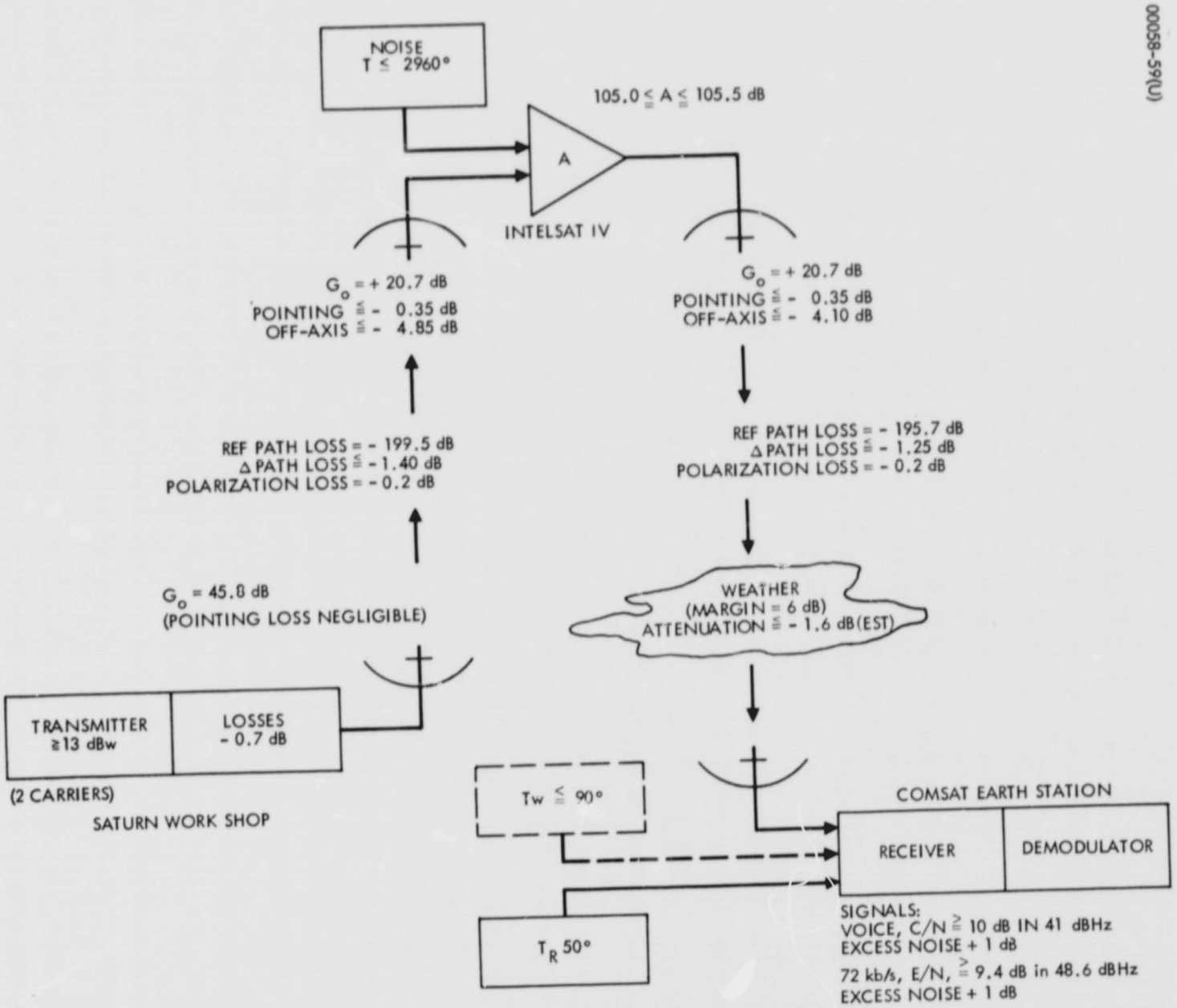

b) Downlink

Figure 5.2-6. Link Power Parameters

respectively. Progressing through the uplink (Figure 5.2-6a) the radiated power may or may not be subject to weather attenuation. Gains and losses evident in the paths to and from Intelsat IV are lumped, as indicated, to simplify the summary presentations of power relations presented in Tables 5.2-1 and 5.2-2. Path losses for the up and down frequencies are first given relative to the subsatellite point (with on-axis gain of the Inteslat IV antenna). Off-axis l sses and range decrements are then separately identified and subtracted (Figure 5.2-5).

The noise power density characteristic of the Intelsat receiver enters the system at the repeater input is amplified with the signal and radiated to the receiving station. Further noise appears at the DRT receiver input, summing with the repeater noise, as shown in Equation 5, before arriving at the demodulator.

The Comsat earth station does not present quite the same situation as the DRT (Figure 5.2-6b). Here, weather attenuating both the desired carrier and repeater noise adds some 90° K to the effective temperature of the earth station receiver.

Throughout this report, "uplink" and "downlink" are understood to be relative to the OA. However, the link power budgets of Tables 5.2-1 and 5.2-2 show signals to and from Intelsat IV, respectively, since it is here that the proper up/downlink power balance is established.

Up and downlink power budgets of Table 5.2-1 follow the formulation of Equation 5 precisely. Two cases are presented for each carrier: the situations that would prevail with the earth station 1) in clear weather and 2) in foul weather resulting in 1.6 dB attenuation of received signals. Uplink power compensation for local weather would be desirable.

To best illustrate the impact of weather, as well as the degree of tolerance of the total system, it has been assumed that both the earth and SWS stations would radiate fixed power, regardless of weather. Transmitter power levels were selected to satisfy the communication requirements within the limits of the stated weather.

5.3 CARRIER SPREADING

The close proximity of the OA to the earth will result in a high probability of occasional interference with terrestrial communication systems operating in the same frequency range as the DRT transmitter. The interference can be limited to DRT sidelobe radiation with little or no degradation of DRT link operation since the DRT will be inhibited from transmitting whenever its mainbeam is incident on the earth' s surface, or, more realistically, whenever the mainbeam is incident upon an imaginary spherical surface at a predetermined altitude.

To assure noninterference with terrestrial systems, maximum levels of radiant energy emanating from a space vehicle and incident upon the earth' s surface have been defined in CCIR Recommendation 358-1; these levels are given as curve b in Figure 5.3-1. The corresponding levels of DRT incident power flux density are shown as curve a. The residual protection required to meet the CCIR recommendations, i.e., the difference between the above two curves, is shown as curve c.

As indicated by curve c of Figure 5.3-1, the maximum residual protection required is 24 dB/4 kHz per dBw of EIRP radiated by the DRT mainbeam. or 24 plus 58 for a total of 82 dB/4 kHz. Sidelobe attenuation (when more than 10 degrees off-axis) provides 35 dB of such protection, leaving the need for an additional reduction of 47 dB. The remaining means for decreasing the incident flux density per unit bandwidth is to spread the radiation over the available bandwidth. The total bandwidth of an Intelsat IV transponder of 36 MHz; 4 MHz has been reserved for the uplink and for a guardband between the up and down links, leaving a total bandwidth of 32 MHz available for spreading the downlink carrier. Relative to 4 kHz, this would provide an improvement of 39 dB, with a net deficit in the protection required to meet CCIR recommendations of 8 dB, as summarized in Table 5.3-1.

TABLE 5.3-1. DOWNLINK POWER FLUX DENSITY SUMMARY

Protection required for worst case path geometry	24 dB/dBw
DRT on-axis EIRP	58 dBw
Pattern discrimination by DRT antenna (> 10 degrees off-axis)	-35 dB
Additional protection required	47 dB
Maximum reduction in power flux density attainable by carrier spreading over available channel bandwidth (32 MHz)	-39 dB
Deficit	8 dB

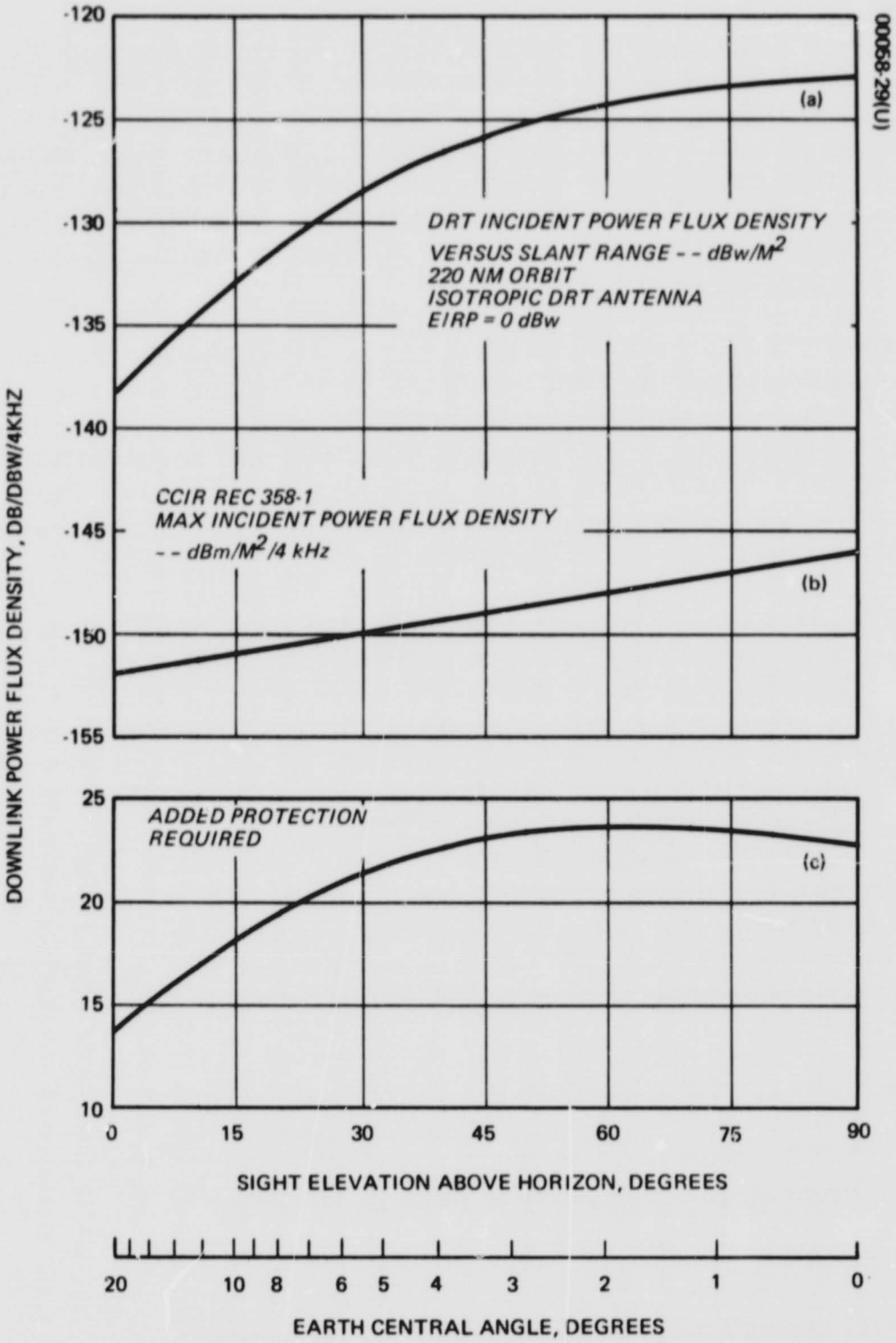

Figure 5.3-1. Downlink Power Flux Density at Surface of Earth

In spite of this deficit, operation of the downlink may be satisfactory. The levels defined in the cited CCIR recommendation are considered by many authorities to be too severe, and at least one proposal for relaxing the levels specified in the CCIR recommendation is under consideration. Further, even if it is assumed that resultant incident flux density is sufficient to interfere with the operation of terrestrial systems, the actual interference with any particular system will occur only for short, infrequently spaced intervals (up to about 5 minutes at a time, and up to twice per day).

A potential interference problem on the uplink (radiation from Intelsat IV to terrestrial system) exists during pauses in voice transmission when no commands are being sent. This can be avoided, however, by transmitting dummy commands to fill the gaps between real commands.

5.4 ANTENNA ACQUISITION AND TRACKING

In its typical operation, the DRT antenna will be required to alternately track each of two Intelsat IV satellites. This will require that the antenna track the appropriate Intelsat IV satellite until line-of-site communication is no longer available. At this time, the antenna on the SWS will be required to slew to the alternate satellite in order to resume tracking. Figure 5.4-1 illustrates the angular variation on the gimbal angles for the DRT antenna for a typical tracking situation.* The figure shows that tracking (Atlantic satellite) occurs for approximately 40 minutes. At this time, it is required to slew the antenna to a new position and again track (Pacific satellite) for approximately 40 minutes. The alternate track/slew procedure continues as indicated in Figure 5.4-1. Relatively small angular variations are required during the tracking phase, and relatively large variations are required during the slew phase. Therefore, some type of general positioning is required by the DRT antenna to position the antenna initially to approximately the right angular coordinates. Once these coordinates have been achieved, the DRT antenna will accomplish a fine acquisition procedure and transfer to the tracking mode.

The material in this section is divided into two parts; the first deals with the tracking of the DRT antenna and the second with the procedures for acquiring the Intelsat IV satellite. Tracking is treated first because the tracking performance establishes the angular pull-in range and thus affects the acquisition mode performance.

5.4.1 Tracking

It is conceptually possible to accomplish both acquisition and tracking either by open-loop computer-controlled orientation of the antenna or by completely automatic means. Open-loop tracking was discarded for this approach because the OA onboard computer is not available for full-time usage by the

*The data plotted in Figure 5.4-1 were obtained with the aid of a computer program, described in Appendix C.

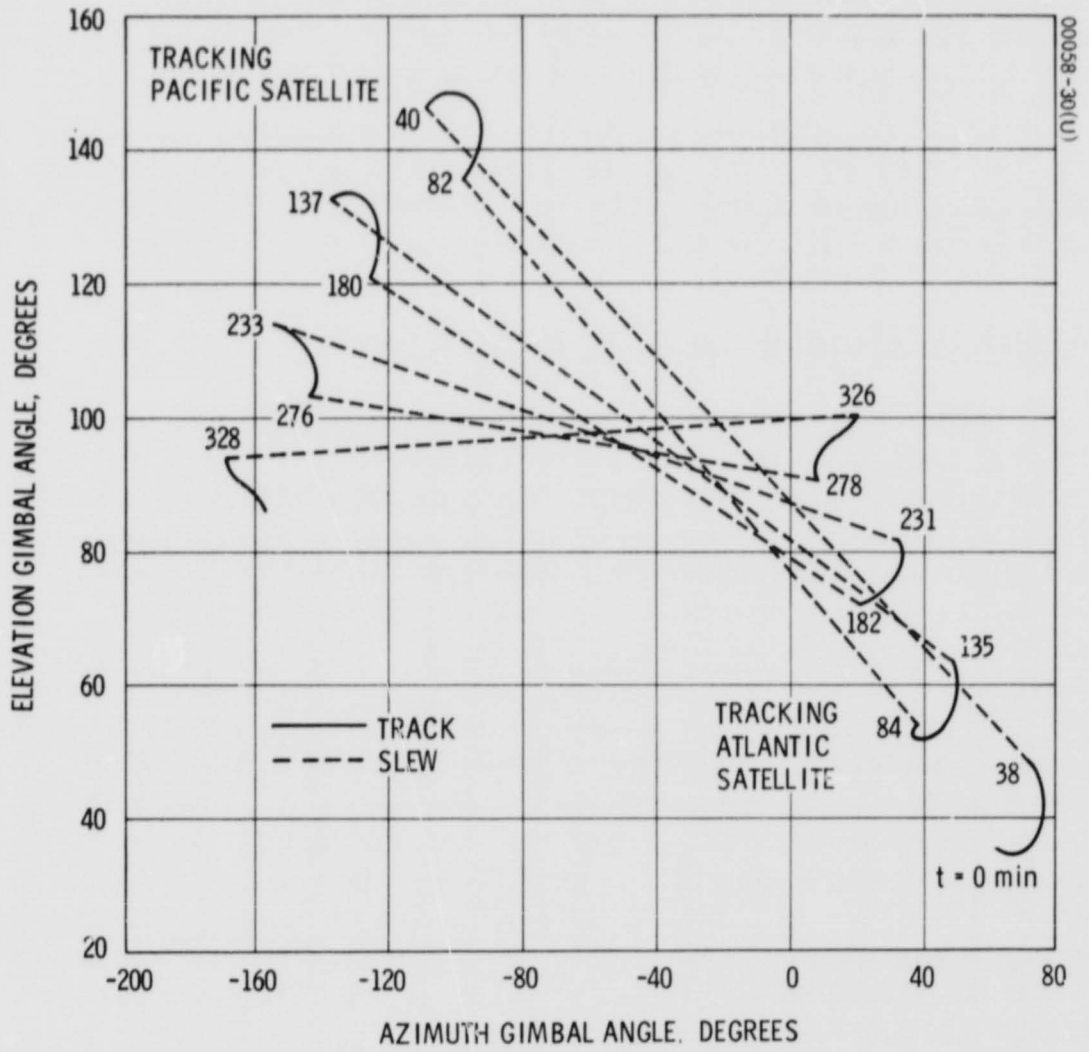

Figure 5.4-1. Typical Tracking Paths for Oriented Spacecraft

DRT, and it is unlikely that pointing commands could be generated with the accuracy required for pointing the narrowbeam antenna. (Acquisition is accomplished by open-loop computer scanning, as described later.) Automatic tracking options include lobing and monopulse systems, both described below.

5.4.1.1 Lobing

Mechanical lobing was used on early tracking systems but has been discarded as a result of mechanical wear and the large lobing loss (1 to 3 dB) resulting from operation with an offset beam. Electronic beam lobing includes the single electronic channel variants described under monopulse systems; the selected time-shared monopulse system is one of these.

5.4.1.2 Monopulse Systems

Three types of monopulse systems were considered. The first is a true monopulse implementation, the second uses frequency multiplexing, and the third uses time multiplexing.

True Monopulse. A true monopulse implementation block diagram is indicated in Figure 5.4-2. Here, a sum and two difference signals from the monopulse feed are each amplified, mixed to an IF frequency, amplified again, and phase detected against the sum channel. The output signals of the phase detectors provide the elevation and azimuth steering signals. As indicated by the dashed lines, a diplexer is required for the transmitter, and low noise preamplifiers may be required. A disadvantage of the true monopulse system is the requirement for IF amplifiers and mixers for three separate channels. Further, the phase and gain characteristics of the three channels must be carefully matched to provide optimum operation of the monopulse implementation. The advantage of the true monopulse system is that it provides maximum gain through the sum channel, which is the channel carrying the communications data.

Quadrature Monopulse. Figure 5.4-3 shows a quadrature monopulse implementation. In this implementation, the two difference channels are frequency multiplexed with the sum channel. Both the azimuth and elevation difference signals are balance modulated against a frequency scanning oscillator. This oscillator has a frequency of a few hundred cycles. The output of the balanced modulator consists of two frequencies separated from the original RF frequency by twice the scanning oscillator frequency. The scanning oscillator drive to the two balanced modulators (elevation and azimuth) is phase shifted by 90 degrees to permit these two signals to be distinguished once they have been added. The outputs of the two balanced modulators are added together, providing the indicated vector sum signals, and then added to the original sum channel. The resultant signal out of the coupler is a carrier signal with two sidebands and is similar to that obtained in a conical scan system.

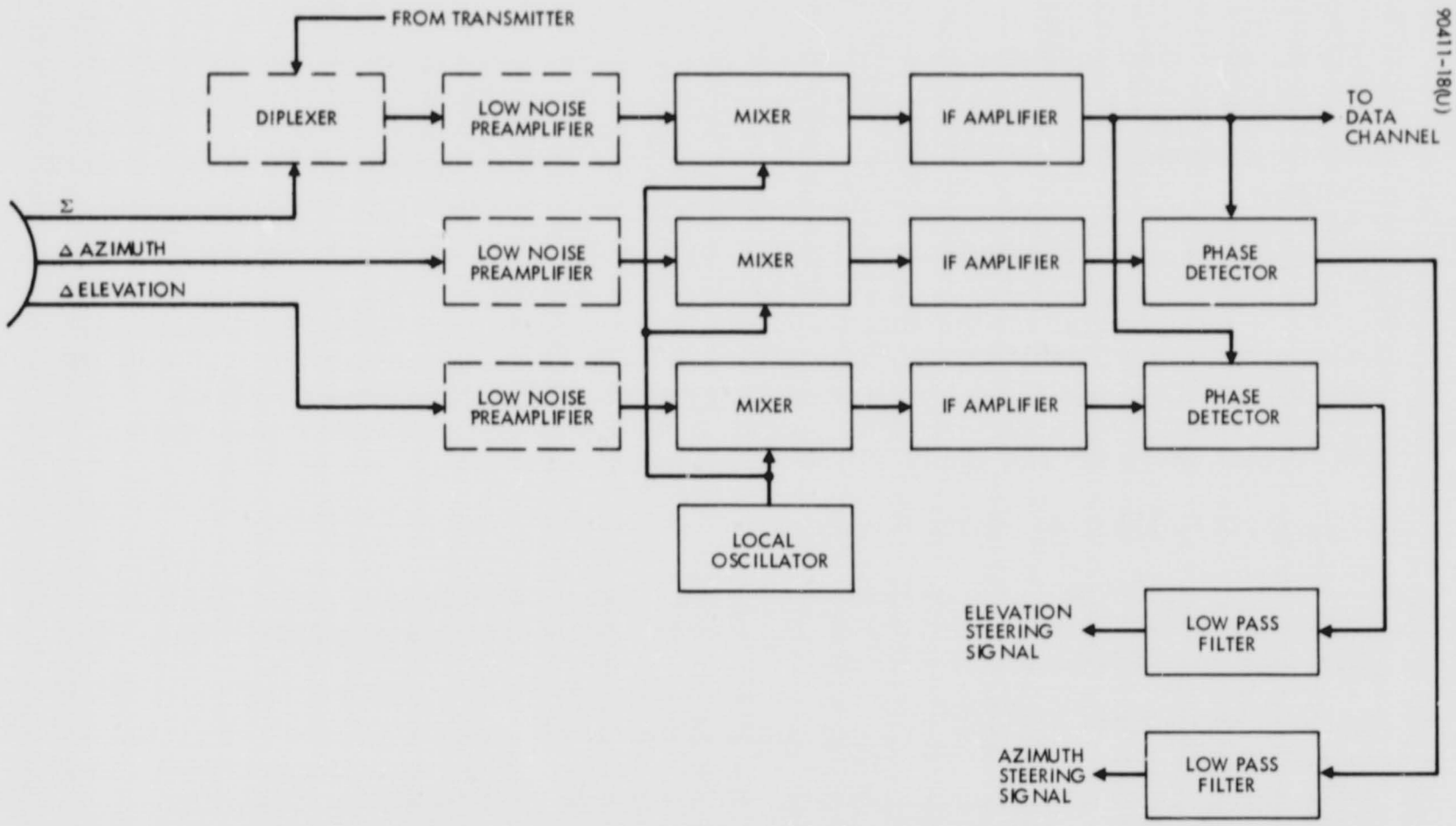

Figure 5.4-2. True Monopulse Implementation

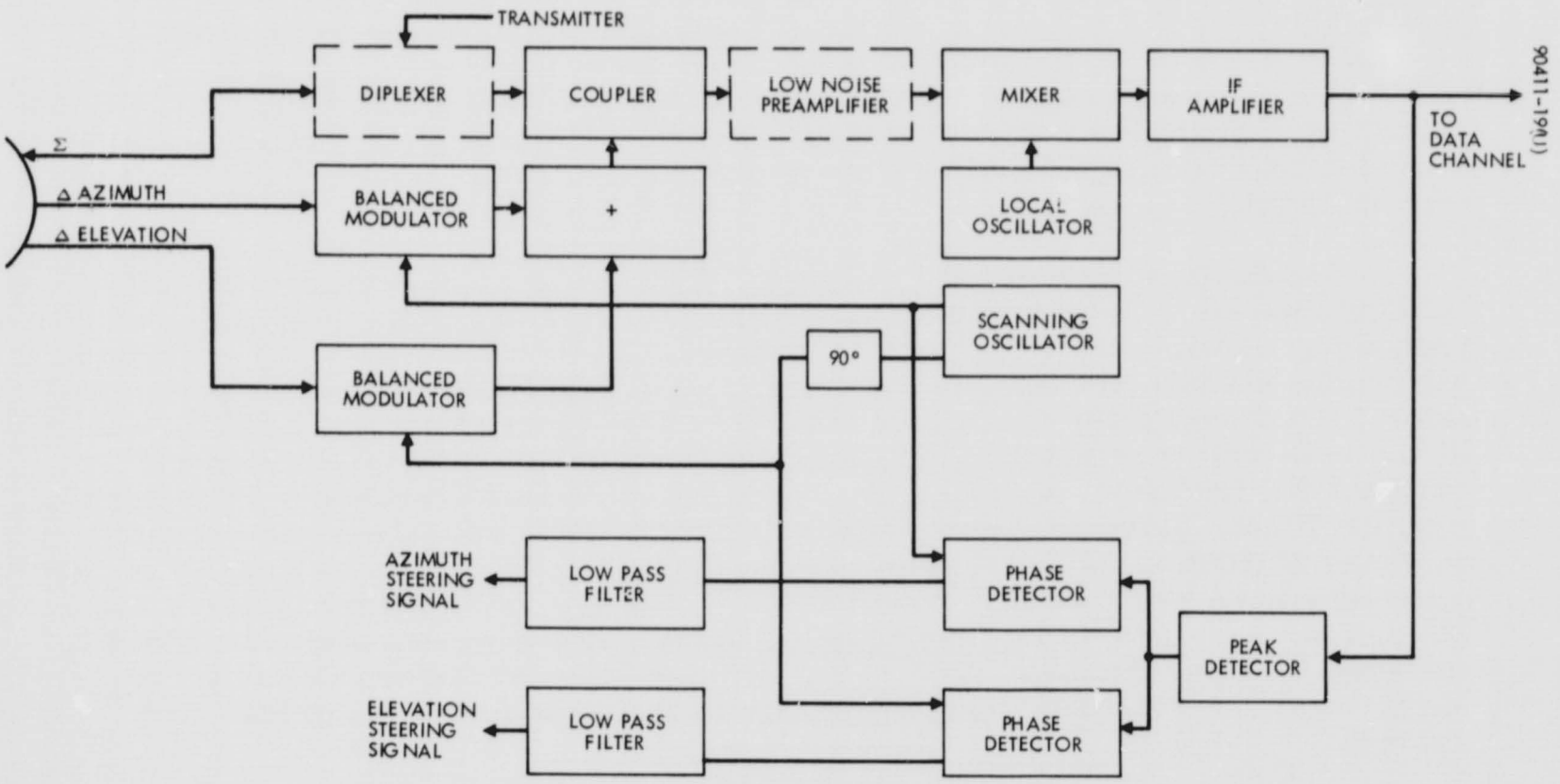

Figure 5.4-3. Quadrature Monopulse Implementation

Once the two difference channels have been added to the sum channel, a common low noise amplifier, mixer, and IF amplifier chain may be used to operate on the composite signal. At the output of the IF amplifier, a peak detector recovers the amplitude modulation which corresponds to the two error signals. The amplitude variation is phase detected against the original scanning oscillator to detect both the azimuth and elevation error signals.

Figure 5.4-4 illustrates the phase frequency relationships among the sum and the two difference signals in such a quadrature monopulse system. As evident, the input signal to all three channels is at the same frequency but of different amplitudes, reflecting the error difference signals in azimuth and elevation and the fact that there is an error signal in both channels. Once the azimuth and elevation signals have passed through the balanced modulator, the output signal (which has its carrier suppressed) consists of two sideband signals above and below the original carrier frequency. (The slant angle of the signals is intended to indicate the phase shift relative to the original phase of the incoming signal.) The outputs of the balanced modulators are added to provide a composite vector sum at the original RF frequency plus and minus the scan frequency. This composite signal is coupled to the sum signal to provide the overall composite signal. The coupler value favors the sum channel at the expense of the difference channel, so there is a strong attenuation of the difference channel sidebands, as indicated. The amplitude of the two sideband channels reflects the input error magnitude, and the phase shift of the two sideband channels indicates the angular position of the error.

Time-Shared Monopulse. A third type of monopulse system is the time-shared monopulse presented in Figure 5.4-5. Here, the two difference channels are sequentially sampled using switch A. While switch A is sampling the azimuth signal, switches B and C switch twice so that a 180 degree phase shift is added into the azimuth signal. Once this has been completed, switch A returns to the elevation signal and again switches B and C cycle twice. Thus, the time switching consists of alternately sampling the azimuth and elevation signals and, while they are being sampled, reversing the signal phase. The time-shared signal is then coupled to the sum channel to provide a multiplex signal that is amplified through a common amplifier chain. At the output of the IF amplifier, an envelope detector detects the amplitude variation on the composite signal and separates this into two channels which are demodulated against the original switching oscillator to detect the azimuth and elevation steering signals.

Figure 5.4-6 illustrates, in vector fashion, the signals found in the block diagram of Figure 5.4-5. Parts a, b, and c correspond to the original input signals from the antenna. Part d shows the azimuth channel after switch A, indicating the azimuth channel is switched on and off by switch A. Part e indicates the alternate switching of the elevation channel after switch A. Parts f and g indicate the phase reversal in both the azimuth and elevation channel switching, and part h indicates the composite signal where parts f and g are added. It is seen that this is an amplitude-varying signal whose amplitude contains a measure of the azimuth and elevation error signals.

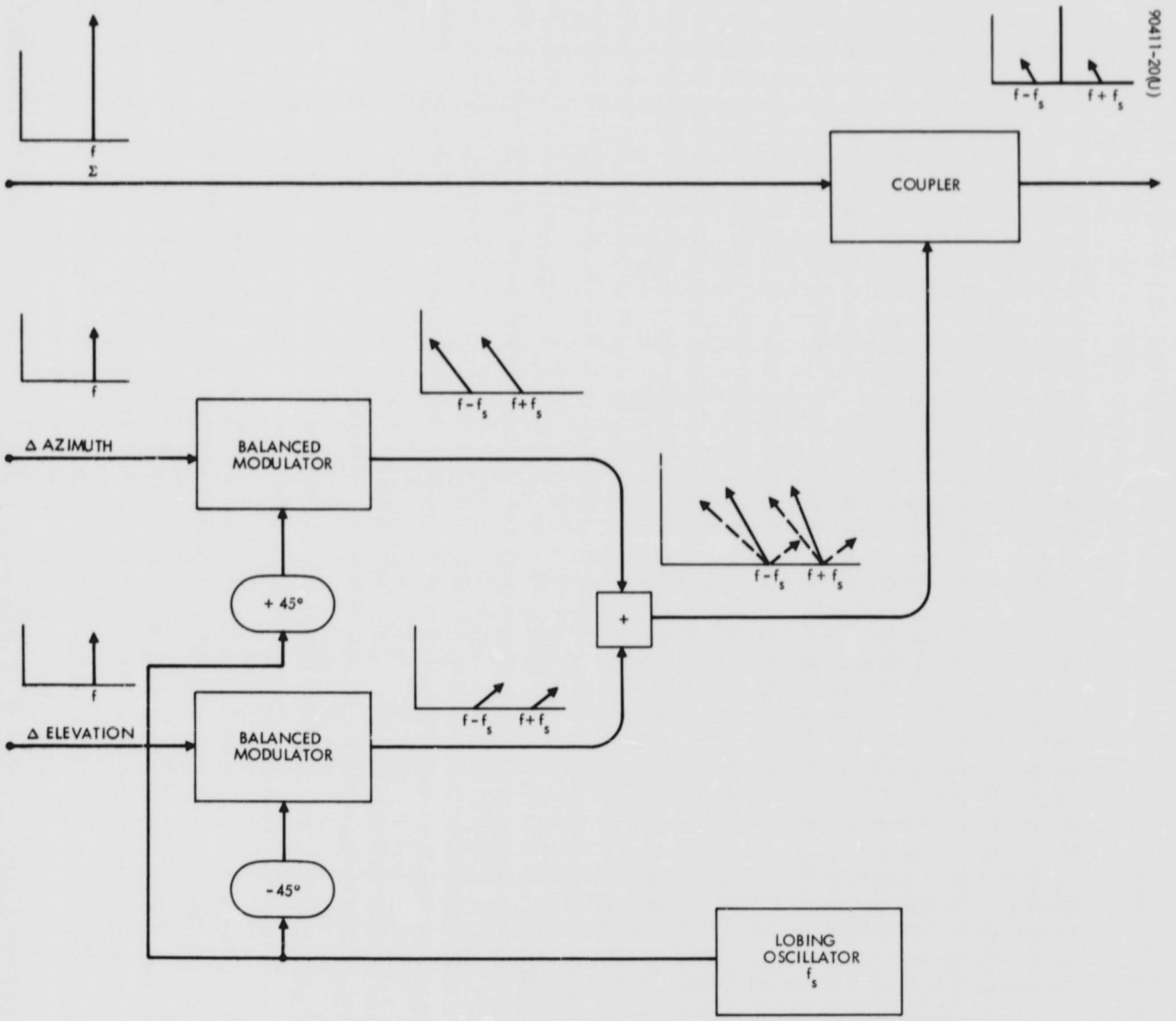

Figure 5.4-4. Quadrature Monopulse Spectra

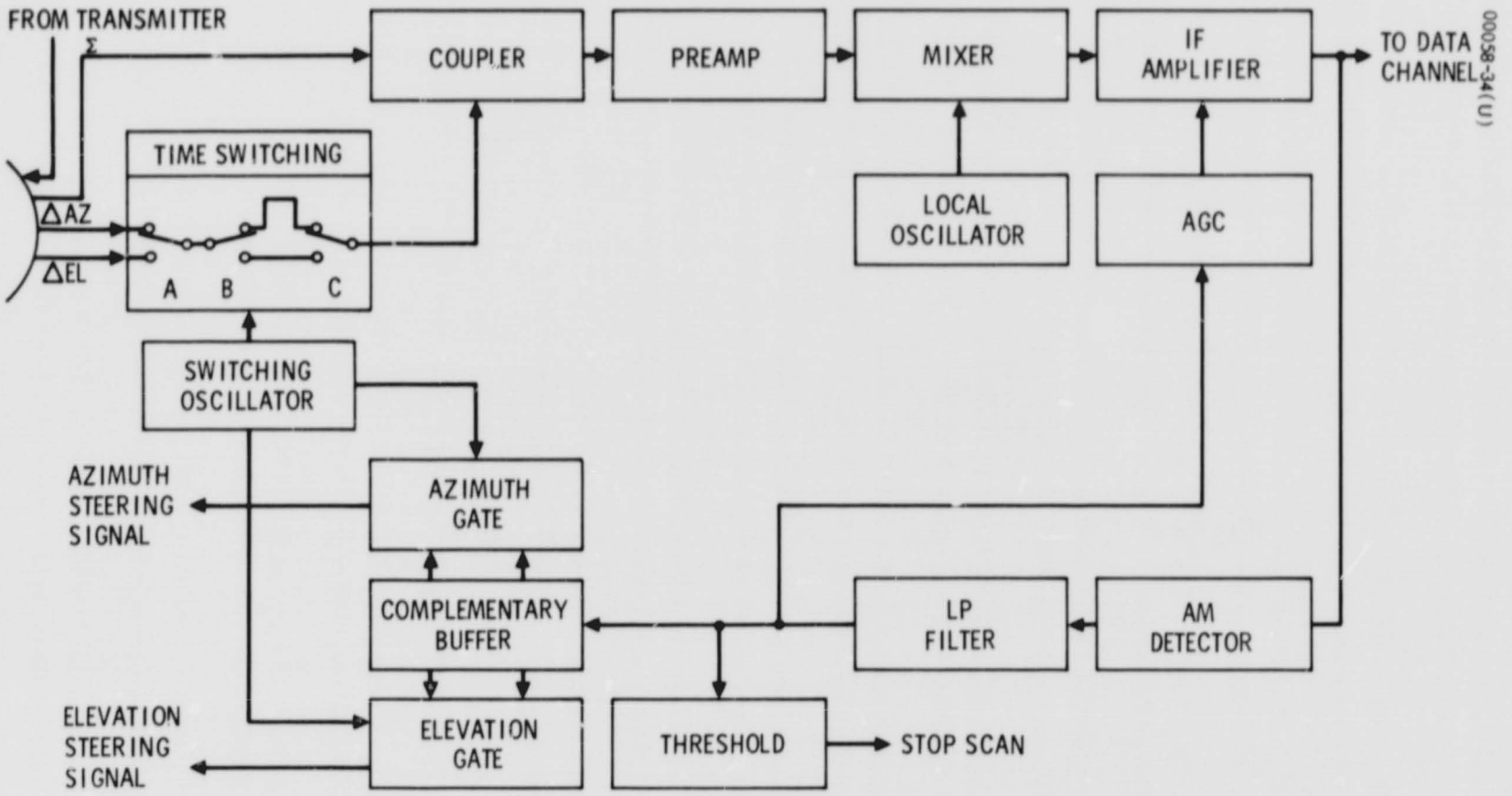

Figure 5.4-5. Time-Shared Monopulse Concept

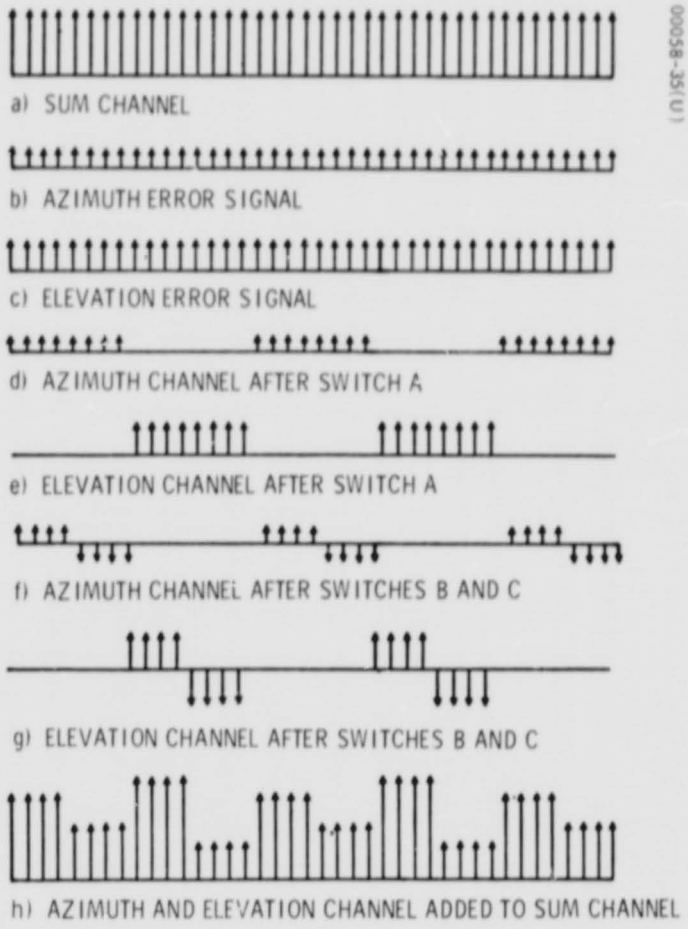

Figure 5.4-6. Time Division Monopulse Vector Diagram

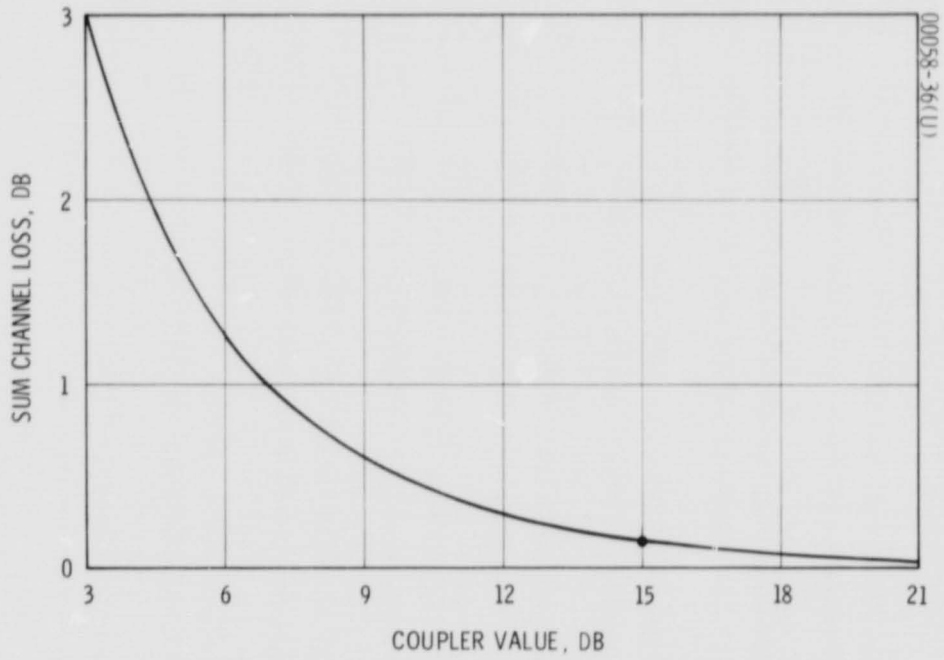

Figure 5.4-7. Dependence of Sum Channel Loss on Coupler Value

The disadvantages of both the quadrature monopulse and time-shared monopulse implementations is that a coupler is in series with the sum channel. This coupler causes a loss in the sum channel, depending on the coupler value. Typically, the coupler value is on the order of 15 to 20 dB, which inserts only a small loss into this sum channel. This loss is indicated in Figure 5.4-7, which shows that once the coupler value is greater than approximately 15 dB, the loss incurred in the sum channel is only a small fraction of a dB. This is adequate for all but receiving systems requiring very low noise levels.

Table 5.4-1 summarizes the advantages and disadvantages of true monopulse and time-shared monopulse implementations. It can be seen that true monopulse provides the best thermal noise performance but is more complex. Time-shared monopulse has less hardware but has a slight degradation in the tracking and communication link due to the coupler loss. A time-shared monopulse implementation has been chosen for the DRT antenna tracking receiver.

TABLE 5.4-1. ADVANTAGES AND DISADVANTAGES OF TRUE MONOPULSE AND TIME-SHARED MONOPULSE

Advantage or Disadvantage	True Monopulse	Time-Shared Monopulse
Advantages	1) Best thermal noise performance for tracking and communication link	1) Less hardware 2) Phase and amplitude balance not required
Disadvantages	1) Requires three channels 2) Requires amplitude and phase tracking between channels as function of frequency and temperature	1) Slight degradation in tracking and communication link performance due to coupling

5.4.1.3 Performance

The performance accuracy of a tracking antenna depends both on the mechanical stepping involved and the noise due to the tracking circuitry.

The tracking error that may be expected using the value of parameters chosen for time division monopulse is given in Figure 5.4-8. The 3σ tracking error is plotted as a function of coupler value, and the coupler design value is 15 dB. Also shown in Figure 5.4-8 are the errors resulting from a true monopulse system. Since a true monopulse implementation does not have a coupler, there is no dependence on the coupler value, and a horizontal line

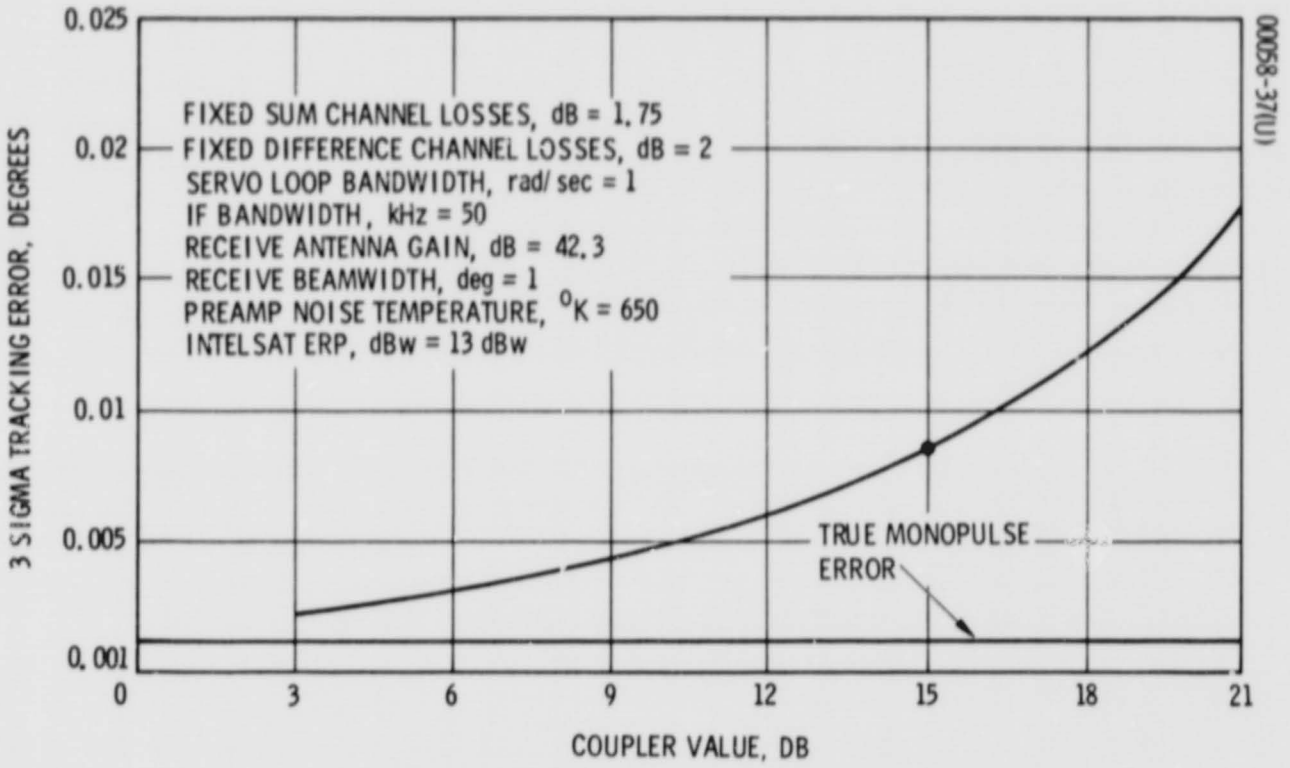

Figure 5.4-8. Tracking Error Due to Thermal Noise for True and Time-Shared Monopulse Systems as Function of Coupler Value

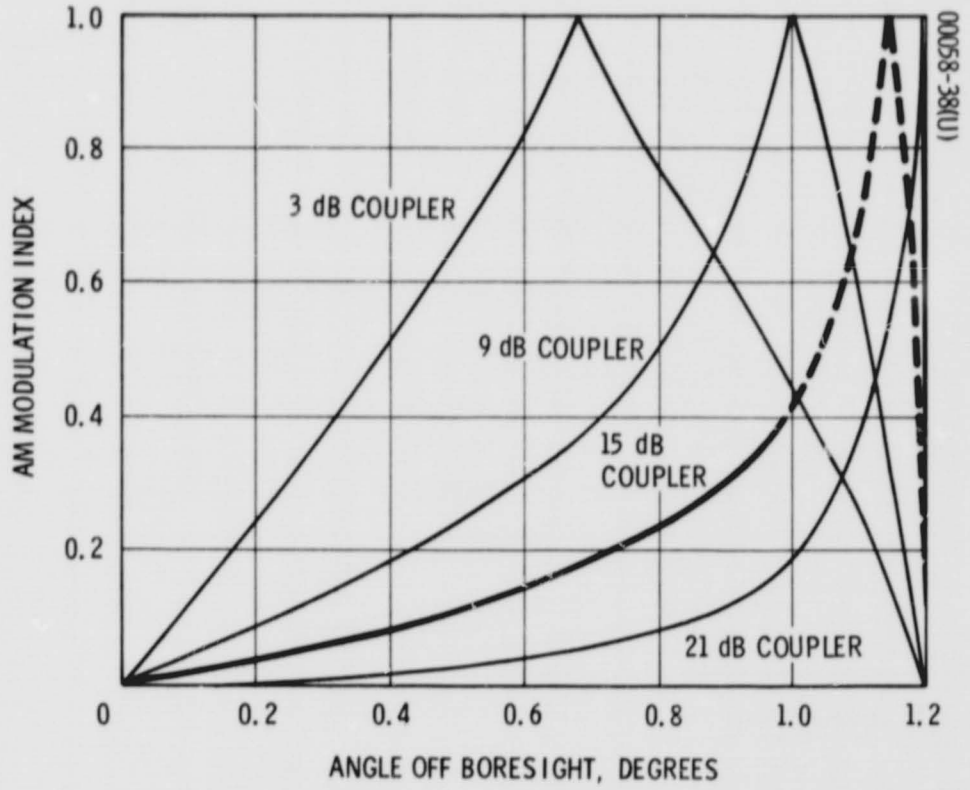

Figure 5.4-9. Monopulse Error Signal

results. As shown, as the coupler value increases, the tracking signal energy in the channel decreases, and the noise increases in the tracking loop. However, this particular example is for a receiving antenna beamwidth of 1 degree and the total 3σ error is less than 0.01 degree for a coupling value up to 15 dB. A coupler of this amount has approximately 0.2 dB insertion loss in the sum channel. From this comparison, the time division multiplex system is preferred to the true monopulse system since only a slight loss is incurred and the error signals are well within the beamwidth of the antenna.

Table 5.4-2 gives the tracking parameters for the time-shared monopulse system used in the DRT. It is possible for a tracking system to lock-on when the angular error of the signal to be tracked is within some fraction of the antenna beamwidth. In order to estimate how large this fraction will be, the AM index of the difference signals upon the sum signals was calculated from the actual antenna sum and difference patterns. Coupler losses in the sum and difference channels and other fixed losses in these two channels were also considered. The modulation index is directly proportional to the antenna angle servo error signal and is plotted in Figure 5.4-9 for several values of the coupler. As shown, the coupler design value of 15 dB provides near linear performance up to 1 degree error. At this point, the mainlobe antenna gain is 27 dB, which is adequate to provide steering signals with a small noise component in the angle error servo. Therefore, an acquisition pull-in range of approximately 1 degree is expected for the DRT antenna.

TABLE 5.4-2. TRACKING PARAMETERS

Intelsat ERP	13 dBw
IF bandwidth	50 kHz
Servo bandwidth	1 rad/sec
Preamplifier noise temperature	650° K
Receive antenna gain	42.3 dB
Receive beamwidth	1 degree
3σ thermal noise error	0.008 degree
Fixed sum channel losses	1.75 dB
Fixed difference channel losses	2 dB

5.4.2 Acquisition

The antenna must acquire the uplink carrier signal from an Intelsat IV after the antenna has been slewed over several tens of degrees. The antenna slewing will be directed by the OA onboard computer. Once the antenna has been positioned to the expected position of the Intelsat IV satellite, the final acquisition procedure takes place. The extent of this final acquisition procedure depends on the accuracy to which the antenna may be initially positioned by the onboard computer. In addition to the computational errors, there are errors in the mechanism between the computer reference point and the actual antenna boresight. These errors will build up to the total estimated error given in Table 5.4-3 for this design. As shown in the table, the maximum sum error is approximately 1 degree in each of the three axes, whereas the expected rms error is on the order of 0.5 degree. This angular error is small enough to allow the antenna pattern itself to be used in the acquisition procedure and thus not require any scanning over an uncertainty area. However, estimates furnished by NASA/Marshall indicate an angular uncertainty of the computer command of ±5 degrees. Therefore, acquisition scanning has been included in the overall acquisition procedure. The scanning pattern will encompass the expected error, which lies some place between ±5 and ±0.5 degrees.

TABLE 5.4-3. INITIAL ACQUISITION POINTING ERRORS

Error	Angle, arcmin		
	Pitch	Yaw	Roll
Space station attitude	4	4	10
Space station thermal deflection	16	16	0
Slew mechanism	3	3	3
Boom alignment	3	3	3
Boom thermal deflection	0	18	18
Gimbal position	3	3	3
Antenna thermal deflection	9	9	9
Antenna boresight	5	5	5
Monopulse phase	5	5	5
Relay satellite orbital position	2	2	2
Maximum sum error	50	68	58
Expected rms error	21	28	24

5.4.2.1 Acquisition Options

When the expected angular position error is greater than the beamwidth of the antenna, some type of search technique must be used to properly orient the antenna. Two general techniques may be considered: a narrow-beam scanning technique and a beam broadening (beam spoiling) technique. Beam spoiling, or broadening, may be used to advantage when the angular sector of uncertainty for the received signal is relatively small, from 2 to 10 times the angular area of the mainbeam. This technique may also be preferable to scanning if system requirements lead to excessive total gimbal travel or scan rates. For this application, the maximum expected uncertainty is on the order of 100 times the normal beam area; therefore, beam spoiling is not attractive.

Typical bar scan and spiral scan patterns are shown in Figure 5.4-10. The bar scan approach has the advantage of relatively simple pointing commands. Its disadvantage is that, for complete coverage of the search area, turnaround occurs outside the search area, thereby increasing scan time. A bar scan is also less efficient in that it begins scanning over an area that has low probability of containing the signal, whereas a spiral scan starts at the point of highest probability of finding the target. A spiral scan is most efficient in terms of early acquisition of the target, and the beam is always in the search area. In addition, this pattern lends itself to a time-varying scan rate. Disadvantages of the spiral scan are the generation of complex drive signals in order to maintain scan rates which vary with the scan radius and the requirement for extremely high torques near the center of search if a constant scan rate were to be used. For the DRT, a square bar raster scan has been selected since the disadvantages of somewhat longer scanning time are overcome by the inherent advantages of a relatively simple search pattern.

5.4.2.2 Acquisition Procedure

The tracking receiver outputs an acquisition status signal. When the receiver indicates no acquisition, the computer will command the antenna to the predicted position of the available Intelsat IV satellite. After a wait at this point for a predetermined length of time, the bar scan will be initiated if a signal is not within the antenna beam. The bar scan is implemented in such a way that only azimuth or elevation commands are changed at a given time. Thus, the antenna scans in azimuth through the length of the bar scan (10 degrees) and then steps in elevation by the beamwidth step. The azimuth scan is then returned to the initial azimuth position. Figure 5.4-11a is a sketch of this bar scan.

The computer drives the scan raster throughout the expected range of azimuth and elevation angles until acquisition is achieved. Acquisition is noted by the acquisition signal indicating the presence of a target. With the present implementation of the stepper motor drive used to move the antenna, the stepper motors will be able to stop the antenna within about 3/8 of a beamwidth after the signal is detected. At this time, the tracking loop is closed and automatic tracking commences.

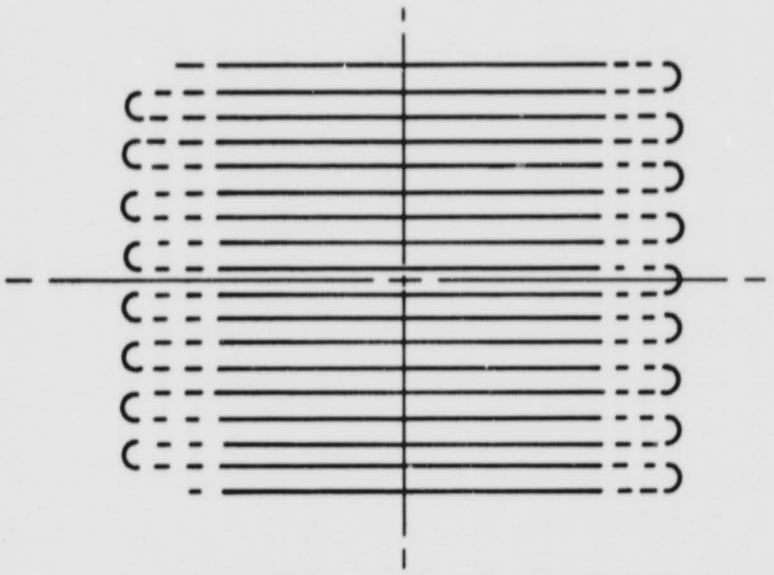

A) SQUARE AREA BAR SCAN

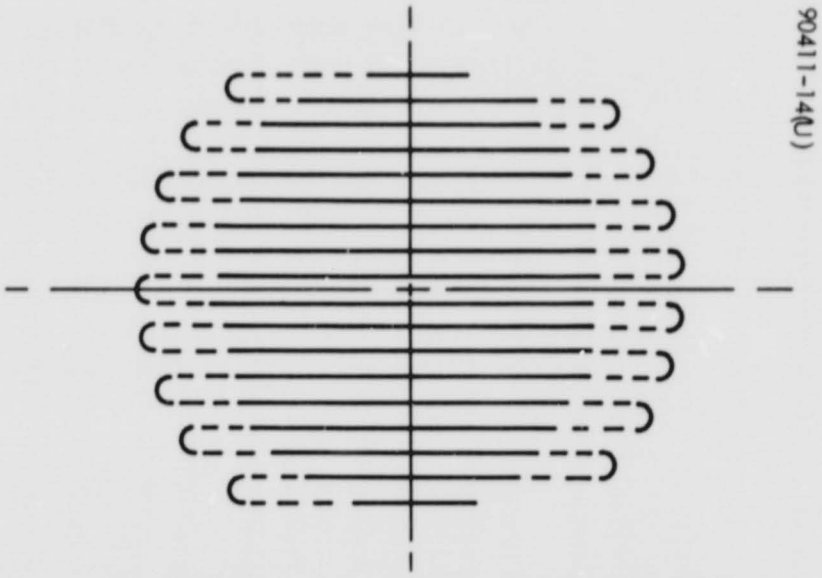

B) CIRCULAR AREA BAR SCAN

90411-14(U)

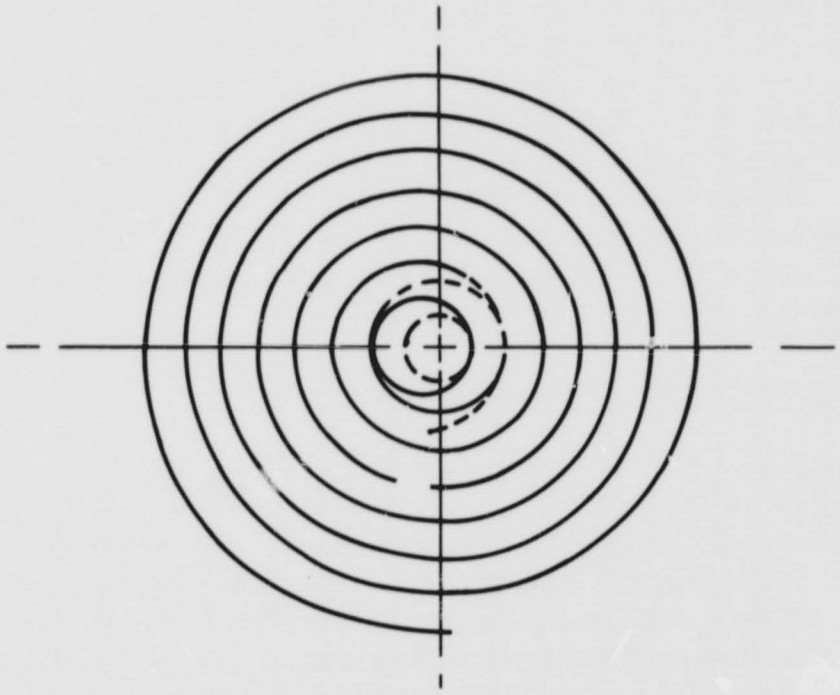

C) SPIRAL SCAN

Figure 5.4-10. Scan Patterns

As shown in Figure 5.4-11b, the displacement between scanning bars is 0.8 degree, as compared to the 1 degree beam size for the antenna. This provides an adequate overlap and assures a high detection probability since the target will always be within the 3 dB point of the antenna beam for a time sufficient for the acquisition circuit to detect the presence of the signal from the Intelsat IV satellite. A scan rate of 150 deg/min will be used for azimuth and elevation. The time per line is estimated at between 4 and 6 seconds as a result of uncertainty in the turnaround time required. Up to 12 lines of scanning may be required, and the maximum time for acquisition will be between 48 and 72 seconds, depending on the turnaround time required.

5.4.2.3 Acquisition Computations

1) Nominal position command

$$Az = \arctan C_1/C_3$$

$$El = \arctan \frac{C_1 \sin (Az) + C_3 \cos (Az)}{C_2}$$

where $\overline{C} = (C_1, C_2, C_3)$ is the vector directed from SWS to Intelsat IV in coordinates centered at SWS and oriented to the gimbal mount (boom position and proper quadrants for Az and El determined by Az-El space mask)

2) Scan generation

Actual position commands are a sequence of points in scan pattern

5.4.2.4 Probability of Acquisition in Presence of Noise

The acquisition probability is a function of the number of angle bins* searched, the probability of signal plus noise exceeding the threshold, and the probability of noise alone exceeding the threshold.

The acquisition beamwidth, σ, must scan over the uncertainty solid angle, Σ. Use of a simplifying assumption relative to beam overlap defines K angle bins where $K = \Sigma/\sigma$. If the probability of the noise exceeding the detection threshold is taken as P_e and the probability of the signal plus noise exceeding the threshold is P_d, then the probability of acquisition, P_{acq}, may be determined as follows:

$$P_{acq} = \sum_{n=1}^{K} P(m) (1-P_e)^{n-1} Pd \qquad (1)$$

*Angle bins denote equal, nonoverlapping, elementary angular regions or resolution elements.

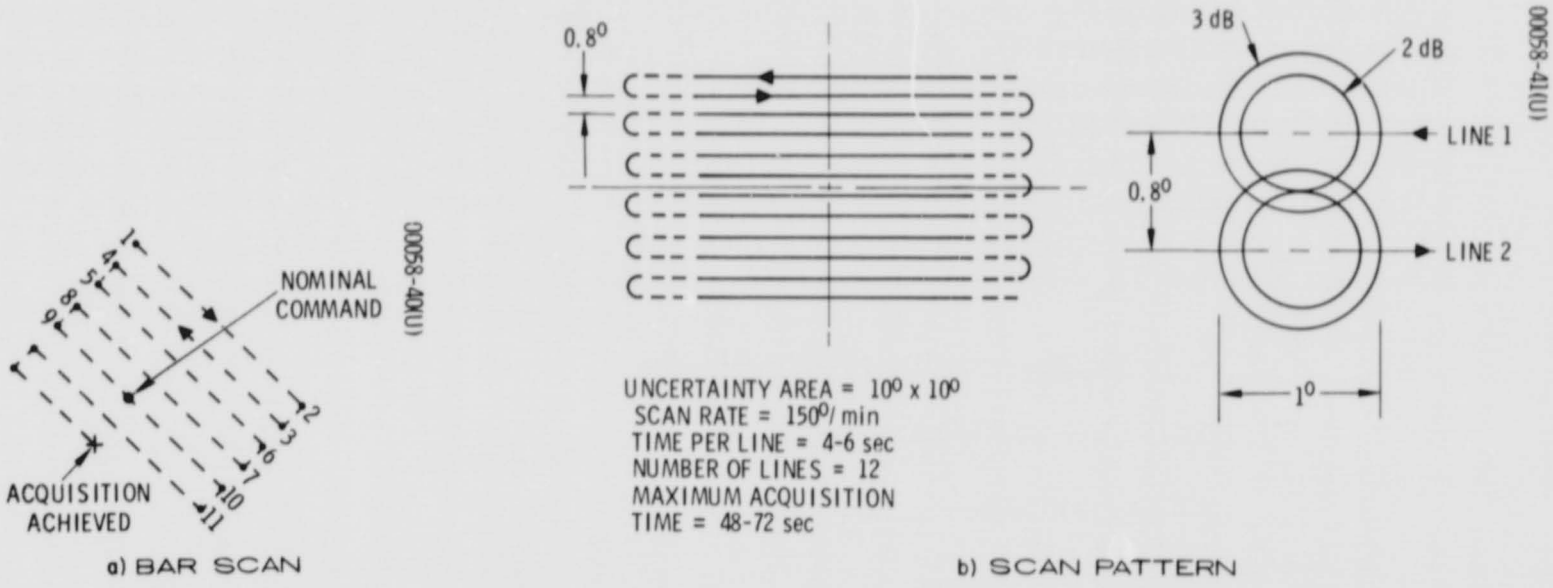

Figure 5.4-11. Acquisition

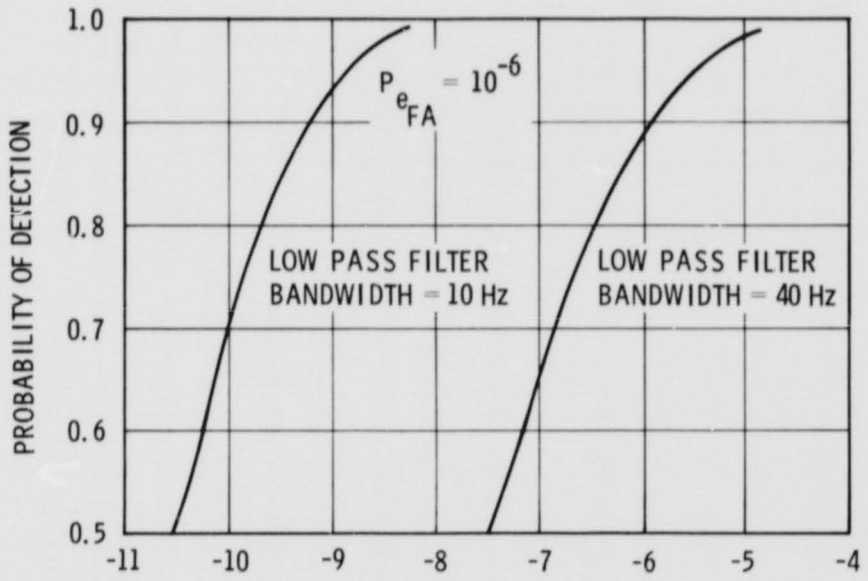

$$P_{ACQ} = K P_{e_{FA}}^{P_d} \left[1 - (1 - P_{e_{FA}})^K\right] = 0.99$$

P_d = 0.99

K = NUMBER OF ANGLE BINS = 144

$P_{e_{FA}} = 10^{-6}$

Figure 5.4-12. Probability of Acquisition

where P(m) is the probability that the signal is the mth bin. The acquisition implementation used is one where the beam is scanned until a target is detected. Thus, the entire frame will not be scanned unless no target is detected. If a false target is detected, the false target angle coordinates are tracked until the nature of the false target is determined. If the simplifying assumption is made that $P(m) = 1/K$, Equation 1 reduces to

$$P_{acq} = \frac{P_d}{K} \sum_{n=1}^{K} (1 - P_e)^{n-1} \qquad (2)$$

This is a geometric series which has as the sum

$$P_{acq} = \frac{P_d}{K} \left[\frac{1 - (1 - P_e)^K}{1 - (1 - P_e)} \right]$$

or

$$P_{acq} = \frac{P_d}{KP_e} \left[1 - (1 - P_e)^K \right]$$

The probability of acquisition, P_{acq}, is a function of P_d, the probability of signal and noise exceeding the threshold, and P_e, the probability of noise only exceeding the threshold as a parameter. P_d and P_e may be a result of several types of statistics.

These probabilities are analyzed below and yield the total probability of acquisition shown in Figure 5.4-12 using the conditions noted there.

To determine P_d as a function of IF signal-to-noise ratio, use is made of the appropriate literature. Emerson* has analyzed a case of interest, i.e., an IF amplifier followed by an envelope detector and a very narrowband low pass filter. He concludes that the detection curves of Marcum** can be used

---

*R. C. Emerson, "First Probability Densities for Receivers with Square-Low Detectors," J. Applied Physics, Vol. 24, 1953, p. 1168.

**J. I. Marcum, A Statistical Theory of Target Detection by Pulsed Radar, Rand Corporation Report RM 754, 1947.

if $(1 + 1/2\ A^2)^{1/2}$ is interpreted as the approximate number of samples averaged by the low pass filter, where A is the ratio of the IF bandwidth to the low pass filter bandwidth.

The results of these computations are shown in Figure 5.4-12 for low pass filter bandwidths of 12 and 35 Hz. The 35 Hz bandwidth is more desirable since it has a faster response time and P_d is adequate (greater than 0.99 for IF signal-to-noise ratios down to -4 dB). Therefore, using the conservative numbers of 0.99 and 10^{-6} for P_d and P_e, respectively, P_{acq} is approximately 0.99.

The principal acquisition parameters are listed in Table 5.4-4.

TABLE 5.4-4. ACQUISITION PARAMETERS

Probability of acquisition	0.99
Scan sector	10° x 10°
Type of scan	Raster
Line separation	0.8 degree
Pointing loss	3 dB
Number of angle bins	144
Maximum acquisition time	≈1 minute
IF signal-to-noise ratio	6 dB

5.5 TWT SELECTION

Summary performance data of available space TWTs that appear feasible for this application are given in Table 5.5-1. Although none of the tubes listed were designed for operation in the 6.2 to 6.4 GHz range, it is expected that all or most of them will operate satisfactorily in that range. Specifically, the Hughes Model 219H was measured at frequencies as low as 5.5 GHz, and the Model 240H was tested down to 6.5 GHz, as shown in Figure 5.5-1. Actually, these two tubes are design variants of each other and were developed over the same time span. The 240H is formally qualified and is currently operational in a Hughes-built communication satellite.

Of the tubes listed, only the Hughes 219H and 240H are at the right power level; the 240H was selected since it has already been space-qualified. For this application, slight changes should be incorporated to optimize tube performance in the 6.2 to 6.4 GHz range; however, these changes are required only in passive circuitry, and neither the tube structure nor the qualification status would be affected. (Partial requalification may be required to account for the AAP booster environment.)

Should a requirement for substantially higher power be developed, the Watkins-Johnson Model 231 might be considered as an alternative to paralleling two of the Hughes 240H TWTs.

5.6 ANTENNA SELECTION

Two antenna configurations suitable for use on the DRT are a two-reflector cassegrain system and a single-reflector prime-focus paraboloid.* The size, weight, and gain of the two types are summarized in Table 5.6-1. The gain of the cassegrain, including transmission line loss, is at least 2.4 dB higher than of the prime-focus design.

The very large frequency band required to cover both transmit and receive frequencies gives the cassegrain configuration a fundamental advantage over the prime-focus configuration. This advantage is that the location of the feed at the vertex of the paraboloid permits the use of a more complicated feed, which, in turn, yields a more efficient antenna than is possible with the prime-focus design. The price for this higher efficiency is a heavier feed. The large frequency band is a disadvantage for the prime-focus design because it requires a four-horn monopulse feed having a relatively large aperture in order to achieve a satisfactory impedance match at both transmit and receive frequencies; and the rather large

---

*The use of phased-array or nonrigid reflector antennas was discounted at the initiation of this study as not being available in time to be implemented for the first SWS. By the time that implementation plans were changed, the terminal design had proceeded to a point at which it was no longer feasible to consider a major design change.

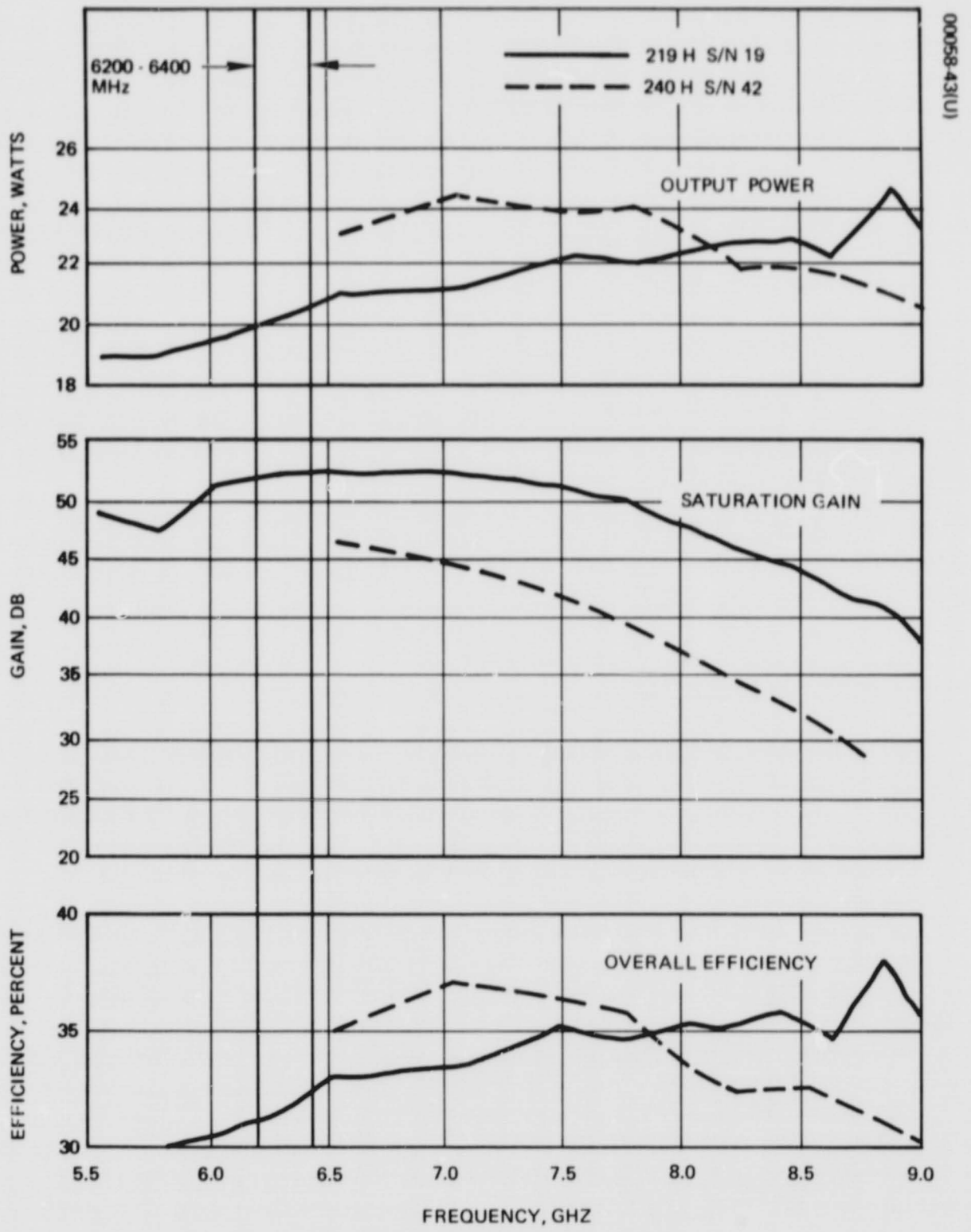

Figure 5.5-1. TWT Data

TABLE 5.5-1. SPACE TWTs NEAR 6200 TO 6400 MHz BAND

Manufacturer	Model	Frequency Range, MHz	Saturation Power Output, watts	Qualification Status	End Use	Remarks
Eimac/ Varian	1066*	7250 to 7300	3.5	Yes	IDCSP	
	1192B*	7950 to 8220	6.2	Yes	Mistram-B	
Watkins-Johnson	130	7250 to 7300	3	Yes	IDCSP	Single field-reversal focusing
	251	7250 to 7750	3	Yes		
	231	7250 to 7400	35			PPM focusing
Hughes	240H	7250 to 7750	20	Yes	TACSAT	
	219H	7500 to 9000	20	Yes	NASA/ Langley	

*TWT and power supply packages.

TABLE 5.6-1. CASSEGRAIN ANTENNA VERSUS PRIME-FOCUS ANTENNA FOR 15 FOOT DIAMETER PARABOLOID

Antenna Type	Feed Type	Feed		F/D	F, inches	Gain, dB	
		Weight, pounds	Length, inches			6350 MHZ	4120 GHz
Cassegrain	Five-horn 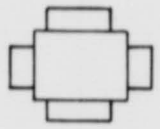	35	36	≥0.4	≥ 72	45.8*	42.3*
Prime focus	Four-horn 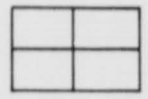	10	15	≥0.6	≥ 108	43.9* 43.4**	40.2* 39.7**

*Does not include transmission line loss.
**Includes transmission line loss.

TABLE 5.6-2. CASSEGRAINIAN DESIGN – ANTENNA LOSS BUDGET AND EXPECTED GAINS, dB SUM PEAK

Parameter	Frequency, MHz	
	6350 ±38	4120 ±38
Area gain	49.6	45.9
Losses		
Aperture efficiency	1.0	0.9
Spillover	0.7	0.7
Hyperboloid blockage	0.5	0.5
Strut (hyperboloid support) blockage	0.2	0.2
Reflector rms surface error (σ_M = 0.040 inch, σ_S = 0.015 inch)	0.4	0.2
Reflector thermal distortion	0.3	0.3
RF circuit (two magic tees, 4 foot waveguide polarizer, power divider, 6/4 orthomode tee)	0.4	0.5
Cross-polarized power	0.3	0.3
Total	3.8	3.6
Expected gain	45.8	42.3

feed aperture would require a large focal length/diameter (F/D) ratio to maximize antenna efficiency. To achieve approximately the same efficiency at both transmit and receive frequencies, the F/D is selected to be optimal at about 5.2 GHz. At the transmit frequency, the paraboloid is "under-illuminated," and at the receive frequency it is "overilluminated." Under-illumination refers to an insufficient power at the outer portion of the dish, and overillumination means too much power at the outer portion. The higher efficiency of the cassegrain system results in a 1.4 dB higher contribution to the gain. Also, the cassegrain system has a very much shorter structure (by approximately 40 inches).

Another factor contributing to the lower gain of the prime-focus antenna is the long transmission line required between the feed and the transmitter/receiver. The additional loss due to this is at least 0.5 dB. Other differences between the two antenna types favor the gain of the cassegrain by at least 0.5 dB relative to the prime-focus feed.

The loss budget for the cassegrain system is shown in Table 5.6-2 and for the prime-focus design in Table 5.6-3.

5.7 ANTENNA FABRICATION

5.7.1 Tooling

The main reflector tool will be a machined mechanite casting. The casting vendor can modify his facility to produce a single piece of this size, or segmented tooling can be used. The tool will be fastened to a suitable carriage for movement between the fabrication and cure facilities.

5.7.2 Material

The composite honeycomb sandwich structure will be fabricated from materials that have been approved for space application. The face structural sheets will be of preimpregnated epoxy-glass cloth, the core will be of lightweight aluminum - (Flexcore - Hexcel Products), and the RF reflective surface will be a metallized dacron mesh.

The syntactic foam is a Hughes-developed material. The honeycomb core segments will be joined with a structural foaming tape adhesive.

5.7.3 Fabrication and Processing

The fabrication process will proceed as follows: A suitable release agent will be applied to the tool surface. Two plies of glass cloth prepreg, the metallized dacron mesh, and two more plies of glass cloth prepreg will be placed against the tool surface. The honeycomb core will be segmented and applied to the tool with foaming tape adhesive at the splice joints. The tape and core segments will be held together with small aluminum clips.

TABLE 5.6-3. PRIME-FOCUS DESIGN – ANTENNA LOSS BUDGET AND EXPECTED GAINS, dB SUM PEAK

Parameter	Frequency, MHz	
	6350 ± 38	4120 ± 38
Area gain	49.6	45.9
Losses		
Aperture efficiency	2.2	0.9
Spillover	0.7	2.2
Feed blockage	0.4	0.4
Strut (feed support) blockage	0.4	0.4
Reflector rms surface error (σ_M = 0.040 inch)	0.4	0.2
Reflector thermal distortion	0.3	0.3
Primary pattern, amplitude and phase	0.2	0.2
Feed, ohmic	0.3	0.3
RF circuit (stripline)	0.5	0.5
Cross-polarized power	0.3	0.3
Transmission line (12 foot waveguide)	0.5	0.5
Total	6.2	6.2
Expected gain	43.4	39.7

The syntactic foam fill is then applied in the desired areas. The four-ply outer skin is assembled next. The warp direction of all plies is staggered to give a balanced construction. The entire assembly is then vacuum bagged and moved into the oven. Bonding pressure of 1/2 to 2/3 atm will be used. The heat cycle will be dictated by cure requirements of the epoxy-face material and the foaming tape adhesive. The epoxy prepreg will act as both the laminating system and the adhesive bonding interface. Cure temperatures will not exceed 350°F.

Upon completion of cure, the assembly will be cleaned of excess materials and trimmed to meet drawing requirements. A handling support ring is then bolted to the back of the dish, and the dish can now be transported to the paint shop for application of thermal control coatings. Acceptability of the antenna contour may have to be based on RF performance since the conventional beam and dial gauge inspection method may be difficult to implement on a dish of this size.

5.7.4 Subreflector

To obtain maximum surface contour accuracy, the subreflector will be fabricated as a solid glass-cloth-epoxy prepreg laminate approximately 0.1 inch thick on a mechanite mold. Vacuum-deposited aluminum will form the RF reflective surface. Inserts will be provided on the backside of the subreflector to interface with the quadripod support tubes.

5.7.5 Quadripod

The subreflector will be supported on four tubular legs. These legs will be fabricated from prepreg cloth with unidirectional graphite fibers added to increase tube stiffness and strength. The quadripod legs will be bolted to the main reflector at the 6 foot diameter opposite the equipment support ring.

5.8 SELECTION OF ANTENNA POSITIONER TRADEOFFS

5.8.1 Motor Selection

Five types of drive motor system were considered: 1) two-phase, 400 cycle servo motors; 2) brushless dc motors; 3) brush-type dc motors; 4) variable reluctance stepper motors; and 5) permanent magnet stepper motors. Tables 5.8-1 and 5.8-2 summarize the advantages, disadvantages, and tradeoff considerations for each of these types.

5.8.1.1 Two-Phase, 400-Cycle

These servo motors have the advantages of a high degree of development, availability from a large number of sources, and a relatively low slewing current. A typical example is the Kearfott size 23, 115 volt,

TABLE 5.8-1. CANDIDATE MOTOR TYPES

Selection	Advantages	Disadvantages
Two-phase ac	Highly developed Low slew power	Requires ac power form Requires extra gears and bearings Requires brake High speed bearings and gears
Brushless dc servo	Linear speed/torque High efficiency	Complex commutation Limited size availability Requires brake Single source
Brush dc servo	Low track power Large selection Linear speed/torque	High slew power Brush lubrication Wear phenomenon Requires brake Brush debris
Variable reluctance stepper	High pulse rate No brushes High efficiency Allows open-loop positioning Compatible with digital system	Limited size availability High peak current Requires brake High ratio gearing
Permanent magnet stepper	Power off holding torque No brushes Allows open-loop positioning Space-qualified vendor Compatible with digital system	Limited pulse rates High peak current Requires commutation for large inertia

TABLE 5.8-2. MOTOR TRADEOFFS

Parameter	Slo-Syn Stepper SS 250	Inland DC Brush T2950	Size 23 Two-Phase 400 Cycle Servo Motor
Motor stall torque, ft-lb	1.17	1.20	0.047
Current at slew room temperature, amperes	1.22	2.9	1.2
Current at track, amperes (0.4 deg/min average)	0.14 (10 percent duty)	0.06	0.6
Average current, amperes, 90 percent track, 10 percent slew	0.25	0.34	0.66
Weight - motor only, pounds	6.50 complete	2.15 Frameless	1.80 Motor
Weight - additional drive elements, pounds	0	3.00 Frame and brake	3.00 2-stage Gear and brake
Power-off brake	29 ft-lb	Friction only	Friction only

CY 40127007 unit with a 10,000 rpm no-load speed, a stalled torque of 9 in-oz, and a weight of 29 ounces. The disadvantages of a drive design based on such a unit are:

- The low torque level and high speed necessitate use of a more complex high-ratio gear box.
- A two-phase 400 cycle power supply and an auxiliary mechanical brake would be required.

5.8.1.2 Brushless DC

These servo motors have the advantages of a linear speed torque relationship and high efficiency. Units with high enough torque to avoid extreme gear ratios are available. Aeroflex units combining the motor and a resolver to commutate through solid state switching are suitable, and the system has been proven on other Hughes programs. Disadvantages are mechanical and electronic complexity in the commutation system and that an auxiliary mechanical brake is required.

5.8.1.3 Brush Type DC

These motors have the advantages of requiring low tracking power, having a linear speed torque characteristic and high efficiency, and being available from several sources. The Inland Motor Corporation T2950, with a torque of 1.2 ft-lb, and a weight of 2.15 pounds would be suitable. Disadvantages of this type of motor are its high slew current (2.9 amperes), use of brushes in a vacuum with resultant brush debris, and the need for a separate brake.

5.8.1.4 Variable Reluctance Stepper

These motors have the advantages of a high pulse rate, no brushes, high efficiency, and allow open-loop positioning compatible with digital control. Their disadvantages is that they are limited to low torque units requiring high ratio gear boxes which increase the complexity and complicate the bearing and gear lubrication problems. A separate brake system would also be required.

5.8.1.5 Permanent Magnet Stepper

These motors have the advantages of no brushes, high efficiency, compatible open-loop positioning with digital control, and they require no auxiliary brake. A Slo-Syn model SS 250, with charactristics as shown in Table 5.8-2, meets the requirements. The system using this motor with positive encoder-controlled solid state commutation has been developed on another Hughes program. The disadvantages are limited pulse rates, high peak current, and the need for a commutation system when used to drive large inertia loads.

5.8.1.6 Selection

Referring to the data of Table 5.8-2, the permanent magnet stepper motor manufactured by Superior Electric Company under the trade name Slo-Syn is preferred because of the advantages named above. The major factors determining this choice are 1) digital controls sytem compatibility, 2) reliable power-off brake, 3) high torque, 4) ability to handle high inertia loads, and 5) minimum power usage.

5.8.2 Gear Reduction

The principal consideration in the selection of the drive train unit is reliability. Lubrication for high loads in a space vacuum is of major concern. Table 5.8-3 shows the tradeoff considerations between a harmonic drive and a four-stage gear box. The key point is the higher reliability anticipated with the harmonic drive. Other reasons for selecting the harmonic drive include:

1) The moving parts count for the harmonic drive is much lower than for a suitable gear drive.

2) Harmonic drives have a large number of teeth simultaneously in contact, and the shape and motion of each tooth gives something more than the line contact of straight gearing. This feature allows for much larger material strength margins.

3) Due to the lower unit pressure in moving contact areas, burnished molybdenum disulfide (MoS_2) lubricant has a demonstrated acceptable life of 2.5 million input revolutions for harmonic drives tested in high vacuum. Other types of gearing would be under relatively heavy unit loads and would require a lubrication replenishment provision.

4) The backlash with a harmonic drive is less than for comparable gearing.

5.8.3 Position Instrumentation

Five available gimbal position readout instrumentation systems were studied, as follows:

1) Digisec optical, Wayne-George Corporation

2) Litton Industries pancake optical

3) American Electronics resolver — two-speed

4) Librascope magnetic V scan

5) Litton brush contact

TABLE 5.8-3. DRIVE TRAIN SELECTION

Requirement	Harmonic Drive	Gears
160/1 ratio	One stage	Four stages
Withstand motor stall 140 ft-lb	320 ft-lb capacity	Large gears
Number of teeth in contact	Many with surface contact	1.6 with line contact
Backlash	≈0	Large
Temperature -90° to +150° F	MoS_2 powder	Bonded MoS_2
Weight	2.5 pounds	High
Reliability	Low parts count	High parts count

Table 5.8-4 compares the significant features of each. The considerations favoring the selection of a two-speed resolver are given in the following paragraphs.

5.8.3.1 Accuracy

All five systems can meet the readout requirement of 0.1 degree.

5.8.3.2 Weight Effect

The Wayne-George optical system showed an 18 pound increase over the other systems. Its large outside diameter increased the housing diameter, and extra weight was required for drive and mounting provisions.

5.8.3.3 Input Power

All units are acceptable; however, the two optical systems require considerably more electric power than do the others (up to 6.7 watts per unit). Most systems have the advantage of a simple dc voltage input, the resolver requires ac excitation, and the magnetic core requires a specialized interrogation pulse.

5.8.3.4 Output Form

All of the systems have a desirable digital output except the two-speed resolver. A digital output is preferred for compatibility with the onboard computer. The output of the resolver is a modulated sine-cosine analog signal which must be digitized.

5.8.3.5 Environmental Adaptation

Environmental adaptation was the most important factor affecting the choice of a system. The American Electronics two-speed resolver was the only system completely meeting environmental requirements in its present form without development liabilities that could increase cost, delay deliveries, or impair performance. All other systems studied require additional development.

5.8.3.6 Reliability

The most reliable devices are those with no contacting mechanisms and no electronics placed in a variable temperature environment. The only device that meets these criteria is the resolver.

5.8.3.7 Cost

The lowest cost system was the Litton brush contact encoder when the cost of the electronics is included. However, except for the resolver, the cost basis for each of the devices is uncertain due to the development required for space application. Although the highest estimated cost is for

TABLE 5.8-4. SUMMARY OF SHAFT POSITION READOUT INSTRUMENTS

Type	Optical	Optical	Magnetic	Magnetic	Brush Contact
Manufacturer	Wayne-George	Litton Industries	American Electronics	Librascope	Litton Industries
Configuration	5.5 inch diameter cylinder	Pancake	Pancake	Size 11 synchro	Size 11 synchro
Operation basis	Incandescent lamps	Gallium arsenide light source	Dual-speed resolver	Magnetic core stable state	Pin-contact V-scan
Accuracy, including electronics, degrees	0.02	0.20	0.20 with Hughes electronics	0.20	0.20
Weight effect per positioner	18 pound increase	Same	Baseline	1 pound decrease	1 pound decrease
Input electrical power	Dc voltage, 6.7 watts	Dc voltage, 1 watt	Sine-cosine, 5 kHz carrier, 0.10 watt	Digital pulse interrogation 1 watt average	Dc voltage, 0.10 watt
Output signal	Natural binary word	Binary decimal code	Sine-cosine modulated waveforms	Magnetic state of each bit	Binary decimal code
Environmental	Redesign for vacuum use, electronic components temperature limiting to -67° F	Electronic components limit low temperature to -67° F	Space-qualified; no electronics in positioner	Vacuum lubrication required for gears and bearings	Vacuum lubrication required for gears and bearings
Reliability	Concern about lamps and electronics in hostile environment	Concern about light source and electronics in hostile environment	High reliability basic materials; no extra bearings; all electronics in redundant APE	Complex mechanization; 32/1 turns; requires gear to drive	Complex mechanization; wearout brushes; 16/1 turns; requires gear to drive
Cost	Medium to high cost unit offset by low cost Hughes electronics	Low to medium cost unit offset by low cost Hughes electronics	High to low cost unit, not higher cost Hughes electronics	Medium to medium cost unit coupled with medium cost Hughes electronics due to complex input	Low to low cost unit coupled with low cost Hughes electronics
Development risk	Redesign for space-compatible materials	New specialized design and package	Lowest space-qualified design; standard circuit methods	Redesign for space lubrication	Redesign for space lubrication

the resolver and its associated processing electronics, there is greater confidence that it will not grow since no further development is required.

5.9 THERMAL ANALYSIS

A summary of the thermal control design requirements and predicted performance for each of the DRT components is presented in Table 5.9-1*. Predicted temperatures for the antenna dish and feed support tubes were utilized in the stress and distortion analysis to determine their acceptability. The analytical results indicate that adequate thermal control of all components can be maintained throughout the mission with passive techniques.

Temperature control of the electronics package will be accomplished by utilizing the outboard surface of the equipment mounting platform as a black radiator ($\alpha^* = 0.96$, $\epsilon = 0.85$) and 30 layers of superinsulation to minimize radiation interchange to the wall and dish interface.

During operation, the antenna gimbal angles resulting from the mission profile provide a solar-terrestial thermal environment that will cause the mounting plate temperature to vary between 45° and 95° F. To maintain mounting plate temperatures below 100° F during extended nonoperational periods, the antenna must be oriented to provide an angle of solar incidence on the radiator greater than 50 degrees.

Black paint offers an adequate finish for the antenna dish in terms of both bulk temperature and temperature gradients. The use of black paint provides a stable and predictable finish, which eliminates the need to consider solar interreflections with other antenna and spacecraft elements. The feed support tubes and gimbal housings can be maintained within their required temperature ranges by surface finishes providing an $\alpha/\epsilon \leq 1.1$ and a Σ of 0.5.

Figure 5.9-1 shows the steady state orbital average bulk temperature of the radiator for 94 consecutive orbits. The upper curve is for continuous operation at 100 watts and the lower for power-off. These curves were generated by assuming alternate tracking of two Intelsat IV satellites with essentially continuous coverage. The assumed initial position of the OA and the two Intelsats relative to the sun is shown in Figure 5.9-1. Since the ratio of the Intelsat period to the SWS period (1440/92) is irrational, this initial position would never exactly repeat. The 94 orbit sample represents five Intelsat orbits; the variation of the electronics temperature appears to be consistent over each Intelsat orbit, and it was assumed that the data are representative for all Intelsat orbits. The thermal capacitance of the system would reduce the amplitude of the minimum

*Table 5.9-1 is the same as Table 4-10 but is reproduced here for convenience of the reader.

TABLE 5.9-1. THERMAL CONTROL SUMMARY

Component	Thermal Design	Control Requirements	Predicted Temperature, °F		
			Description	Maximum	Minimum
Electronics package	Black radiator	Operational	Power on	95	45
	(α* = 0.96, ϵ = 0.85)	0/+100	Power off	0	-20
	30 layers of silicon	Survival	(Boresight pointed at sun)		
		-40/+140			
Antenna	Both sides black	Acceptability of bulk temperatures and ΔTs determined by stress and distortion analysis	Gradient, °F/in	50	μ_o
Dish			Bulk temperature	180	-90
			ΔT across dish	225	μ_o
			ΔT through core	30	μ_o
Feed support	Assumed black for worst case ΔTs		Bulk temperature	190	-150
			ΔT between strut	225	μ_o
Gimbal assembly	α/ϵ = 0.5	-200° to +200° F	Bulk temperature	150	- 90

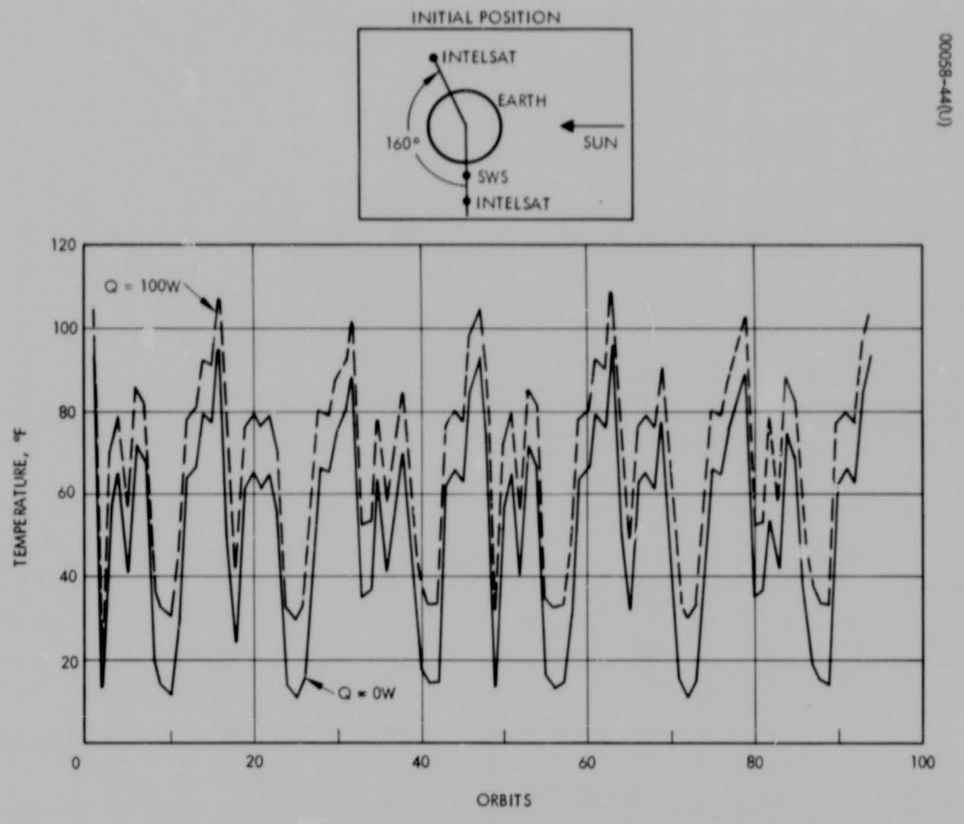

Figure 5.9-1. Equilibrium Orbital Average Temperature of Radiator

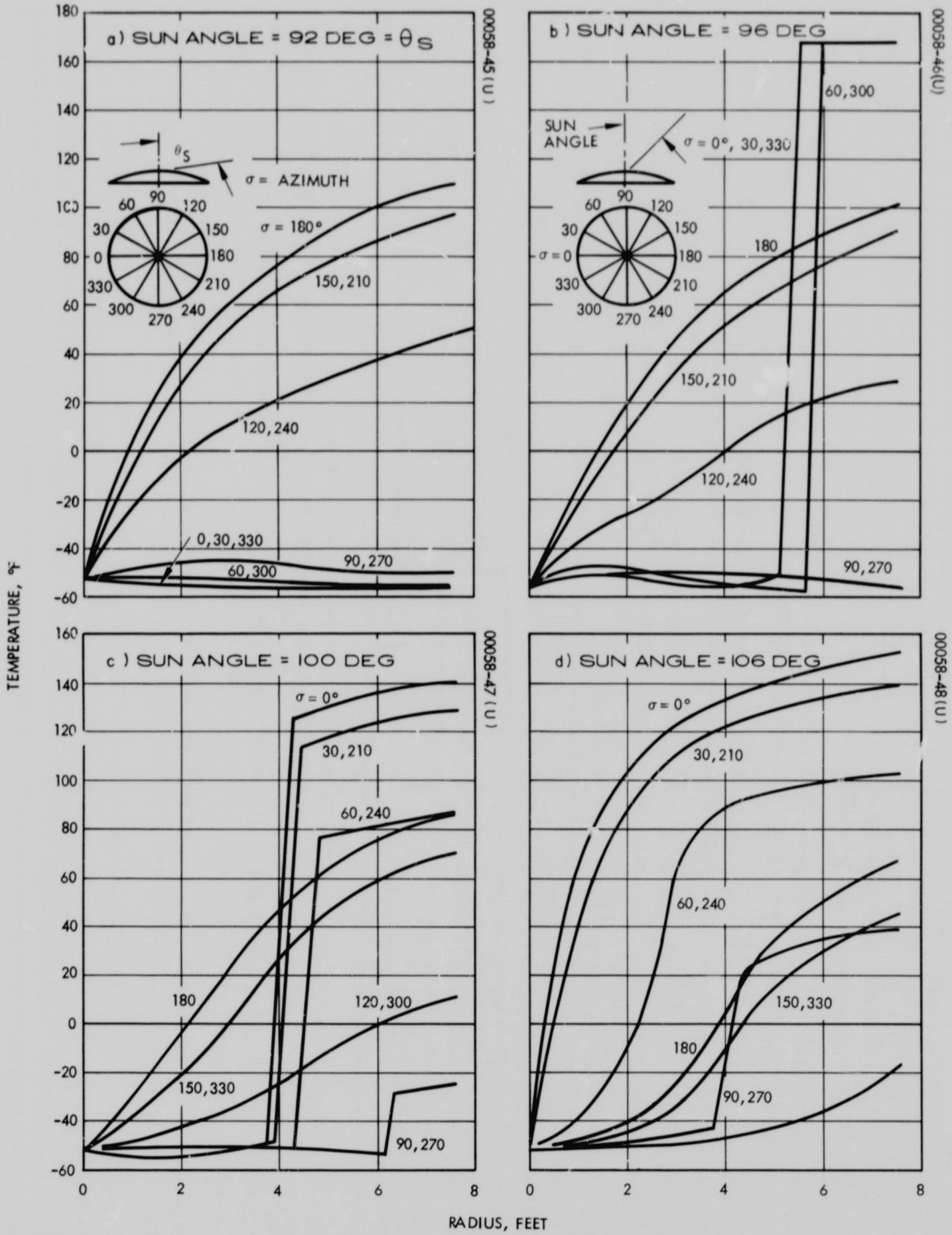

Figure 5.9-2. Antenna Temperatures

and maximum steady state temperatures to 70° ± 25° F during operation and to 50° ± 25° F for zero dissipation. Extended shutdown periods (no tracking) require pointing the antenna so that the angle of solar incidence on the radiator is greater than 50 degrees. A 50 degree incidence angle results in an orbital average temperature of 100° F. Any desired orbital average temperature (-40° to +100° F) can be maintained (±10° F) during shutdown by selecting the appropriate orientation of the radiator with respect to the sun. Table 5.9-1 shows that a temperature of -10° ± 10° F would result if the radiator were pointed away from the sun (incidence angle = 180 degrees).

The antenna dish analysis utilized results obtained from a 60-node model of a similar antenna that included conduction and radiation between nodes. To define a conservative thermal environment which provides an upper bound on the maximum temperature gradients, it was assumed that there was no thermal interaction with the SWS and that the albedo was zero. These two effects would result in higher bulk temperatures but reduced gradients; since the latter result is more significant in distortion analysis, these results give the desired upper limit. Examination of the analytical data indicated that the severest gradients occur at sun angles between 92 and 100 degrees. Radial temperature distributions with azimuth angle as the parameter for sun angles of 92, 96, 100, and 106 degrees are presented in Figures 5.9-2a through d, respectively. Definition of the sun angle is also included in these figures. It can be seen from Figure 5.9-2b that the maximum gradient (radial or azimuth) will be about 50° F/inch across the shadow line on the antenna. The maximum ΔT through the core will be 30° F when the sun is normal to the segment of the dish. Table 5.9-1 summarizes the significant results obtained from this analysis.

The feed support tubes were assumed to be black for analytical conservatism; predicted performance is shown in Table 5.9-1. Bulk temperatures are steady state values for normal illumination of a strut (170° F) and for eclipse (-150° F), assuming a 50 percent view factor to the dish. The temperature differential between two struts, one illuminated and the other shadowed, is 225° F. Surface finishes with α/ϵ less than 1.1 would reduce the maximum bulk temperature and the ΔT but not affect the minimum temperature.

A limiting case analysis similar to that performed on the struts was employed on the gimbal assembly. As shown in Table 5.9-1, steady state bulk temperatures of the housing are predicted to be 150° F (normal illumination) and -90° F (eclipse). These results assume an α/ϵ of 0.5, a 50 percent view factor to the SWS, and that heat dissipation during nominal operation has a negligible influence on bulk temperature.

APPENDIX A. SELECTION OF INTELSAT IV TRANSPONDER CHANNELS AND FREQUENCIES

HUGHES AIRCRAFT COMPANY
AEROSPACE GROUP
SPACE SYSTEMS DIVISION
EL SEGUNDO, CALIFORNIA
P.O. Box 92919 Airport Station
Bldg. 366, Mail Station C-1081
Los Angeles, California 90009

3 November 1969

Bellcomm, Inc.
955 L'Enfant Plaza North, S.W.
Washington, D.C. 20024

Attn: R. K. Chen:

When you visited us on October 23, you indicated that it would be helpful if we presented our views on frequency allocation for the OWS microwave link.

To provide adequate redundancy for the OWS microwave link, it is suggested that two transmit frequencies t_1 and t_2 (primary and alternate) and two receive frequencies r_3 and r_4 (primary and alternate) be assigned, with the links 1 and 3 passing through a common Intelsat-4 channel (primary channel), and 2 and 4 passing through a second Intelsat-4 channel (alternate channel), as shown in Figure 1. (Since each Intelsat-4 channel is provided with fully redundant circuitry, frequency-flexibility involving more than two Intelsat-4 channels seems pointless.)

The question remains as to which channels of the Intelsat 4 satellite should be assigned. It appears that two channels chosen from among channels 9 - 12 would be the best operational match with the Intelsat 4, since these four channels lack spot-coverage transmit capability, a capability which the OWS link cannot use. Moreover, it would help substantially to have two adjacent channel assignments, to lessen the frequency flexibility required of the OWS terminal. Finally, it would help even more if links 1 and 3 were located near the upper edge of the lower channel, and links 2 and 4 were located near the lower edge of the upper channel of the Intelsat 4.

We have examined the ramifications of various frequency assignments, and found them as follows:

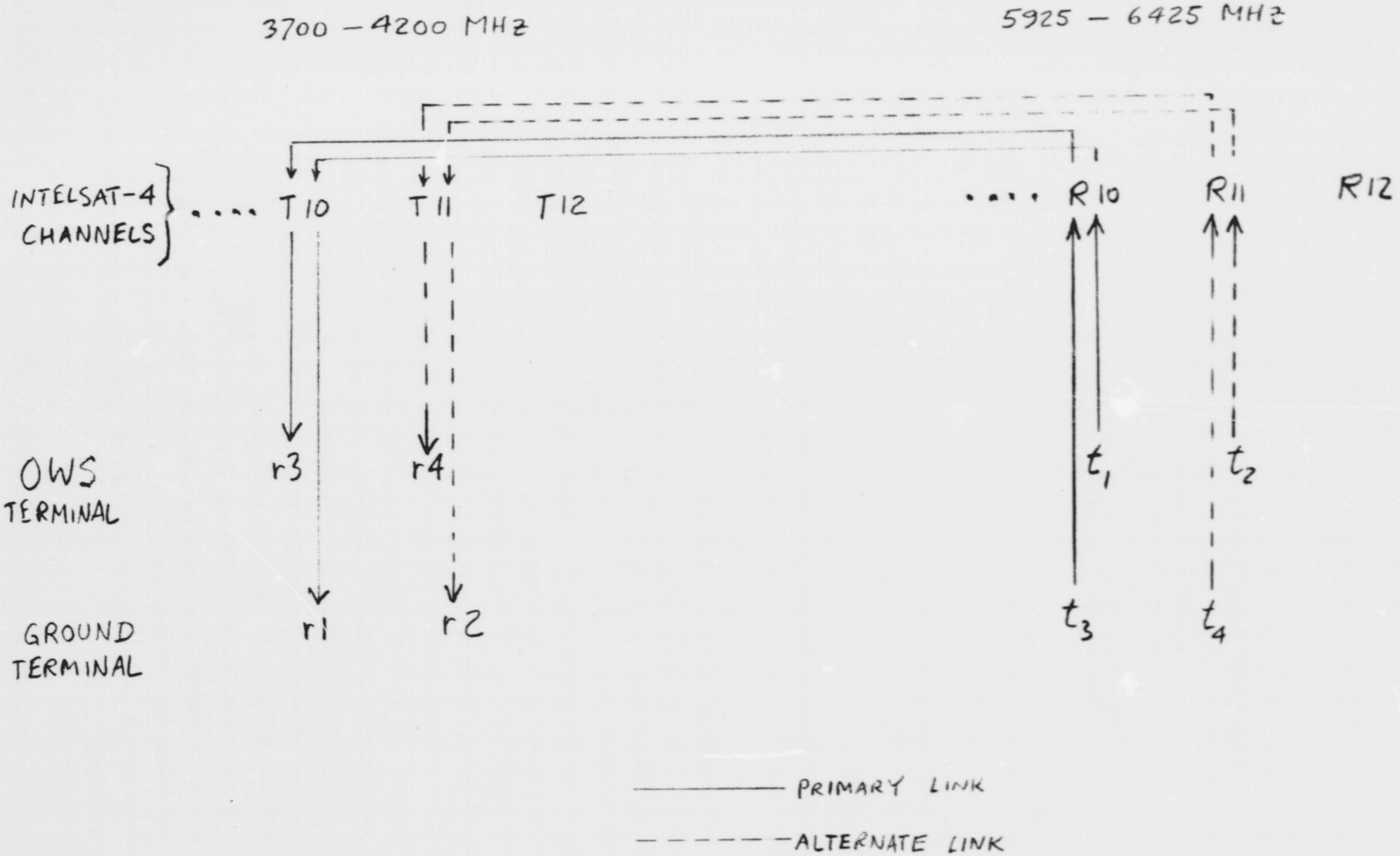

Fig. 1 -- Frequency Scheme for the OWS microwave link.

OWS Antenna and Feed

Alternative	Intelsat 4 Channels Assigned	Nominal Frequency Range, MHz	Relative Gain, db	Relative Sidelobe Level, 6-GHz Band, db	Relative Development Cost
1	Two adjacent channels	R 4100-4200 T 6300-6400 } typical	Ref.	-16	1.00
2	Any two channels, Channels 9-12	R 4000-4200 T 6200-6400	-0.2	-16	1.05
3	Any two channels, Channels 1-12	R 3700-4200 T 5900-6400	-1.0	-15	1.25

This summary indicates that either alternative 1 or 2 would be satisfactory, in that no significant penalty in performance or cost of the antenna results.

OWS Receiver and Transmitter

1-A) Frequencies Near Adjacent Edges of Adjacent Channels.

For frequencies r_3 and r_4 near the upper edge of the lower channel, and near the lower edge of the upper channel, respectively, the frequency separation can be kept under 40 MHz or so (i.e., 1 percent of receive bandwidth, less on transmit), which permits sharing of all receive r-f filters and harmonic-chain multipliers. Frequency selection is effected by simply switching between quartz-crystal oscillators.

1-B) Frequencies Near Opposite Edges of Adjacent Channels.

If it is necessary to place r_3 and r_4 at opposite edges of adjacent channels, this will result in frequency separation of up to 76 MHz (or to 86 MHz for channels 6 and 7, which are more widely spaced). This is 2-percent bandwidth for the receiver LO chain, which is probably the limit of what can be done with simple multiplier chains. In the case of the preamp, a 2-percent bandwidth would be no problem for a TDA, but may constrain the design of a paramp.

2) Frequencies in Top Four Channels.

If it is necessary to accept any allocation from among the top four channels, this implies a bandwidth of 156 MHz. The exciter and the transmitter LO chains will require 2 - 3 times the development and alignment effort of alternatives 1 and 2. A parametric preamp for the receiver will probably not be practical; a TDA, while still possible, will be difficult. A requirement for such broad frequency flexibility for the receiver will probably necessitate a double conversion scheme in order to avoid image problems.

3) Frequencies in Any Two Channels, Out of 12.

Should it be necessary to cover any two channels, space anywhere among the 12 channels provided by the Intelsat 4, two completely separate receivers may have two be provided to cover the frequency range (on top of whatever redundancy provisions must be made).

From the above, the desirability of alternative 1 is quite apparent.

We hope that the information provided will prove helpful, and remain.

Very truly yours

L P Reiche

L. P. Reiche

LPR:dt

cc: G. A. Carnegis
E. F. Shatz
L. M. Gould
R. C. Winterbottom
L. S. Stokes
S. W. Fordyce/NASA Hq.

APPENDIX B. AAP/SWS SPACE TERMINAL STRUCTURAL DESIGN CRITERIA AND REQUIREMENTS

The attached document presents preliminary basic criteria, requirements, and other information governing the structural design of the AAP/SWS space terminal. Included in the document are the following:

- Basic facts pertinent to the structural design
- Basic objectives for the structural design criteria
- Conditions and mechanical environments for which the structure must be investigated and designed
- Requirements for establishing loads and other environmental factors for the design conditions

The document also includes the MDAC design goal that the space terminal have a fundamental mode frequency above 12 cps. A fundamental mode lower than this requires Hughes to give them a mathematical model of the space terminal for their coupled booster-spacecraft analysis. This document will be revised as required.

HUGHES AIRCRAFT COMPANY
Space Systems Division
El Segundo, California

Report No. 2222.3/1035

AAP/SPACE TERMINAL STRUCTURAL DESIGN AND ENVIRONMENTAL CRITERIA

October 1969

By: H. H. Cooley

M. M. Frisman

M. M. Frisman, P.E.
Structural Mechanics Dept.

Approved: C D Knauer

C. D. Knauer, Head
Dynamics Section
Structural Mechanics Department

TABLE OF CONTENTS

		PAGE
1.0	INTRODUCTION	1
	1.1 Scope	1
	1.2 Definitions	1
	1.2.1 Limit Load	1
	1.2.2 Ultimate Load	1
	1.2.3 Factor of Safety	1
	1.2.4 Applied Temperature	1
	1.2.5 Load Factor	2
	1.2.6 Critical Condition	2
	1.2.7 Failure	2
	1.2.8 Excessive Deformations	2
	1.3 Coordinate System	2
	1.3.1 Space Terminal Subsystem	2
2.0	GENERAL DESIGN CRITERIA	3
	2.1 Design Conditions	3
	2.1.1 Dynamic Loads	3
	2.1.2 Load and Thermal Fatigue	3
	2.1.3 Vibration and Acoustical Loadings	3
	2.2 Design Requirements	3
	2.2.1 The General Design Requirement	3
	2.2.2 Strength Requirement	4
	2.2.2.1 Applied Loads	4
	2.2.2.1.1 Limit Loads	4
	2.2.2.1.2 Ultimate Loads	4
	2.2.3 Dynamic Requirements	4
	2.2.4 Factors of Safety	5
	2.3 Required Analysis	5
	2.3.1 Loads Analysis	5
	2.3.1.1 Preliminary Loads Analysis	5

TABLE OF CONTENTS (Continued)

		PAGE
3.0	BOOST	6
3.1	Temperature	6
3.2	Acoustic Field	6
3.3	Vibration	6
3.3.1	Space Terminal	6
3.3.2	Saturn Workshop Floor/Ceiling Mounted Components	6
3.4	Shock	6
3.5	Sustained Acceleration	7

FIGURE

1	AAP/Space Terminal	8
2	Random Vibration Qualification Levels for Space Terminal	9
3	Component Random Qualification Vibration Level for Saturn Workshop	10
4	Shock Spectrum for Space Terminal	11

TABLE

1	Acoustic Environment	12
2	Sinusoidal Vibration Test Specification	13

APPENDIX

Douglas Dynamic Environments 14

1.0 INTRODUCTION

1.1 Scope

This document presents basic criteria, detailed requirements, and other information governing the structural design of the AAP/Space Terminal Antenna and components to be launched by a Saturn V launch vehicle.

Included herein are:

(a) Basic facts and references pertinent to the structural design

(b) Basic objectives for the criteria of structural design

(c) Conditions and environments for which the structure must be investigated and designed. Two (2) areas are considered:

1) Within the Saturn Workshop where electronic components are located

2) Within the interstage adapter where the antenna is mounted.

(d) Requirements for establishing loads and other environmental factors for the design conditions

1.2 Definitions

1.2.1 Limit Load

Limit load is the maximum anticipated load, or combination of loads, which a structure may be expected to experience during the performance of specified missions in specified environments. Since the actual loads that are experienced in service are occasionally random in nature, statistical methods for predicting limit loads, usually the three-sigma level, shall be employed wherever appropriate.

1.2.2 Ultimate Load

Ultimate load is obtained by multiplying the limit load by the ultimate factor of safety.

1.2.3 Factor of Safety

The factor of safety is an arbitrary factor meant to account for uncertainties and variations from item to item in material properties, fabrication quality and details, and internal and external load distributions.

1.2.4 Applied Temperatures

Applied temperatures are maximum and/or minimum calculated temperatures to which the structure will be subjected during the performance of specified missions in specified environments.

1.2.5 Load Factor

Load factor is the ratio of the external forces (other than weight) acting on a mass to the weight of the mass.

1.2.6 Critical Conditions

A critical condition is a loading and/or temperature condition which dictates the design of a portion of the structure.

1.2.7 Failure

A structure is considered to have failed when it can no onger perform its intended function. Failure of a structure may result in he loss of the spacecraft, or any part thereof, or may present a hazard to personnel.

1.2.8 Excessive Deformations

Deformation, either elastic or inelastic, resulting from application of loads and temperatures are excessive when any portion of the spacecraft structure can no longer perform its intended function without reducing the probability of successful completion of the mission.

1.3 Coordinate Systems

The AAP/Space Terminal coordinate system is shown pictorially in Figure 1.

1.3.1 Space Terminal

The AAP/Space Terminal Antenna subsystem will have the coordinate system of the Saturn launch vehicle. The $\pm$X axis is longitudinal and positive in the forward direction. The mutually perpendicular Y and Z axis form a right-handed coordinate system.

2.0 GENERAL DESIGN CRITERIA

2.1 Design Conditions

The environmental phenomena corresponding to each design condition shall include all factors which can influence the structural design, and typically include temperature, vibration, shock and acoustics in addition to quasi-static and dynamic loads. Requirements presented in this specification shall be used in the design of the structure where applicable.

External loads such as those resulting from launch transients and boost shall be determined by analysis of the design environment. The effects of structural flexibility on the distribution and intensity of loads shall be investigated by rational analytical methods.

Loads shall be distributed internally throughout the structure taking into account the effects of flexibilities, non-linearities and temperatures on internal load distribution.

2.1.1 Dynamic Loads

Dynamic Loads shall be determined for all non-steady state phenomena expected in each design environment. The calculation of all dynamic loads shall include the effects of total vehicle structural flexibilities and damping, and coupling of structural dynamics with the control system and the external environment.

2.1.2 Load and Thermal Fatigue

The effects of repeated loads for all life phases and elevated temperature will be considered in the structural design.

2.1.3 Vibrational and Acoustical Loadings

The response of the dynamic system to the vibrational and acoustical environments shall be included in the design analysis where applicable.

2.2 Design Requirements

2.2.1 The General Design Requirement

The structure shall possess sufficient strength, rigidity and other necessary characteristics required to survive the critical loading conditions that exist within the envelope of mission requirements. It shall survive those conditions with sufficient margin so as not to reduce whatsoever the probability of the successful completion of the mission.

The structure shall be designed for either the flight conditions or the dynamic testing requirements, whichever is critical. In general, protective devices will assure that the non-flight conditions and environments will not influence the structural design. Exceptions will be permitted only in those cases where they are dictated by cost and weight considerations.

2.2.2 Strength Requirement

The structure shall be designed to withstand, without degredation, simultaneous application of loads, temperatures, and other accompanying environmental phenomena during boost, ascent and orbit. No factor of safety is applied to any environmental phenomena except loads.

The strucutral design shall be such that comparison of the applied load (or stress) to the allowable load (or stress) shall result in a positive margin of safety, M.S.

$$M.S. = \frac{1}{R} - 1$$

where R is the ratio of applied load (or stress, when applicable) to the allowable load (or stress). In determining the factor R, the effects of combined loads or stresses (interaction) shall be included.

For minimum weight, the structural design shall strive for the smallest permissible margins of safety, which shall be zero, except in certain specific instances where specified finite values may be required.

2.2.2.1 Applied Loads

2.2.2.1.1 Limit Loads

The structure shall experience no permanent deformations greater than .2% in/in at limit loads in the appropriate design environment.

In particular, the minimum stiffness of all portions of the spacecraft shall be great enough that deflection under limit loads shall not produce contact or interference between adjacent parts of the spacecraft or between the spacecraft and fairing or between the spacecraft and the booster interface.

2.2.2.1.2 Ultimate Loads

The structure shall be designed to withstand simultaneously the ultimate loads, applied temperature, and other accompanying environmental phenomena without fracture or any other mode of failure as defined in Section 1.2.7.

2.2.3 Dynamic Requirements

The design goal for the spacecraft payload fundamental frequency shall be 12 cps, with 10 cps being the minimum acceptable. This requirement is necessary to avoid the more severe vibration inputs in the 7-8 cps area.

Component brackets with components attached should have their minimum frequency above 100 cps.

2.2.4 Factors of Safety

The loads specified in the loads document are obtained by applying the factors of safety tabulated below to the maximum anticipated values obtained by analysis or test. These factors are higher than normally encountered in load specifications due to the requirement that all hardware be man-rated.

	LIMIT	ULTIMATE
(1) Flight Loads	2.00	3.0
(2) Non-Flight Loads		
Dangerous to Personnel	2.00	4.0
Remote to Personnel	2.00	3.0

2.3 Required Analysis

2.3.1 Loads Analysis

From the quasi-static and vibration loads and associated environments, the critical loads and/or critical combinations of loads and temperatures on the structure shall be used in an internal loads analysis to obtain the loads for the space terminal. The interactions of the various structural components shall be considered in the internal loads analysis. The internal loads shall include the shears, bending moments, axial forces, and torsional moments acting on a structural element or component defined by the dynamic model.

Thermally-induced structural loads shall be examined for both steady-state and transient temperature conditions. Test data, if available, shall be used along with theoretical analyses to obtain the temperature distribution throughout the antenna and supporting structure and components.

Dynamic loads analysis shall be conducted in all cases where rapidly applied loads give rise to dynamic elastic response of the vehicle or its component parts. The interaction of control system dynamics and structural dynamics shall be considered.

2.3.1.1 Preliminary Loads Analysis

Preliminary ascent loads in the form of lateral and longitudinal load factors shall be initially used to permit preliminary sizing of the payload structure. The current values of these ultimate load factors are specified as 25 G's in both longitudinal and lateral directions. The values given in Section 3.5 are included in these levels with consideration given to dynamic amplification and safety factors.

If the fundamental payload frequency is below 12 cps Douglas requires that a mathematical model of the payload be given to them for their coupled booster/spacecraft analysis.

3.0 BOOST ENVIRONMENTS

3.1 Temperature

The Space Terminal shall be designed to withstand the large heat flux emanating from the four (4) retro-engines mounted on the interstage adapter. Heat flux of 140 BTU - FT^2/SEC has been measured at a Cornell Aeronautical Lab test accompanied by a .18 psia over-pressure. The engines are fired for about one (1) second duration in flight.

The structure shall also be designed to withstand thermal inputs after liftoff due to aerodynamic heating of the nose fairing and free molecule heating after nose fairing separation. In orbit, the structure shall be able to withstand the thermal environments.

3.2 Acoustic Field

The antenna structure and Saturn Workshop mounted components will encounter acoustic excitation as described in Table 1. The subsystem in a total payload test will be subjected to 154.2 db overall.

3.3 Vibration

3.3.1 Space Terminal

The Space Terminal is subjected to sinusoidal and random vibration. The sinusoidal portion arises from system test and modal survey requirements. These are delineated in Table 2 (see also Appendix).

Random vibration, primarily caused by motor or engine generated acoustics and aerodynamic buffeting excitations, will be encountered. Vibrations of maximum severity may occur for periods of a few seconds near liftoff, through the transonic region, near the period of maximum dynamic pressure and at ignition and burnout of each stage. These environments modified for testing, are described in Figure 2 (see also Appendix).

3.3.2 Saturn Workshop Floor and Ceiling Mounted Components

The components mounted to the floor and ceiling of the Saturn Workshop are subject to the random vibration qualification specification of Figure 3 (see also Appendix).

The basic chassis of individual components and their immediate support structure (excluding trusses) shall have fundamental resonant frequencies greater than 100 cps. In those cases where vibration isolators are employed or where significant weight penalties would be incurred, these requirements will be amended.

3.4 Shock

Shock loads will be encountered due to engine ignition, motor and engine shutdown, and stage separation. Additional shocks will be experienced due to the shaped-charge pyrotechnic fairing and explosive bolt separation

techniques. These shocks will exhibit the form of complex decaying sinusoids which may result in equipment component (resonant) response acceleration peaks. This shock response spectrum at the satellite/interstage interface will be approximately enveloped by the response spectrum specified in Figure 4.

3.5 Sustained Acceleration

Satellite components shall be designed for the following conditions in sustained flight (limit values given):

DIRECTION	COMBINED LOADING CONDITION 1 (G's)	COMBINED LOADING CONDITION 2 (G's)
LONGITUDINAL	+5	-2
LATERAL	3	3

The above values form the basis for the design load factors given in Section 2.3.1.1 after amplification and safety factors have been applied.

AA/P SPACE TERMINAL

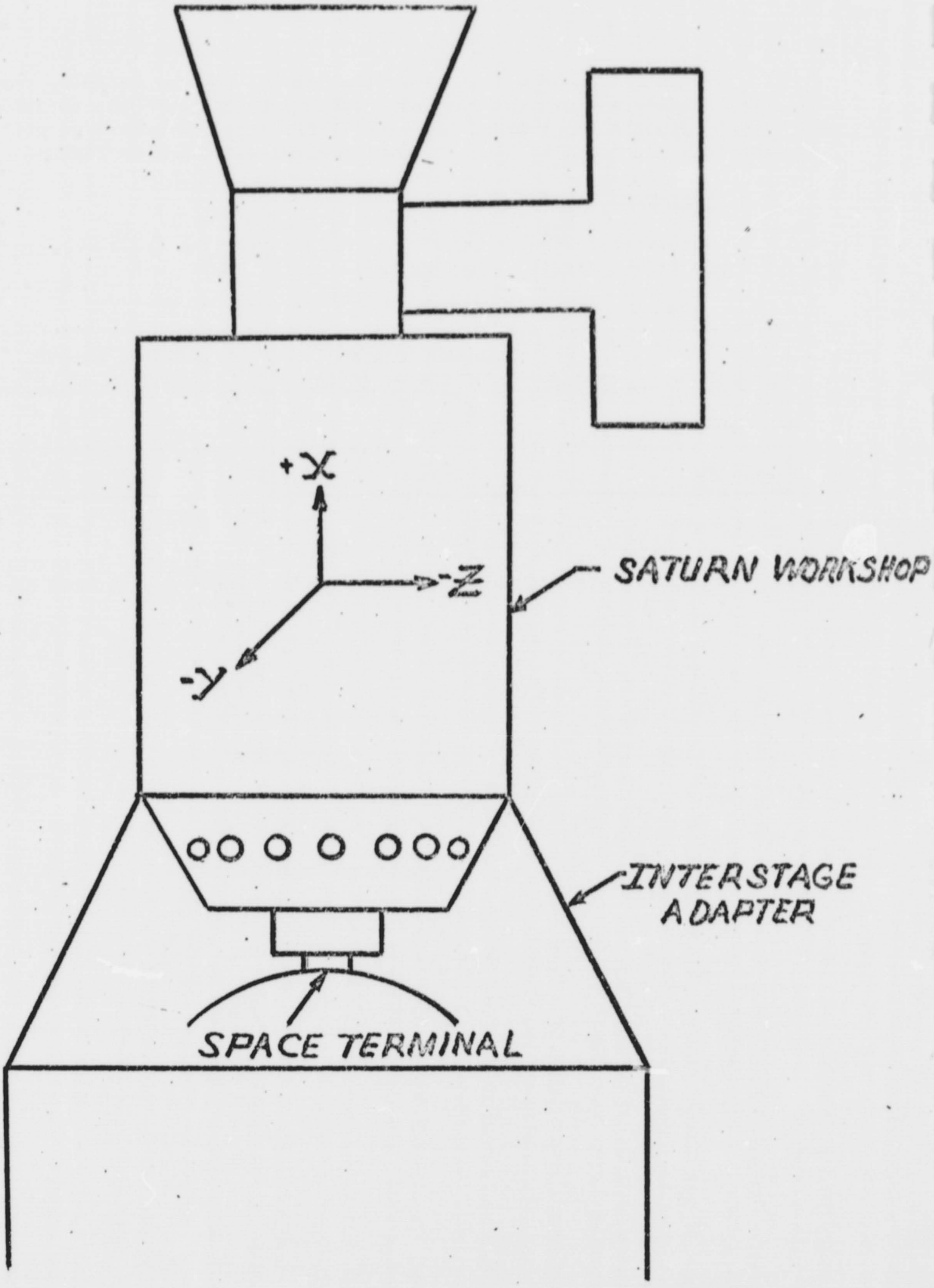

FIGURE I

RANDOM VIBRATION QUALIFICATION LEVELS FOR SPACE TERMINAL

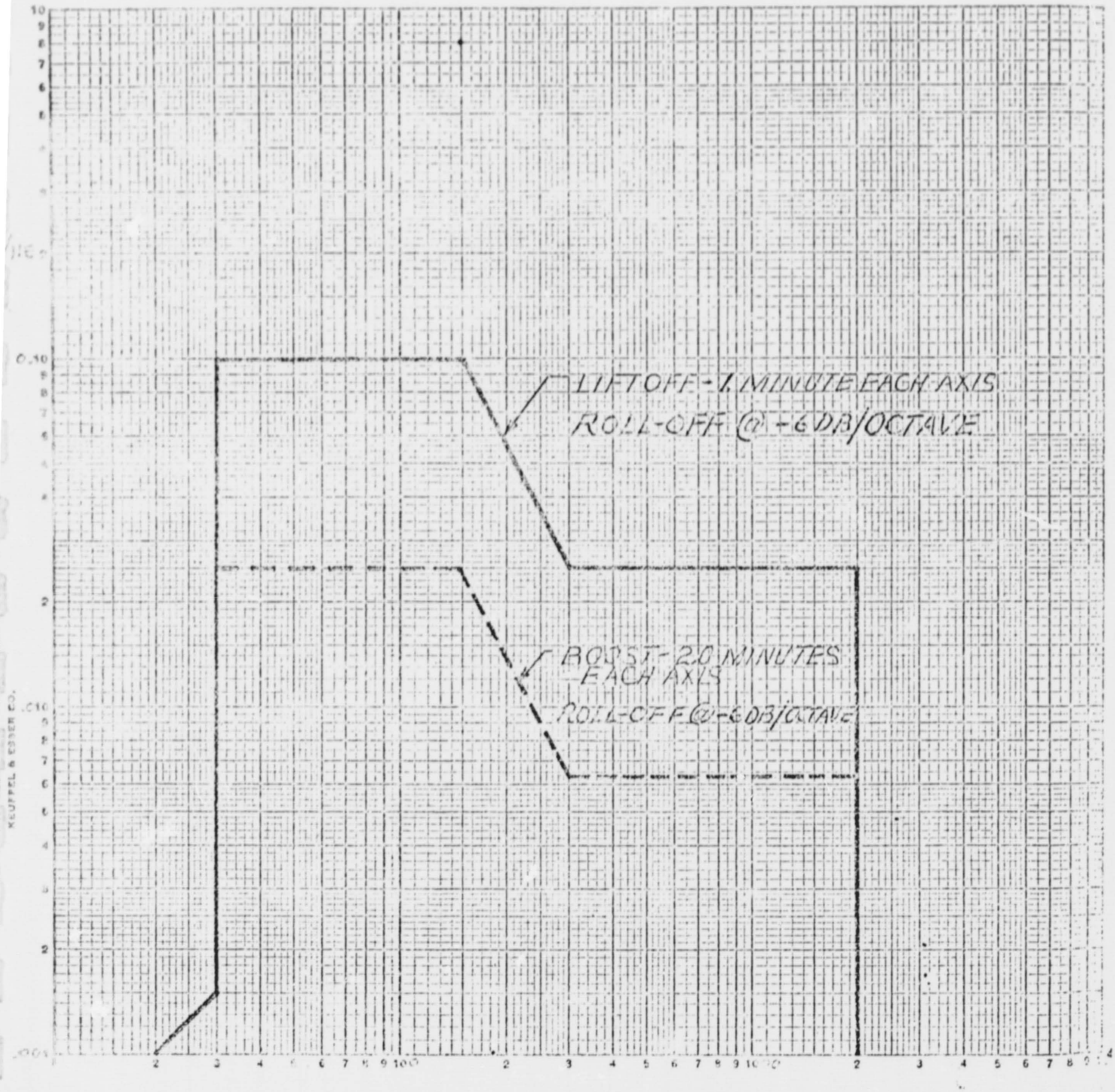

COMPONENT QUALIFICATION RANDOM SPECIFICATION FOR SATURN WORKSHOP

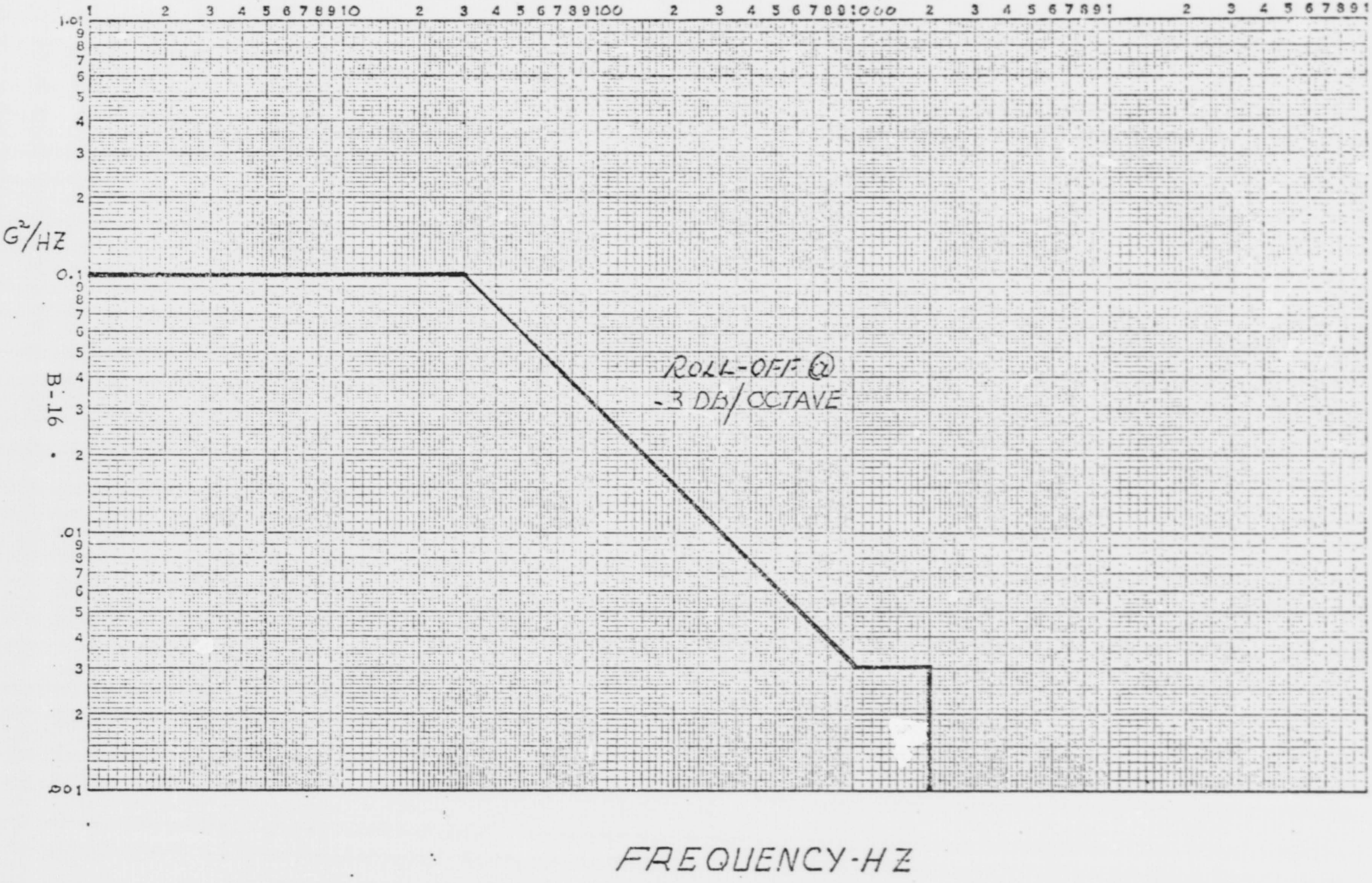

FIGURE

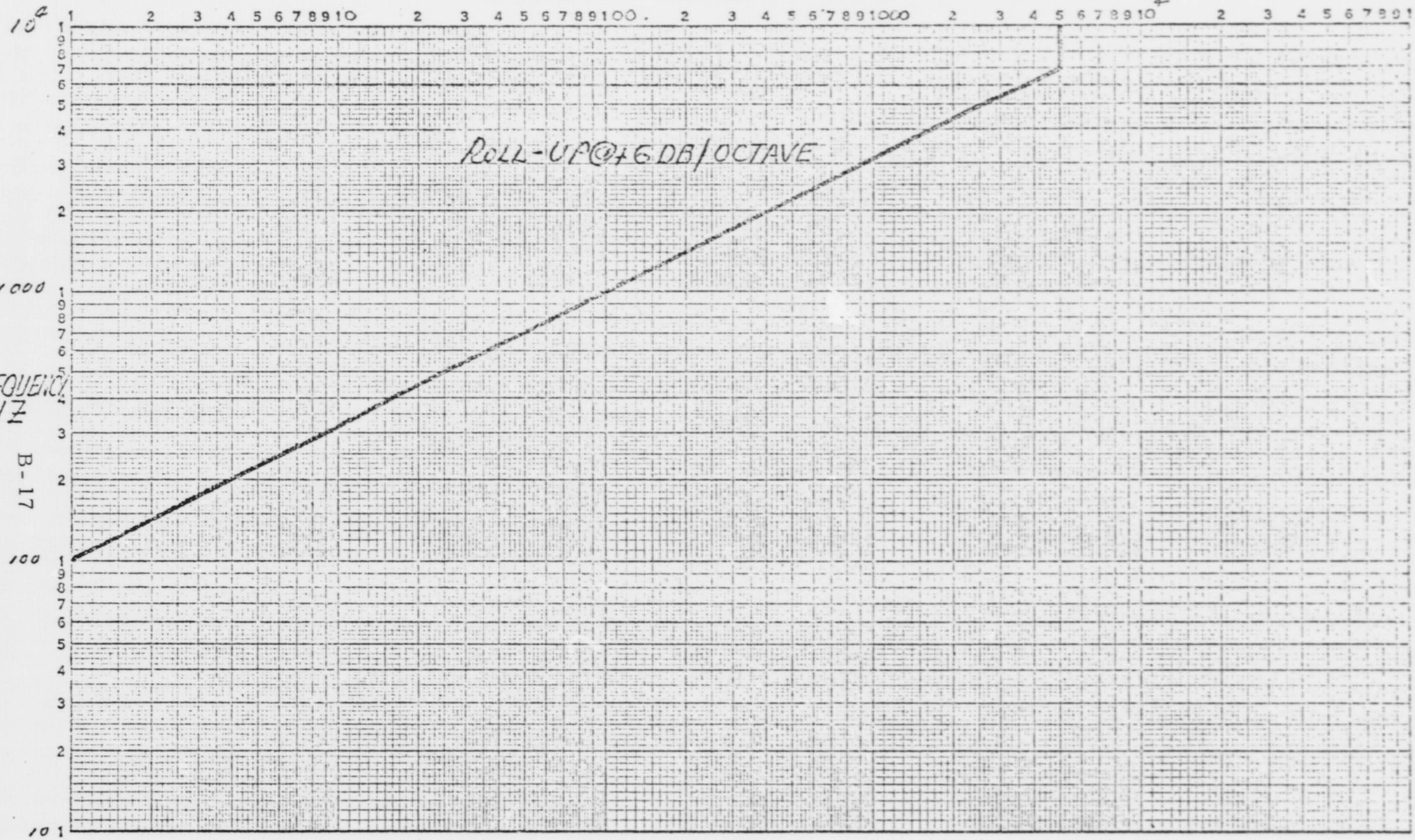
SHOCK SPECTRUM FOR SPACE TERMINAL
ROLL-UP @ +6 DB/OCTAVE
FREQUENCY -HZ
B-17
10⁴
1000
100
10
1 2 3 4 5 6 7 8 9 10 2 3 4 5 6 7 8 9 100 2 3 4 5 6 7 8 9 1000 2 3 4 5 6 7 8 9 10⁴ 2 3 4 5 6 7 8 9 1
G - PEAK

FIGURE 4

TABLE 1

ACOUSTIC ENVIRONMENT FOR INTERSTAGE ADAPTER AREA

FREQUENCY THIRD OCTAVE BAND GEOMETRIC MEAN FREQ. (Hz)	3 MINUTE TEST DURATION LEVEL (db RE.0.002 dynes/CM^2)
5.0	129.5
6.3	131.0
8.0	132.0
10.0	134.0
12.5	135.0
16.0	136.0
20.0	138.0
25.0	139.5
31.5	141.0
40.0	143.0
50.0	144.5
63.0	146.0
80.0	147.0
100.0	145.0
125.0	143.0
160.0	141.0
200.0	138.0
250.0	135.0
315.0	133.0
400.0	132.0
500.0	131.0
630.0	130.0
800.0	129.5
1000.0	129.0
1250.0	128.0
1600.0	127.0
2000.0	126.0
2500.0	125.0
3150.0	124.0
4000.0	123.0
5000.0	122.0
6300.0	121.0
8000.0	120.0
10000.0	119.0
	154.2 db (Overall)

TABLE 2

SINUSOIDAL VIBRATION TEST SPECIFICATION

Vehicle Dynamic Criteria Limit Loads

Scan the given frequency range, logarithmically, at the rate of 3.0 octaves/minute from the low frequency to the high frequency in the flight axis (5 Hz to 50 Hz)

5 - 50 Hz at 0.3 g peak

Scan the given frequency range, logarithmically, at the rate of 3.0 octaves/minute from the low frequency to the high frequency in the lateral axes (1.5 Hz to 20 Hz)

1.5 - 4.5 Hz at 0.4 g peak

4.5 - 10 Hz at 0.4 inches D.A. Disp. (D.A. = Double Amplitude)

10 - 20 Hz at 2.0 g peak

Sinusoidal Vibration Evaluation Criteria

Scan the given frequency range, logarithmically, at the rate of 1.0 octave/minute from the low frequency to the high frequency in three mutually perpendicular directions (20 Hz to 2,000 Hz)

20 - 100 Hz at 0.002 inches D.A. Disp.

100 - 2000 Hz at 1 g Peak

Zone 2-1-2 Thrust Structure Mounted Component

Total Weight of Component 40 to 150 lbs.

Vehicle Dynamic Criteria

Scan the given frequency range, logarithmically, at the rate of 3.0 octaves/minute from the low frequency to the high frequency in the flight axis. 5 Hz to 50 Hz (3-1/3 octaves).

5 - 50 Hz at 0.3 g peak

Scan the given frequency range, logarithmically, at the rate of 3.0 octaves/minute from the low frequency to the high frequency in the lateral axes.. 1.5 Hz to 20 Hz (3.7 octaves).

1.5 - 4.5 Hz at 0.4 g peak
4.5 - 10 Hz at 0.4 inches D.A. Disp.
10 - 20 Hz at 2.0 g peak

Sinusoidal Vibration Evaluation Criteria

Scan the given frequency range, logarithmically, at the rate of 1.0 octave/minute from the low frequency to the high frequency in three mutually perpendicular directions. 20 Hz to 2,000 Hz (6-2/3 octaves).

20 - 100 Hz at 0.002 inches D.A. Disp.
100 - 2000 Hz at 1 g Peak

Liftoff Level Random Vibration Criteria

Subject the specimen to the specified random vibration for 1.0 minute in each of the three mutually perpendicular directions. The excitation shall be applied as one input over the frequency interval from 20 to 2,000 Hz.

20 - 30 Hz at + 3dB/Octave
30 - 150 Hz at 0.1 g^2/Hz
150 - 300 Hz at - 6dB/octave
300 - 2000 Hz at 0.025 g^2/Hz

Boost Level Random Vibration Criteria

Subject the specimen to the specified random vibration for 2.0 minutes in each of three mutually perpendicular directions. The excitation shall be applied as one input over the frequency interval from 20 to 2,000 Hz.

20 - 30 Hz at + 3dB/octave
30 - 150 Hz at 0.025 g^2/Hz
150 - 300 Hz at - 6dB/octave
300 - 2000 Hz at 0.0063 g^2/Hz

Shock Criteria

Not applicable.

VIBRATION CRITERIA INTELSAT ANTENNA SUPPORT ELECTRONICS INSTALLED ON WORKSHOP FLOOR & CEILING

Zone 4-5-2 Workshop Floor and Ceiling

Vehicle Dynamic Criteria

Scan the given frequency range, logarithmically, at the rate of 3.0 octaves/minute from the low frequency to the high frequency in the flight axis. 5 Hz to 50 Hz (3-1/3 octaves).

5 - 50 Hz at 0.84 g peak

Scan the given frequency range, logarithmically, at the rate of 3.0 octaves/minute from the low frequency to the high frequency in the lateral area. 1.5 Hz to 20 Hz (3.7 octaves).

1.5 - 2.5 Hz at 1.5 inches D.A. Disp.
2.5 - 8 Hz at 0.5 g peak
8 - 20 Hz at 0.154 inches D.A. Disp.

Sinusoidal Vibration Evaluation Criteria

Scan the given frequency range, logarithmically, at the rate of 1.0 octave/minute from the low frequency to the high frequency in three mutually perpendicular directions. 20 Hz to 2,000 Hz (6-2/3 octaves).

20 - 100 Hz at 0.002 inches D.A. Disp.
100 - 2000 Hz at 1 g peak

Liftoff Level Random Vibration Criteria

Subject the specimen to the specified random vibration for 1.0 minute in each of the three mutually perpendicular directions. The excitation shall be applied as one input over the frequency interval from 20 to 2,000 Hz.

Thrust			Lateral Axes		
2	-	5 Hz at + 6dB/octave*	2	-	34 Hz at 0.01 g^2/Hz*
5	-	30 Hz at 0.1 g^2/Hz*	34	-	60 Hz at + 6dB/octave
30	-	1000 Hz at - 3dB/octave	60	-	2000 Hz at 0.03 g^2/Hz
1000	-	2000 Hz at 0.003 g^2/Hz			

Boost Level Random Vibration Criteria (Maximum q)

Subject the specimen to the specified random vibration for 2.0 minutes in each of three mutually perpendicular directions. The excitation shall be applied as one input over the frequency interval from 20 to 2,000 Hz.

Thrust			Lateral Axes		
2	-	5 Hz at + 6dB/octave*	2	-	34 Hz at 0.0025 g^2/Hz*
5	-	30 Hz at 0.025 g^2/Hz*	34	-	60 Hz at + 6dB/octave
30	-	1000 Hz at - 3dB/octave	60	-	200 Hz at 0.0075 g^2/Hz
1000	-	2000 Hz at 0.0007 g^2/Hz	200	-	600 Hz at + 6dB/octave
			600	-	2000 Hz at 0.03 g^2/Hz

Shock Criteria

Not applicable.

*Tests not required below 20 Hz - design criteria only.

APPENDIX C. GIMBAL ANGLES FOR LOW ALTITUDE SATELLITE ANTENNA TRACKING A SYNCHRONOUS SATELLITE

C.1 INTRODUCTION

A computer program (ST-1) for generating the track of elevation over azimuth gimbal angles for tracking a series of up to three synchronous satellites from a low altitude inclined circular orbit has been written for this study. However, the program may be used as is, or with simple modification, for many related applications.

The program automatically provides for switching to the next available synchronous satellite when the line of sight to the satellite currently being tracked intercepts the earth's atmosphere. The atmospheric altitude to be cleared is one of the input parameters to the program (DRE).

The computations used in the programs are derived in Section C.2. A listing of the gimbal angle program (in Fortran IV) is attached as Section C.3. Tabulated and plotted outputs for a typical run are shown in Sections C.4 and C.5, respectively. Section C.6 is a list of program symbol definitions.

C.2 COMPUTATION DERIVATIONS

C.2.1 SWS Configuration

As shown in Figure C-1, the antenna boom is nominally assumed to be parallel to the AAP/SWS Y axis (Ya). However, provision is made in the program to offset from this position by inputting the angle DD, corresponding to a simple rotation of the boom about the Xa. (Provision is also made for any arbitrary orientation of the antenna by the definition of a Q matrix. As programmed, Q is prestored as a unit matrix.)

The first gimbal rotation, azimuth (Az), is about the boom, or No. 2 axis*. The zero azimuth position corresponds to the elevation axis parallel to the Xa axis.

---

*All coordinate references in this analysis, except for direct reference to the AAP/SWS axes, use numeric subscripts 1, 2, and 3 corresponding to nominal right-handed X, Y, and Z axes, respectively.

The second gimbal rotation, elevation (El), is about a No. 1 axis. (Rotations will be positive in the usual right-handed convention.)

C. 2. 2 X Coordinate Reference

The basic coordinate set, X = [X1, X2, X3] is a geocentric system with X3 directed northward along the polar axis; X2 is along the AAP/OA orbit line of nodes, directed toward the descending node; and X1 is perpendicular to X2 and X3 so as to make a right handed system, as shown in Figure C-2.

C. 2. 3 Communication Satellite Position

The position of the communication relay satellite is given by the vector $\bar{C}$. Its components, in the X system are:

$$CX_1 = R_c \cos (2\pi T/TC + \theta_c (NSAT))$$

$$CX_2 = R_c \sin (2\pi T/TC + \theta_c (NSAT))$$

$$CX_3 = 0 \qquad (1)$$

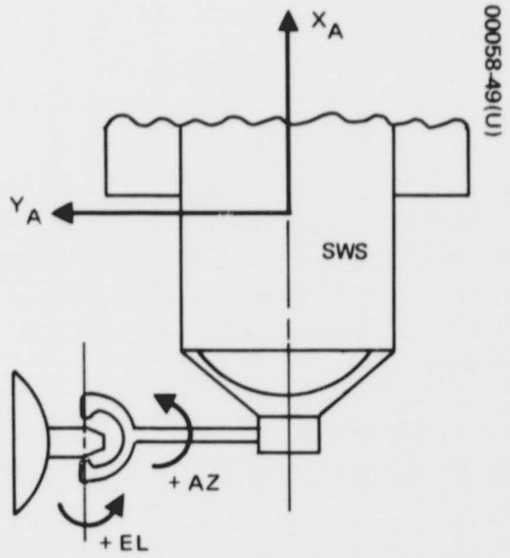

Figure C-1

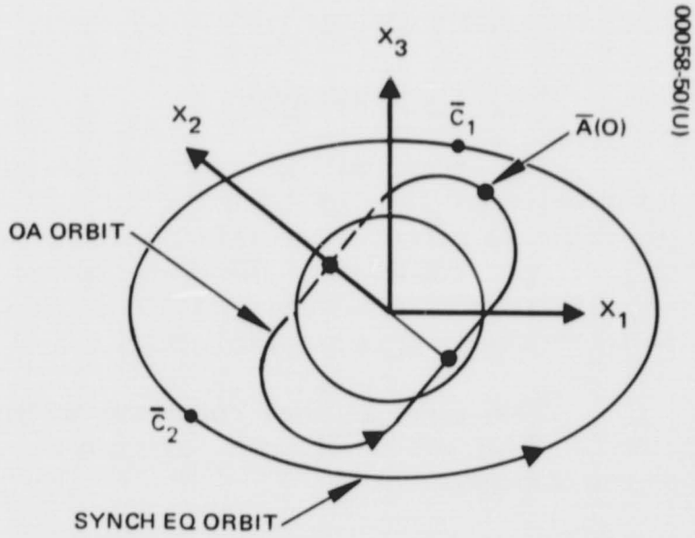

Figure C-2

where

R_c is the synchronous orbit radius (22,771 n.mi.)

T_c is the synchronous orbit period (1440 minutes)

and

θ_c is the sum of an initial phase angle establishing the longitudinal orientation of the OA orbit relative to earth at time t = 0, plus the station longitude of the particular synchronous satellite being tracked. (The computer program will accept three satellite longitudes.) NSAT is an index variable identifying the particular communication satellite currently being tracked.

(Note: The quantities R_c and T_c are prestored in the computer program. The longitudinal references, THETAC, relating the AAP/OA orbit to the earth at time T = 0, and the locations of the communication satellites, DTHETA(NSAT), are inputted by data cards.)

C.2.4 Y' Coordinate Reference

A Y' reference is obtained by a negative rotation about the X_2 axis of the angle i, the inclination of the AAP/OA orbit, or

$$\overline{Y}' = [T1]\,\overline{X} \tag{2}$$

where

$[T1] = RM(2, -i)^*$

C.2.5 AAP/OA Position

The position of the AAP/OA is given by the vector $\overline{A}$. Its components in the Y' coordinates, are

$$AY_1 = RA \cos(2\pi T/TA)$$

$$AY_2 = RA \sin(2\pi T/TA)$$

$$AY_3 = 0 \tag{3}$$

*RM (NAXIS, ANGLE) is a rotation matrix corresponding to a positive rotation about principal axis numbered NAXIS and through a displacement ANGLE. The rotation matrices for each of the three principal axes are defined in Section C.2.14.

where

RA is the orbit altitude (220 n. mi.)

TA is the orbit period (92 min.)

(Note: Values of the quantities RA and TA are prestored in the computer program.)

For later use, the components, in X coordinates, are

$$AX_1 = AY_1 \cos i$$

$$AX_2 = AY_2$$

$$AX_3 = AY_1 \sin i \qquad (4)$$

C.2.6 O/A Orientation

In its normal mode, the AAP/OA is in a sun-inertial orientation, with its first axis (XA) in the orbit plane and its third axis (ZA) directed toward the sun. The sun direction is inputted to the computer as a unit vector, $\overline{S}$, whose components, in the X reference, are SX_1, SX_2, and SX_3. (For the attached case, SX = (1, 0, 0.)

To accomplish the desired orientation, the OA will be rotated about its Ya axis (Y_2') through an angle B, followed by a rotation about the Xa axis through an angle Dl. As intermediate steps, the Y, Z, and U coordinate references will be defined.

C.2.7 Y Coordinate Reference

The Y reference differs from the Y' (defined in Section C.2.4) only by a translation corresponding to the position of the OA, namely:

$$\overline{Y} = \overline{Y}' - \overline{A} \qquad (5)$$

C.2.8 Z Coordinate Reference

The Z axes are obtained by a rotation about Y_3 through the angle B.

$$Z = [T2]\ Y \tag{6}$$

where

$$[T2] = RM(3,\ B)$$

C.2.9 U Coordinate Reference

The U reference is obtained by a rotation about Z through the angle D. The angle D = D1 + DD, where D1, defined in Section C.2.6, is the spacecraft roll required to orient the OA Za axis toward the sun, and DD is the angular displacement, about the Xa axis, of the antenna boom relative to the Ya axis, as discussed in Section C.1. Then

$$U = [T3]\ Z \tag{7}$$

where

$$[T3] = RM(1,\ D)$$

C.2.10 Determination of Angles B and D1

$$Su = [T3']\ [T2]\ Sy \tag{8}$$

where

$$Sy = [T1]\ Sx \tag{9}$$

and [T3'] is the same as [T3] except for the substitution of angle D1 for D. Expanding Equation 8 into its component equations:

$$Su_1 = \cos B \cdot SY_1 + \sin B \cdot SY_2 \tag{8.1}$$

$$Su_2 = \sin B \cdot \cos D \cdot SY_1 + \cos B \cdot \cos D \cdot SY_2 + \sin D \cdot SY_3 \tag{8.2}$$

and

$$Su_3 = \sin B \cdot \sin D \cdot SY_1 - \cos B \cdot \sin D \cdot SY_2 + \cos D \cdot SY_3 \tag{8.3}$$

To establish the desired sun-inertial orientation, the angles B and Dl must be such that the sun vector, $\bar{S}u = (0, 0, 1)$. Using this criterion, Equation 8.1 is solved for

$$B = \arctan - SY_1/SY_2 \tag{10}$$

B may be limited to the range of $-\pi/2 \leq B \leq +\pi/2$ without any loss of capability. Proceeding, Equation 11.2 is solved for

$$Dl = \arctan \frac{\sin B \cdot SY_1 - \cos B \cdot SY_2}{SY_3} \tag{11}$$

At this point, rotations [T2] and [T3] are fully defined.

C.2.11 Earth Shadowing

Referring to Figure C-3, a particular communication satellite located at the end of vector $\bar{C}$(NSAT) is visible to the SWS, at position $\bar{A}$, if the line of sight from $\bar{A}$ to $\bar{C}$ does not penetrate the effective atmosphere of the earth. The radius of the effective atmosphere is defined as

$$REA = RE + DRE \tag{12}$$

where

RE is the earth surface radius

and

DRE is the effective altitude of the earth's atmosphere, as shown in Figure C-3

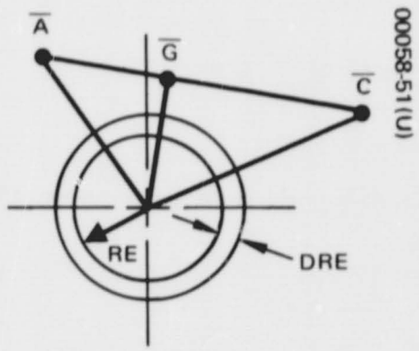

Figure C-3

To determine atmospheric penetration, the vector $\bar{G}$, perpendicular to the line of sight from $\bar{A}$ to $\bar{C}$, is defined as

$$\bar{G} = \bar{A} + K_1 (\bar{C} - \bar{A}) = K_1 \bar{C} + (1 - K_1) \bar{A} \tag{13}$$

Because of its perpendicularity,

$$\bar{G} \cdot (\bar{C} - \bar{A}) = 0 \tag{14}$$

Substituting the value of $\bar{G}$ from Equation 13 and performing the dot product of Equation 14:

$$0 = [\bar{A} + K_1 (\bar{C} - \bar{A})] \cdot (\bar{C} - \bar{A})$$

$$= \bar{A} \cdot (\bar{C} - \bar{A}) + K_1 (\bar{C} - \bar{A}) \cdot (\bar{C} - \bar{A})$$

$$= \bar{A} \cdot \bar{C} - \bar{A} \cdot \bar{A} + K_1 (\bar{C} - \bar{A}) \cdot (\bar{C} - \bar{A}) \tag{15}$$

However,

$$\bar{A} \cdot \bar{A} = \left|A\right|^2 = R_a^{\,2} \text{ and } (\bar{C} - \bar{A}) \cdot (\bar{C} - \bar{A}) = \left|\bar{C} - \bar{A}\right|^2 = R^2$$

where R is the range between the OA and the communication relay satellite. Solving Equation 15:

$$K_1 = \frac{R_a^{\,2} - \bar{A} \cdot \bar{C}}{R^2} \tag{16}$$

where

$$\bar{A} \cdot \bar{C} = AX_1 \cdot CX_1 + AX_2 \cdot CX_2 + AX_3 \cdot CX_3 \tag{17}$$

and

$$R^2 = (AX_1 - CX_1)^2 + (AX_2 - CX_2)^2 + (AX_3 - CX_3)^2 \qquad (18)$$

If $K_1 < 0$, the geometry is as shown in Figure C-4, and atmospheric penetration obviously cannot occur.

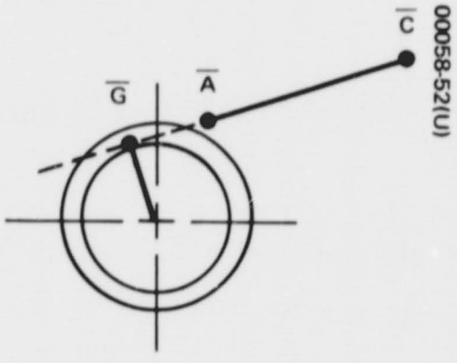

Figure C-4

When $K_1 \geq 0$, interception will occur only if $|G| < REA$, where

$$|G|^2 = \sum_{i=1}^{3} (K_1\, CX_i + (1 - K_1)\, AX_i)^2$$

In performing this computation on the computer, the satellite most recently observed will be tested first. If visibility exists, the computation proceeds. Otherwise, the remaining satellites are tested until visibility is established. If no satellite is visible, the process will be repeated at intervals of time, DT, until some satellite becomes visible, or until an interval of 0.7 TA has elapsed, in which case an error stop is programmed.

C.2.12 Arbitrary Rotation - V Coordinate Reference

To provide for a redefinition of the antenna boom orientation, or any other rotation which may be derived, an arbitrary rotation matrix, Q, is defined, such that

$$\bar{V} = [Q]\ \bar{U} \qquad (20)$$

For the initial study, Q is defined as a unity matrix, i.e.,

$$Q = \begin{bmatrix} 1 & 0 & 0 \\ 0 & 1 & 0 \\ 0 & 0 & 1 \end{bmatrix}$$

C.2.13 Determination of Gimbal Angles (Az, El)

Achievement of the desired gimbal angles is characterized by the components of the satellite position vector $\bar{C}$, expressed in W coordinates, satisfying the condition

$$\bar{C}W = (0, R, 0) \tag{21}$$

where the W coordinates are established by a rotation about V_2, through the angle Az, followed by a rotation about V_1', through the angle El, i.e.,

$$\bar{W} = [T5]\,[T4]\,\bar{V} \tag{22}$$

where

$$[T4] = \begin{bmatrix} \cos Az & 0 & -\sin Az \\ 0 & 1 & 0 \\ \sin Az & 0 & \cos Az \end{bmatrix} = RM(2, Az) \tag{23}$$

and

$$[T5] = \begin{bmatrix} 1 & 0 & 0 \\ 0 & \sin El & \sin El \\ 0 & -\cos El & \cos El \end{bmatrix} = RM(1, El) \tag{24}$$

Expanding Equation 22 into its components and substituting the components of CW from Equation 21:

$$CW_1 = 0 = \cos Az \cdot CV_1 - \sin Az \cdot CV_3 \tag{25}$$

$$CW_2 = R = \sin Az \cdot \sin El \cdot CV_1 + \cos El \cdot CV_2 = \cos Az \cdot \sin El \cdot CV_3 \tag{26}$$

and

$$CW_3 = 0 = \sin Az \cdot \cos El \cdot CV_1 - \sin El \cdot CV_2 = \cos Az \cdot \cos El \cdot CV_3 \tag{27}$$

Solving Equation 25,

$$Az = \arctan CV_1/CV_3 \tag{28}$$

and, from Equation 27,

$$El = \arctan \frac{\sin Az \cdot CV_1 + \cos Az \cdot CV_3}{CV_2} \tag{29}$$

As an error check, the value of R determined by Equation 26 is compared with the value determined by Equation 18. If the difference exceeds 1 n. mi., an error stop is programmed.

C. 2. 14 Definition of Rotation Matrices

The rotation matrices, RM (NAXIS, ANGLE) are defined as follows:

Let

c = cos (angle)

s = sin (angle)

Then

$$RM(1, \text{angle}) = \begin{bmatrix} 1 & 0 & 0 \\ 0 & c & s \\ 0 & -s & c \end{bmatrix}$$

$$RM(2, \text{angle}) = \begin{bmatrix} c & 0 & -s \\ 0 & 1 & 0 \\ s & 0 & c \end{bmatrix}$$

$$RM(3, \text{angle}) = \begin{bmatrix} c & s & 0 \\ -s & c & 0 \\ 0 & 0 & 1 \end{bmatrix}$$

C.3 COMPUTER PROGRAM

C.3.1 List of Program ST-1

```
C      FORTRAN DECK
CST1C                AAP/SWS SPACE TERMINAL GIMBAL ANGLES
      REAL I, K1, K2
      DIMENSION CX(3), CY(3), CV(3) , AX(3), AY(3), SX(3), SY(3), T1(3,3
     1), T2(3,3), T3(3,3), P(3,3), Q(3,3), THETA(3), DTHETA(3), PI(3,3),
     2CY1(3), AZ(600), EL(600)
      DATA  ((Q(J,K), K=1,3), J=1,3) / 1., 3*0., 1., 3*0., 1. /
      DATA  RC,TC, RE, PI       / 22771., 1440., 3441., 3.141859        /
      PI = ATAN  (1.)*4.
      READ (5,1) RA, TA, I
      READ (5,2) NS1, DTHETA
      READ (5,2) NCASE, SX, DD
      READ (5,2) NCASE, DRE
   74 READ (5,2) NCASE, THETAC, DT, T,TMAX
    2 FORMAT( I2, 6F10.2)
    9 X= -THETAC
      AZ2 = 0.
      AZDOT1 = 0.
      ELDOT1 = 0.
      WRITE (6,201) RA, TA, I, I, X
      WRITE (6,202) RC, TC, NS1, (DTHETA(J), J= 1,NS1)
      WRITE (6,203) RE, DRE, DD
  201 FORMAT (1H1 9X, 24HAAP/SWS ORBIT PARAMETERS //19X 12HORBIT RADIUS
     1 6X  F6.1, 7H N. MI./ 19X 12HORBIT PERIOD 6X F6.1, 9H MIN. /19X
     2 17HORBIT INCLINATION  6X F6.1, 8H DEGREES //19X 26HTHE SUB-ORBIT
     3POINT AT TIME T = 0 IS  F6.1,21H DEGREES, N. LATITUDE /46X 5HAND
     4 F6.1, 23H DEGREES, W. LONGITUDE. ///)
  202 FORMAT( 10X,34HCOMMUNICATION SATELLITE PARAMETERS // 19X 12HORBIT
     1RADIUS F8.1,  7H N. MI. / 19X 12HORBIT PERIOD  F6.1, 9H MIN. / 19X
     2 I1, 65H SATELLITES ARE EMPLOYED.  THEIR LOCATIONS, IN DEGREES, N.
     3 LONG., / 19X 3HARE  3F12.2)
  203 FORMAT(///10X 16HOTHER PARAMETERS  // 19X 12HEARTH RADIUS F14.1,7H
     1N. MI. /19X 20HEFFECTIVE ATMOSPHERE F6.1, 7H N. MI. / 19X 56HOFFSE
     2T OF THE ANTENNA BOOM RELATIVE TO THE S/C Y AXIS IS F6.1,5H DEG.
     3///)
      RPD = PI/180.
      PI2 = 2.*PI
C  SWS ORBIT INCLINATION ROTATION MATRIX (T1)
      SI  = SIN(I*RPD)
      CI  = COS(I*RPD)
      XX = -I * RPD
      CALL RMAT (2,XX,T1)
C  SUN INERTIAL ORIENTATION
      CALL MXMP(T1,SX,3,3,3,1,SY)
      IF(SY(2).EQ.0.) GO TO 22
      B = ATAN ( -SY(1)/SY(2))
   23 CB = COS(B)
      SB = SIN(B)
      B  = B/RPD
      D1= ATAN2( (SB*SY(1) - CB*SY(2)) , SY(3) )
      D = D1 +DD * RPD
      D1= D1/RPD
```

```
      CD= COS(D)
      SD= SIN(D)
      WRITE (6, 101)  SX, B, D1
C  SUN INERTIAL ROTATION MATRICES (T2,T3)
      CALL RMAT (2, B,T2)
      CALL RMAT (1, D,T3)
      WA  = PI2/TA
      WC  = PI2/TC
C  MISC. INITIALIZION (NOT TIME VARYING)
      DO 21 J=1,3
   21 THETA(J)=(THETAC + DTHETA(J))*RPD
      CX(3) = 0.
      AY(3)=0.
      NP = 1
      NS = 0
      NSAT = 1
      NSAT1 = 0
      R1 = 0.
      EL1 = 0.
      AZ1 = 0.
      TDOT= 0.
      REA= RE + DRE
      NXFR = 0
      CALL MXMP(T3,T2,3,3,3,3,P1)
      CALL MXMP(Q ,P1,3,3,3,3,P )
      WRITE(6, 110)
C  POSITION OF SAT AND S/C AT TIME T
   43 CC = WC*T + THETA(NSAT)
      AA = WA*T
      CX(1) = RC*COS(CC)
      CX(2) = RC*SIN(CC)
      AY(1) = RA*COS(AA)
      AY(2) = RA*SIN(AA)
C  SELECTION OF COMM. SAT. IN VIEW (EARTH INTERCEPT SOLUTION)
      AX(1) = AY(1)*CI
      AX(2) = AY(2)
      AX(3) = AY(1)*SI
      RSQ=0.
      AC =0.
      DO 31 J=1,3
      RSQ = RSQ + ( CX(J)- AX(J) )**2
   31 AC  = AC +  AX(J)*CX(J)
      K1 =  (RA**2 - AC)/RSQ
      K2 =  1. - K1
      IF (K1.LT.0.) GO TO 41
      G = 0.
      DO 42 J=1,3
   42 G = G + (K1*CX(J)+K2*AX(J))**2
      G = SQRT (G)
      IF (G.GT.REA) GO TO 41
      NXFR = NXFR + 1
      IF (NXFR.GE.NS1) GO TO 99
```

```
 44   NS = MOD(NS + 1, NS1)
      NSAT= NS + 1
      GO TO 43
 41   NXER = 0
      IF (TOUT.GT.0.) WRITE (6,109) TOUT
      TOUT= 0.
C  DETERMINATION OF GIMBAL ANGLES
      CALL MXMP(T1, CX, 3,3, 3,1, CY1)
      CALL MXSB(CY1, AY, 3,1, CY)
      CALL MXMP(P, CY, 3,3, 3,1, CV)
      XAZ = ATAN2(CV(1), CV(3))
      IF(ABS(XAZ).LT.PI-0.1) GO TO 79
      IF(AZ2/XAZ.GE.0.) GO TO 79
      XAZ =SIGN (PI2 - ABS(XAZ), AZ2 )
 79   AZ2 = XAZ
      CAZ = COS(XAZ)
      SAZ = SIN(XAZ)
      AZ(NP) = XAZ/RPD
      IF(CV(2).EQ.0.) GO TO 52
 50   XEL = ATAN2( (SAZ*CV(1) + CAZ*CV(3)),CV(2))
 53   CEL = COS(XEL)
      SEL = SIN(XEL)
      EL(NP) = XEL/RPD
      R = ABS( SAZ*SEL*CV(1) + CEL*CV(2) + CAZ*SEL*CV(3) )
      RERR = R - SQRT(RSQ)
      RERR = ABS(RERR)
      IF(RERR.GT.1.) GO TO 93
      IF (NSAT.NE.NSAT1) GO TO 81
      IF (T.GT.TDOT + 1.5*DT) GO TO 81
      RDOT = (R - R1)/DT
      ELDOT = (EL(NP) - EL1)/DT
      AZDOT = (AZ(NP) - AZ1)/DT
      WRITE (6,111) T, R, AZ(NP), EL(NP), NSAT, RDOT, AZDOT, ELDOT
      IF(ABS(AZDOT).LE.AZDOT1) GO TO 89
      AZDOT1 = ABS(AZDOT)
      TAZDOT = T
 89   IF(ABS(ELDOT).LE.ELDOT1) GO TO 82
      ELDOT1 = ABS(ELDOT)
      TELDOT = T
 82   R1 = R
      NSAT1 = NSAT
      EL1 = EL(NP)
      AZ1 = AZ(NP)
      TDOT = T
      IF (T.GT.TMAX) GO TO 51
      T = T + DT
      NP= NP+ 1
      GO TO 43
 51   CALL CPLOT2 (1, AZ, 9.,30HAZIMUTH GIMBAL ANGLE (DEGREES), 30, 9.,
     1 32HELEVATION GIMBAL ANGLE (DEGREES), 32, NP, EL )
      WRITE (6, 102) AZDOT1, TAZDOT, ELDOT1, TELDOT
      IF (NCASE.NE.0) GO TO (71, 72, 73, 74),      NCASE
```

```
 59   STOP
 71   READ (5,2) NCASE, I
      T = 0.
      GO TO  9
 72   READ (5,2) NCASE, SX, DD
      T = 0.
      GO TO  9
 73   READ (5,2) NCASE, DRE
      T = 0.
      GO TO  9
 22   B= SIGN (PI/2., -SY(1))
      GO TO 23
 81   WRITE (6,11?) T, R, AZ(NP), EL(NP), NSAT
      GO TO 82
 99   T= T+DT
      TOUT = TOUT + DT
      NXFR=0
      IF(TOUT.LT. 0.7*TA) GO TO 44
      WRITE(6, 97)  T, TOUT
      STOP
 32   XEL= SIGN(PI/2., XEL)
      GO TO 53
 98   XRSQ= SQRT(RSQ)
      WRITE (6,96)  T, R, XRSQ, RERR
      CALL PDUMP
 96   FORMAT(1H0,5F15.5)
      STOP
  1   FORMAT( 7F10.2)
 97   FORMAT(/// 10X13HERROR MESSAGE // 10X 34HUNABLE TO ACQUIRE COMM SA
     1T AT TIME  F7.1, 44H MIN.  NO SAT HAS BEEN OBSERVED FOR THE LAST
     2F7.1, 5H MIN.)
 101  FORMAT(   10X22HFOR A SUN VECTOR SX = ( 3F10.5,  1H) // 10X23HTHE
     1SWS MUST BE ROTATED  F7.1, 25H DEGREES ABOUT ITS Z AXIS
     2                    /22X11HAND ROTATED F7.1, 25H DEGREES ABOUT S/C X
     3 AXIS/ 22X33HTO ORIENT S/C Z AXIS TOWARDS SUN. ////)
 102  FORMAT(///10X 41HTHE MAXIMUM GIMBAL RATES (ABS. VALUE) ARE // 10X
     1 7HAZDOT =  F6.1, 27H DEG/MIN, WHICH OCCURRED AT  F6.0,10H MIN., A
     2ND // 10X  7HELDOT =  F6.1, 27H DEG/MIN, WHICH OCCURRED AT  F6.0,
     3 5H MIN. )
 109  FORMAT(/ 10X 50HTIME OUTAGE DUE TO LACK OF SATELLITE VISIBILITY IS
     1 F6.0, 5H MIN.  //)
 110  FORMAT( 8X 4HTIME  3X5HRANGE  3X7HAZIMUTH 5X5HELEV. 6X4HSAT. 5X5HR
     1 DOT 4X6HAZ DOT 4X6HEL DOT / 8X4HMIN. 3X5HN.MI. 6X4HDEG. 6X4HDEG.
     2 7X3HNO. 2X8HN MI/MIN 3X7HDEG/MIN 3X7HDEG/MIN //)
 111  FORMAT( F12.1, F8.0, 2F10.1, I10, F10.1, 2F10.2)
      END
```

C.3.2 List of Subroutine RMAT

RMAT is a subroutine for generation of rotation matrices about a principal axis.

```
$      OPTION  FORTRAN
$      FORTRAN LSTOU,DECK,COMDK
       SUBROUTINE RMAT (NAXIS, ANGLE, RM)
C&R                ROTATION MATRIX
C
C  NAXIS IS THE NUMBER OF THE PRINCIPAL AXIS ABOUT WHICH THE ROTATION IS
C        TO BE MADE
C
C  ANGLE IS THE ANGULAR ROTATION, IN RADIANS
C
C  RM    IS THE (3 X 3) ROTATION MATRIX
C
       DIMENSION RM(3,3)
       C= COS(ANGLE)
       S= SIN(ANGLE)
       IF(NAXIS-2)1,2,3
    1  RM(1,1)= 1.
       RM(1,2)= 0.
       RM(1,3)= 0.
       RM(2,1)= 0.
       RM(2,2)= C
       RM(2,3)= S
       RM(3,1)= 0.
       RM(3,2)=-S
       RM(3,3)= C
       RETURN
    2  RM(1,1)= C
       RM(1,2)= 0.
       RM(1,3)=-S
       RM(2,1)= 0.
       RM(2,2)= 1.
       RM(2,3)= 0.
       RM(3,1)= S
       RM(3,2)= 0.
       RM(3,3)= C
       RETURN
    3  RM(1,1)= C
       RM(1,2)= S
       RM(1,3)= 0.
       RM(2,1)=-S
       RM(2,2)= C
       RM(2,3)= 0.
       RM(3,1)= 0.
       RM(3,2)= 0.
       RM(3,3)= 1.
       RETURN
       END
```

C. 3. 3 Data Input for Sample Case

```
$       EXECUTE
$       LIMITS  5,24000,,5000
        1.          0.          0.          15.
       20.
 2     24.5       -174.        -62.5
        0.          1.          0.         100.
$       ENDJOB
```

SX,DD
DRE
DTHETA
MISC

C.4 TABULATED COMPUTER OUTPUT

AAP/SWS ORBIT PARAMETERS

ORBIT RADIUS 3661.0 N. MI.
ORBIT PERIOD 92.0 MIN.
ORBIT INCLINATION 35.0 DEGREES

THE SUB-ORBIT POINT AT TIME T = 0 IS 35.0 DEGREES, N. LATITUDE
AND -15.0 DEGREES, W. LONGITUDE.

COMMUNICATION SATELLITE PARAMETERS

ORBIT RADIUS 22771.0 N. MI.
ORBIT PERIOD 1440.0 MIN.
2 SATELLITES ARE EMPLOYED. THEIR LOCATIONS, IN DEGREES, W. LONG.,
ARE 24.50 -174.00

OTHER PARAMETERS

EARTH RADIUS 3441.0 N. MI.
EFFECTIVE ATMOSPHERE 20.0 N. MI.
OFFSET OF THE ANTENNA BOOM RELATIVE TO THE S/C Y AXIS IS 15.0 DEG.

FOR A SUN VECTOR SY = (1.00000 0. 0.)

THE SWS MUST BE ROTATED -90.0 DEGREES ABOUT ITS Z AXIS
AND ROTATED -125.0 DEGREES ABOUT S/C X AXIS
TO ORIENT S/C Z AXIS TOWARDS SUN.

TIME MIN.	RANGE N.MI.	AZIMUTH DEG.	ELEV. DEG.	SAT. NO.	R DOT N MI/MIN	AZ DOT DEG/MIN	EL DOT DEG/MIN
0.	20653.	-70.3	66.0	1			
1.0	20491.	-70.0	65.9	1	-161.7	0.25	-0.06
2.0	20330.	-69.7	65.9	1	-152.0	0.28	-0.03
3.0	20198.	-69.4	65.9	1	-141.5	0.32	-0.00
4.0	20068.	-69.1	65.9	1	-130.1	0.35	0.03
5.0	19959.	-68.7	66.0	1	-118.0	0.37	0.06
6.0	19844.	-68.3	66.1	1	-105.1	0.39	0.09
7.0	19753.	-67.9	66.2	1	-91.6	0.41	0.12
8.0	19675.	-67.5	66.3	1	-77.5	0.43	0.15
9.0	19613.	-67.0	66.5	1	-62.8	0.44	0.18
10.0	19565.	-66.6	66.7	1	-47.7	0.44	0.21
11.0	19533.	-66.2	67.0	1	-32.3	0.44	0.24
12.0	19516.	-65.7	67.2	1	-16.7	0.44	0.26
13.0	19515.	-65.3	67.5	1	-0.8	0.43	0.29
14.0	19530.	-64.9	67.8	1	15.0	0.41	0.31
15.0	19561.	-64.5	68.1	1	30.8	0.39	0.33
16.0	19607.	-64.1	68.5	1	46.4	0.37	0.35
17.0	19669.	-63.8	68.9	1	61.7	0.34	0.37
18.0	19746.	-63.5	69.2	1	76.7	0.31	0.38
19.0	19837.	-63.2	69.6	1	91.2	0.28	0.39
20.0	19942.	-62.9	70.0	1	105.2	0.25	0.40

21.0	20861.	-62.7	70.4	1	118.6	0.21	0.40
22.0	20192.	-62.6	70.8	1	131.3	0.17	0.40
23.0	20335.	-62.4	71.2	1	143.2	0.13	0.40
24.0	20480.	-62.3	71.6	1	154.3	0.09	0.40
25.0	20654.	-62.3	72.0	1	164.6	0.04	0.39
26.0	20828.	-62.3	72.4	1	174.0	0.00	0.38
27.0	21010.	-62.3	72.8	1	182.4	-0.04	0.37
28.0	21200.	-62.4	73.1	1	190.0	-0.08	0.36
29.0	21397.	-62.6	73.5	1	196.5	-0.13	0.35
30.0	21599.	-62.7	73.8	1	202.1	-0.17	0.33
31.0	21806.	-62.9	74.1	1	206.8	-0.21	0.32
32.0	22016.	-63.2	74.4	1	210.5	-0.25	0.30
33.0	22230.	-63.5	74.7	1	213.2	-0.28	0.28
34.0	22445.	-63.8	75.0	1	215.0	-0.32	0.26
35.0	22661.	-64.1	75.2	1	215.9	-0.36	0.25
36.0	22877.	-64.5	75.4	1	215.9	-0.39	0.23
37.0	23092.	-65.0	75.7	1	215.1	-0.42	0.21
38.0	23305.	-65.4	75.8	1	213.3	-0.45	0.19
39.0	23516.	-65.9	76.0	1	210.8	-0.48	0.17
40.0	21417.	117.0	113.9	2			
41.0	21232.	117.1	114.1	2	-184.9	0.10	0.19
42.0	21053.	117.2	114.3	2	-179.1	0.14	0.17
43.0	20881.	117.4	114.4	2	-172.4	0.18	0.15
44.0	20716.	117.6	114.5	2	-164.7	0.22	0.12
45.0	20560.	117.9	114.6	2	-156.2	0.26	0.10
46.0	20413.	118.2	114.7	2	-146.9	0.29	0.07
47.0	20276.	118.5	114.8	2	-136.7	0.32	0.04
48.0	20151.	118.9	114.8	2	-125.7	0.35	0.01
49.0	20037.	119.2	114.7	2	-114.0	0.38	-0.02
50.0	19935.	119.6	114.7	2	-101.6	0.40	-0.05
51.0	19846.	120.1	114.6	2	-88.6	0.42	-0.08
52.0	19771.	120.5	114.5	2	-75.0	0.43	-0.11
53.0	19711.	120.9	114.4	2	-60.9	0.44	-0.15
54.0	19664.	121.4	114.2	2	-46.4	0.45	-0.18
55.0	19633.	121.8	114.0	2	-31.6	0.45	-0.21
56.0	19616.	122.3	113.7	2	-16.5	0.44	-0.24
57.0	19615.	122.7	113.5	2	-1.3	0.43	-0.26
58.0	19629.	123.1	113.2	2	13.9	0.42	-0.29
59.0	19658.	123.5	112.9	2	29.1	0.40	-0.31
60.0	19702.	123.9	112.5	2	44.1	0.37	-0.33
61.0	19761.	124.2	112.2	2	58.9	0.35	-0.35
62.0	19834.	124.5	111.8	2	73.3	0.32	-0.37
63.0	19922.	124.8	111.4	2	87.4	0.28	-0.38
64.0	20022.	125.1	111.0	2	100.9	0.25	-0.39
65.0	20136.	125.3	110.6	2	113.8	0.21	-0.40
66.0	20262.	125.5	110.2	2	126.1	0.17	-0.40
67.0	20400.	125.6	109.8	2	137.6	0.13	-0.40
68.0	20548.	125.7	109.4	2	148.5	0.08	-0.40
69.0	20707.	125.7	109.0	2	158.5	0.04	-0.40
70.0	20874.	125.7	108.6	2	167.6	-0.00	-0.39
71.0	21050.	125.7	108.3	2	175.9	-0.05	-0.39
72.0	21234.	125.6	107.9	2	183.3	-0.09	-0.38
73.0	21423.	125.4	107.5	2	189.8	-0.13	-0.36
74.0	21619.	125.3	107.2	2	195.4	-0.17	-0.35
75.0	21819.	125.0	106.8	2	200.0	-0.21	-0.34
76.0	22023.	124.8	106.5	2	203.7	-0.25	-0.32
77.0	22229.	124.5	106.2	2	206.6	-0.29	-0.30

78.0	22438.	124.2	105.9	2	208.5	-0.33	-0.29
79.0	22647.	123.8	105.7	2	209.5	-0.36	-0.27
80.0	22857.	123.4	105.4	2	209.7	-0.40	-0.25
81.0	23066.	123.0	105.2	2	209.0	-0.43	-0.23
82.0	23273.	122.5	105.0	2	207.5	-0.46	-0.21
83.0	23479.	122.0	104.8	2	205.2	-0.49	-0.19
84.0	23681.	121.5	104.6	2	202.1	-0.52	-0.17
85.0	23228.	-95.1	71.1	1			
86.0	23005.	-95.4	71.0	1	-223.0	-0.30	-0.14
87.0	22780.	-95.7	70.9	1	-225.3	-0.26	-0.13
88.0	22554.	-95.9	70.8	1	-226.6	-0.22	-0.12
89.0	22326.	-96.1	70.7	1	-227.1	-0.19	-0.10
90.0	22099.	-96.2	70.6	1	-226.6	-0.15	-0.09
91.0	21874.	-96.4	70.5	1	-225.1	-0.11	-0.07
92.0	21652.	-96.4	70.4	1	-222.6	-0.07	-0.06
93.0	21433.	-96.4	70.4	1	-219.1	-0.02	-0.04
94.0	21218.	-96.4	70.4	1	-214.5	0.02	-0.02
95.0	21009.	-96.4	70.4	1	-208.9	0.06	-0.00
96.0	20807.	-96.3	70.4	1	-202.2	0.10	0.02
97.0	20612.	-96.1	70.4	1	-194.5	0.14	0.04
98.0	20427.	-95.9	70.5	1	-185.7	0.18	0.06
99.0	20251.	-95.7	70.6	1	-175.8	0.22	0.08
100.0	20086.	-95.5	70.7	1	-165.0	0.25	0.11
101.0	19933.	-95.2	70.8	1	-153.1	0.29	0.13

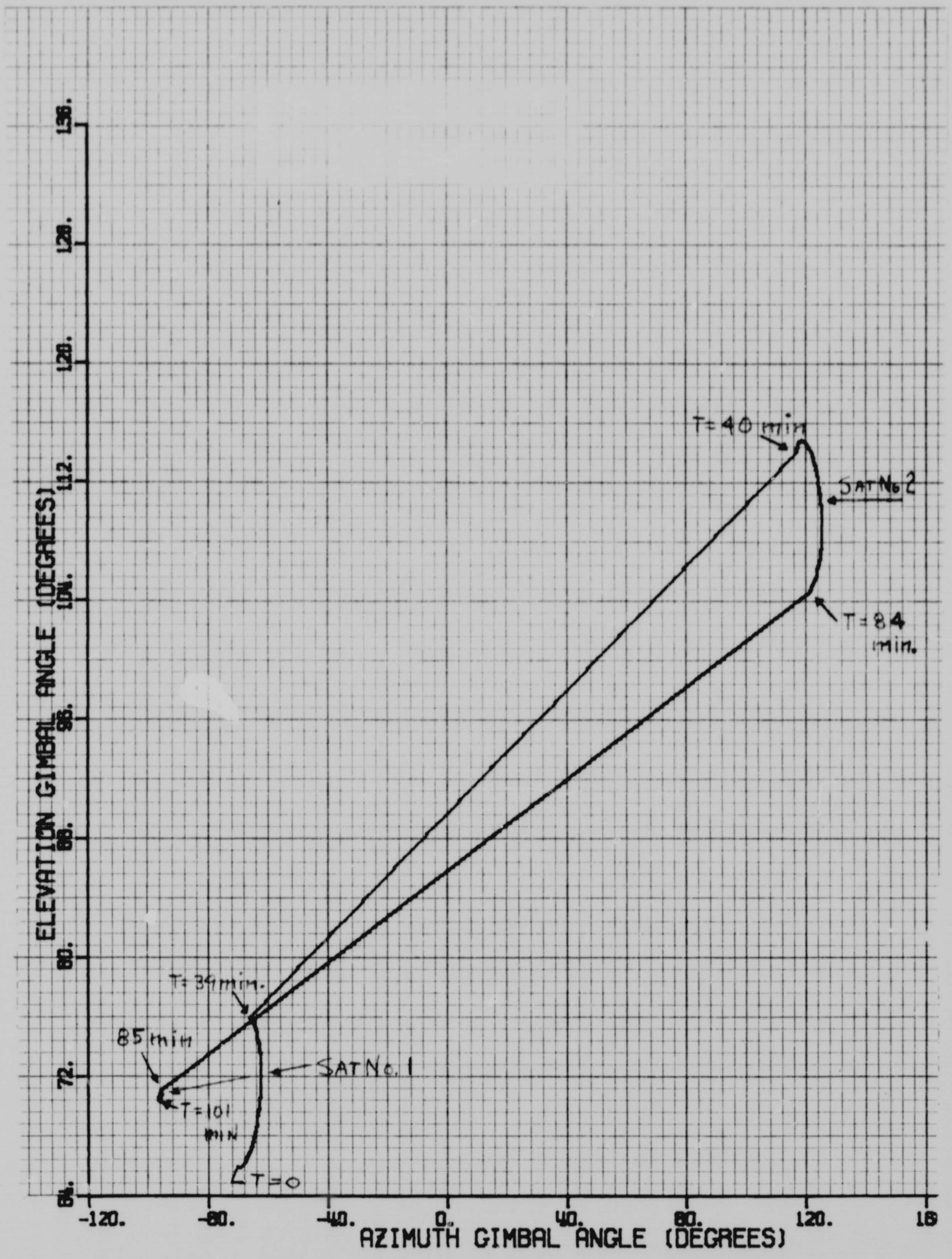
ELEVATION GIMBAL ANGLE (DEGREES)
136.
128.
120.
112.
104.
96.
88.
80.
72.
64.
-120.
-80.
-40.
0.
40.
80.
120.
160
AZIMUTH GIMBAL ANGLE (DEGREES)
T=40 min
SAT No 2
T=84 min.
T=34 min.
85 min
SAT No. 1
T=101 min
T=0

C.6 LIST OF SYMBOLS

SYMBOL DEFINITIONS

AA = DUMMY VARIABLE-COMM. RELAY ORBIT ANGLE (RADIANS

AC = DOT PRODUCT OF VECTORS A AND C

AX = S/C VECTOR (X COORD)

AY = S/C VECTOR IN Y PRIME COORDINATES

AZ = FIRST (AZIMUTH) GIMBAL ANGLE

AZDOT AZIMUTH GIMBAL RATE ((AZ(T) - AZ(T-DT))/DT)

B = ROTATION (FROM NORTH) OF S/C X AXIS TO PERMIT AIMING Z TO SUN (DEG)

CC = DUMMY VARIABLE-COMM. RELAY ORBIT ANGLE (RADIANS)

CV = COMM SAT VECTOR IN V COORD.

CX = COMM. SAT. VECTOR IN X COORDINATES

CY = COMM SAT VECTOR IN Y COORD.

CY1 = COMM SAT VECTOR IN Y PRIME COORD

D = (D1+DD) * RPD (RADIANS)

D1 = ROTATION OF S/C ABOUT X AXIS TO ORIENT Z TOWARDS SUN (DEGREES)

DD = RADIAL ORIENTATION OF ANT BOOM RELATIVE TO S/C Z AXIS (DEGREES)

DRE = INCREMENT IN EARTH RADIUS TO CLEAR ATMOS AND/OR MAIN BEAM

IT = COMPUTATIONAL TIME INCREMENT (MINUTES)

DTHETA = RELATIVE LONGITUDES OF COMM SATS

EL = SECOND (ELEVATION) GIMBAL ANGLE

ELDOT ELEVATION GIMBAL RATE ((EL(T) - EL(T-DT))/DT)

G = VECTOR FROM EARTH CENTER NORMAL TO LOS BETWEEN SWS AND SAT.

I = S/C ORBIT INCLINATION (DEGREES)

K1,K2 = COEFFICIENTS USED IN EARTH INTERCEPT SOLUTION (K2=1-K1)

NP = INDEX OF STORED DATA TO BE PLOTTED

NS = NSAT -1 (DUMMY VARIABLE USED FOR INDEXING NSAT)

NSAT = NO. OF COMM SAT BEING TRACKED

NSAT1 NUMBER OF SATELLITE BEING TRACKED ON PREVIOUS ITERATION

NXFR TEST VARIABLE USED IN SEARCHING FOR VISIBLE SATELLITE

P = INTERMEDIATE ROTATION MATRIX - P=Q*T3*T2

P1 = INTERMEDIATE MATRIX USED IN EVALUATING P

PI = PI (3.14159)

PI2 = 2*PI

Q = ARBITRARY ROTATION

R = COMPUTED DISTANCE BETWEEN S/C AND COMM SAT

R1 = COMPUTED RANGE IN PREVIOUS ITERATION

RA = RADIUS OF APOLLO S/C ORBIT (N. MI.)

RC = RADIUS OF COMM. SAT. ORBIT (N. MI.)

RDOT = RANGE RATE ((R(T) - R(T-DT))/DT)

RE = EARTH RADIUS (3441 W. MI.)

REA = RADIUS OF EARTHS ATMOS. (RE + DRE)

RERR = DIFFERENCE IN CPMPUTED VALUES OF RANGE

RPD = RADIANS PER DEGREE CONVERSION FACTOR

RSQ = RANGE (R) SQUARED

SX = UNIT VECTOR DEFINING SUN ANGLE (X COORD)

SY = UNIT VECTOR - SUN ANGLE (Y COORD)

T = TIME (MINUTES)

T1 = FIRST ROTATION

T2 = SECOND ROTATION

T3 = THIRD ROTATION

TA = PERIOD OF APOLLO S/C ORBIT (MINUTES)

TC = PERIOD OF COMM. SAT. ORBIT (MINUTES)

TDOT = TEST VARIABLE (TDOT = T - DT)

THETAC = PHASE ANGLE OF SYNCH. RELAY SATELLITE

THETA = ORBITAL PHASE ANGLE OF COMM SATS AT T=0

TMAX = TIME TO TERMINATE COMPUTATION (MINUTES)

TOUT = OUTAGE TIME (WHEN SATELLITE IS NOT VISIBLE)

WA = ANGULAR RATE OF S/C ORBIT (RAD/MIN)

WC = ANGULAR RATE OF COMM. SAT. ORBIT (RAD./MIN.)

XAZ INTERMEDIATE STORAGE OF AZ

XEL INTERMEDIATE STORAGE OF EL

XRSQ RANGE (SQRT(RSQ))